STUDY OF PHYSICAL PROPERTIES OF LIQUID CRYSTALS AND THEIR MIXTURES

THESIS SUBMITTED FOR THE DEGREE OF
DOCTOR OF PHILOSOPHY (SCIENCE)
OF THE
UNIVERSITY OF NORTH BENGAL

BY
NAVIN KUMAR PRADHAN

JUNE 1998

LIQUID CRYSTAL RESEARCH LABORATORY
DEPARTMENT OF PHYSICS, NORTH BENGAL UNIVERSITY
RAJA RAMMOHUNPUR, DARJEELING, WEST BENGAL
734 430-INDIA

STOCK TAKING - 2011

This work is dedicated to

my beloved father,

Late Bir Bahadur Pradhan.

DEPARTMENT OF PHYSICS
UNIVERSITY OF NORTH BENGAL
P.O. NORTH BENGAL UNIVERSITY
DIST. DARJEELING (WB)
PIN : 734430 INDIA

Railway Station : New Jalpaiguri (NFR)
Airport : Bagdogra
Phone : 0353-450414* Fax : 0353-450546*
E-mail : root @ nbu. ernet. in

local : omit 0353
International : replace 0353 by +91353

(TO WHOM IT MAY CONCERN)

This is to certify that the work reported in this thesis entitled " STUDY OF PHYSICAL PROPERTIES OF LIQUID CRYSTALS AND THEIR MIXTURES" by Mr. Navin Kumar Pradhan has been carried out by the candidate himself under my direct supervision and guidance. Mr. Navin Kumar Pradhan has fulfilled all the requirements for the submission of the thesis for Ph.D. degree of the University of North Bengal. Some part of the research work presented in this dissertation has been performed in collaboration with others. However, even in those works his contribution is very substantial. In character and disposition Mr. Navin Kumar Pradhan is fit to submit the thesis for the Ph. D. degree.

Date: 29th June 1998

(Ranjit Paul)
Professor of Physics and Supervisor.

Acknowledgements

I express my deep sense of gratitude to Prof. Ranjit Paul, Dept. of Physics, North Bengal University, who not only introduced me to the mysterious and fascinating world of Liquid Crystals but also supervised me whole-heartedly at every stage of my research work. I take this opportunity to express my gratefulness to Dr. (Mrs.) Sukla Paul, Reader, Dept. of Physics, N. B. U., for her active guidance and untiring support to complete my work.

I must express my gratitude to Prof. R. Dabrowsky, Military Institute of Technology, Warsaw, Poland, for donating Liquid Crystal samples used in my research work. My thanks are also due to E. Merck, U. K. and Hoffmann-La Roche Co., Basel, Switzerland for donating Liquid Crystal samples used in my research work.

I would like to extend my gratefulness to Mr. Sajal Kr. Sarkar, Senior Technical Assistant, Dept. of Physics, N. B. U. for his constant co-operation for designing and repairing the instruments used in my research. Mr. P. Tamang, Senior Technical Assistant, Dept. of Physics, N. B. U. is thankfully acknowledged for his spontaneous help during my experiments.

I am also thankful to Dr. P. Mandal, Dr. M. K. Das, Dr. B. Adhikari, Dr. A. Nath, Mr. P. Sarkar and Miss. S. Ghosh for their co-operation during my experiments. I would like to thank all the staffs of the University Science and Instrumentation Centre for availing me the various workshop facilities. I am really thankful to Mr. S. K. Giri, for his constant help when my experiment was in progress and also during the preparation of this manuscript.

I wish to convey my gratefulness to the Head of the Dept. of Physics, N. B. U. for allowing me to avail the laboratory facilities to persue my research work. I am also indebted to the Principal, St. Joseph's College and the Jesuit Community, Darjeeling, for sanctioning me the leave to complete my research work.

I wish to convey my sincere thanks to the University Grant Commission, New Delhi, for providing me financial assistance under F.I.P. scheme to carry out research work at North Bengal University for one-year.

I shall fail in my duty if I do not express my gratefulness to Mr. D. Lama, Senior Lecturer, Dept. of Botany, St. Joseph's College Darjeeling, for his co-operation at every stage of preparation of this thesis.

I am indebted to all whose name have not been mentioned but have substantial contributions in my research work without their realisation.

A word for my beloved Mother - "I am here today because of her."

Finally it is more than a pleasure once more to acknowledge my indebtedness to my loving wife, sons, daughter and other members of my families for their unfailing encouragement and loving co-operation in my work. I thank them for their forbearance towards my frequent spells of late-comings and outgoing when my research work was in progress.

Navin Kr. Pradhan

June 1998.

(Navin Kumar Pradhan)
Senior Lecturer in Physics,
St. Joseph's College,
Darjeeling - 734 104.

Contents

CHAPTER-1

Introduction

Introduction:

Liquid crystalline materials are generally organic compounds having physical properties intermediate between crystalline solids and isotropic liquids. The liquid crystalline phase was first observed in 1888 by F. Reinitzer [1] and O. Lehmann [2]. Friedel [3,4] suggested the term "mesomorphic phase" or "mesophase" to the liquid crystalline matter. At present several thousands of organic compounds are known to exhibit mesophases [5,6]. Few organo-metallic compounds [7,8] as well as some inorganic compounds [9] are also found to exhibit liquid crystalline properties.

Liquid crystals are fluids in which there occur a certain order in the arrangement of the molecules. As a result there is anisotropy in the mechanical, electrical, magnetic and optical properties. Although liquid crystals combine certain properties of a solid and an isotropic liquid, they exhibit very specific electro-optical magneto-optical phenomena. The molecules of the compound that shows mesophases are geometrically highly anisotropic in shape, like a rod or a disc. In the crystalline solid the centre of mass of the molecules are located on a three dimensional lattice while in the liquid state the three dimensional translational symmetry disappears and there only remains some short range order between the centres of mass of the molecules. In the liquid crystalline state the three dimensional translational symmetry of the centres of mass of the molecules is partially or fully absent but some degree of orientational order of the molecules is still present. Some of the books and review articles on liquid crystals which give details regarding molecular structure and physical properties of the compound exhibiting mesophases are listed in the references [5, 6, 8, 13-20]. Recent developments in the field of liquid

crystals and applications are also available in the recent publications [21-25].

1. Classification of Liquid Crystals:

Liquid crystals are broadly classified into two types, viz. 'Lyotropic' and ' Thermotropic'.

1.1 Lyotropic mesophase :

Lyotropic liquid crystals are solutions of rod like molecules in a normally isotropic solvent [26-29]. In such mesophase the amount of the solvent is the most important variable. Soap solution in water is a common example of lyotropic mesophase and its behaviour appears as a function of either concentration or temperature. The lyotropic mesophase is also exhibited by solution of deoxyribonucleic acid ; certain viruses in appropriate solvent (usually water) in suitable concentration.

Although lyotropic liquid crystals play an important role in living systems and are of great biological interest [22], the present work is restricted to the study of the thermotropic liquid crystals only.

1.2 Thermotropic mesophase:

Thermotropic liquid crystals are those where mesomorphic behaviour are exhibited due to the change of temperature. Thermotropic liquid crystals in which the mesophases are stable at temperatures above the melting point, both during heating and during cooling are called enantiotropic. In certain cases the liquid crystalline state is stable only at temperatures below the melting point and can be obtained only during cooling of the compound, phases of this kind are called monotropic. Friedel

[30], from his detailed optical and X-ray studies subdivided the thermotropic liquid crystals into three types, viz. nematic, cholesteric and smectic. The thermotropic liquid crystals can also be classified according to the shape of the constituent molecules. Calamitic liquid crystals have rod like molecules, where as discotic liquid crystals have disc shaped molecules. I shall confine myself to calamitic liquid crystals in the rest of this section 1.2.

1.2a Nematic mesophase :

The word nematic comes from the Greek word νημα which means thread. When a thin layer of nematic liquid crystal is observed between crossed polarisers under a polarising microscope then a characteristic pattern known as texture, is observed. The textures of nematic liquid crystals are generally thread - like, hence the name nematic. Nematic liquid crystals are characterised by long-range orientational order of the molecules but they do not have long range translational order, thereby possessing fluid like behaviour. Although there is no long range correlation between the centres of mass of the molecules, but still it differs from isotropic liquid in that the molecules are, on an average, aligned with their long axes parallel to each other. Thus, in nematic liquid crystals a preferred direction known as the director denoted by **n** is defined whose direction in space is in general arbitrary. The molecules in the nematic phase rotate about their long axes very fast ($\sim 10^{-11}$ sec) and hence the nematic phase can be assumed to be uniaxial. The axis of uniaxial symmetry has no polarity, i.e., **n** and **-n** are equivalent. Fig 1.1 shows the schematic diagram of molecular order of nematic and isotropic phase. Another characteristic of nematic phase is that the constituent molecules are identical to its mirror

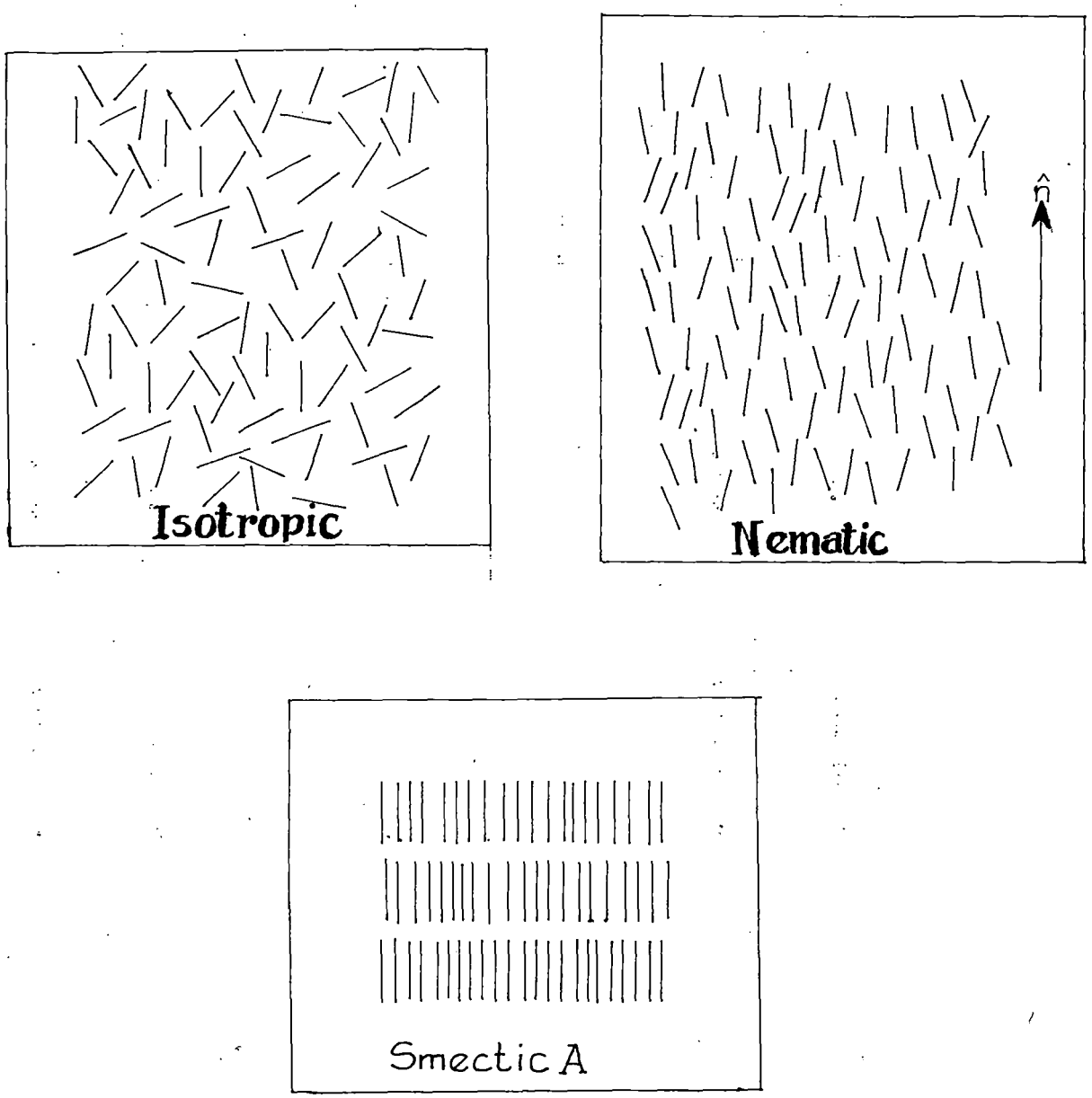

Figure 1.1. Schematic representation of molecular order in the isotropic, nematic and smectic phase.

image (achiral) or the system may be considered as a racemic mixture of left- and right-handed species. X-ray studies [32,38,39] indicates that some nematics consists of clusters of molecules, called the cybotactic groups. In each cluster the molecular long axes are parallel to each other and the molecular centres are arranged in more or less well defined layers. When the molecular long axes is normal to the layer then the phase is known as normal cybotactic nematic phase and if it is tilted with respect to the layer then the phase is known as skewed cybotactic nematic phase. The so called cybotactic groups may be thought of as smectic fluctuation in the nematic phase. Another type of nematic phase call the fibre type nematic [33] is also identified in some of the liquid crystalline compounds. In this type of mesophase there is one dimensional correlation of molecules along the director, **n**, thus leading to the existence of strings of molecules or fibres in the nematics. Furthermore, a biaxial modification of the nematic liquid crystals has been discovered in certain polymeric liquid crystals [34] and lyotropic systems [35]. Figure 1.2 shows the schematic diagram of molecular order in different types of nematic liquid crystals.

1.2b Cholesteric or Chiral nematic phase :

The cholesteric liquid crystals are so called because many derivatives of cholesterol belong to this class of mesophase. The cholesteric mesophase is also a nematic type of liquid crystal except that it is composed of optically active molecules. As such they are also termed as chiral nematics [36-38]. The molecules of this class of mesophase have long range orientational order together with the spatial variation of the director leading to a helical structure. The helical structure (Fig 1.3) can be described by an intrinsic non-constant director.

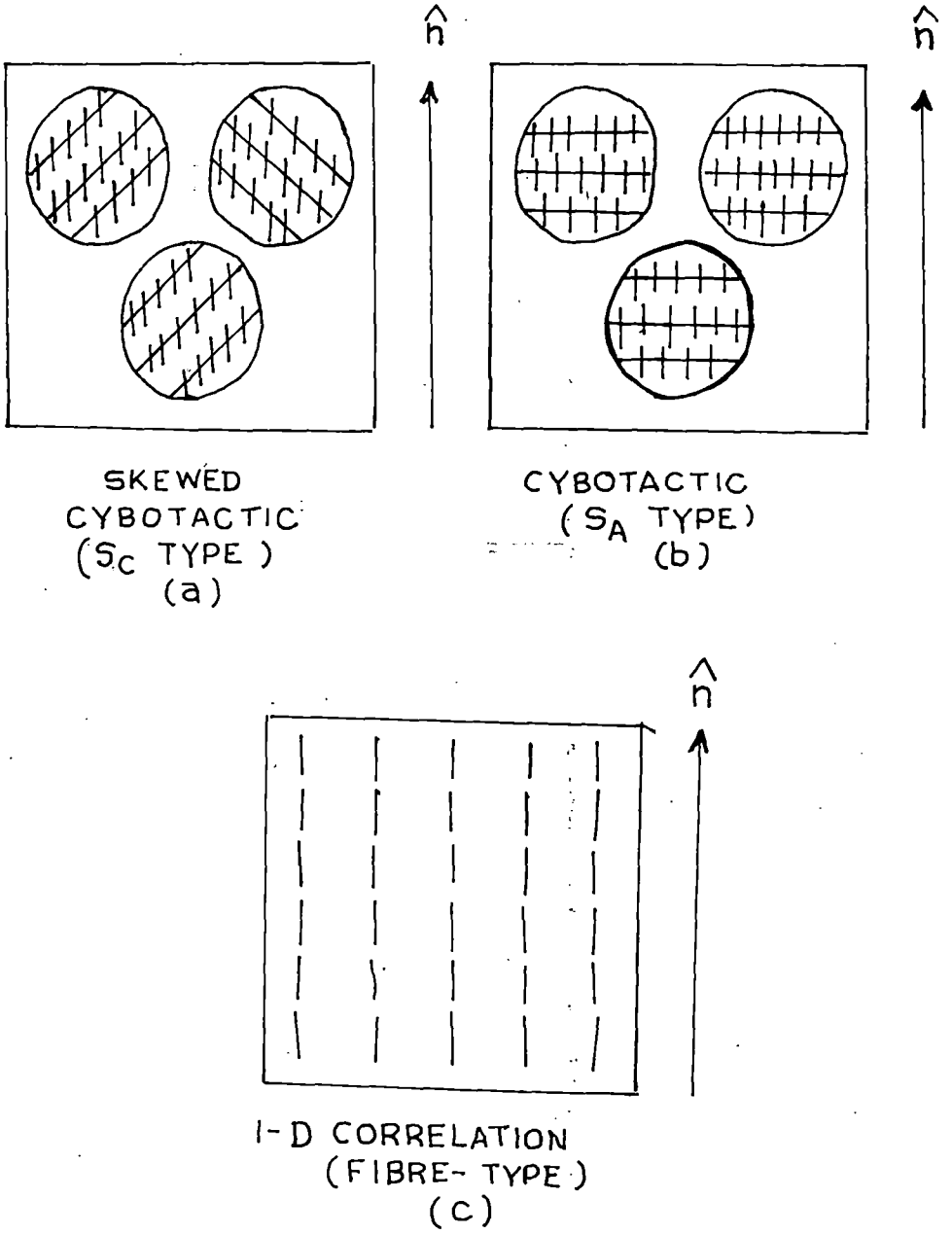

Figure. 1.2. Schematic representation showing molecular arrangements in nematics having three types of short range order.

$n_x = \cos (q_o z + c)$

$n_y = \sin (q_o z + c)$

$n_z = 0$

c being a constant

The helix axis is taken parallel to the z-axis. The pitch of the helix may be defined as the linear distance along the helix axis in which the full rotation of the director **n** is completed. The pitch (p) is given by :

$$p = 2\pi / | q_o |$$

However, n and -n are equivalent, the pitch in chiral nematics is given by :

$$p = \pi / | q_o |$$

The sign of q_o distinguishes between left-handed and right-handed chiral nematics. When $q_o = 0$, then the pitch is infinite and it corresponds to normal nematic phase. No liquid crystalline compounds are known to have phase transition from nematic to chiral nematic phase, however the application of electric or magnetic field may cause phase transition from chiral to nematic. Moreover the addition of small amount of chiral compound to nematic compound changes a nematic phase into a long pitch chiral nematic phase.

1.2c Smectic mesophase :

Smectic liquid crystals have stratified structures and variety of molecular arrangement are possible within each stratification. Within the layer, the long axes of the molecules are parallel to each other thereby exhibit orientational order as in the nematic phase. In addition to this the centre of the molecules are, on the average, arranged in equidistant planes showing one degree of translational order. In most smectic phases, the molecules are mobile in two directions and can rotate about one axis. The

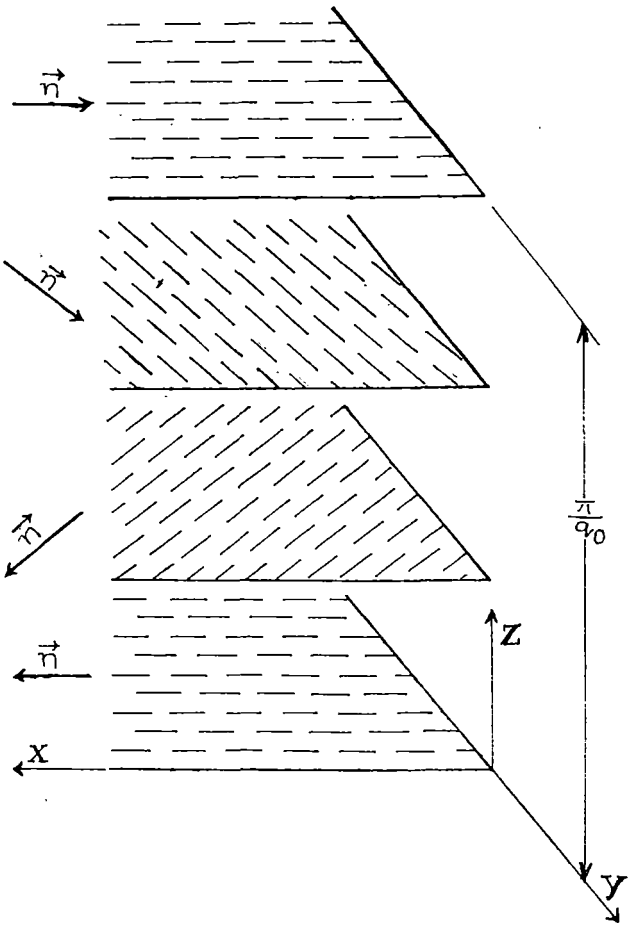

Figure 1.3. Schematic representation of the helical structure of the cholesteric liquid crystals.

inter-layer attractions are weak compared with the lateral forces between the molecules, and the layers are able to slide over one another relatively easily. Consequently, the smectic phase have fluid properties, but are much more viscous than the nematic phase. Smectics are much more ordered than the nematics and consistent with their higher order, the smectic phases always occur at temperatures below the nematic domain. Classification of the smectic mesophases are generally done by three different methods, viz. ; miscibility, texture, and x-ray diffraction studies. The various types of smectic mesophases that have been identified [40-49] are designated as follows [50] :

S_A , S_B , S_C, S_E, S_F, S_G, S_H, S_k, $S_{l, etc.}$ ----------

Since the present work deals mostly with smectic A phase and smectic A_d phase, only these phases are discussed.

1.2 c1 Smectic A phase :

Smectic A is the simplest type of smectic phase. The smectic A mesophase is made up of layers which move freely with respect to each other. With in the layers, the long axes of the molecules lie almost parallel to one another, their mean direction being normal to the plane of the layer. The molecules are free to rotate about their long axes, and the distribution of the molecules with in the layers are random [43,51,52]. Thus, within the layers the molecules have a low degree of translational order, each layer being a two - dimensional liquid. The molecular arrangement of smectic A phase is shown in Fig 1.1.

The smectic A phase has the highest temperature of the smectic phase and on heating it undergoes a transition to the nematic or cholesteric mesophase, or directly to the isotropic phase. At thermal equilibrium the

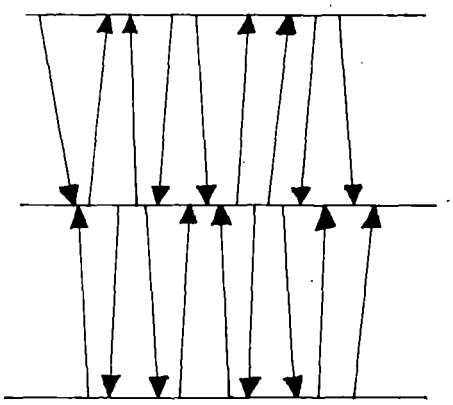

A_1

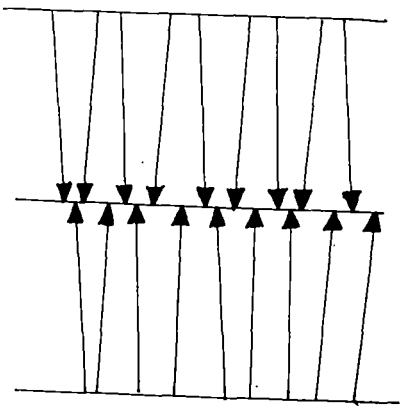

A_2

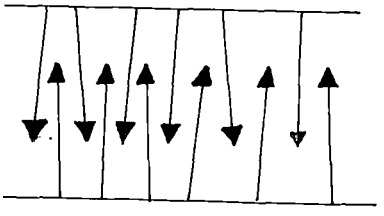

A_d

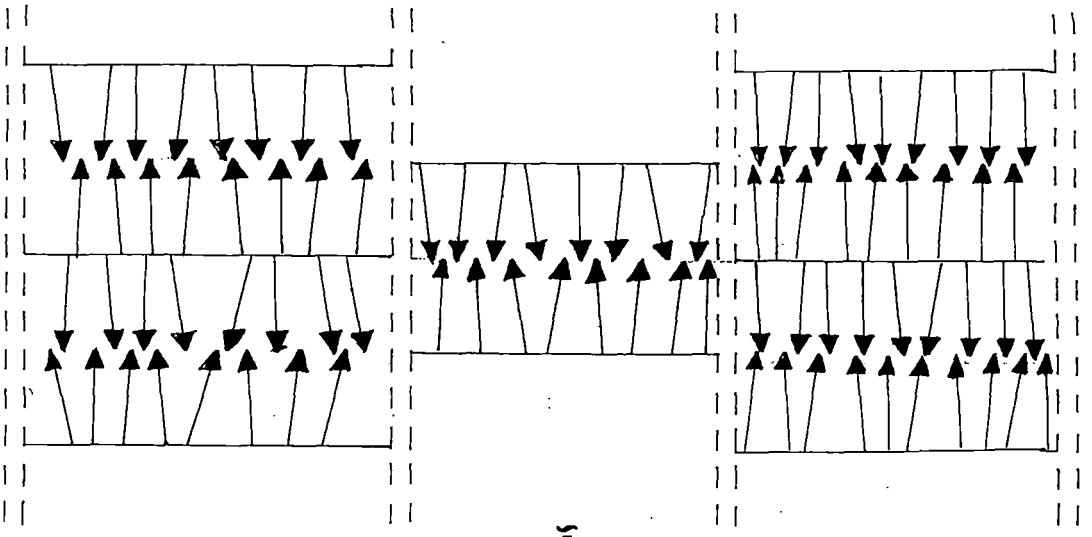

$\tilde{A}$

Figure 1.4. Schematic representation of the molecular arrangement in the different forms of smectic A phase composed of polar molecules; monolayer A_1, bilayer A_2, partially bilayer A_d and antiphase $\tilde{A}$.

smectic A phase is optically uniaxial [53] due to the infinite fold rotational symmetry about the axis parallel to the layer normal. Apart from the focal conic textures [54-60] smectic A also exist in homeotropic texture [54-60]. Smectic A phase can be further subdivided into several distinct phases [61-67] such as monolayer smectic A_1, bilayer smectic A_2, partially bilayer smectic A_d and smectic antiphase $\tilde{A}$. In the monolayer smectic A_1 phase the layer spacing (d) is approximately equal to the molecular length (l) whereas in the bilayer smectic A_2 phase the layer spacing (d) is approximately in between l and 2l. The structures of these phases are represented schematically in Fig. 1.4. When the molecules, possess a dipole moment positioned at the end of the molecules, then the molecules can minimise their dipole interaction via antiparallel dipole correlation. Consequently smectic A_d phases can be formed with a layer thickness, that is approximately given by $d \approx a + 2b$, where a and b are the length of the aromatic head and the aliphatic tail, respectively. Typically this leads to $d \approx 1.4\,l$ where $l = a + b$. The dipole - dipole interaction has a profound effect on many physical properties. The details regarding polymorphism in smectic A are discussed in references [68-75].

1.3 Some new liquid crystalline phases:

1.3a Discotic phase:

A new type of mesophase has been discovered [74] which cannot be classified either as a nematic or as a smectic. This phase is formed in materials with molecules which are approximately disc-shaped. The disc are packed together in columns, although their arrangement within an individual column can be either ordered or random. Such mesophase are called discotic liquid crystals and its structure may be classified into three

groups, viz. the columnar, the nematic and the lamellar. Previously very similar disc-like mesogens have been observed in petroleum and coal tar [75,76]. At present remarkable progress have been achieved in the field of discotic liquid crystals [77-81].

1.3b Blue phases :

For chiral nematics with a relatively short pitch (less than 7000Å), several different types of phases have been observed between the isotropic and the chiral nematic phase and these are known as the 'blue phases'. The temperature region in which these blue phases are stable is very small (approximately 0.1 °C). Compounds with relatively high pitch can display upto three different types of blue phases [82]. Blue phase shows optically isotropic structure with colours in reflected light. The structure of blue phase is not yet completely explained but it is clear that they exhibit cubic symmetry and the basic structure is related to cholesteric phase. The most probable model to explain the structure of the blue phase is in terms of the defect in a cubic array. Blue phases do not possess double refraction, however, they show optical activity and selective reflection of circularly polarised light.

1.3c Chiral tilted smectic phases :

Liquid crystalline compounds which exhibit optical activity can form a chiral smectic C mesophase in which each successive layer is rotated through a certain angle with respect to the tilt direction so that a twisted structure is formed. This structure has ferro-electric (FE) properties when positively oriented molecular dipoles are present. Ferri electric (FI) and anti-ferro electric (AF) phases are also observed. [83]. The ferroelectric

structures possess two fold-rotational axis of symmetry parallel to the smectic layer and perpendicular to the director **n**. In the twisted form, the lateral dipole moments of the molecules are cancelled on average. If a lateral dipole moment is present, each smectic layer possess an electric polarisation parallel to the two fold axis of symmetry. Hence the director and the polarisation spiral together along the helix axis, leading to an overall zero bulk polarisation. By interaction with the walls or in electric or in magnetic fields, the twist can be unrolled and this form the phase can show ferroelectric properties which originates from a summation of many lateral molecular dipole moments. In the FI phase the local dipole moments are partially compensated whereas in the AF phase, the adjacent layers of the molecules are oppositely tilted. Recently both AF phase [84] and FI phase [85] have been observed in a substance MHPOBC. Ferroelectric liquid crystal has attracted much attention for fast switching electro-optical display devices.

1.3d Injected smectic phase :

By mixing two pure nematic liquid crystals it is possible for us to obtain the so called injected or induced smectic phase [90-91]. As such, the formation of injected smectic phase is accompanied by a marked deviation of the nematic isotropic transition temperature from a linear dependence on composition. Induced smectic phase can generally be formed in a binary mixture in which one of the constituent have a strong terminal polar group while the other have a non-polar terminal group [92-107]. In binary mixtures, dipole-induced dipole interaction is responsible for the phase stabilisation. However injected smectic phase has also been observed in a mixture of other type of molecules [108-110]. A quantitative theory of

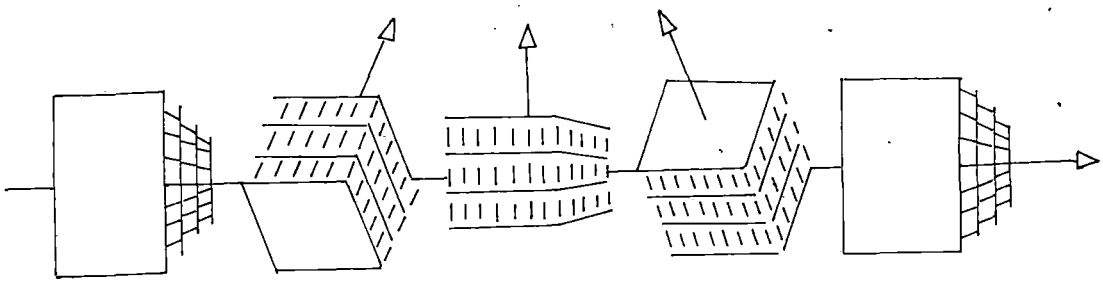

Figure 1.4a Schematic representation of the structure of smectic A* phase.

formation of injected smectic phase is difficult as it would require the inclusion of position dependent attractive and repulsive interactions for both the components. A molecular model of the induced smectic phase has been discussed by de Jeu et al [111].

1.3e Smectic A* phase:

The term smectic A* phase was coined by Goodby et. al [134]. Smectic A* phase consists of regular array of dislocations which is being formed in the smectic A under an imposed twist or bend distortion. Smectic A* is composed of optically active molecules and its helical axis is parallel to the layers. For this reason smectic A* structure may be imagined as a series of smectic A blocks or grains separated by twist grain boundaries, the director being rotated by a constant angle on going from one grains to the next. The pitch of the helix axis is found to be about 1μm [135] and the grain size obtained from x-ray measurement [135] is about 180 Å. Furthermore, Renn and Lubensky [136] termed this phase as the "twist grain boundary phase". The structure of the smectic A* phase is shown schematically in Figure (1.4a).

1.3f Re-entrant phase:

When a compound exhibits both smectic and nematic phase, then as a rule, the nematic phase occurs at the higher temperature. In 1975 Claudis [112] discovered exception to this rule in certain strongly polar materials, the so called phenomenon of re-entrant polymorphism. The nematic re-entrant phase was first observed on binary mixtures of two cyano compounds. The phase sequence of transition on cooling was as follows :-

Isotropic → Nematic → Smectic A_d → Nematic re-entrant → Crystal.

Claudis [114,115] reported the re-entrant nematic phase in pure terminal polar compounds (octyloxy cyano biphenyl) at elevated pressures. The re-entrant nematic phase has been observed in some pure compound at atmospheric pressure [116-123]. More complex example of multiple re-entrant polymorphism have been found in a pure substance [108]. The re-entrant phase have been found also in non-polar compounds [93-96].

From the molecular point of view, a simple model has been proposed by Cladis [129-131] which gives an approximate qualitative explanation of the re-entrant phenomenon. a more elaborate model, which take into account attractive forces and hard core repulsions, dipole-induced dipole interactions etc. have been proposed by Longa and de Jeu [111]. S. Chandrasekhar [133] has also discussed qualitatively the re- entrant phenomenon based on the molecular point of view.

References:

1) F. Reinitzer, Monatsh. Chem., 9, 421 (1888), Liq. Cryst., 5, 7 (1989).

2) O. Lehmann, Z. Physik. Chem., 4, 462 (1889).

3) G. Friedel, In Colloid Chemistry, Ed. J. Alexander, Vol. 1, p-102ff. The chemical catalogue company, Inc., N. Y., (1926).

4) G. Friedel and E. Friedel, Z. Krist., 79, 1 (1931).

5) W. Kast, Landelt-Bornstein Tables, Vol. 2, 6th edition, p-266, Springer-Verlag (1969).

6) D. Demus and H. Demus, Flussige Kristalle in Tabellen, VEB Deutscher Verlag fur Grundstoffindustrie, Leipzig (1974).

7) G. H. Brown, J. Electronic Materials, 2, 402 (1973).

8) H. Kelker and R. Hartz, Hand book of Liquid Crystals, Verlag Chemie, Weinheim, p. 67 (1980).

9) H. Zocher, Liquid Crystals (2), part 1, ed. G. H. Brown, G & Bscience Publisher, Inc. N. Y. , 115 (1969).

10) I. G. Chistyakov, Zhidkie Kristally (Liquid Crystals), Nauka, Moscow (1966).

11) P. G. de Gennes, The Physics of Liquid Crystals, Clarendon Press, Oxford, (1974).

12) L. M. Blinov, Usp. Fiz. Nauk, 114, 67 (1974) [Sov. Phys. Usp., 17, 658 (1975).]

13) G. W. Gray, Molecular structure and the properties of liquid crystals, Academic Press (1962).

14) E. B. Priestley, P. J. Wojtowicz and P. Sheng, eds., Introduction to liquid crystals, Plenum, New York, 1974.

15) S. Chandrasekhar, Liquid Crystals, Cambridge University Press, Cambridge, (1977).

16) G. W. Gray and P. A. Winsor (Editor) Liquid crystals, Vol. 1 and 2, Ellis Horwood Limited, (1974).

17) G. Vertogen and W. H. de Jue, Thermotropic Liquid Crystals, Fundamentals, Springer-Verlag (1988).

18) P.S. Pershan, Structure of Liquid Crystal Phases, World Scientific, (1988).

19) G.W. Gray and J. W. Goodby (Editors), Smectic Liquid Crystals, Leonard-Hill (1984).

20) G. R. Luckhurst and G. W. Gray, (Editors), The Molecular Physics of Liquid Crystals, Academic Press (1979).

21) Advances in Liquid Crystals ed. G. W. Brown, Vol. 1-6, Academic Press, (1975-1983).

22) Liquid Crystals, Applications and uses, (Ed. B. Bahadur, World Scientific (1991). Vol. 1, 2 and 3.

23) Thermophysical properties of liquid crystals, A. L. Tsykalo, Gordon and Breach Science Publishers.

24) Modern topics in Liquid Crystals, (Ed. A. Buka). World Scientific (1993).

25) Physics of Liquid Crystalline Materials, (Ed. I. C. Khoo and K. Simoni), Gordon and Breach Science Publishers.

26) A. S. C. Lawrence, "Lyotropic Mesomorphism in Lipid-water Systems, Mol. Cryst. Liq. Cryst. 7, 1 (1969).

27) P. A. Winsor, Chem. Rev. 68, 1 (1968).

28) P. Ekwall, L. Mandell and K. Fontell, Mol. Cryst. Liq. Cryst. 8, 157 (1969).

29) V. Luzzati and F. Reiss-Husson, Nature, 210, 1351 (1966).

30) G. Friedel, Ann Physique, 18, 273 (1922).

31) H. Sachmann and D. Demus, Mol. Cryst. Liq. Cryst. , 21, 239 (1973).

32) A. de Vries, Mol. Cryst. Liq. Cryst. 10, 31 (1970) ; ibid 10, 219 (1970); ibid 11, 36 (1970).

33) K. Usha Deniz, A. S. Paranjpe, V. Amirthalingam and K. V. Muralidharan, Mol. Cryst. Liq. Cryst. (Letters), 49, 265 (1979).

34) K. Praefcke, B. Kohne, B. Gundogan, D. Singer, D. Demus, S. Diele, G. Pelzl and U. Bakowsky, Mol. Cryst. Liq. Cryst., 198, 393 (1991).

35) L. Y. Lu and A. Saupe, Phys. Rev. Lett., 45, 1000 (1980).

36) G. H. Brown, Amer. Scientist, 60, 64 (1972).

37) T. Nakagiri, H. Kodama and K. K. Kobayashi, Phys. Rev. Lett. , 27, 564 (1971).

38) I. G. Chistyakov, Sov. Phys. Ups. , 9, 551 (1967).

39) G. W. Stewart and R. M. Morrow, Phys. Rev. , 30, 332 (1927).

40) K. Herrmann and A. H. Krummacher, Z. Kristallogr. Mineral. Petrogr., A 81, 317 (1932).

41) G. Friedel, C. R. Acad. Sci., Paris, Ser. A. B., 180, 269 (1925).

42) H. Sackmann and D. Demus, Mol. Cryst. Liq. Cryst., 21, 171 (1973).

43) S. Diele, P. Brand and H. Sackmann, Mol. Cryst. Liq. Cryst., 16,105 (1972).

44) D. Demus, G. Kunicke, J. Neelson and H. Sackmann, Z. Naturforsch., 23a, 84 (1968).

45) D. Demus, S. Diele, M. Klapperstuck, V. Link and H. Zaschke, Mol. Cryst. Liq. Cryst., 15, 161 (1971).

46) A. de Vries, Mol. Cryst. Liq. Cryst., 24, 337 (1974).

47) J. Falgueirettes and P. Delord, in Liquid and Plastic Crystals, Vol. 2, (Eds. G. W. Gray and P. A. Winsor), Halstead, New York, 1974, p. 62.

48) A. de Vries and D. L. Fishel, Mol. Cryst. Liq. Cryst., 16, 311 (1972).

49) A. de Vries, in proceedings of the International Liquid Crystal Conference, Bangalore, December, 1973, Pramana Supplement I, p. 93.

50) H. Kelkar and R. Hatz, Handbook of Liquid Crystals, Verlag Chemie, Chapter 1, p.6 (1980).

51) G. C. Fryberg, E. Gelerinter and D. L. Fisher, Mol. Cryst. Liq. Cryst., 16, 39 (1972).

52) G. R. Luckhurst and A. Sanson, Mol. Cryst. Liq. Cryst., 179 (1972).

53) P. G. de Gennes, The Physics of Liquid Crystals, Clarendon, Oxford, 1974.

54) H. Sackmann and D. Demus, Mol. Cryst. Liq. Cryst., 2, 81 (1966).

55) H. Sackmann and D. Demus, Fortschr. Chem. Forsch., 12, 349 (1973).

56) G. H. Brown, J. W. Doane, and V. D. Neff, A Review of the Structure and Physical Properties of Liquid Crystals, Crc Press, Cleveland, Ohio, (1971).

57) P. G. de Gennes, Mol. Cryst. Liq. Cryst., 21, 49 (1973).

58) H. Sackmann and D. Demus, Mol. Cryst. Liq. Cryst., 21, 239 (1973).

59) H. Sackmann, Pure and Applied Chem., 38, 505 (1974).

60) A. Saupe, in Liquid Crystals and Plastic Crystals, Vol. 1 (G. W. Gray and P. A. Winsor, eds.), Halstead, New York, p. 8, (1974).

61) A. M. Levelut, R. J. Tarento, F. Hardouin, M. F. Achard and G. Sigaud, Phys. Rev. A, 24, 2180 (1981).

62) G. Sigaud, F. Hardouin, M. F. Achard and A. M. Levelut, J. Physique, 42, 107 (1981).

63) F. Hardouin, N. H. Tinh, , M. F. Achard and A. M. Levelut, J. Physique, 43, L.327 (1982).

64) C. Druon and J. M. Wacrenier, Mol. Cryst. Liq. Cryst., 98, 201 (1983).

65) I. Hatta, Y. Nagai, T. Nakayama and S. Imaizumi, J. Phys. Soc. Jpn., 52, Suppl. 47 (1983).

66) C. Chiang and C. W. Garland , Proc. of Tenth International Liquid Crystal Conference, New York, July, (1984), Abstract no. E20.

67) F. Hardouin, A. M. Levelut, M. F. Achard and G. Sigaud, J. de Chemie Physique, 80, 53 (1983).

68) T. R. Taylor, J. L. Fergason and S. L. Arora, Phys. Rev. Lett. 24, 359 (1970).

69) R. Pindak, D. E. Moncton, S. C. Davey and J. W. Goodby, Phys. Rev. Lett., 46, 1135 (1981).

70) M. Cheng, J. H. Ho, S. W. Hui and R. Pindak, Phys. Rev. Letts. 59, 1112 (1987).

71) M. Lambert and A. M. Levelut in Anharmonic Lattices, Structural Transitions and Melting (Ed. T. Riste), Noordhoff, Leiden, p. 375, (1974).

72) H. M. Richardson, A. J. Leadbetter and J. C. Frost., Ann. Phys., 3, 177 (1978).

73) A. J. Leadbetter, M. A. Mazid and R. M. Richardson, Liquid Crystals, (Ed. S. Chandrasekhar), Heyden, London, p. 65 (1980).

74) S Chandrasekhar, B. K. Sadashiva and A. K. Suresh, Pramana, 9, 471 (1977).

75) J. E. Zimmer and J. L. White, Mol. Cryst. Liq. Cryst., 38, 177 (1977).

76) J. D. Brooks and G. H. Taylor, Carbon, 3, 185 (1965).

77) D. Guillon, A. Skoulios, C. Piechocki, J. Simon and P. Weber, Mol. Cryst. Liq. Cryst., 100, 275 (1983).

78) J. Luz, Tenth Int. Conf. on Liquid Crystals, York, July (1984), Abstract no. H2.

79) P. G. de Gennes, J. de Phys. (Lett.), 44, 657 (1983).

80) A. C. Ribeiro and A. F. Martins, Tenth Int. Conf. on Liquid Crystals, York, July, (1984), Abstract no. H6.

81) C. Destrade, H. Gasparoux, P. Foucher, N. H. Tinh, J. Malthete and J. Jacques, J. Chem. Phys., 80, 137 (1983).

82) S. Meiboom, M. Sammon, Phys. Rev. Lett., 44, 882 (1980).

83) M. Glogarova in Modern Topics in Liquid Crystals (Ed. A. Buka), World Scientific, p. 271 (1993)

84) A. D. L. Chandani, Y. Ouchi, H. Takezoe, A. Fukada, K. Terashima, K. Furukawa and A. Kishi, Jpn. J. Appl. Phys. , 28, L1261 (1989).

85) E. Gorecka, A. D. L. Chandani, Y. Ouchi, H. Takezoe, A. Fukada, Jpn. J. Appl. Phys., 29, L111 (1990).

86) R. B. Meyer, L. Libert, L. Strzelecki and P. Keller, J. Physique Lett., 36, L69 (1975).

87) J. W. Doane, A. Golemme, J. L. West, J. B. Whitehead, Jr. , and B. G. Wu, Mol. Cryst. Liq. Cryst., 165, 511 (1988).

88) P. S. Drzaic, J. Appl. Phys., 60, 2142 (1986).

89) G. P. Montgomery, Jr. in large-area Chromogenics: Materials and Devices for Transmittance Control, C. M. Lampert and G. G. Granqvist (Ed. SPIE).

90) J. S. Dave, P. R. Patel and K. L. Vasant, Mol. Cryst. Liq. Cryst., 8, 93 (1969).

91) C. S. Oh, Mol. Cryst. Liq. Cryst., 42, 1 (1977).

92) J. W. Park, C. S. Bak and M. M. Labes, J. Amer. Chem. Soc., 97, 4398 (1975).

93) A. C. Griffin, T. R. Britt, N. W. Buckley, R. F. Fisher, S. J. Havens and D. W. Goodman, Liquid Crystals and Ordered Fluids, Vol. 3, Eds. J. F. Johnson and R. S. Porter , Plenum Press, New York, p. 61, (1978).

94) B. Engelen and F. Schneider, Z. Naturforsch., 33A, 1077 (1978).

95) B. Engelen, G. Heppke, R. Hopf and F. Schneider, Ann. Phys., 3, 403 (1978).

96) L. J. Yu and M. M. Labes, Mol. Cryst. Liq. Cryst., 54, 1 (1979).

97) M. Domon and J. Billard, J. Phys. (Paris), 40, C3-413 (1979).

98) K. P. L. Moodithaya and N. V. Madhusudana in "Liquid Crystals", Proc. Int. Liq. Cryst. Conf., Bangalore, Dec. 8, (1979), Ed. S. Chandrasekhar, Heyden, London, p. 297, (1980).

99) F. Schneider and N. K. Sharma, Z. Naturforsch., 36a, 62 (1981).

100) F. Schneider and N. K. Sharma, Z. Naturforsch., 36a, 1086 (1981).

101) K. Araya and Y. Matsunaga, Mol. Cryst. Liq. Cryst., 67, 153 (1981).

102) G. Derfel, Mol. Cryst. Liq. Cryst., 82, 277 (1982).

103) J. Szabon and S. Diele, Crystal Res. Tech., 17, 1325 (1982).

104) K. W. Sadowska, A. Zywocinski, J. Stecki and R. Dabrowski, J. Phys. (Paris), 43, 1673 (1982).

105) W. Waclawek, R. Dabrowski and A. Domagala, Mol. Cryst. Liq. Cryst., 84, 255 (1982).

106) A. Boij and P. Adomenas, Mol. Cryst. Liq. Cryst., 95, 59 (1983).

107) E. Chino and Y. Matsunaga, Bull Chem. Soc. Japan, 56, 3230 (1983).

108) N. K. Sharma, G. Pelzl, D. Demus and W. Weissflog, Z. Phys. Chem. (Leipzig), 261, 579 (1980).

109) J. W. Goodby, T. M. Leslie, P. E. Cladis and P. L. Finn. Proc. ASC Symposium on Liquid Crystals and Ordered Fluids, Las Vegas, (1982), Ed. A. C. Griffin and J. F. Johnson, Plenum, New York, p. 89, (1984).

110) N. V. Madhusudana, V. A. Raghunathan and M. Subramanya Raj Urs, Mol. Cryst. Liq. Cryst., 106, 161 (1984).

111) W. H. de Jue, L. Longa and D. Demus, J. Chem. Phys., 84, 6140 (1986).

112) P. E. Cladis, Phys. Rev. Lett., 35, 48 (1975).

113) D. Guillon, P. E. Cladis and J. Stamatoff, Phys. Rev. Lett., 41, 1598 (1978).

114) P. E. Cladis, R. K. Bogardus, W. B. Daniels and G. N. Taylor, Phys. Rev. Lett., 39, 720 (1977).

115) P. E. Cladis, R. K. Bogardus and D. Aadsen, Phys. Rev. Lett., A18 2292 (1978).

116) F. Hardouin, G. Sigaud, M. F. Achard and H. Gasparoux, Solid St. Commun., 30, 265 (1979), Phys. Lett., 71A, 347 (1979).

117) N. V. Madhusudhana, B. K. Sadashiva and K. P. L. Moodithaya, Curr. Sci., 48, 613 (1969).

118) F. Hardouin, G. Sigaud, M. F. Achard and H. Gasparoux, Phys. Lett., 3, 71A, 347 (1979).

119) 15. N. H. Tinh and H. Gasparoux, Mol. Cryst. Liq. Cryst., 49, 287 (1979).

120) K. P. L. Moodithaya, and N. V. Madhusudhana, Proc. Int. Liq. Cryst. Conf., Bangalore, Dec. 8, (1979), Ed. S. Chandrasekhar.

121) J. C. Dubois, N. H. Tinh, A. Zann and J. Billard, Nouv. J. Chimie, 2, 647 (1978).

122) B. K. Sadashiva, Proc. Int. Liq. cryst. Conf. , Bangalore, Dec. 8, (1979), Ed. S. Chandrasekhar, Heyden, p-165 (1980).

123) C. Legrand, J. P. Parneix and A. Chapton, Tenth Int. Conf. on Liquid Crysts. , New York, (1984), Abstract no.-E 18.

124) Nguyen Hun Tinh, F. Hardouin and C. Destrade, J. Phys.(Orsay, Fr.), 43, 1127 (1982).

125) G. Pelzl, S. Diele, I. Latif, W. Weißflog and D. Demus, Cryst. Res. Technol., 17, K82 (1982).

126) S. Diele, G. Pelzl, I. Latif and D. Demus, Mol. Cryst. Liq. Cryst. (Lett.), 92, 27 (1983).

127) G. Pelzl, I. Latif, S. Diele, M. Novak, D. Demus, H. Sackmann, Mol. Cryst. Liq. Cryst., 139, 333 (1986).

128) L. K. M. Chen, G. W. Gray, D. Lacey, S. Srilhauratana and K. J. Toyne, Mol. Cryst. Liq. Cryst., 150B, 335 (1985).

129) P. E. Cladis in "Liq. Crystals", Proc. Int. Conf. Bangalore, (1979), Ed. S. Chandrasekhar , Heyden, London, p-105, (1980).

130) P. E. Cladis, Mol. Cryst. Liq. Cryst., 67, 177 (1981).

131) P. E. Cladis, D. Guillon, F. R. Bouchet and P. L. Finn, Phys. Rev., 23a, 2594 (1981).

132) L. Longa and W. H. de Jue, Phys. Rev. A, 26, 1632 (1982).

133) S. Chandrasekhar, Mol. Cryst. Liq. Cryst., 124, 1 (1985).

134) J. W. Goodby, M. A. Waugh, S. M. Stein, E. Chin, R. Pindak and J. S. Patel, Nature (London), 337, 449 (1989); J. Am. Chem. Soc., 111, 8119 (1989).

135) G. Srajer, R. Pindak, M. A. Waugh, J. W. Goodby and J. S. Patel, Phys. Rev. Lett., 64, 1545 (1990).

136) S. R. Renn and T. C. Lubensky, Phy. Rev., A38, 2132 (1988).

CHAPTER-2

Theoretical background and experimental methods

2.1 Theories of liquid crystalline phases:

The theories of liquid crystalline phase have been described in detail in several books of which some are listed in the references [1-5]. In present work I have tried to compare the experimental values of the order parameters of nematics and smectics with those obtained from Maier-Saupe mean field theory and McMillan theory respectively. As such I have discussed, in short, Maier Saupe mean field theory [6] and McMillan theory [7,8] respectively.

2.2 Maier-Saupe mean field theory of nematic phase of rod like molecules:

Maier and Saupe have given a molecular statistical theory of the nematic phase with one order parameter. Suppose that the liquid crystal is composed of rod-like molecules in which the long axis of the molecules tend to align parallel to the director **n** in mesophase. The stability of the nematic liquid crystal phase arises from the existence of the anisotropic part of the dispersion interaction energy between the molecules. This energy originates from the intermolecular electrostatic interaction. For the sake of simplicity Maier and Saupe approximated the electrostatic interaction by the first term of its multipole expansion and assumed that:

a/ the influence of the permanent dipoles can be neglected as far as long range nematic order is concerned.

b/ only the effect of the induced dipole-dipole interaction need to be considered.

c/ the molecules may be considered to be cylindrical symmetric about its long axis.

d/ with respect to a given molecule the distribution of the centre of mass of the remaining molecules may be taken to be spherical symmetric.

The distribution of the molecular long axis about the director is given by an orientational distribution function f(cosθ). As the molecules have no head to tail asymmetry, f (cosθ) is an even function of cosθ. The general expression for the orientational distribution function can be written as [9]:

$$f(\cos\theta) = \sum_{\text{L-even}} (2L+1)/2 \langle P_L(\cos\theta)\rangle P_L(\cos\theta) \qquad 2.1$$

where $P_L(\cos\theta)$ are the L^{th} even order Legendre polynomials, and

$\langle P_L(\cos\theta)\rangle$ are the statistical average given by :-

$$\langle P_L(\cos\theta)\rangle = \int_0^1 P_L(\cos\theta)\, f(\cos\theta)\, d(\cos\theta) \qquad 2.2$$

$\langle P_L\rangle$ are called the orientational order parameters. The expression for the potential of a single molecule in the generalised mean field approximation can be written as

$$V(\cos\theta) = \sum_{\text{L-even}} U_L \langle P_L\rangle P_L(\cos\theta) \qquad 2.3$$

where U_L are the functions of distance between the central molecule and its neighbours only.

Putting $L = 2$ in equation 2.2 we have :

$$\langle P_2(\cos\theta)\rangle = \int_0^1 P_2(\cos\theta)\, f(\cos\theta)\, d(\cos\theta) \qquad 2.4$$

$\langle P_2 \rangle$ is generally called the order parameter. $\langle P_2 \rangle = 0$ for isotropic liquid and $\langle P_2 \rangle = 1$ for perfectly ordered sample.

Equation 2.3 can be written in the expanded form as :

$$V(\cos\theta) = U_2 \langle P_2 \rangle P_2(\cos\theta) + U_4 \langle P_4 \rangle P_4(\cos\theta) + U_6 \langle P_6 \rangle P_6 \cos\theta) + \ldots\ldots \qquad 2.5$$

In the mean field theory of Maier and Saupe, only the first term of the equation 2.5 is retained, so that the expression for the potential energy of a single molecule can be written as :

$$V(\cos\theta) = -v\, P_2(\cos\theta)\, \langle P_2 \rangle \qquad 2.6$$

where $v = -U_2$

The orientational distribution function corresponding to the single molecule is given by :

$$f(\cos\theta) = Z^{-1} \exp[-V(\cos\theta)/kT] \qquad 2.7$$

where Z is the single molecule partition function given by :

$$Z = \int_0^1 \exp[-V(\cos\theta)/kT]\, d(\cos\theta) \qquad 2.8$$

and k is the Boltzmann's constant.

Substituting the value of $f(\cos\theta)$ and $V(\cos\theta)$ from equation 2.7 and equation 2.6 into equation 2.4 we have :

$$\langle P_2(\cos\theta) \rangle = \frac{\int_0^1 P_2(\cos\theta) \exp[P_2(\cos\theta) \langle P_2 \rangle / T^*]\, d(\cos\theta)}{\int_0^1 \exp[P_2(\cos\theta) \langle P_2 \rangle / T^*]\, d(\cos\theta)} \qquad 2.9$$

where $T^* = k T / v$

equation 2.9 is a self consistent equation. For every temperature T^* we can obtain the value of $\langle P_2 \rangle$ that satisfies the self consistence equation. $\langle P_2 \rangle = 0$ is a solution at all temperatures that corresponds to normal isotropic liquid. when $T^* < 0.22284$, two other solutions of $\langle P_2 \rangle$ appear and the state that has minimum free energy will be stable. It has been found that the nematic phase with $\langle P_2 \rangle > 0$ is stable when the T^* satisfies the condition $0 \leq T^* \leq 0.22019$. When $T^* > 0.22019$, the isotropic phase with $\langle P_2 \rangle = 0$ is stable.

The order parameter $\langle P_2 \rangle$ decreases from unity to a minimum value of 0.4289 at $T^*=0.22019$. The nematic isotropic transition takes place at $T^*=0.22019$ and it is a first order phase transition as the order parameter discontinuously changes from $\langle P_2 \rangle = 0.4289$ to $\langle P_2 \rangle = 0$. Although approximation are involved in Maier-Saupe theory, for a number of nematic liquid crystals, the experimental values of $\langle P_2 \rangle$ agree quite well with those predicted by the theory.

2.2 McMillan's theory for smectic phase:

McMillan proposed a simple and elegant description of smectic A by extending the Maier-Saupe theory to include an additional order parameter for characterising the one dimensional translational periodicity of a layered structure. In smectic A phase, there is a periodic density variation along the layer normal (z-direction) in addition to the orientational distribution of the molecular axes. Therefore, the normalised distribution function can be written as:

$$f(\cos\theta) = \sum_{L,\,\text{even}} \sum_{n} A_{L,n}\, P_L(\cos\theta)\, \cos(2\pi n z / d) \qquad 2.10$$

where d is the layer thickness.

The normalising condition for the distribution function is given by:

$$\int_{-1}^{1} \int_{0}^{d} f(\cos\theta, z)\, dz\, d(\cos\theta) = 1 \qquad 2.11$$

McMillan [7,8] following Kobayashi [10,11] expressed the pair potential as:

$$V_M(\cos\theta, z) = -V [\, \delta\alpha\tau \cos(2\pi z / d) + \{\eta + \alpha\delta \cos(2\pi z / d)\} P_2(\cos\theta)] \qquad 2.12$$

where α and δ are the two parameters of the potential. α increases with increasing length of the molecules and δ is the ratio of the translational part of the potential to the orientational part of it. $\eta = \langle P_2(\cos\theta)\rangle$, $\tau = \langle\cos(2\pi z/d)\rangle$ and $\sigma = \langle P_2(\cos\theta)\cos(2\pi z/d)\rangle$ are the orientational, translational and mixed order parameters respectively, and $\langle\ \rangle$ denotes the statistical average of the quantities inside.

The single particle distribution function can be written as:

$$f_M(\cos\theta, z) = Z^{-1} \exp[-V_M(\cos\theta, z) / kT] \qquad 2.13$$

where Z is the partition function given by:

$$Z = \int_{0}^{1} \int_{0}^{d} \exp[-V_M(\cos\theta, z) / kT]\, d(\cos\theta)\, dz \qquad 2.14$$

Once again, three self consistent equations containing η, τ and σ can be written and solved iteratively.

Out of several possible solutions, the thermodynamically stable solution is selected by the criterion of lowest free energy. Depending on the values of the coupling parameters, the following three type of solution are possible:

a/ $\eta = 0, \tau = 0, \sigma = 0$, this solution describes the isotropic liquid phase;

b/ $\eta \neq 0, \tau = 0, \sigma = 0$, this solution describes the nematic phase in accordance with the Maier Saupe theory;

c/ $\eta \neq 0, \tau \neq 0, \sigma \neq 0$, this solution describes the smectic A phase.

For $\alpha > 0.98$, the smectic A phase transforms directly into the isotropic phase, while for $\alpha < 0.98$ there is a smectic A-nematic transition followed by a nematic-isotropic transition at higher temperature. Although nematic-isotropic transition temperature is always first order according to McMillan theory, the smectic A-nematic transition can be either first order or second order. For $T_{AN} / T_{NI} < 0.87$, the smectic A - nematic transition is second order while for $T_{AN} / T_{NI} > 0.87$, the smectic A - nematic transition is first order. T_{AN} and T_{NI} are the smectic A - nematic and nematic - isotropic transition temperature respectively.

2.4 X - ray diffraction from mesophases:

The structure and hence the properties of the liquid crystalline compound can best be understood from the x-ray diffraction studies of the liquid crystal compounds. Although a number of review articles are available in this field, Vainshtein [14] and Leadbetter [17] have given the theoretical interpretation. From x-ray experiment, the Fourier image of the

correlation density function can be determined, the reconstruction of which from the scattered data yields information both on the mutual arrangement of molecules in a liquid crystal and the specific features of the orientational and translational order.

X-ray diffraction of the unoriented nematic phase consists of a uniform halo just like that of an isotropic liquid. The reason behind this is that a nematic liquid crystal generally consists of a large number of domains, the molecules being ordered within each domain along the director **n**, but there is no preferred direction for the sample as a whole so that the diffraction pattern has a symmetry of revolution around the direction of the x-ray beam. However, application of suitable magnetic or electric field can produce a 'monodomain' or 'aligned' or 'oriented' sample of liquid crystal.

The small angle x-ray diffraction pattern from a nematic liquid crystal oriented perpendicular to the direction of the incident x-ray beam is shown in the Figure 2.1a. In the diffraction pattern, the main halo splits into two crescents for each of which intensity is maximum in the equatorial direction, i.e. perpendicular to the director. These crescents are formed mainly due to the intermolecular scattering and the corresponding Bragg angle is a measure of lateral intermolecular distance. The angular distribution of the x-ray intensity (Fig. 2.1a), I (ψ) vs. ψ curve, also gives the orientational distribution function f($\cos\theta$) and order parameter $\langle P_L \rangle$, (L= 2, 4).

In the meridional direction, parallel to the director, two crescents are also observed at much smaller angle and the corresponding Bragg angle is a measure of apparent molecular length. Sometimes, the inner diffuse crescents are replaced by sharp spots and the corresponding

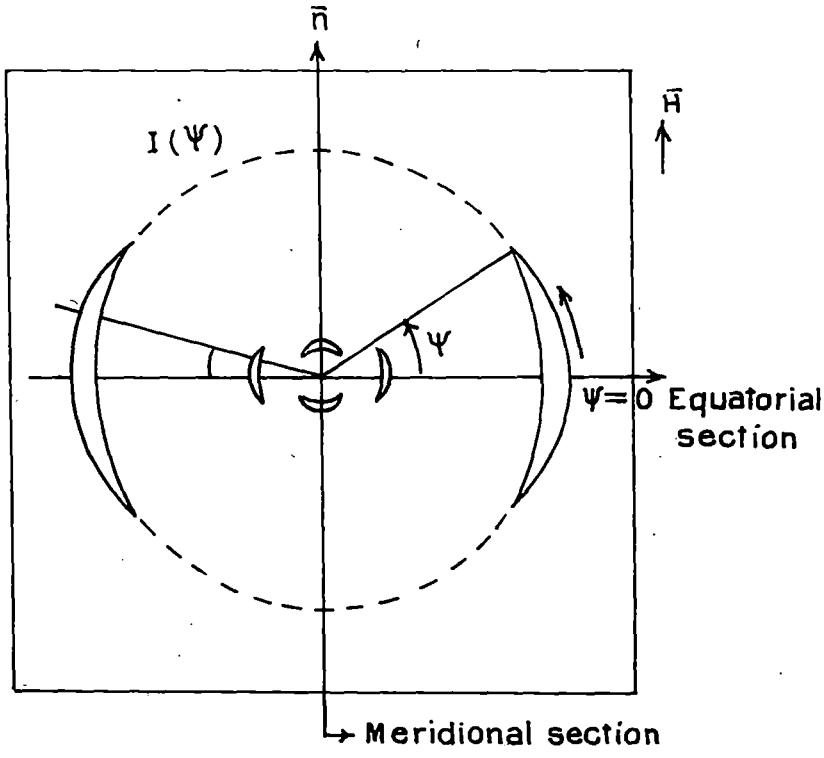

Figure 2.1a. Schematic representation of the x-ray diffraction pattern of an oriented nematic liquid crystal.

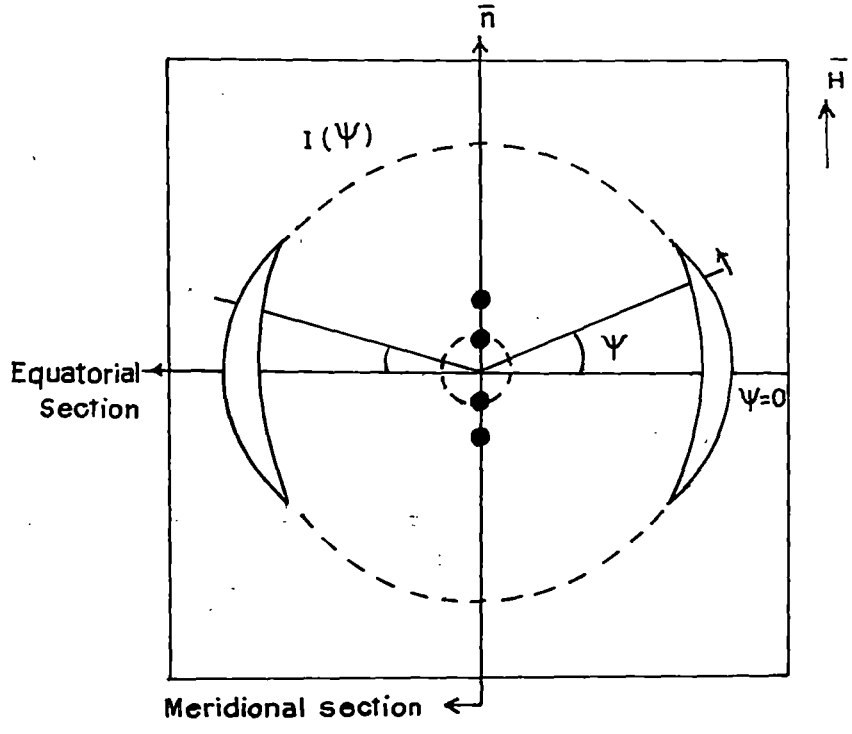

Figure 2.1b. Schematic representation of the x-ray diffraction pattern of an oriented smectic A liquid crystal.

phase is called "cybotactic phase". The presence of the sharp spots indicates smectic like clusters in the nematic phase which are called "cybotactic" groups [20].

The x-ray diffraction pattern of smectic A phase is shown in Figure 2.1b. The meridional spots are formed due to Bragg reflection from the layers and provide the value of layer thickness. Since smectic A can have only quasi-long range order along its layer normal [3,21], the second order Bragg reflections in the meridional direction are generally very weak and are often absent in the x-ray photographs. When present, these second order reflections provide a method for calculating τ, the translational order parameter.

In our x-ray photographs of the liquid crystals, sometimes other faint diffuse spots are also present, which may be due to (a) intra-molecular atomic scattering (b) next nearest neighbour intermolecular scattering and (c) effect of white radiation contained in Ni filtered Cu-radiation. However, we do not consider such diffraction patterns in our analysis.

2.5 Experimental technique and data analysis; X-ray diffraction studies:

The x-ray diffraction set up has been designed and fabricated in our laboratory by Jha and Paul [22]. The schemetic representation of the whole set up is shown in Figure 2.2. The brief description of the set up is as follows:

The x-ray generator is that of Radon house (India) and the x-ray tube with copper - target is used. The set up has flat-plate camera provided with the

sample holder (8) having heating arrangement. The sample holder is fitted with a changeable collimator (2) and is well insulated from the surroundings by asbestos cement. The sample holder is supported by four brass posts (16) that are rigidly attached to the heavy brass plate (12). The brass plate is also fitted with the film cassette holder (11) and the space between the film cassette and the sample holder are separated by adjustable spacer (15). The sample was taken in a thin walled lithium glass capillary of diameter 1mm and is introduced into the sample holder. The camera is then placed between the pole pieces of an electromagnet in such a way that the sample remains at the centre of the pole pieces (17). The magnetic field acts along the axis of the capillary and the pole pieces can be brought very close to each other to provide strong magnetic field of about 5 Kilogauss. The strength of the magnetic field was measured by sensitive Gaussmeter (ECIL model GH 867). For better collimation of the x-ray beam, levelling screws (13) are provided on the brass plate. At first the sample was heated to the isotropic phase and was slowly cooled to the desired temperature in presence of the magnetic field. The temperature of the sample holder and hence the sample was maintained constant within ± 0.5 °C by a temperature controller (Indotherm model IT401D2). The film cassette is loaded with new film and is then placed on the cassette holder. The film is then exposed to x-ray diffracted from the sample, the direct beam being stopped by a beam stop. The magnetic field was kept on during the exposure of the film. The exposure time in our experiment was about three hours. Also, all the x-ray photographs were taken by using Ni-filter of thickness 0.009 mm which gives mainly the monochromatic Cu K_α radiation of wavelength 1.5418 Å. Furthermore, the incoming x-ray beam was collimated by a collimator of aperture 0.8 mm. X-ray photographs were taken for the same

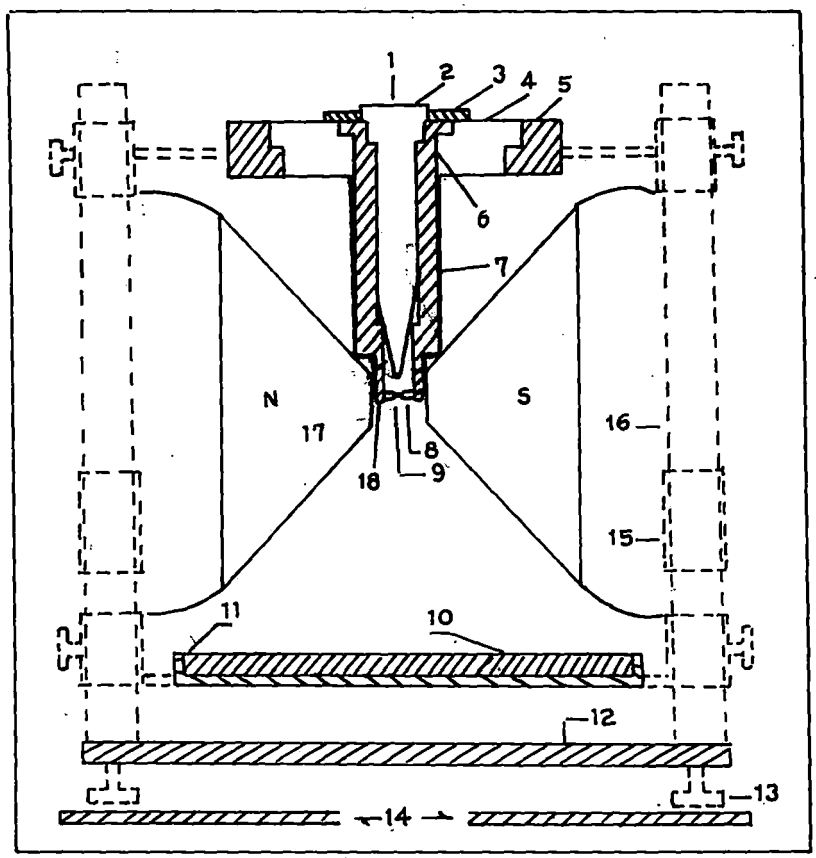

Figure 2.2 Sectional diagram of the X-ray diffraction camera.

1. X-ray 2. Collimator 3. Brass ring 4. Ring of syndanyo board 5. Brass ring 6. Cylindrical brass chamber 7. Asbestos insulation and heater winding 8. Specimen holder and thermocouple 9. Sample 10. Film Cassette 11. Film cassette holder 12. Base plate 13. Levelling screw 14. Brass plates over the coils of the electromagnet 15. Removable spacer 16. Supporting brass stand 17. Pole peices 18. Asbestos insulation.

sample at various temperatures. In my experiment, the sample to film distance was varied from 8 cm to 10 cm depending upon the sample.

The spacer gives only apparent distance between the sample and the film. To get the exact sample to film distance, I have taken aluminium powder photograph. The Bragg angle corresponding to the hkl reflecting plane for the aluminium (F.C.C structure) can be determined from the equation [23]:

$$\sin\theta' = \lambda (h^2 + k^2 + l^2)^{1/2} / 2a \qquad 2.15$$

Thus measuring the diameter of the diffraction rings corresponding to (111) and (200) reflections [22] and the values of Bragg angle from equation 2.15, the actual distance between the sample and the film can be obtained from the relation :

$$\tan (2\theta') = \text{Radius of the ring / Sample to film distance} \qquad 2.14$$

The correction term was calculated and the apparent distance given by spacer was corrected to get the exact value of sample to film distance.

a/ Conversion of optical density to x-ray intensity:

The optical density of the x-ray photographs were measured by a Carl Zeiss Microdensitometer (MD100) which has potentiometric recording (k200) facility for linear scanning. The optical density values obtained from the densitometric scan were then converted to relative intensity values by a method explained by Klug and Alexander [24]. A strip of film was kept inside a film holder provided with a rectangular

opening on a lead sheet and was kept at a fixed distance from the x-ray tube. Multiple film technique was used to prepare an intensity scale by exposing different portion of the film to x-rays coming through the rectangular opening with different exposure times (5sec, 10sec, 20sec,...etc.). The optical densities of these spots were measured with the help of microdensitometer. Since the microdensitometer zeroing was adjusted on unexposed x-ray film, we need not subtract the optical density of unexposed film from the measured data. A graph is then plotted with optical density vs. time in seconds. Since x-ray intensity is proportional to the time of exposure, the optical density vs. time in second curve actually corresponds to x-ray intensity and hence it is used as calibration curve to convert x-ray intensity to optical density.

b/ Circular scanning of x-ray photographs:

To perform circular scanning of the x-ray film, densitometer is provided with the rotating stage, fabricated in our laboratory, to facilitate 360°-scanning of the photographs. Photographs were scanned to measure angular intensity distribution $I(\psi)$ which was used to calculate the orientational distribution function $f(\beta)$ and order parameters $< P_2 >$ and $< P_4 >$. Reading of the circular scan of the outer diffraction arc were taken from $\psi = 0$ to $\psi = 360°$ at 1° interval near the peak and at larger intervals elsewhere. The optical density values, thus obtained, were converted into corresponding x-ray intensity with the help of the calibration curve. The experimental intensities values were then corrected for the background intensity values arising due to the air scattering. The peak intensity position which corresponds to $\psi = 0$ was determined from intensity $I(\psi)$ vs. angle (ψ) curve. $I(\psi)$ vs. ψ curve were smoothed, and nineteen values of $I(\psi)$

were taken from $\psi = 0$ to $\psi = 90^{\circ}$ at 5° intervals. From the values of $I(\psi)$, we have calculated the distribution function $f(\beta)$, and order parameters ($\langle P_2 \rangle$ and $\langle P_4 \rangle$) by Lead better's expression. A computer program was written in our laboratory for these calculations.

c/ Linear Scanning of x-ray photographs:

The linear scan of the x-ray photographs were performed by using the potentiometric recorder and the recorder plotted a graph of optical density vs. linear distance. The distance between the peak position gives the diameter of the diffraction ring.

2.6 Orientational distribution functions and order parameters:

As it has been mentioned in Chapter-1, the liquid crystals are composed of rod like molecules which are cylindircally symmetric about their long axes. Both the nematic and smectic A phases have uniaxial symmetry which is parallel to the unit vector **n** called the director. The orientational distribution function describes how the moleculer long axes are distributed about the director; it gives the probability of finding a molecule at some prescribed angle β from **n**. The x-ray diffraction pattern of an oriented sample consists of equatorial arcs. The orientational distribution function is related to the distribution of x-ray intensity along the diffused equatorial axes according to the following equation [17]:

$$I(\psi) = c \int_{\beta=\psi}^{\pi/2} f_d(\beta) \sec^2 \psi \, [\tan^2 \beta - \tan^2 \psi]^{-1/2} \sin \beta \, d\beta \qquad 2.16$$

where $f_d(\beta)$ describes the distribution function of the directors of clusters in which the molecules are perfectly aligned. The equation 2.16 can be numerically inverted to give $f_d(\beta)$ which are assumed to be close to the singlet distribution function $f(\beta)$.

The orientational order parameter $\langle P_2 \rangle$ and $\langle P_4 \rangle$ were calculated by using the following equation :

$$\langle P_L \rangle = \int_0^1 P_L(\cos\beta)\, f_d(\beta)\, d(\cos\beta) \Big/ \int_0^1 f_d(\beta)\, d(\cos\beta) \qquad 2.17$$

where, $L = 2,4$.

The method of obtaining intensity values $I(\psi)$ from the measured optical densities of the x-ray diffraction photographs has been described in section 2.5b. To calculate $f_d(\beta)$ and order parameter we need $I(\psi)$ values from $\psi = 0$ to $\psi = 90^0$ i.e. one quadrant. I have measured $I(\psi)$ values of four quadrants separately and the average values of $I(\psi)$ is considered to calculate $f(\beta)$ as well as $\langle P_2 \rangle$ and $\langle P_4 \rangle$ for all the samples. The errors in the calculation of $\langle P_2 \rangle$ and $\langle P_4 \rangle$ in our experiment are estimated to be within $\pm$ 0.02.

2.7 Molecular parameters from x-rays studies:

a/ Intermolecular distance:

The average lateral distance between the neighbouring molecules (D) is related to the corresponding Bragg angle (2θ) according to the formula [20];

$$2\, D \sin\theta = k\, \lambda \qquad 2.18$$

where, 2θ is the Bragg angle for the equatorial diffraction, λ is the wave length of the x-ray and k is a constant which comes from the cylindrical symmetry of the system. Recent calculation [30] have shown that the value of k depends on the order parameter of the sample under consideration. For perfectly ordered state k = 1.117 as given by de Vries [20]. Since the variation of k with $< P_2 >$ is small, I have used the value k = 1.117 for all the calculations.

b/ Apparent molecular length or layer thickness:

To calculate the apparent molecular length (or layer thickness) (d), I have used the Bragg equation ($2\ d \sin\theta = \lambda$), where θ is the Bragg angle for the meridional diffraction crescent (or spots) for an aligned sample or for the inner halo (or ring)in the case of unaligned sample.

2.8 Refractive index of mesophases:

Most of the nematic liquid crystals are optically uniaxial and strongly birefringent. A uniaxial liquid crystal has two principal refractive indices viz. ordinary refractive index (n_0) and extraordinary refractive index (n_e). The birefringence is defined by the following equation:

$$\Delta n = n_e - n_o \qquad 2.19$$

The first birefringence measurement were made by E. Dorn [31] and its theoretical explanation was given by O.Weiner [33] and H.Zocher [34,35]. Birefringence is positive for conventional nematics with its value lying between 0 to 0.4, while it is negative for chiral nematics. Refractive indices of the smectic phases have also been measured [43-45]. To evaluate the molecular polarisabilities of the liquid crystal it is necessary to consider the anisotropic internal field that arises due to anisotropic

molecular arrangements in the liquid crystals. Hence, in case of liquid crystals the well known Lorentz-Lorentz formula for isotropic media is replaced by Neugebauer formula [46] or Vuks formula [47]. Saupe and Maier [48] also applied a more elaborate internal field suggested by Neugebauer.

I have measured the ordinary and extra ordinary refractive index of the nematic liquid crystals, smectics as well that of the re-entrant nematic phase and then calculated the effective polarisabilities α_0 and α_e of the anisotropic liquid crystals by using the two different internal field models [46,47]. Finally orientational order parameter $\langle P_2 \rangle$ was calculated.

a/ Neugebauer Method:

Neugebauer [46] extended Lorentz-Lorentz equations for an isotropic system to an anisotropic system. In this model the effective polarisabilities α_0 and α_e of the liquid crystals are related to the refractive indices n_e and n_0 according to the following equations:

$$n_e^2 - 1 = 4\pi N \alpha_e (1 - N \alpha_e \gamma_e)^{-1} \qquad 2.20$$

and $$n_0^2 - 1 = 4\pi N \alpha_0 (1 - N \alpha_0 \gamma_0)^{-1} \qquad 2.21$$

where, γ_o and γ_e are the respective internal field constants for ordinary and extraordinary rays, N is the number of molecules per c.c. and n_e and n_0 are the extraordinary and ordinary refractive indices respectively. The relevant equations for calculating polarisabilities (α_0, α_e) as obtained from the equations 2.20 and 2.21 are as follows:

$$1/\alpha_e + 2/\alpha_o = [4\pi N/3] [\{ (n_e^2 + 2) / (n_e^2 - 1)\} + \{2 (n_o^2 + 2) / (n_o^2 - 1) \}] \qquad 2.22$$

and

$$\alpha_e + 2\,\alpha_o = [9/4\pi N]\,[(n^2 - 1)/(n^2 + 2)] \qquad 2.23$$

where,

$n^2 = (2n_o^2 + n_e^2)/3$, n is the mean refractive index.

α_o and α_e values are obtained by directly solving equations 2.22 and 2.23.

b/ Vuks method:

Vuks has derived another formula for polarisabilities associated with anisotropic molecules by assuming that the internal field is independent of orientation. The Vuks formula relating the molecular polarisabilities (α_o, α_e) and refractive indices (n_o, n_e) are as follows :

$$(n_o^2 - 1)/(n^2 + 2) = 4\pi N\alpha_o/3 \qquad 2.24$$

and

$$(n_e^2 - 1)/(n^2 + 2) = 4\pi N\alpha_e/3 \qquad 2.25$$

where,

$n^2 = (2n_o^2 + n_e^2)/3$, n is the mean refractive index.

α_o and α_e can be calculated directly from the refractive index values.

2.9 Calculation of order parameter from the polarisabilities:

The relation between orientational order parameter $\langle P_2 \rangle$ and the principal polarisabilities are given by de Gennes [49] as :

$$\alpha_e = \bar{\alpha} + (2/3)\,\alpha_a \langle P_2 \rangle \qquad 2.26$$

$$\alpha_o = \bar{\alpha} - (1/3)\,\alpha_a \langle P_2 \rangle \qquad 2.27$$

where,

$\bar{\alpha} = (2\alpha_o + \alpha_e)/3$ is the mean polarisability

and

$\alpha_a = (\alpha_\parallel - \alpha_\perp)$ is the molecular polarisability anisotropy where $\alpha_\parallel$ and $\alpha_\perp$ are the principal polarisabilities, parallel and perpendicular to the long axes of the molecules in the crystalline state. Due to strong absorption in the solid phase, we could not measure α_a directly. to get the value of α_a, Haller's extrapolation method [50] was adopted. The graph was plotted with $\log(\alpha_e-\alpha_o)$ vs. $\log(T_c-T)$ giving a straight line which is extrapolated to $\log(T_c)$ where T_c corresponds to nematic isotropic transition temperature. the limiting value of $(\alpha_e-\alpha_o)$ at $T = 0\ ^oK$ is assumed to correspond to $(\alpha_\parallel-\alpha_\perp)$.

From equation 2.26 and 2.27 we have

$$\langle P_2 \rangle = \frac{\alpha_e - \alpha_o}{\alpha_\parallel - \alpha_\perp} \qquad 2.28$$

For a given sample, α_e and α_o are calculated at various constant temperatures from which $(\alpha_\parallel-\alpha_\perp)$ is obtained. The order parameter $\langle P_2 \rangle$ is then calculated by using equation 2.28.

2.10 Measurement of refractive indices :

Refractive indices (n_o, n_e) of a liquid crystal for ordinary and extra-ordinary rays were measured by using thin hallow prisms with the refracting angle less than 2^o. The details of the preparation of the prism and the experimental procedure have already been reported by Zemindar et al [51]. To prepare prism optically flat glass plates are taken, and they are first cleaned by conc. HNO_3 and then by acetone. One surface of the glass plates was rubbed on bond paper in a direction parallel to one of their

edges. The rubbed surface is then coated with thin layer of 1 % solution of polyvinyl alcohol and then dried. The preferred direction on the substrate can be obtained by rubbing the same surface in the same direction again by a tissue paper. The prism was then prepared by placing the rubbed surfaces inside, with the rubbing direction parallel to the refracting edge of the prism. A thin glass spacer was introduced between one of the vertical edge of the prism for getting the desired refracting angle of the prism. The glass plate of the prism were sealed together by using high temperature adhesive and were baked in an oven. Liquid crystal sample was introduced into the prism from its top open side by melting. The system was alternately heated to isotropic phase and cooled slowly so that the liquid crystals were perfectly aligned with its optic axis parallel to the refraction edge of the prism. The prism was then placed inside a brass oven provided with transparent opening at the centre and the temperature of the oven was maintained constant at a desired value by a temperature controller (Indotherm model IT401D2) within an accuracy of ±0.5 °C. The refractive indices (n_o, n_e) were measured for four different wavelengths (λ = 6907Å, 5890Å, 5461Å, 4358 Å), corresponding to mercury source by means of a precision spectrometer and an optical monochromator.

2.11 Measurements of densities:

The densities of the liquid crystals were measured with the help of a dilatometer of the capillary type. A weighed amount of the liquid crystal was introduced inside the dilatometer which was kept immersed in a thermostated liquid bath. The height of the liquid crystal column was measured at different temperatures with the help of a travelling microscope. But before taking the reading, sufficient time was given to

attain equilibrium at any desired temperature. The densities were then calculated by making corrections for the expansion of glass capillary. The accuracy of density measurement lies within ± 0.1 %.

2.12 Magnetic susceptibility measurements:

Introduction:

The determination of diamagnetic properties is of great importance in the study of liquid crystals. All anisotropic properties of liquid crystals are related to the orientational order parameter $\langle P_2 \rangle$ in a more or less complicated way. Since the molecular susceptibility of a liquid crystal is anisotropic the orientational order parameter is related to the magnetic susceptibility [52-55] in a more or less straight forward way. It is considered to be one of the best methods for studying the variation of order parameter with temperature despite the experimental difficulties in measuring the susceptibility. The theoretical treatment regarding the effect of external magnetic field on liquid crystal was given by J.P.Dias [56] and the magnetic alignment of the liquid crystal was explained by J.O.Kessler [57]

To investigate the effect of external magnetic field on liquid crystal materials we first define the magnetisation **M** induced by the applied magnetic field **H** according to the following equation:

$$M_\alpha = \chi_{\alpha\beta} H_\beta \qquad 2.29$$

$$\alpha,\beta = x, y, z$$

where $\chi_{\alpha\beta}$ is an element of the magnetic susceptibility tensor $\bar{\chi}$ and the summation convention over repeated index is followed.

For uniaxial phase like nematic or smectic A phase and choosing the director along the **n** along the z-axis we have:

$$\bar{\chi} = \begin{bmatrix} \chi_\perp & 0 & 0 \\ 0 & \chi_\perp & 0 \\ 0 & 0 & \chi_\parallel \end{bmatrix}$$

The subscript $\parallel$ and $\perp$ indicates the component parallel and perpendicular to the director respectively. The average susceptibility is given by

$$\bar{\chi} = (1/3) \sum_{\gamma} \chi_{\gamma\gamma}$$

$$= (1/3)(\chi_\parallel + 2\chi_\perp) \qquad 2.30$$

The magnetic susceptibility anisotropy is defined as :

$$\Delta\chi = \chi_\parallel - \chi_\perp$$

$$= (3/2)(\chi_\parallel - \bar{\chi}) \qquad 2.31$$

Hence the susceptibility tensor has only two different non zero elements, and we find :

$$\mathbf{M} = \chi_\parallel \mathbf{H}, \text{ if } \mathbf{H} \parallel \mathbf{n}$$

$$\mathbf{M} = \chi_\perp \mathbf{H}, \text{ if } \mathbf{H} \perp \mathbf{n}$$

For an arbitrary angle (θ) between **H** and **n** we derive for total magnetisation

$$\mathbf{M} = \chi_\perp \mathbf{H} + \Delta\chi (\mathbf{H}.\ \mathbf{n})\mathbf{n} \qquad 2.32$$

Therefore the free energy in a magnetic field is given by:

$$F_{magn} = -\int_0^H \mathbf{M}.\, d\mathbf{H}$$

$$= -(1/2)\chi_\perp H^2 - (1/2)\Delta\chi\ (\mathbf{H}.\mathbf{n})^2$$

2.33

Since the first term of the above equation is free from **n**, it may be omitted as far as orientation related problems are concerned. For positive anisotropy i.e. $\Delta\chi > 0$, the last term is minimised when **H** is collinear with **n**. Therefore the liquid crystal with positive $\Delta\chi$ tend to align with their molecular long axes along the direction of the applied magnetic field. However, for liquid crystal with negative $\Delta\chi$, the molecules tend to align perpendicular to the applied magnetic field. Hence the coupling to the director occurs through the anisotropy of the molecular susceptibility.

2.13 Relation between order parameter and magnetic anisotropy:

The order parameter **Q** is defined by considering the anisotropic part of the susceptibility χ as follows :

$$Q_{\alpha\beta} = \chi_{\alpha\beta} - \delta_{\alpha\beta}\ \bar{\chi} \qquad 2.34$$

where, $\alpha, \beta = x, y, z$ and $\delta_{\alpha\beta}$ is the kronecker delta function, **Q** is a second rank tensor, which is diagonal.

If we choose the director **n** along the z-axis, then **Q** has zero trace and vanishes for the isotropic phase. If we consider uniaxial symmetry around **n**, it is sufficient to consider only one element Q_{zz} of **Q**.

Equation 2.34 can also be written in the form:

$$Q_{\alpha\beta} = \chi_{\alpha\beta} - (1/3)\delta_{\alpha\beta} \sum_{\gamma} \chi_{\gamma\gamma} \qquad 2.35$$

Therefore,

$$Q_{zz} = \chi_{zz} - (1/3)\{\chi_{xx} + \chi_{yy} + \chi_{zz}\}$$
$$= (2/3)(\chi_{\parallel} - \chi_{\perp}) \qquad 2.36$$

Here we assume

$$\chi_{xx} = \chi_{yy} = \chi_{\perp} \text{ and } \chi_{zz} = \chi_{\parallel}$$

In order to relate **Q** to the microscopic order parameter S, let **K** be the tensor of the molecular magnetic polarisability which is assumed to be diagonal in the molecule - fixed co-ordinate system ξ,η,ζ.

Therefore,

$$\chi_{\alpha\beta} = N \sum_{i,j} K_{ij} \langle i_\alpha j_\beta \rangle \qquad 2.37$$

where $i, j = \xi,\eta,\zeta$.

$\alpha, \beta = x, y, z$.

i_α is the α - component of a unit vector along ξ,η,ζ axes, N is the number of molecules per unit volume and the bracket $\langle\ \rangle$ stands for statistical average.

Using equation 2.37, the order parameter represented by equation 2.35 can be expressed as :

$$Q_{\alpha\beta} = N \sum_{i,j} K_{ij} \langle i_\alpha j_\beta - (1/3)\ \delta_{\alpha\beta}\delta_{ij} \rangle \qquad 2.38$$

Therefore,

$$\begin{aligned} Q_{zz} &= N \sum_{i,j} K_{ij} \langle i_z j_z - (1/3)\ \delta_{ij} \rangle \\ &= (2/3) N \sum_{i,j} K_{ij}\ (1/2) \langle 3\, i_z j_z - \delta_{ij} \rangle \\ &= (2/3) N \sum_{i,j} K_{ij}\ S_{i,j} \end{aligned} \qquad 2.39$$

where,

$S_{i,j} = (1/2) \langle 3\, i_z j_z - \delta_{ij} \rangle$ is the generalised order parameter.

From equation 2.36 and 2.39 we have:

$$\begin{aligned} Q_{zz} &= (2/3)(\chi_{\parallel} - \chi_{\perp}) \\ &= (2/3) N \sum_{i,j} K_{ij}\ S_{i,j} \end{aligned} \qquad 2.40$$

As S_{ij} is diagonal in a molecular fixed co-ordinate system ξ, η, ζ with the ζ-axis as the long molecular axis and has zero trace, there are two independent scalar order parameter, for which we choose $S = S_{\zeta\zeta}$ and $D = S_{\eta\eta} - S_{\zeta\zeta}$.

Thus equation 2.40 can be written as :

$$(\chi_{\parallel} - \chi_{\perp}) / N = \{K_{\zeta\zeta} - (1/2)(K_{\eta\eta} + K_{\zeta\zeta})\} S + (1/2)(K_{\zeta\zeta} - K_{\eta\eta}) D \qquad 2.41$$

where S is the order parameter which have a value between 0 and 1.

Therefore,

$$S = 1/2 < 3\zeta_z^2 - 1 >$$
$$= 1/2 < 3\cos^2\theta - 1 >$$

where 'θ' is the angle between z and ζ axes.

Furthermore,

$$D = (1/2) < 3\xi_z^2 - 1 > - (1/2) < 3\eta_z^2 - 1 >$$
$$= (3/2) < \xi_z^2 - \eta_z^2 >$$
$$= (3/2) < \sin^2\theta \cos 2\psi >$$

where ψ is the Euler angle specifying the rotation around the ζ-axis. D measures the difference in tendency of the two transverse molecular axes to project on the z-axis. By considering the molecule to be axially symmetric, we have D = 0.

Now equation 2.41 can be written as :

$$(\chi_{\parallel} - \chi_{\perp}) = (\chi_l - \chi_t) S \qquad 2.42$$

where $\chi_l = N K_{\zeta\zeta}$ and $\chi_t = (1/2) N (K_{\eta\eta} + K_{\zeta\zeta})$

Equation 9.42 is known as Tsvetkov's expression for order parameters [44,45]. To determine the order parameter (S) we need the value of

(χ_l - χ_t) which can be obtained from solid single crystal measurements. An alternative method to estimate(χ_l - χ_t) is against temperature due to Haller et al [50] A logarithmic plot of (χ_l - χ_t) against ln(T_c-T) often gives straight line, and (χ_l - χ_t) is obtained by extrapolating to T = 0 and assuming S = 1 at that point. I have adopted Haller's method to estimate the value of order parameter.

2.14 Determination of $\Delta\chi$:

The magnetic susceptibility have been measured by the classical Faraday-Curie method. The total force (F) experienced by a sample in an inhomogeneous magnetic field with a gradient in the horizontal x-direction is given by:

$$F = (1/2)\,(m\chi - m_o\,\chi_o)\,(dH^2/dx)_{av} \qquad 2.43$$

where χ, m are the mass susceptibility and the mass of the sample and χ_o, m_o are those of air driven out of the sample. The subscript 'av' indicates the average value. If we assume that the sample is replaced by almost same volume of the reference sample and is placed at more or less at the same position between the pole pieces of the magnet, then (dH^2/dx) will be same for both the cases. By indicating the reference sample with the subscript 'r', the force acting on the reference sample is given by:

$$F = (1/2)\,(m_r\chi_r - m_o\,\chi_o)\,(dH^2/dx)_{av} \qquad 2.44$$

From equation 2.43 and 2.44 we can write:

$$\chi(t) = \frac{F}{F_r}\,\frac{m_r}{m}\left[\chi_r - \frac{\rho_o(t_o)}{\rho_r(t_o)}\,\chi_o(t_o)\right] + \frac{\rho_o(t)}{\rho(t)}\,\chi_o(t) \qquad 2.45$$

where ρ, ρ_r and ρ_o are densities of the experimental sample, reference sample and air respectively; t_o is the temperature at which the measurement of the reference sample is made.

The sample was taken in a cylindrical quartz container having a volume of nearly 0.1 cm^3. It was hung by a glass capillary between the pole pieces, the value of (dH^2/dx) being 1.1 K. $gauss^2$ / cm. approximately. The value of (dH^2/dx) is constant within 1% for 1cm. length along x-direction while along y and z direction (dH^2/dx) is practically constant over sufficiently large distances. The temperature of the sample was maintained constant within $\pm 0.5^oC$ by temperature controller (Indotherm model 401 D2). The whole system is evacuated to avoid disturbance to the balance due to convection in air. The accuracy of measurement using this balance is about 1%.

I have used trans-decaline ($\chi_r = 0.779 \times 10^{-6}$ c.g.s.unit) [58] a non-volatile liquid at room temperature as a reference substance. Density of reference sample is 0.869 gm/c.c. [59]. Using the magnetic susceptibility of air ($\chi_o = 106.3 \times 10^{-6}$ c.g.s.unit at 20^oC) [60], the curie law $\chi_o \sim 1/T$, the tabulated density of air [61], the necessary correction as given by equation 2.43 can be calculated. Error due to the influence of dissolved oxygen has been discussed and ignored by de Jeu et al [62]. I have also neglected the influence of dissolved oxygen.

In the experimental arrangement, the force on the sample is exactly balanced by the force exerted on the horizontal coil, rigidly attached to the balance beam, placed inside the hollow permanent magnet with a uniform radial field and carrying a suitable current i. This force due to the field on the coil is given by :

$$F = 2\pi rniH$$

where, n = number of turns in the coil, r = radius of the coil, H = magnetic field intensity.

In general the suspended system will experience a pull even in the absence of any magnetic sample to balance the pull, we must pass an initial current i_o through the coil. In our set up, instead of the current we measured voltage drop across a standard resistance of the order of 10 K. ohms with the help of high precision digital voltmeter. So the final expression for the susceptibility becomes:

$$\chi(t) = \frac{(v - v_o)}{(v_r - v_o)} \frac{m_r}{m} \left[\chi_r - \frac{\rho_o(t_o)}{\rho_r(t_o)} \chi_o(t_o) \right] + \frac{\rho_o(t)}{\rho(t)} \chi_o(t) \qquad 2.46$$

All the values of magnetic susceptibilities given by me in this thesis are mass susceptibility in c.g.s. unit (erg gauss^{-2} gm^{-1}).

2.15 Description of the experimental set-up for determination of diamagnetic anisotropy ($\Delta\chi$):

The electromagnetic balance for measuring susceptibilities have been designed and fabricated in our laboratory by M. Mitra and R. Paul [63]. Basically the instrument is of the Curie type, the movement of the arms being restricted to the horizontal plane. the schematic diagram of the apparatus is shown in Figure 2.3.

It consists of a horizontal light glass beam A, kept suspended at the middle with vertically stretched phosphor-bronze strips. The upper strip B, is soldered to a torsion head T used for adjusting the position of the beam, whereas, the lower one B′ terminates in an elliptic spring E secured to a universal adjustable holder H which can be moved horizontally in two

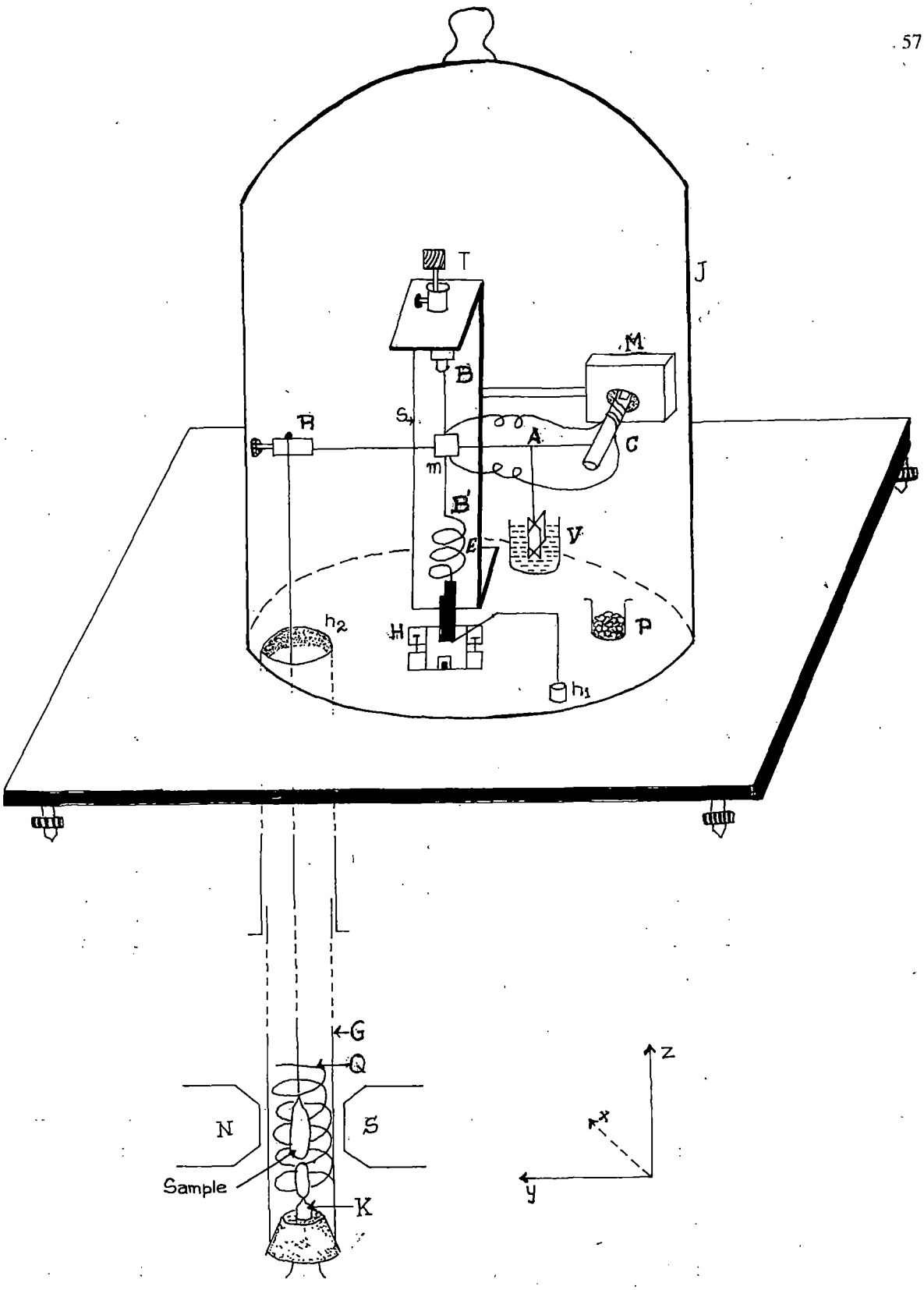

Figure 2.3 Schematic diagram of the apparatus for measuring magnetic susceptibility. T- Torsion head, S- Brass pillar, B, B′ - Phospher-bronze strip, m- mirror, A- Balance beam, M- Magnet, C- Coil, E- Spring, G- Glass tube, Q- Heater, K- Thermo-couple, P- Beaker Containing calcium chloride, V- Vane, H- Adjustable platform, J- Bell-jar, p- Brass plate, R- Perspex block.

directions. The torsion head is fixed to a brass pillar S and the holder H is fixed on a flat brass plate b resting on levelling screws.

A small perspex block R is attached to one end of an arm of the balance beam and has a vertical hole to which is attached a long capillary tube carrying a sample holder. A damping vane V made of thin mica sheet dipping into diffuse pump oil fixed to the other side of the glass beam effectively damps out all spurious vibrations. On the same side of the balance beam is attached a balancing coil of 50 turns of 42 s.w.g. enamelled copper wire wound over a hollow perspex cylinder C and the coil is free to move inside a hollow magnet M having a radial field of about 200 gauss. The phosphor -bronze strips acts as a suspension wire as well as electric connection of the coil. The balance assembly is covered with a greased ground bell jar J. Two holes h_1 and h_2 are drilled in the base plate. In one of this hole, is fixed an ebonite block with binding terminal, sealed vacuum tight with araldite, for leading in the coil currents. The other terminal of the coil is attached to the brass plate. The second aperture h_2 about 3 cm in diameter is fitted with a brass collar for fitting the glass tube extension of the experimental chamber. The joint of the glass tube G and brass tube is made vacuum tight with o-ring. A heater Q of constantant wire and a thermocouple K is fixed through a rubber stopper and is introduced into the glass tube which is made vacuum tight. The sample holder, thermocouple and the heater are placed between the pole pieces of an electromagnet. The brass tube is also provided with a side tube (t) through which the balance chamber and the experimental chamber can be evacuated. The sucksmith form of a pole piece is adopted and any change in the position of the sample was detected with the help of a pair of matched photocells.

It should be notated that since the director of the mesogens aligns itself in the direction of the magnetic field ($\Delta\chi > 0$) in most samples, the magnetic susceptibility determined by this method is $\chi_{\parallel}$ in mesophase and $\bar{\chi}$ in isotropic phase. Since non-metallic organic mesogens are diamagnetic, $\bar{\chi}$ should be independent of temperature. Hence, using equation 2.31 we get $\Delta\chi = 1.5\ (\chi_{\parallel} - \bar{\chi})$, $\Delta\chi$ being the magnetic susceptibility anisptropy. Order parameter is then calculated using equation 2.42.

2.16 Elastic constant and deformation free energy of nematic liquid crystal:

The elastic constants of a liquid crystal are restoring torque which become apparent when the system is perturbed from its equilibrium configuration. In display devices, the electric or the magnetic field induces the initial perturbation and as such the balance between elastic and electric or magnetic forces determines the static deformation pattern of a liquid crystal.

Although various properties of mesophase transitions could be explained in terms of molecular theories but its use to explain the elastic phenomena of the liquid crystal is not obvious as it involves the response of bulk liquid crystal samples to external disturbances. Elastic behaviour of the liquid crystal can be more conveniently explained by regarding liquid crystal as a continuous medium with a set of elastic constants. Based on this viewpoint, Zocher [65], Oseen [66], and Frank [67] developed a phenomenological continuum theory of liquid crystals which can successfully explain the various magnetic or electric field induced effect of liquid crystals.

According to the continuum theory of liquid crystals, the elastic part of the internal energy density of a perturbed liquid crystal is given by the equation:

$$F_{def} = (1/2)\,[\,K_{11}\,(\nabla.\,\mathbf{n})^2 + K_{22}\,(\mathbf{n}.\,\nabla \times \mathbf{n})^2 + K_{33}\,(\mathbf{n} \times \nabla \times \mathbf{n})^2\,] \qquad 2.47$$

where the constants K_{11}, K_{22}, K_{33} are, respectively, termed as the splay, twist, and bend elastic constants and are named collectively known as the Frank elastic constants. **n** is the director. Furthermore, F_{def} must be positive in order to give stability for the uniformly aligned state, all the elastic constants (K_{11}, K_{22}, K_{33}) must be positive.

2.17 Freedericksz transition:

The elastic constants of the liquid crystals can be determined by various methods, of which Freedericksz transition is one of the simplest and convenient methods. The term Freedericksz transition refers to the deformation of a thin layer of nematic liquid crystal sample with a uniform director pattern in an external electric [68-71] or magnetic field [72-79]. Freedericksz observed that when a planar surface aligned nematic liquid crystal cell is subjected to magnetic field normal to the director then the cell undergoes an abrupt change in its optical properties if the strength of the external field exceeds the threshold value, known as the critical field. If the nematic liquid crystals have positive diamagnetic anisotropy or dielectric anisotropy, then as the field exceeds the critical value, the director starts to align along the external field. Depending on the geometry of the arrangement, we can determine, splay, twist or bend elastic constants

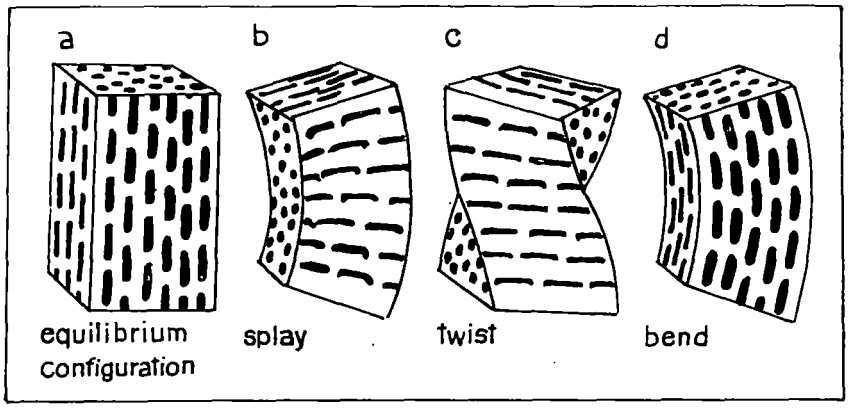

Figure 2.4. (a) An ordered liquid crystal in equilibrium configuration. The deformation states ---- (b) splay, (c) twist, (d) bend.

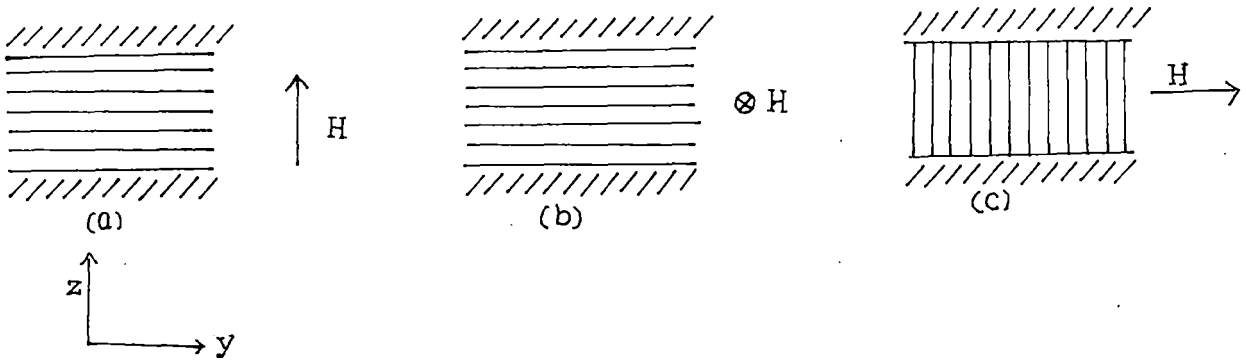

Figure 2.5 Schematic experimental set-up for the determination of the elastic constants from Freedericksz transition: (a) splay, (b) twist and (c) bend.

from Freedericksz transition in the magnetic field. It is shown schematically in Figures 2.4 and 2.5 respectively.

To explain the Freedericksz transition, I have considered a uniform planer layer i.e. is splay mode of nematogenic sample, and is shown in Figure (2.5a). Suppose the magnetic field is applied along the z-axis. When the field increases there is a gradual change in the director pattern once H exceeds a threshold value H_c. When $H < H_c$, the equilibrium state is shown in Figure 2.6(a) where the director is everywhere parallel to the y-axis. In this case a small fluctuation of the director will be damped because the stabilising elastic torque is greater than the de-stabilising magnetic torque. When $H > H_c$, the system will undergo transition to unstable equilibrium state whereby at the slightest fluctuation the system jumps to one of the two stable states as shown in Figures 2.6(b) and 2.6(d).

The threshold magnetic field for the splay, bend or twist deformation is related to the elastic constants by the equation:

$$(H_c)_i = (K_{ii} / \Delta\chi)^{1/2} \quad (\pi / d) \qquad 2.48$$

where d is the sample thickness, $\Delta\chi$ is the diamagnetic anisotropy and $(H_c)_i$ is the respective critical magnetic field.Also the subscript i =1,2,3. refers to the splay, twist and the bend deformation respectively.

2.18 Description of Experimental set-up for determination of K_{11} and K_{33}:

The apparatus of the determination of the elastic constants (K_{11} and K_{33}) has been designed and fabricated in our laboratory by M. K. Das and R. Paul [64]. The block diagram of the set-up has been shown in Figure 2.7.

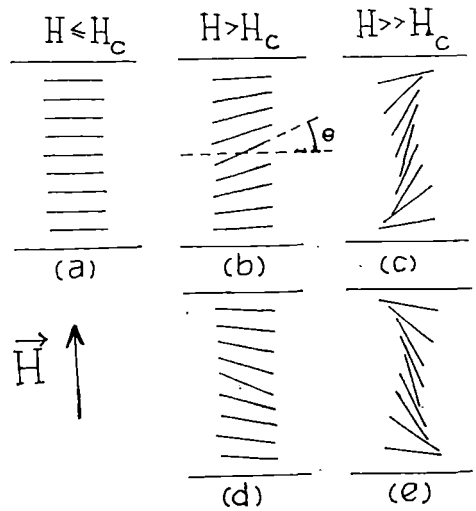

Figure 2.6. Schematic representation of the deformation of the director pattern when $H > H_c$ in the case of the splay mode.

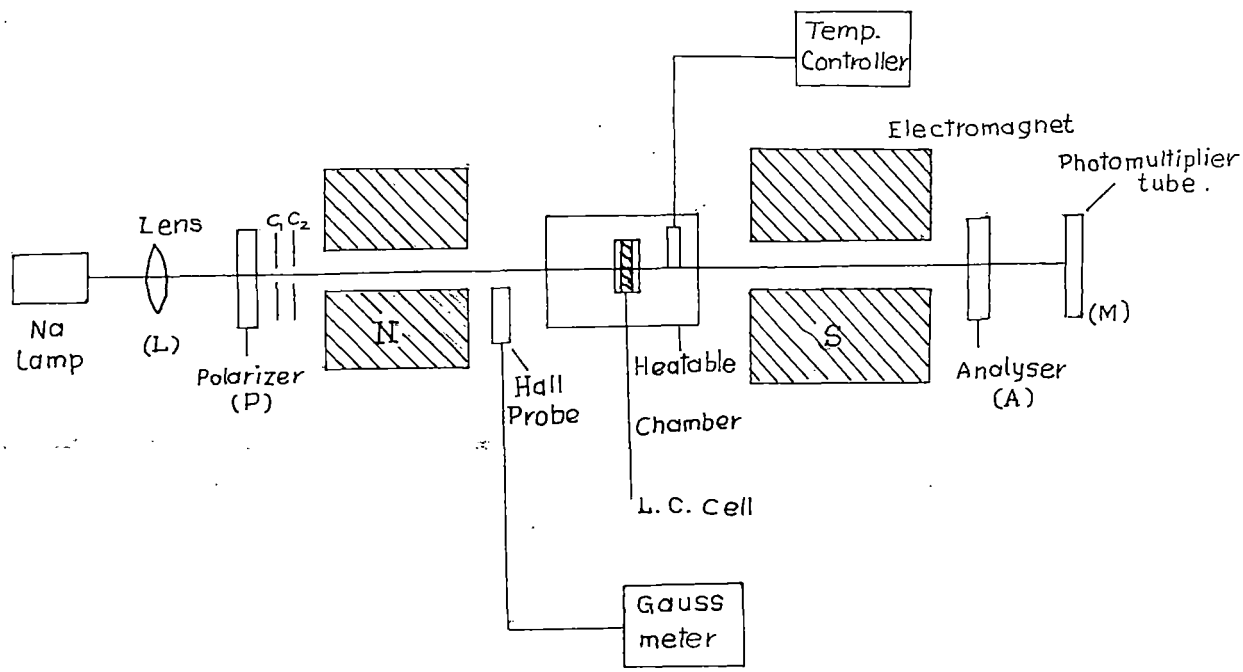

Figure 2.7 Schematic representation of the experimental set-up for elastic constant measurements.

The experimental sample was taken in a glass cell prepared from microscope slides. The cell was housed in a solid brass oven which has a groove at the proper angle and it also acts as a thermostat. The temperature was measured and controlled within an accuracy of $\pm 0.5\ ^0$C by means of a copper-constantan thermocouple inserted in the brass block and a temperature regulator (Indotherm model 457). A sodium D light was used as a source which was allowed to incident on the sample through a lens (L), polarizer (P) and collimating circular slits (C_1,C_2). The polarizer (P) and the analyser (A) were crossed at $\pm 45^0$ relative to the vertical axis. The transmitted light intensity was monitored by a photomultiplier tube (M) whose output was also measured by a nano-ammeter. The magnetic field was applied perpendicular to the director. For the Freedericksz transition to occur, the director must be truly oriented at right angle to the external field. In order to ensure this exact alignment, the brass oven was mounted on a specially constructed platform whose alignment with respect to the field could be adjusted to an accuracy of 1-2′ of arc. Further, the platform itself rested on levelling screws so that the alignment of the sample could be varied in every possible manner. The magnetic field intensity was varied slowly so that the nematic orientation remains in equilibrium with the applied magnetic field. The intensity of transmitted light was measured as the function of the applied magnetic field for any desired temperature. It was observed that when the field (H) exceeds a critical value (H_c) then there was an abrupt change in the optical properties of the sample. Thus we could measure the threshold field intensity (H_c) from the field versus intensity curve within an accuracy of $\pm$ 10 Gauss. The magnetic field was measured using a Hall-probe Gaussmeter (Model DGM-102).

The cell used in the experiment was made of two pieces of glass cut out from microscope slides with sides of 1 inch and 3/4 inch. The glass plates were cleaned by different cleaning agents and subsequently dried and treated for homeotropic or homogenous alignment as required. The smaller glass piece was centred on the larger piece separated by a thin glass-spacer of 150μm thickness. The actual thickness of the sample was measured by a microscope. The splay elastic constant (K_{11}) was measured by using homogenous planar aligned cell which was prepared by treating the inside surface of the glass plate with 1% aqueous solution of polyvinyl alcohol dried and then rubbed the layer in one direction with tissue paper. The bend elastic constant (K_{33}) was measured by using homeotropic cells which were prepared by the surface treatment of the glass plates with lecithin.

When the magnetic field intensity was increased beyond the critical value H_c, the transmitted light intensity exhibits oscillations due to the change of the phase retardation.

The threshold field for twist deformation cannot be detected optically when viewed along the twist axis. Due to the large birefringence of the medium for this direction of propagation, the state of polarisation of the transmitted beam is indistinguishable from that of the emerging beam from the untwist nematics. A total internal reflection technique can be used to measure the K_{22} values of the twist deformation. In my present work however, I have measured only K_{11} and K_{33} for ten different nematic liquid crystals.

Structure and chemical name of the liquid crystals studied:

The chemical names of the liquid crystals studied in the present investigation and their structural formula are given below:

1 & 2. 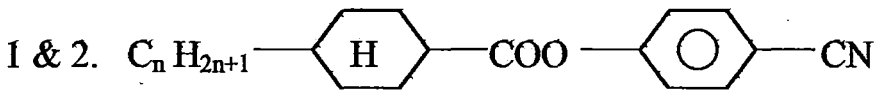

(i) n = 3, p-cyanophenyl trans- 4 - propyl cyclohexane carboxylate.
(CPPCC in short).

(ii) n = 4, p-cyanophenyl trans- 4 - butyl cyclohexane carboxylate.
(CPBCC in short).

3. 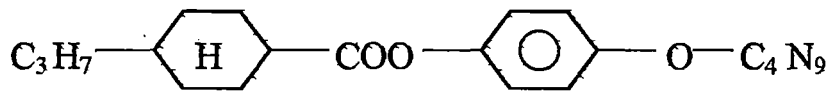

p- butoxyphenyl trans- 4 - propyl cyclohexane carboxylate.
(BPPCC in short).

4. 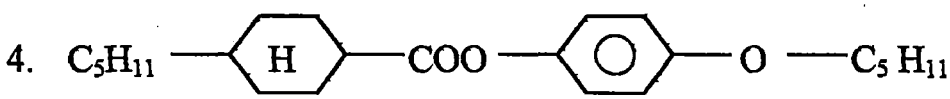

p- pentoxyphenyl trans- 4 - pentyl cyclohexane carboxylate.
(PPPCC in short).

5 & 6. 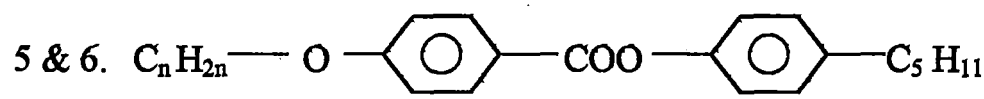

(i) n= 5, 4 -n-pentyl phenyl- 4 - n' pentyloxy benzoate.
(ME 5O.5 in short).

(ii) n= 6, 4 -n-pentyl phenyl- 4 - n' hexyloxy benzoate.
(ME 6O.5 in short).

7. 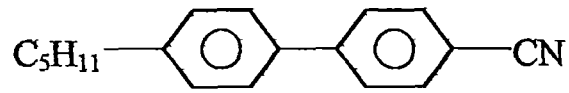

4 - n - pentyl - 4 - n'- cyanobiphenyl. (5CB in short).

8 & 9. 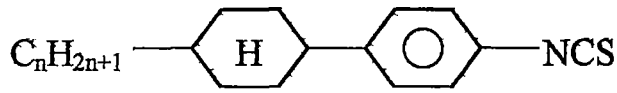

(i) n= 10, 4 - (trans - 4'- n- decyl cyclohexyl) isothiocyanatobenzene.
(10 CPS in short).

(ii)n=12, 4 - (trans - 4'- n- dodecyl cyclohexyl) isothiocyanatobenzene.
(12 CPS in short).

10. 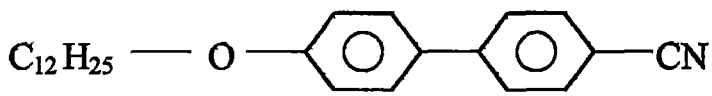

4 - dodecyloxy - 4'- cyanobiphenyl. (12OCB in short).

11. 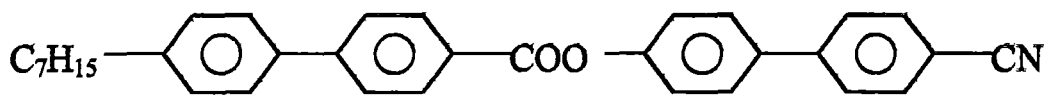

4 - cyanobiphenyl - 4'- yl - 4 - heptylbiphenyl - 4 - carboxylate.
(7CBB in short).

12 & 13. 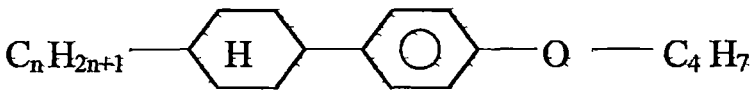

(i) n=3, 3E-n-butene-phenyl-(4-cyclohexane-4′-n-propane)-ether
{ 3CPOd (3)1 in short }

(ii) n= 5, 3E-n-butene-phenyl-(4-cyclohexane-4′-n-pentane)-ether
{ 5CPOd (3)1 in short }

The liquid crystals 1, 2, 3, 11 & 12 were obtained from Hoffmann-La Roche, Basel, Switzerland; the liquid crystals 4, 5 & 6 were obtained from E. Merck, UK; and the crystals 7, 8, 9 & 10 were donated by Prof. R. Dabrowski, Institute of Chemistry, Military University of Technology, Warsaw, Poland. All the samples were obtained in the pure state and were studied without further purification.

References:

1) E. B. Priestley, P. J. Wojtowicz and P. Sheng, Eds. Introduction to Liquid Crystals, Plenum, New York, (1974).
2) S. Chandrasekhar, Liquid Crystals, Cambridge University Press, Cambridge, (1977).
3) G. Vertogen and W. H. de Jue, Thermotropic Liquid Crystals, Fundamentals, Springer-Verlag (1988).
4) G. R. Luckhurst and G. W. Gray, (Editors) The Molecular Physics of Liquid Crystals, Academic Press (1979).
5) P. G. de Gennes, The Physics of Liquid Crystal, Clarendon Press, Oxford, (1974).
6) A. Saupe and W. Maier Z. Natureforsch, 14a, 882 (1959) and 15a, 287 (1960).
7) W. L. McMillan, Phys. Rev., A4, 1238 (1971).
8) W. L. McMillan, Phys. Rev., A6,936 (1972).
9) E. B. Priestley, P. S. Pershan, R. B. Meyer and D. H. Dolphin, Vijnana Parishad Anushandhan Patrika, 14, 93 (1971).
10) K. K. Kobayashi, J. Phys. Soc. (Japan), 29, 101 (1970).
11) K. K. Kobayashi, Mol. Cryst. Liq. Cryst., 13, 137 (1971).
12) D. Demus and L. Richter, Textures of Liquid Crystals, Verlag Chemie, New York (1978).
13) Advances in Liquid Crystals, Vol. 6, Ed. G. H. Brown, Academic Press (1983), Chapter 1.
14) B. K. Vainstein and I. G. Chistyakov, Problem of Modern Crystallography, Nauka, Moscow (1975).

15) A. J. Leadbetter, The Molecular Physics of Liquid Crystals, Eds. G. R. luckhurst & G. W. Gray, Chap.13, Academic Press (1979).

16) A. de Vries, Liquid Crystals, Ed. F. D. Saeva, M. Dekker Inc., NY.

17) A. J. Leadbetter and E. K. Norris, Mol. Phys., 38, 669 (1979).

18) A. de Vries, J. Chem. Phys., 56, 4489 (1972).

19) H. Kohli et al, Z. Physik, B24, 147 (1976).

20) A. de Vries, Mol. Cryst. Liq. Cryst., 10, 219 (1970).

21) P. S. Pershan, Structure of Liquid Crystal Phases, World Scientific (1988).

22) B. Jha and R. Paul, Proc. Nucl. Phys. Solid State Phys. Symp., India, 19c, 491 (1970).

23) C. Kittel, Int. to Solid State Physics, Wiley Eastern, Chap. 2 (1976).

24) H. P. Klug and L. E. Alexander, X-ray diffraction procedures, John Wiley and Sons, N.Y., p.114 and 473 (1974).

25) S. Ergun, J. Appl. Cryst., 1, 19 (1968).

26) R. Bruinsma and D. R. Nelson, Phys. Rev. B. , 23, 1, 402 (1981).

27) E. Gorecka, Li Chen, O. Lavrentovich and W. Pyzuk, Europhysics Letters, 27(7), 507, 1994.

28) R. J. Birgeneau and J. D. Litster, J. Phys. Letts., 39, L399, (1978).

29) B. K. Vainstein, Diffraction of x-rays by Chain Molecules, Elsevier Pub. Co. (1966).

30) R. Paul and G. Chaudhuri, Abstract in the 14th International Liquid Crystal Conference, Pisa, 1992, Abs.no.- H-P23.

31) E. Dorn, Z. Physik, 11, 111 (1910).

32) W. H. Pness, S. A. Teukolsky, W. T. Vellering and B. P. Flannery, Cambridge University Press, 1986, Chap. 15.

33) O. Weiner, S. Ber. Sachs. Ges. Wissensch., 61, 113 (1909).

34) H. Zocher, Naturwiss., 13, 1015 (1925).

35) H. Zocher, Z. Krist., 79, 122 (1931).

36) F. Grandjean, Compt. Rend., 168, 408 (1919).

37) N. V. Madhusudana, R. Sashidhar and S. Chandrasekhar, Mol. Cryst. Liq. Cryst., 13, 61 (1971).

38) Y. Poggi , J. Robert and J. Borel, Mol. Cryst. Liq. Cryst., 29, 31, (1975).

39) R. Chang, Mol. Cryst. Liq. Cryst., 30, 155 (1975).

40) C. C. Huang, R. S. Pindak and J. J. Ho, J. Phys. Lett. (Paris), 35, 185 (1974).

41) W. Kuczynski and B. Stryla, Mol. Cryst. Liq. Cryst., 31, 267 (1975).

42) M. Laurent and R. Journeaux, Mol. Cryst. Liq. Cryst., 36, 171 (1976).

43) G. Pelzl and H. Sackmann, Mol. Cryst. Liq. Cryst., 15, 75 (1971).

44) G. Pelzl and H. Sackmann, Symp. Faraday Soc., No. 5, 68 (1971).

45) Y. Galerne, S. T. Lagerwall and I. W. Smith, Opt. Commun., 19, 147 (1976).

46) H. E. Neugebauer, Canad. J. Phys., 32, 1 (1954).

47) M. F. Vuks, Optics and Spectroscopy, 20, 361 (1966).

48) A. Saupe and W. Maier, Z. Natureforsch, 16a, 816 (1961).

49) P. G. de Gennes, , Mol. Cryst. Liq. Cryst., 12, 193 (1971).

50) I. Haller, H. A. Huggins, H. R. Lilienthal and T. R. McGuire, J. Phys. Chem., 77, 950 (1973).

51) A. K. Zeminder, S. Paul and R. Paul, Mol. Cryst. Liq. Cryst. , 61, 191 (1980).

52) P. G. de Gennes, The Physics of Liquid Crystal, Clarendon Press, Oxford, p.31 (1974).

53) W. H. de Jue, Physical Properties of Liquid Crystalline Materials, Gordon Breach, NY, p. 24 (1980).

54) V. Tsvetkov, Acta Physicochim. USSR, 16, 132 (1942).

55) A. Saupe and W. Maier, Z. Natureforsch, 16a, 816 (1961).

56) J. P. Dias, C. R. Acad. Sci., Se'r, A282, 71 (1976).

57) J. O. Kessler, Liq. Cryst. Ord. Fluids, p. 361 (1970)

58) CRC Handbook of Chemistry and Physics, 58th edition, p.E-128. (1977- 78),

59) CRC Handbook of Chemistry and Physics, 58th edition, p.C-270 (1977- 78),.

60) A. Burris and C.D. Hause, J. Chem. Phys., 11, 442 (1943).

61) CRC Handbook of Chemistry and Physics, 58th edition, p. F-9. (1977- 78),

62)W. H. de Jue and W. A. P. Claassen, J. Chem. Phys., 68, 102 (1978).

63) M. Mitra and R. Paul, Mol. Cryst. Liq. Cryst., 148, 185 (1987).

64) M. K. Das and R. Paul, Mol. Cryst. Liq. Cryst., 259, 13 (1995).

65) H. Zocher, Trans Faraday Soc., 29, 945 (1933).

66) C. W. Oseen, Trans Faraday Soc., 29, 883 (1933).

67) F. C. Frank, Faraday Soc.Discussion, 25, 19 (1958).

68) H. Gruler, T. J. Schiffer and G. Meier, Z. Natureforsh, 27a, 966 (1972).

69) H. Gruler and L. Cheung, J. Appl. Phys., 46, 5097 (1975).

70) H. Deuling in Liquid Crystals, Solid State Physics Suppl. no. 14, ed. L. Liebert, Academic Press, NY, p. 77.

71) M. J. Bradshaw and E. P. Rayens, Mol. Cryst. Liq. Cryst., 72, 35 (1980).

72) V. Freedericksz and V. Tsvetkov, Phy. Z. Soviet Union, 6, 490 (1934).

73) V. Freedericksz and V. zolina, Trans. Faraday Soc., 29, 919 (1933).

74) P. P. Karat and N. V. Madhusudana, Mol. Cryst. Liq. Cryst., 40, 239 (1977).

75) H. P. Schad, M. A. Osman, J. Chem. Phys., 75 (2), 880 (1981).

76) F. Leenhouts, H. J. Boeber, A. J. Dekker and J. J. Jonker, J. Phys. (Paris) Colloque.,40, C3-291 (1979).

77) H. P. Schad, G. Bauer and G. Maier, J. Chem. Phys., 67, 3705 (1977).

78) F. Leenhouts and A. J. Dekker, J. Chem. Phys., 74, 1956 (1981).

79) H. P. Schad, M. A. Osman, J. Chem. Phys., 75 (2), 880 (1978).

80) L. Pohl and U. Finkenzeller in B. Bahadur (Ed.) Liquid Crystals, Application and Uses, Vol. 1, World Scientific, p. 166 (1990)

CHAPTER- 3

X-ray diffraction studies and measurement of density, refractive indices, magnetic susceptibility anisotropy, splay and bend elastic constants of four cyclohexane carboxylate compounds.

In this chapter, I shall present experimental data on four liquid crystalline compounds. The compound studied with their chemical structures and transition temperatures are given below:

I. p-cyanophenyl trans-4-propyl cyclohexane carboxylate.

(CPPCC in short)

C3H7-Cy-COO-Ph-CN

$$K \underset{47\ ^{\circ}C}{\overset{54.5\ ^{\circ}C}{\rightleftharpoons}} N \overset{70\ ^{\circ}C}{\longleftrightarrow} I$$

II. p-cyanophenyl trans-4-butyl cyclohexane carboxylate.

(CPBCC in short)

C4H9-Cy-COO-Ph-CN

$$K \underset{<29.5\ ^{\circ}C}{\overset{55\ ^{\circ}C}{\rightleftharpoons}} N \overset{68.3\ ^{\circ}C}{\longleftrightarrow} I$$

III. p-butoxyphenyl trans-4-propyl cyclohexane carboxylate.

(BPPCC in short)

C3H7-Cy-COO-Ph-O-C4H9

$$K \overset{43\ ^{\circ}C}{\longleftrightarrow} N \overset{72.6\ ^{\circ}C}{\longleftrightarrow} I$$

IV. p-pentoxyphenyl trans-4-pentyl cyclohexane carboxylate.

(PPPCC in short)

C5H11-Cy- COO-Ph-O-C5H11

$$K \overset{33.5\ ^{\circ}C}{\longleftrightarrow} S \overset{35.4\ ^{\circ}C}{\longleftrightarrow} N \overset{75\ ^{\circ}C}{\longleftrightarrow} I$$

(Ph= Phenyl ring, Cy = Cyclohexyl ring)

The transition temperatures were recorded by observing the textures under a polarising microscope using Mettler FP 80/ 82 hot stage. The transition temperatures agreed with those given in the literature [1] and the compounds were used without further purification. The physical properties studied were density, refractive index, magnetic susceptibility anisotropy, and bend and splay elastic constants. X-ray diffraction photographs of all the compounds in their mesophase were also taken. All the experiments covered the full mesomorphic temperature ranges of the substances. The respective experimental procedures have been described in detail in Chapter 2 of this thesis.

Figures 3.1- 3.4 give the temperature variation of density of CPPCC, CPBCC, BPPCC and PPPCC. For all the compounds the density decreases monotonically with increasing temperature and there is a small density change at the nematic-isotropic transition temperature. Only PPPCC has a smectic phase and it appears that the density changes continuously at the smectic to nematic transition.

The temperature variation of ordinary and extraordinary refractive indices for CPPCC, CPBCC, BPPCC and PPPCC at four different wavelengths are given in Figures 3.5 to 3.8. The density and refractive indices (at different wavelengths) of CPPCC, CPBCC and PPPCC have already been reported by Takahashi et al [2] and their values agree with our values within experimental errors. However, they have not calculated order parameters from their data, whereas we have calculated the order parameters and compared these values with those obtained from magnetic susceptibility and x-ray diffraction studies.

The values of densities, ordinary and extraordinary refractive indices at different temperatures for CPPCC, CPBCC, BPPCC and PPPCC at

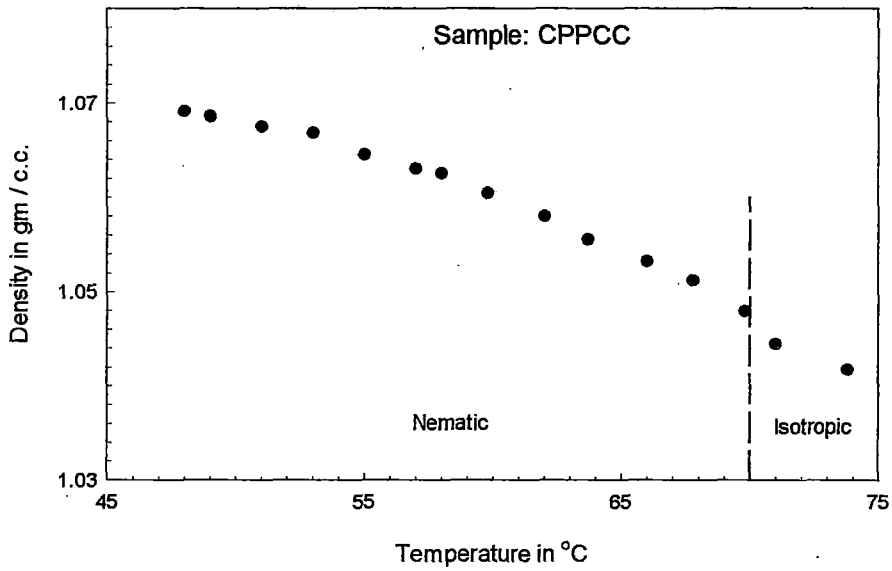

Figure 3.1. Density values as a function of temperature.

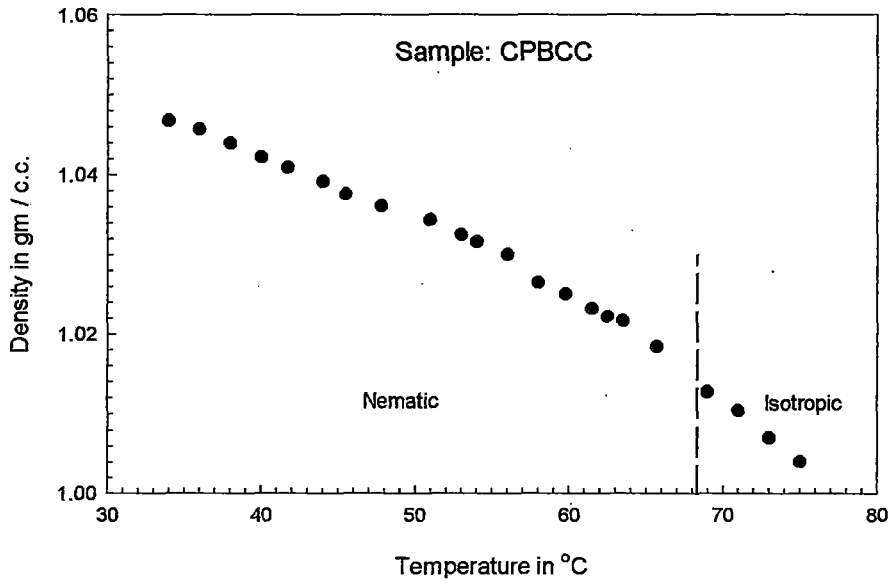

Figure 3.2. Density values as a function of temperature.

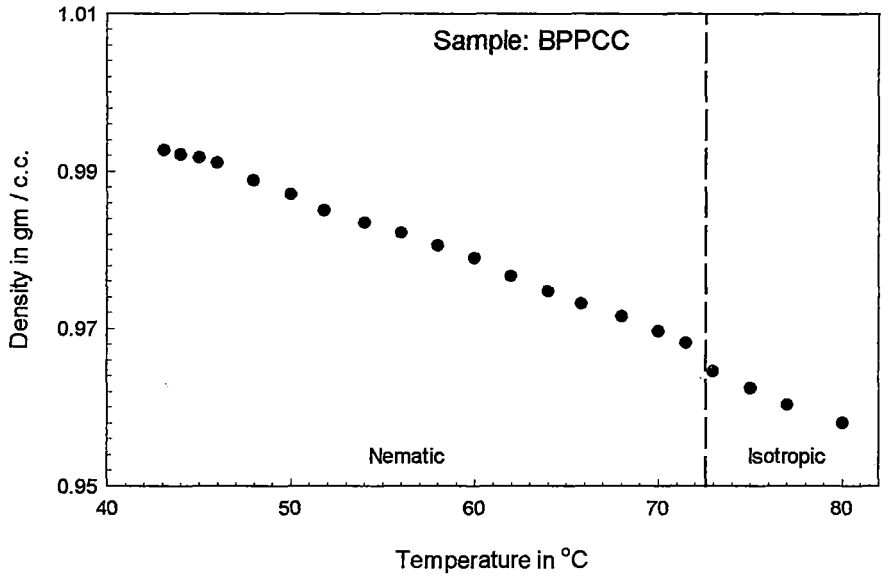

Figure 3.3. Density values as a function of temperature.

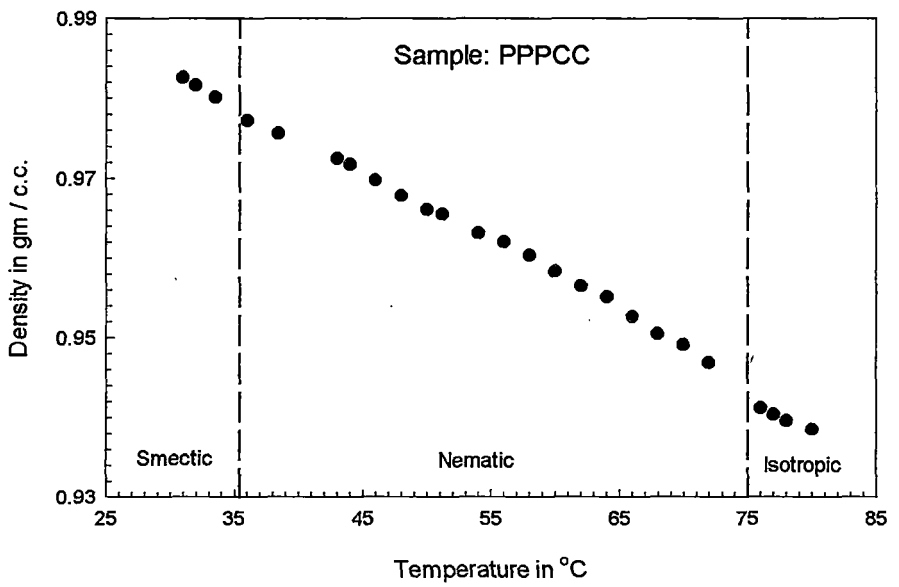

Figure 3.4. Density values as a function of temperature.

wavelengths of 4358 Å, 5461 Å, 5780 Å and 6907 Å are given in Tables 3.1 to 3.4. The respective polarisabilities calculated for these four mesogens using Vuks procedure (equation 2.24 & 2.25) are tabulated in Tables 3.5 to 3.8. The same polarisabilities calculated following Neugebauer method (equations 2.22 &2.23) are given in Tables 3.9 to 3.12. The polarisability anisotropies in the perfectly aligned ($< P_2 > = 1$) samples have been determined by Haller's extrapolation procedure (Chapter 2) and have been given in the respective Table. The order parameters calculated using Vuks polarisability values are tabulated in Tables 3.13 to 3.16 for CPPCC, CPBCC, BPPCC and PPPCC. Finally, the order parameters of these four mesogens using Neugebauer polarisability values are given in Tables 3.17 to 3.20. Though for all the four compounds the polarisability anisotropy calculated from Vuks method are larger than those calculated from Neugebauer procedure, the order parameters from these two methods agree within ± 0.01 % . Mitra et al [3], for some other mesogens, also observed that the Vuks and Neugebauer procedures give almost same order parameter values, though the polarisability anisotropies were different.

The x-ray diffraction photographs from the mesophases of CPPCC, CPBCC, BPPCC and PPPCC at different temperatures are shown in plates 3a-3i. The samples were aligned in a magnetic field of about 5 Kilogauss. The angular distribution of x-ray intensities (in arbitrary scale), after correction for background and conversion from optical densities to x-ray intensities, for the outer diffraction arc for CPPCC at five different temperatures are tabulated in Table 3.21. The corresponding orientational distribution functions calculated by Leadbetter method (equation 2.16) are shown in Table 3.22. Similarly Tables 3.23 and 3.24 give the x-ray intensities and distribution function respectively for CPBCC. For BPPCC

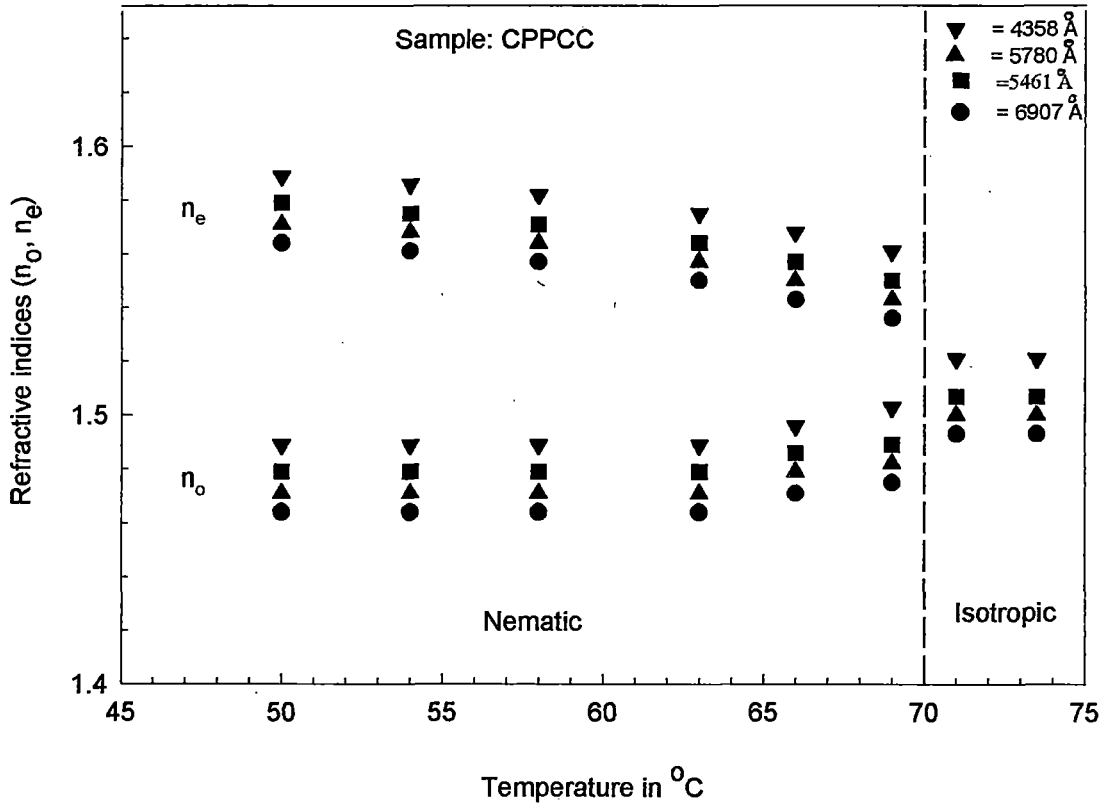

Figure 3.5. Variation of refractive indices (n_O, n_e) with temperature.

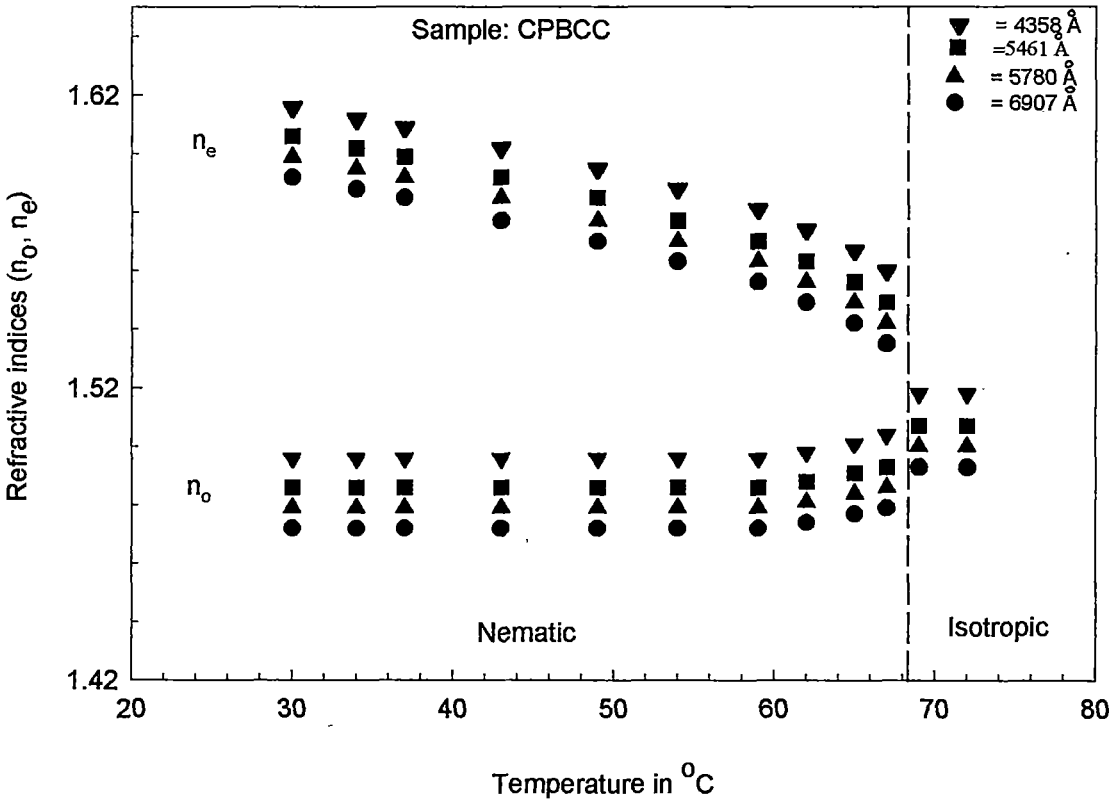

Figure 3.6. Variation of refractive indices (n_O, n_e) with temperature.

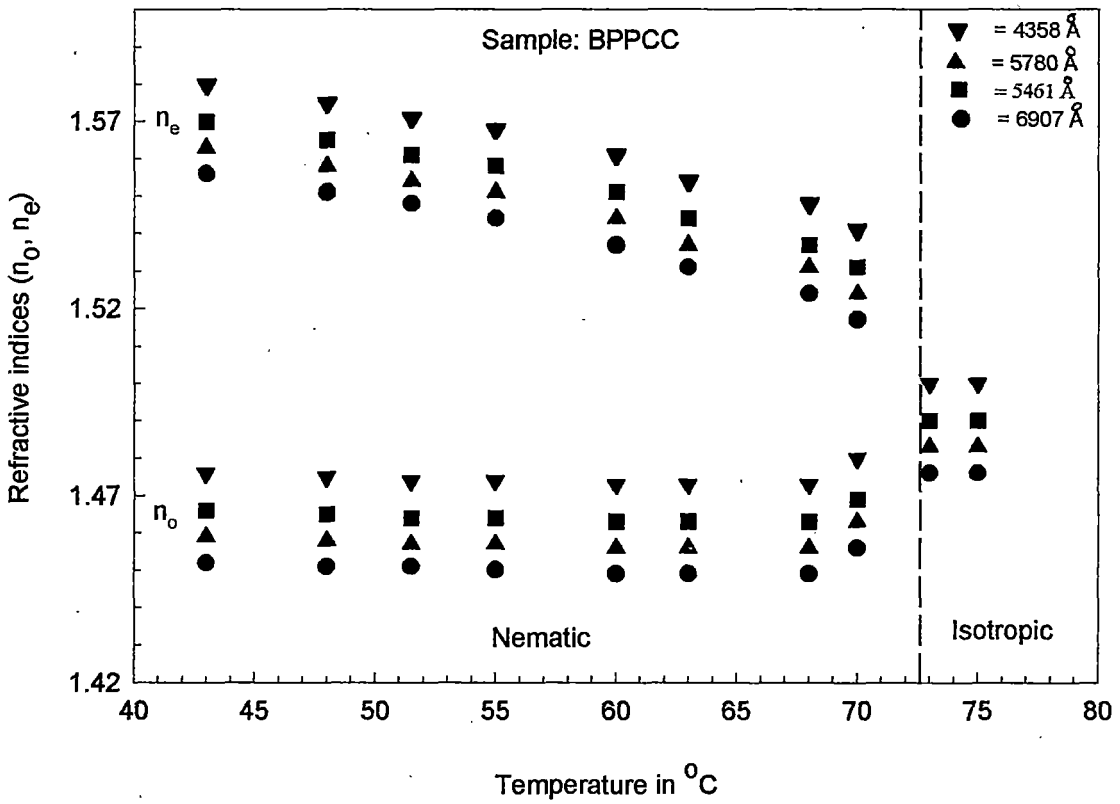

Figure 3.7. Variation of refractive indices (n_o, n_e) with temperature.

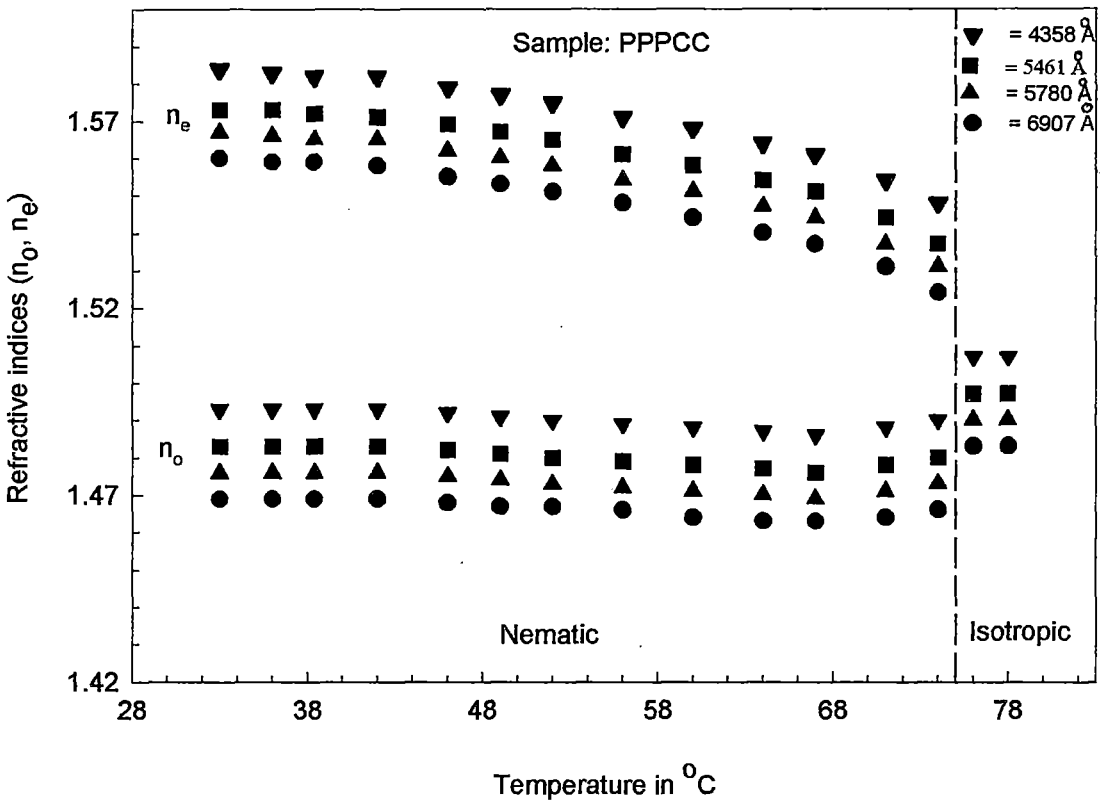

Figure 3.8. Variation of refractive indices (n_O, n_e) with temperature.

the corresponding values are tabulated in Tables 3.25 and 3.26. Tables 3.27 and 3.28 similarly give the x-ray intensity and distribution function values for PPPCC. The orientational order parameters $< P_2 >$ and $< P_4 >$ of CPPCC, CPBCC, BPPCC and PPPCC at different temperatures are tabulated in Tables 3.29 to 3.32.

The apparent molecular lengths of CPPCC and CPBCC in the mesophase, as obtained from the inner x-ray diffraction arc are given in Table 3.33 and 3.34. Tables 3.35 and 3.36 give the corresponding apparent molecular lengths for BPPCC and PPPCC respectively. The temperature variation of the apparent molecular lengths of all the four mesogens are shown in Figure 3.9a to 3.9d. The model lengths of these molecules in their fully extended form have been determined and are noted in the respective tables. It can be seen that for the two cyano compounds (CPPCC and CPBCC) the ratio of apparent molecular lengths to their model molecular lengths are nearly 1.4, showing formation of a molecular association (dimers) in the mesophase. This is in accordance with x-ray diffraction observation on cyanobiphenyls [4], where this ratio of apparent to model molecular lengths are also about 1.4. The other two compounds have no terminal polar groups and the ratio of apparent to model molecular lengths are 1.09 and 1.15 for BPPCC and PPPCC respectively, showing that even if there are association of molecules in the mesophase of these compounds, their apparent length is almost equal to the model length of single molecule. In fact, PPPCC forms cybotactic nematic phase, that means its molecules form small smectic like clusters. It may be mentioned that in PPPCC, we have observed a smectic phase between 33.5 ^{0}C to 35.4 ^{0}C from texture studies. However, the smectic phase could not be identified from x-ray diffraction pattern (Plate 3g) since the sample could

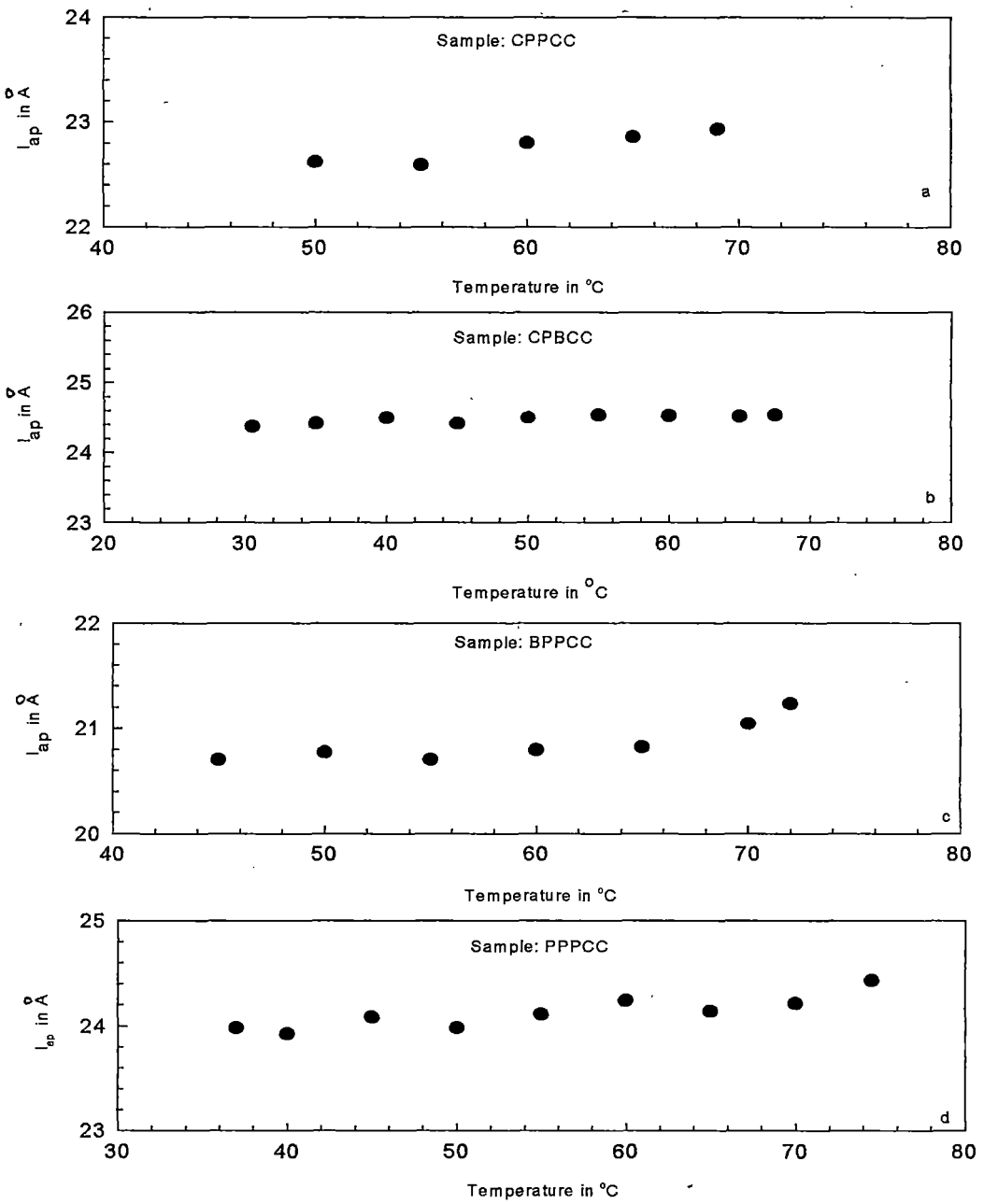

Figure (3.9a - 3.9d). Temperature variation of apparent molecular length (l_{ap}).

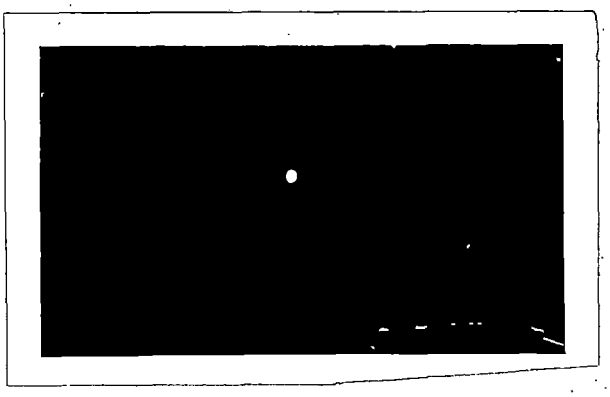

Plate 3a: X-ray diffraction photograph of the oriented sample in the nematic phase of CPPCC at 50°C.

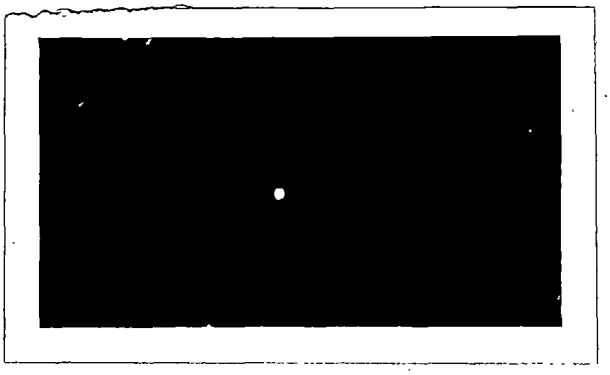

Plate 3b: X-ray diffraction photograph of the oriented sample in the nematic phase of CPPCC at 69°C.

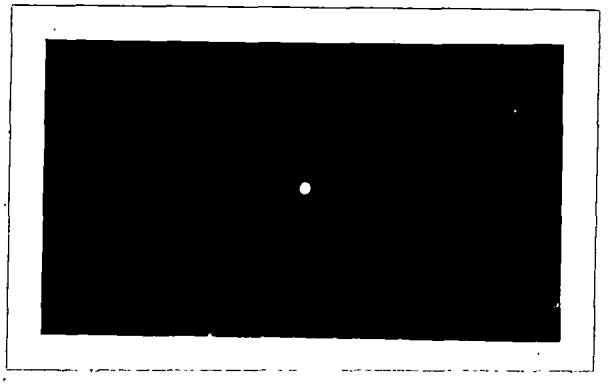

Plate 3c: X-ray diffraction photograph of the oriented sample in the nematic phase of CPBCC at 30.5°C.

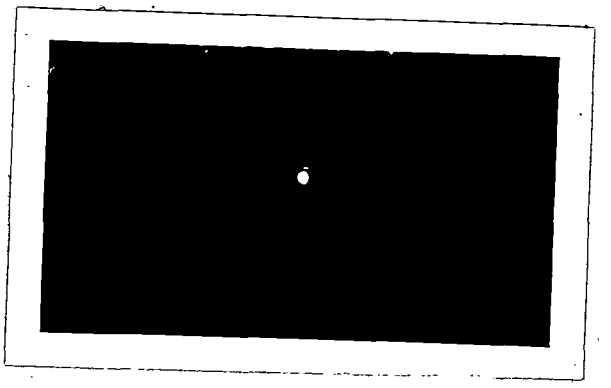

Plate 3d: X-ray diffraction photograph of the oriented sample in the nematic phase of CPBCC at 65°C.

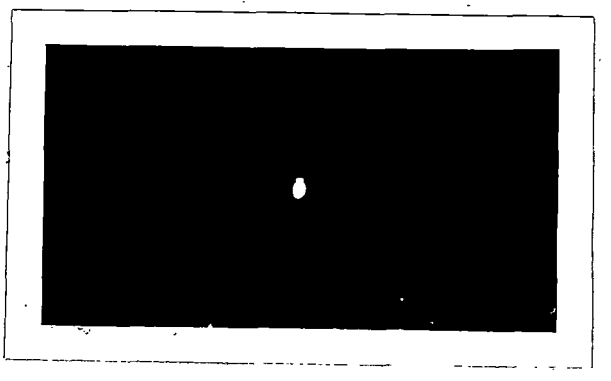

Plate 3e: X-ray diffraction photograph of the oriented sample in the nematic phase of BPPCC at 45°C.

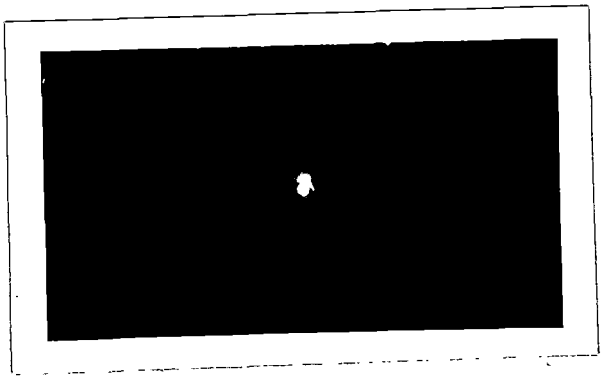

Plate 3f: X-ray diffraction photograph of the oriented sample in the nematic phase of BPPCC at 70°C.

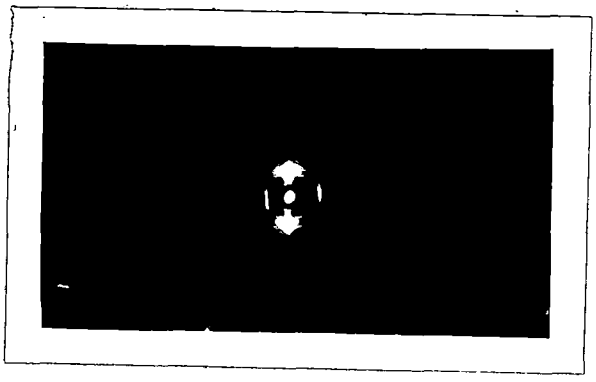

Plate 3g: X-ray diffraction photograph of the partially oriented sample in the smectic phase of PPPCC at 35°C.

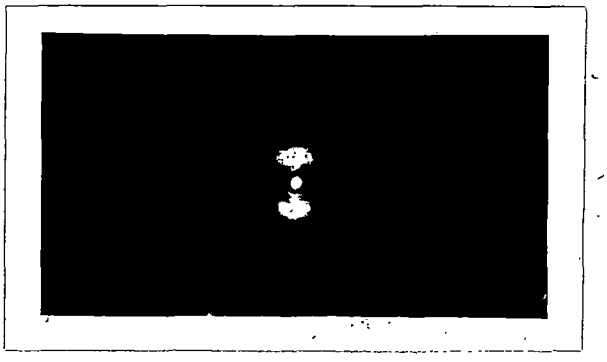

Plate 3h: X-ray diffraction photograph of the oriented sample in the nematic phase of PPPCC at 40°C.

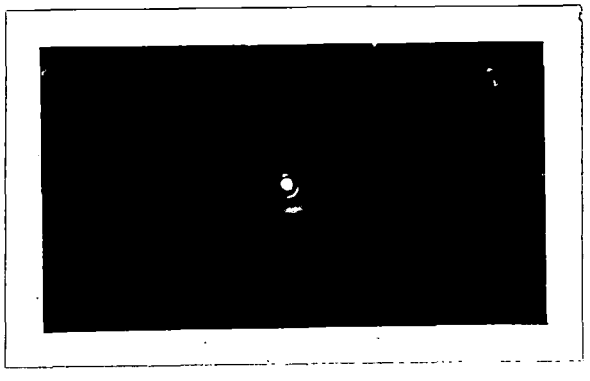

Plate 3i: X-ray diffraction photograph of the oriented sample in the nematic phase of PPPCC at 74.5°C.

not be aligned in the applied magnetic field of about 5 Kilogauss. Moreover, even in the nematic phase of this compound, strong smectic like inner spot were observed in the x-ray pattern upto 40 ^{0}C(Plate 3h). Hence, PPPCC has cybotactic nematic phase below 40 ^{0}C. Above 40^{0}C the x-ray diffraction pattern is like normal nematic(Plate3i).

The experimental magnetic susceptibility values at different temperatures along the director for CPPCC, CPBCC, BPPCC and PPPCC are tabulated in Tables 3.37 to 3.40. The values of respective magnetic susceptibilities in the isotropic phases are also given in these Tables. The magnetic susceptibility anisotropies in the perfectly ordered state, $\Delta\chi_0$, have been determined by Haller's extrapolation (Chapter 2) procedure and are noted in the respective Table. The calculated magnetic susceptibility anisotropy ($\Delta\chi$) and order parameter values are also shown in these tables. The temperature variation of magnetic anisotropy for all these four mesogens have been shown in Figures 3.10 to 3.13. In all these compounds $\Delta\chi$ decreases monotonically with increasing temperature and shows a discontinuity at the nematic to isotropic phase transition.

The temperature variation of order parameter values obtained from refractive index, magnetic susceptibility and x-ray diffraction studies for CPPCC, CPBCC, BPPCC, and PPPCC are shown in Figures 3.14, 3.15, 3.16 and 3.17 respectively. The theoretical Maier-Saupe order parameter values are also shown in these figures. For all the mesogens the trend is similar. At temperatures much below the nematic to isotropic transition, the experimental order parameter values are somewhat greater than the Maier-Saupe calculated values. Near the transition temperature the values of order parameters obtained from refractive index and magnetic susceptibility studies decreases rapidly with increasing temperature, so that

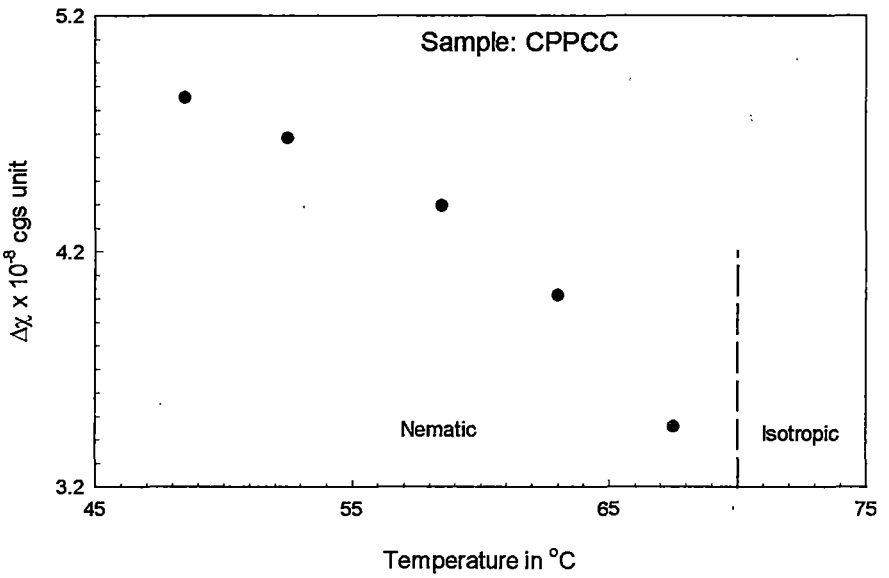

Figure 3.10. Temperature variation of the anisotropy of the diamagnetic susceptibility ($\Delta\chi$).

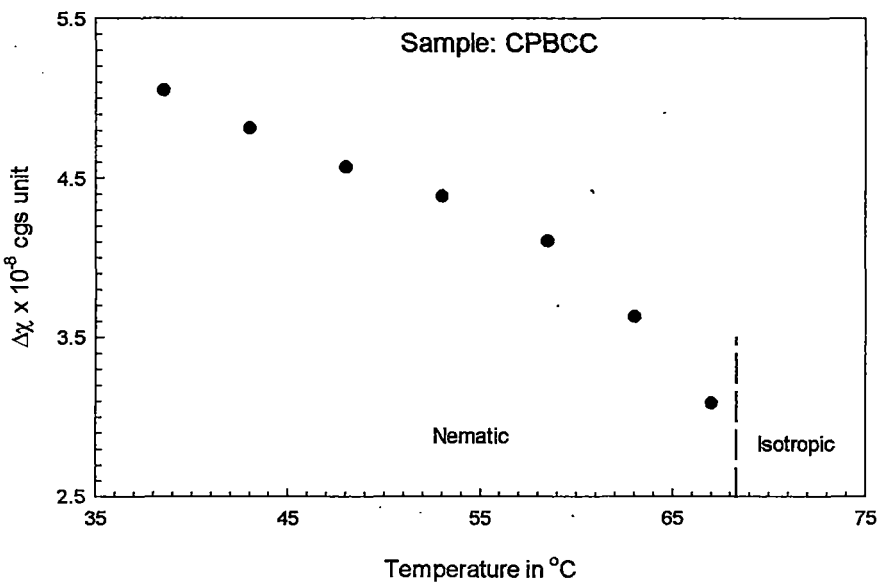

Figure 3.11. Temperature variation of the anisotropy of the diamagnetic susceptibility ($\Delta\chi$).

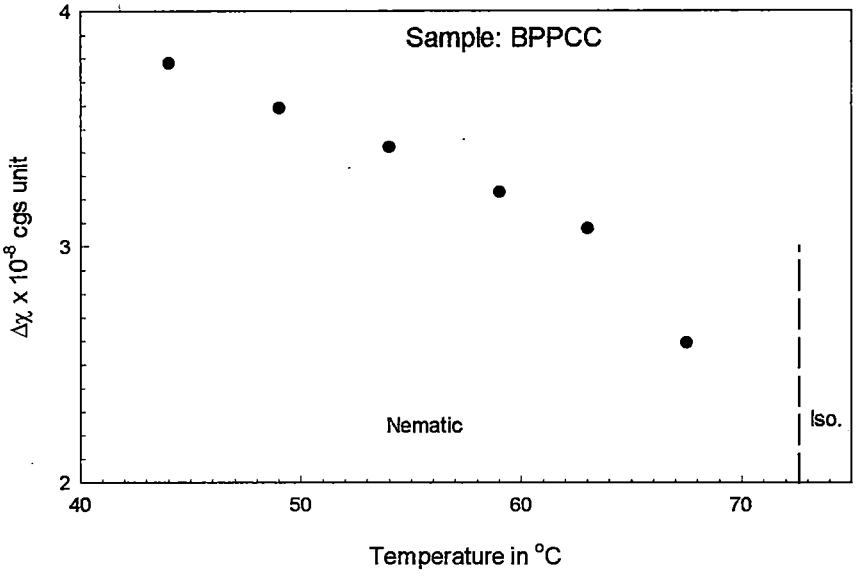

Figure 3.12. Temperature variation of the anisotropy of the diamagnetic susceptibility ($\Delta\chi$).

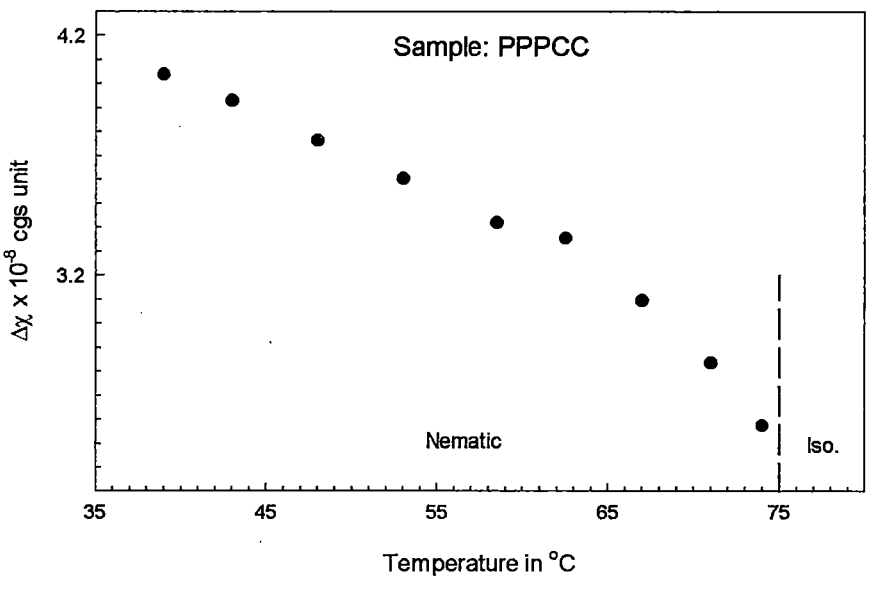

Figure 3.13. Temperature variation of the anisotropy of the diamagnetic susceptibility ($\Delta\chi$).

these values are lower than the theoretical values. The order parameters from x-ray diffraction studies on the other hand follow the Maier-Saupe values closely near the clearing temperature. The rapid variation of $< P_2 >$ obtained from refractive index and magnetic susceptibility data near the N-I transition temperature has been observed by many workers [5-9]. This may be due to fluctuations of the director, which is more pronounced near the transition temperature. Moreover, in the present study all the four compounds have cyclohexane ring, which may vibrate more with the rise of temperature and thus lower the order parameter in addition to the lowering effect due to the aliphatic chain vibrations. However, x-ray studies do not show such rapid decrease of order parameter near the transition. This may be due to the fact that the x-ray diffraction pattern (outer arc) is due to the neighbouring molecules, hence we essentially measure the short range order parameter, which changes less rapidly near the transition temperature. In effect, we are measuring different order parameters depending upon the experimental method used and hence this discrepancy between different experimentally determined order parameter values.

The splay and bend elastic constants of CPPCC, CPBCC, BPPCC and PPPCC have been determined by observing Freedericksz transition in a magnetic field. The full experimental details of the experiment have been given in Chapter 2. The splay and bend elastic constant values together with the critical magnetic fields at different temperatures for the compound CPPCC are given in the Tables 3.41 and 3.42 respectively. The sample thicknesses and the interpolated values of the magnetic susceptibility anisotropy are also given in the Tables. Similarly K_{11} and K_{33} values of CPBCC are shown in Tables 3.43 and 3.44 respectively. The

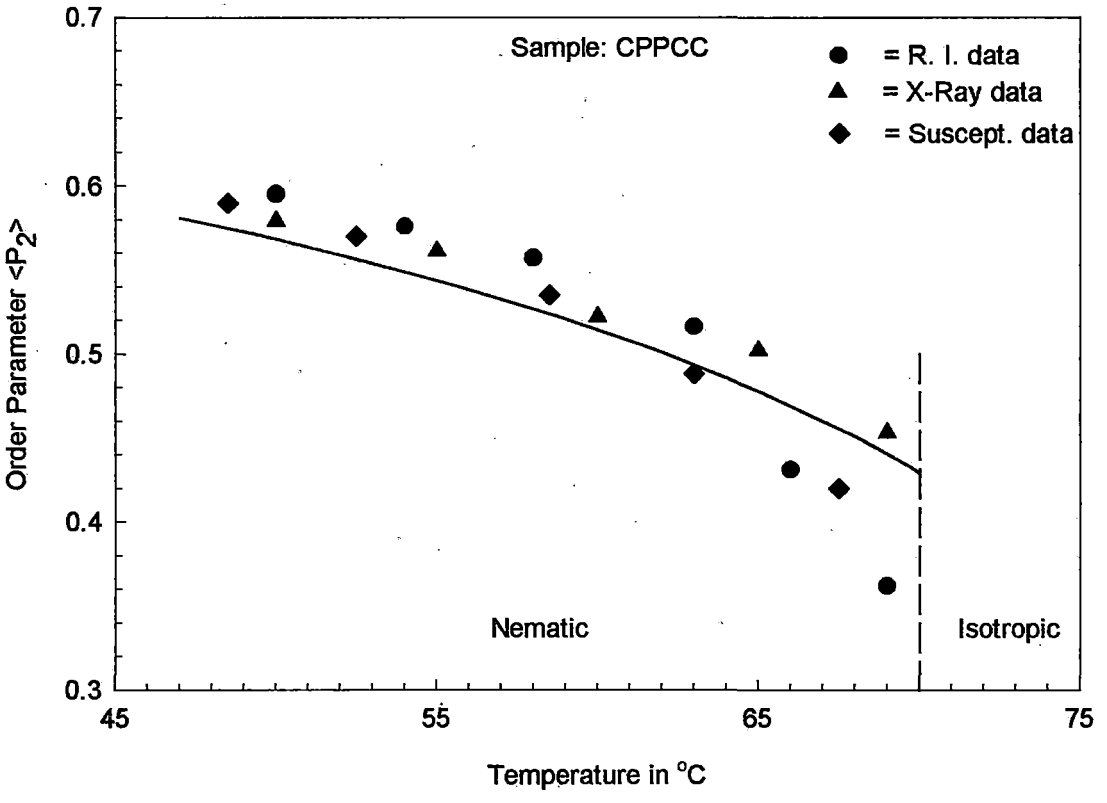

Figure 3.14. Temperature variation of Order Parameter $<P_2>$. Continuous curve corresponds to Maier-Saupe theoretical values.

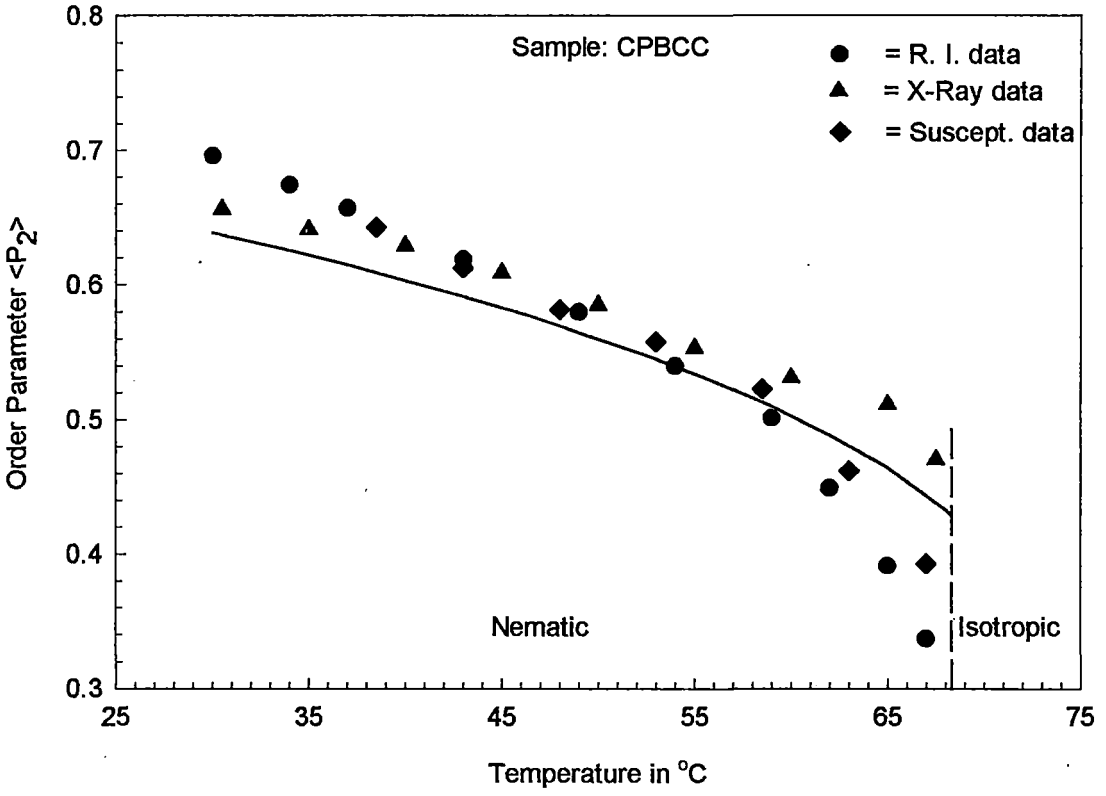

Figure 3.15. Temperature variation of Order Parameter $\langle P_2 \rangle$. Continuous curve corresponds to Maier-Saupe theoretical values.

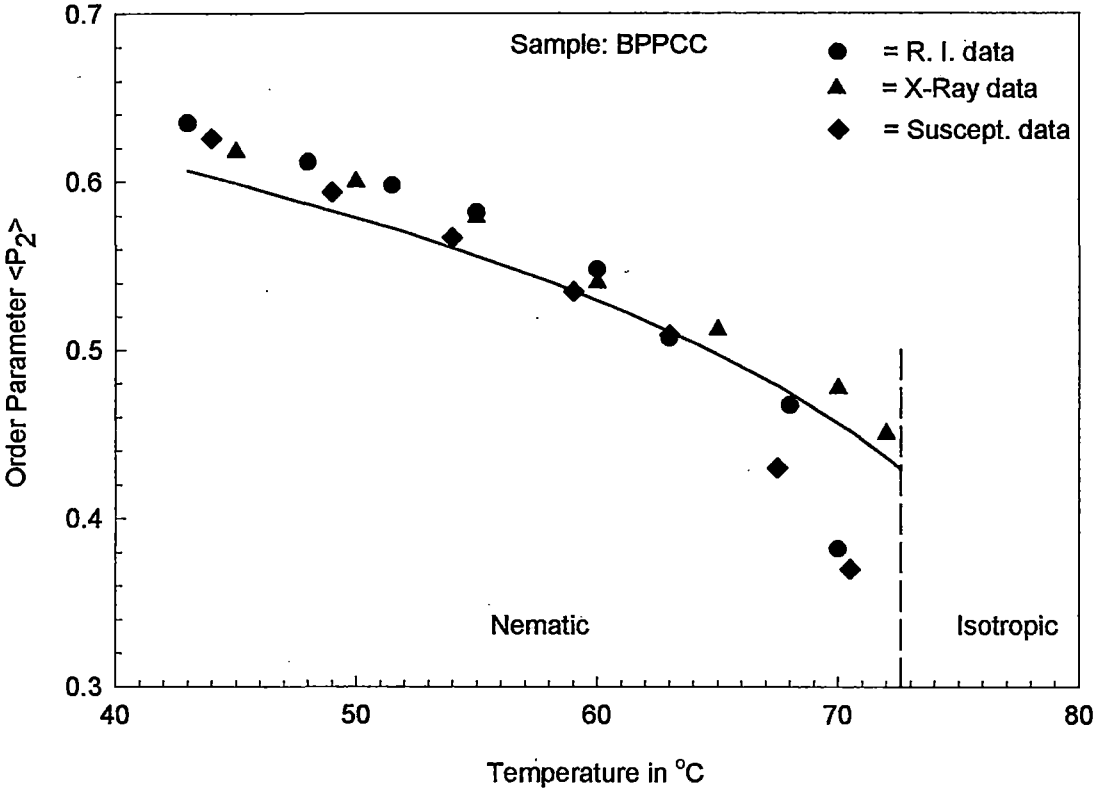

Figure 3.16. Temperature variation of Order Parameter $<P_2>$. Continuous curve corresponds to Maier-Saupe theoretical values.

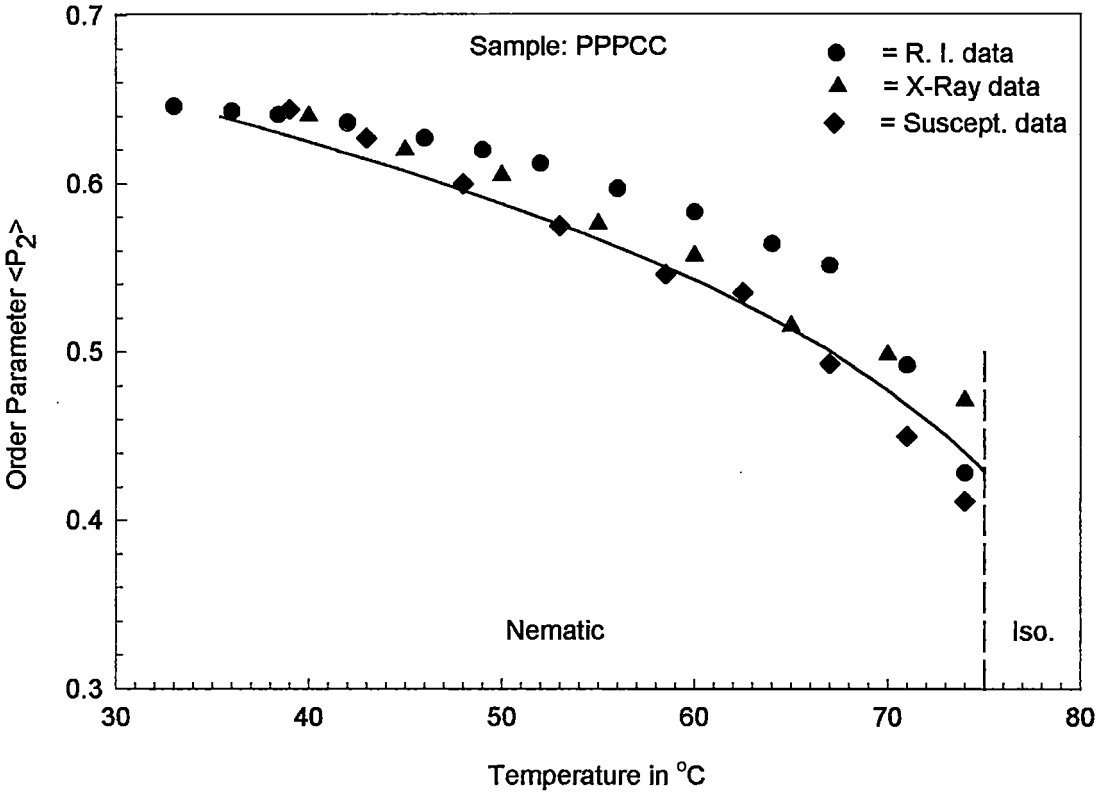

Figure 3.17. Temperature variation of Order Parameter $\langle P_2 \rangle$. Continuous curve corresponds to Maier-Saupe theoretical values.

splay and bend elastic constant values for BPPCC and PPPCC are tabulated in Tables 3.45 to 3.48. The ratios of bend to splay elastic constants (K_{33}/K_{11}) at different relative temperatures for these four mesogens are given in Tables 3.49 and 3.50. The temperature variation of splay and bend elastic constants for CPPCC, CPBCC, BPPCC, and PPPCC are shown in Figures 3.26 to 3.29. Scharkowski et al [10] have given a figure showing the variation of K_{33}/K_{11} with reduced temperature for the two cyano compounds (CPPCC and CPBCC) studied by us. However, they have not given the values of K_{11} and K_{33} separately, so we cannot compare our splay and bend elastic constant values with their values directly. Our bend to splay ratios show similar temperature variations as observed by Scharkowski et al [10]. In both CPPCC and CPBCC the ratios are always greater than 1 and increases with decreasing temperatures. The ratios are somewhat larger for CPPCC than for CPBCC. However, our bend to splay elastic constant ratios are almost 15% smaller than those given by Scharkowski et al. We are unable to explain this discrepancy, since individual K_{11} and K_{33} values are not given by them. The other two mesogens (BPPCC and PPPCC) have the bend to splay ratios less than 1 at all temperatures. Schadt et al [11] have also reported that K_{33}/K_{11} is less than 1 for related compound 5CEPO3 in which the pentyloxy group in PPPCC has been replaced by propyloxy group. In BPPCC the K_{33}/K_{11} ratio increases slowly as the temperature decreases as in CPPCC and CPBCC. However, in PPPCC the bend to splay ratio decreases quite rapidly with decreasing temperatures. It may be mentioned that from the x-ray diffraction studies PPPCC shows cybotactic nematic phase. In the cybotactic nematic phase small groups of molecules show smectic like order. It has been pointed out by Bradshaw et al [12] that smectic like

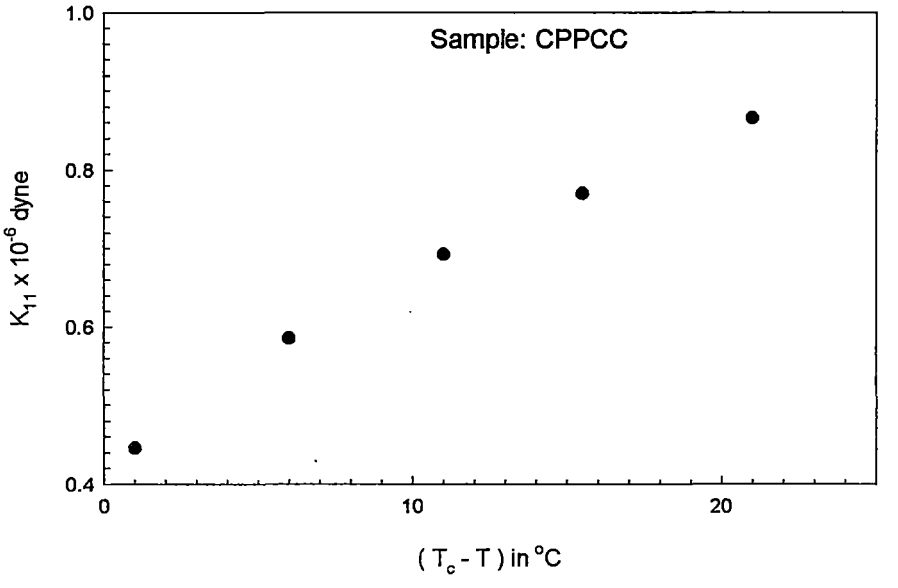

Figure 3.18. Splay elastic constant (K_{11}) as a function of relative temperature (T_c - T).

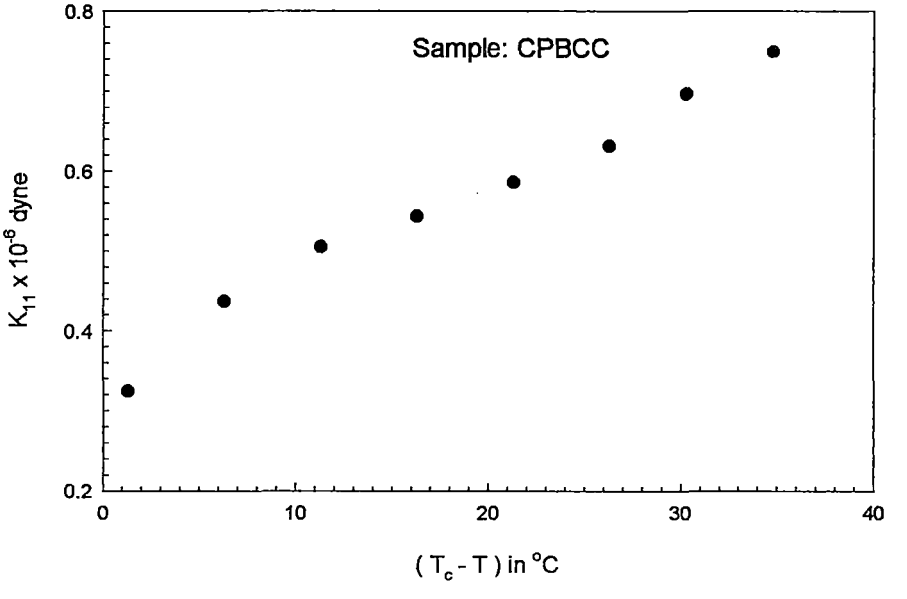

Figure 3.19. Splay elastic constant (K_{11}) as a function of relative temperature (T_c - T).

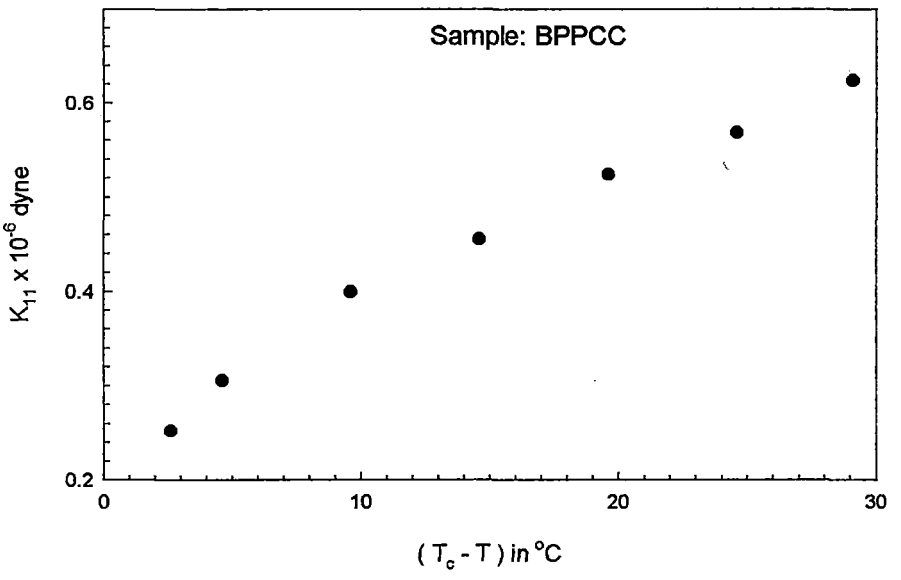

Figure 3.20. Splay elastic constant (K_{11}) as a function of relative temperature (T_c - T).

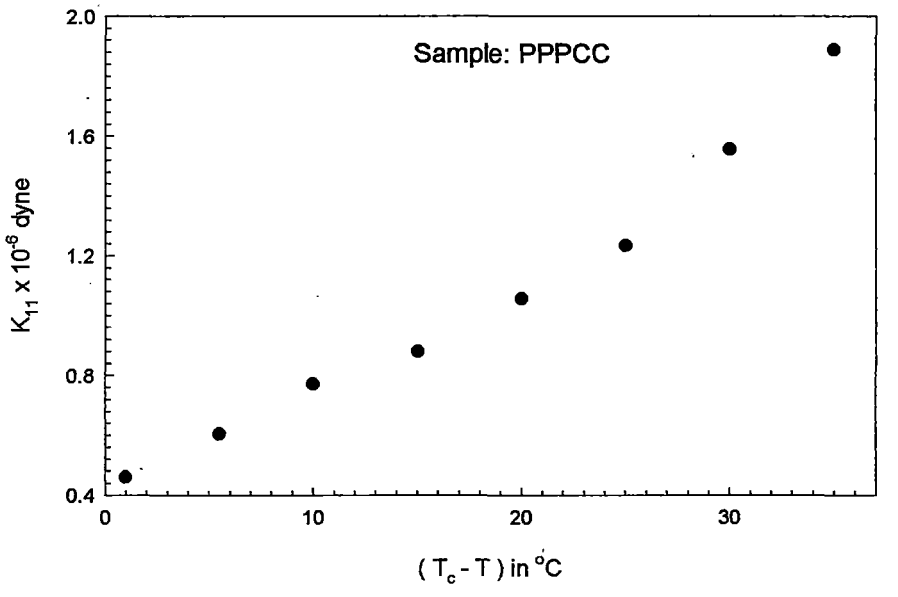

Figure 3.21. Splay elastic constant (K_{11}) as a function of relative temperature (T_c - T).

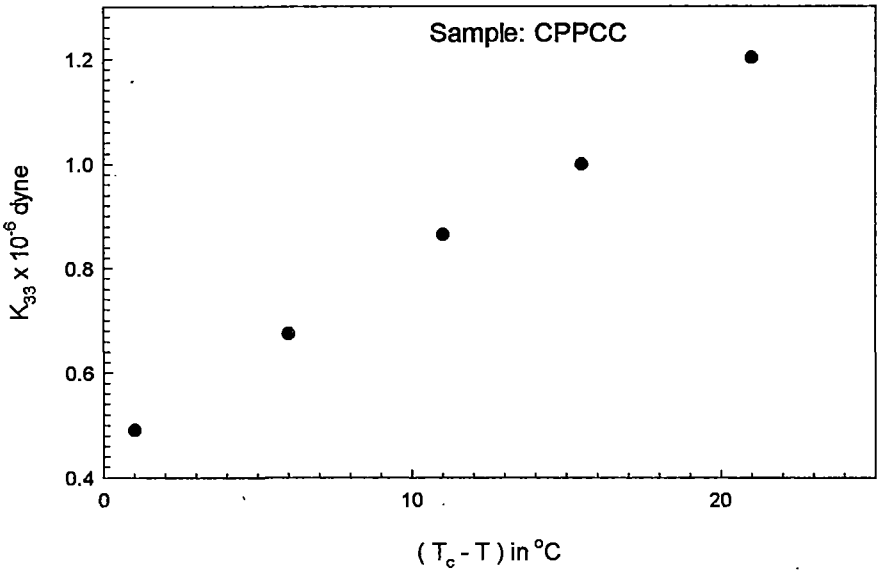

Figure 3.22. Bend elastic constant (K_{33}) as a function of relative temperature (T_c - T).

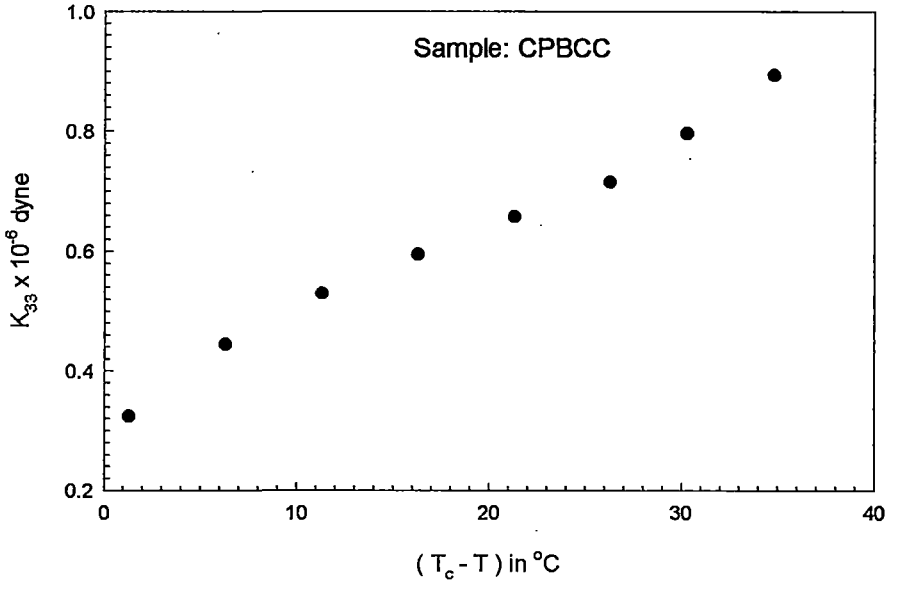

Figure 3.23. Bend elastic constant (K_{33}) as a function of relative temperature (T_c - T).

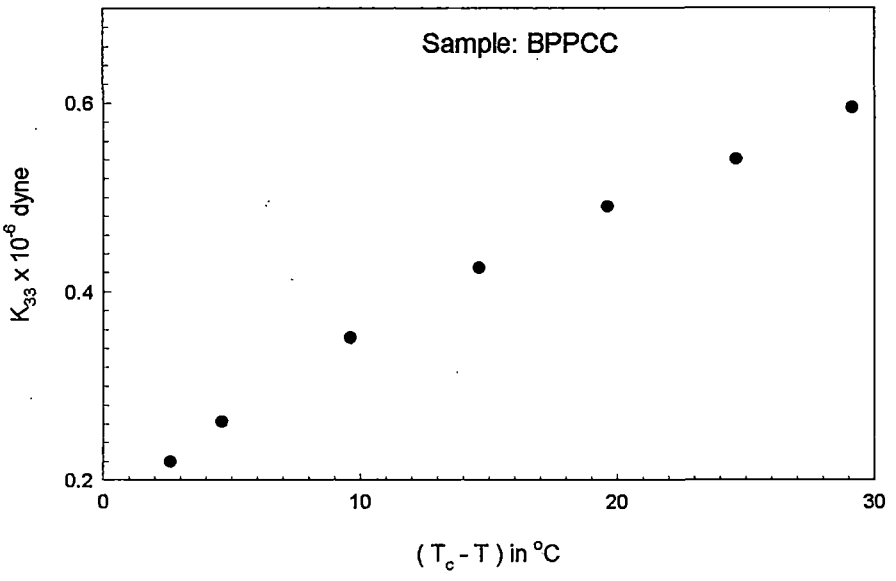

Figure 3.24.Bend elastic constant (K_{33}) as a function of relative temperature (T_c - T).

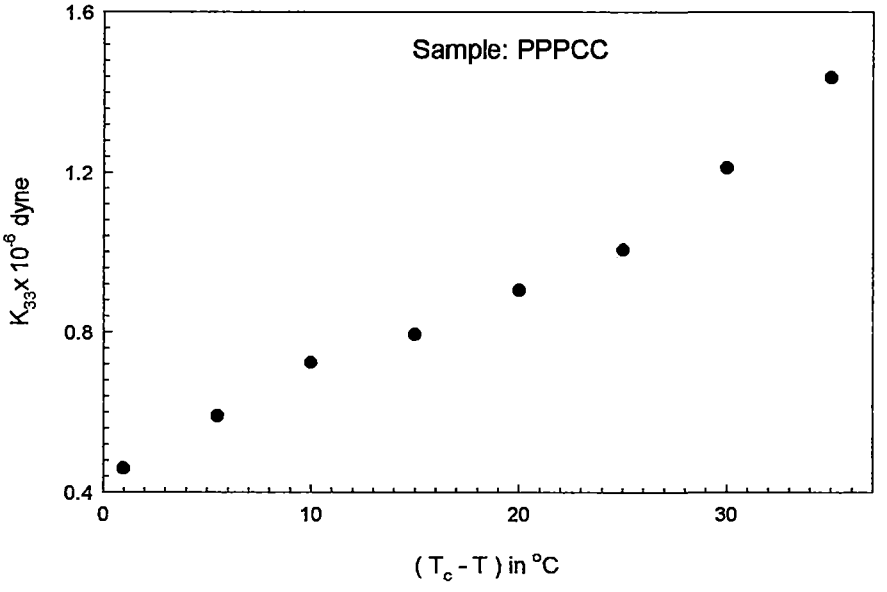

Figure 3.25. Bend elastic constant (K_{33}) as a function of relative temperature (T_c - T).

local ordering in nematogens increases K_{11} and thus lowers the value of K_{33}/K_{11}. The temperature variation of K_{11} in PPPCC indeed shows rapid change (Figure 3.21). Hence the decrease in the K_{33}/K_{11} ratio in PPPCC with decreasing temperature can safely be attributed to the presence of smectic like cybotactic groups.

According to Schadt et al [11], the K_{33}/K_{11} ratio in polar compounds are larger than non-polar compounds having related structure. Thus we find that polar CPPCC and CPBCC have K_{33}/K_{11} greater than 1, whereas in their related non-polar compounds BPPCC and PPPCC the same ratio is less than 1.

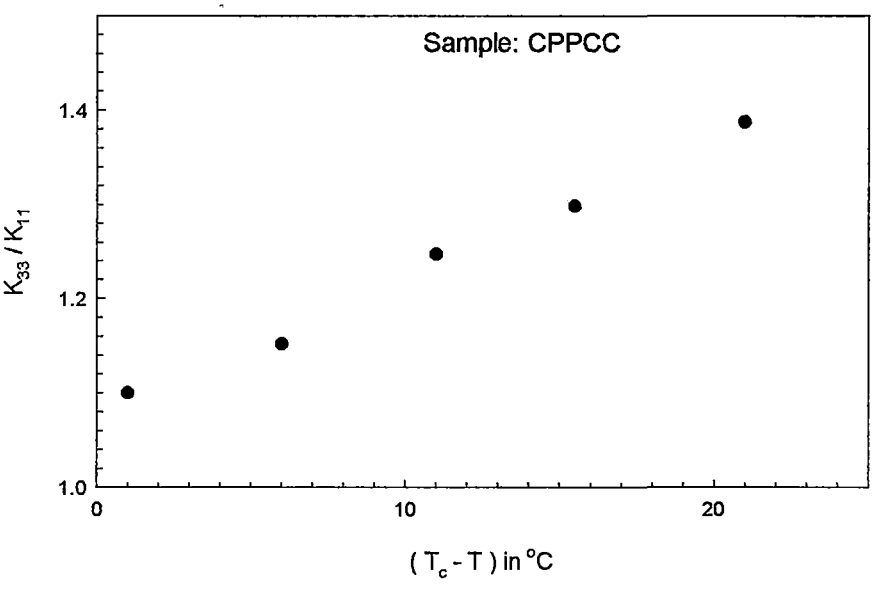

Figure 3.26. Bend to Splay elastic constant ratio (K_{33} / K_{11}) as a function of relative temperature (T_c - T).

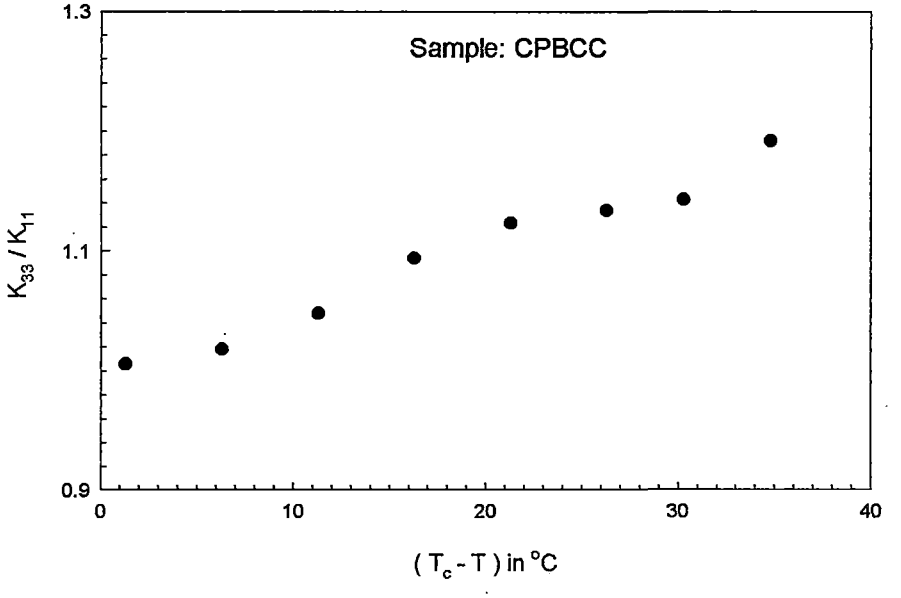

Figure 3.27. Bend to Splay elastic constant ratio (K_{33} / K_{11}) as a function of relative temperature (T_c - T).

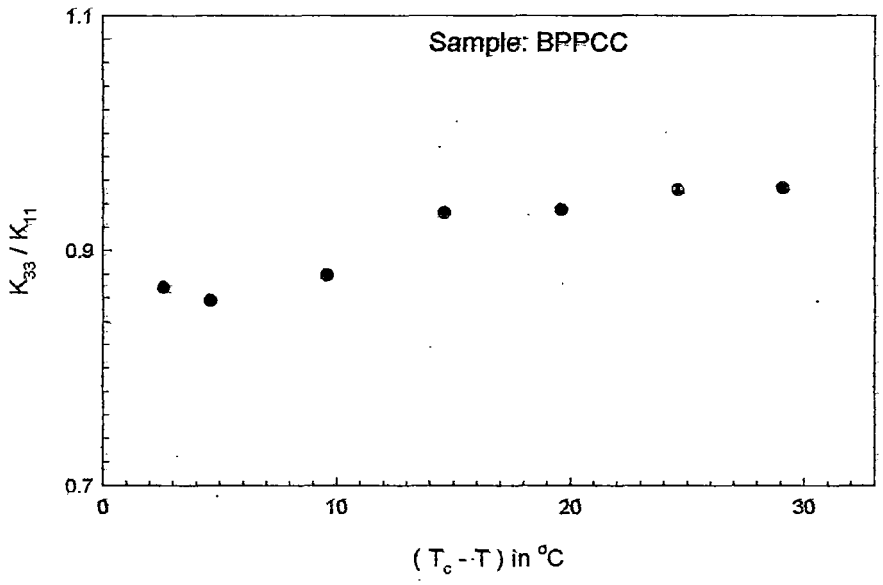

Figure 3.28. Bend to Splay elastic constant ratio (K_{33} / K_{11}) as a function of relative temperature (T_c - T).

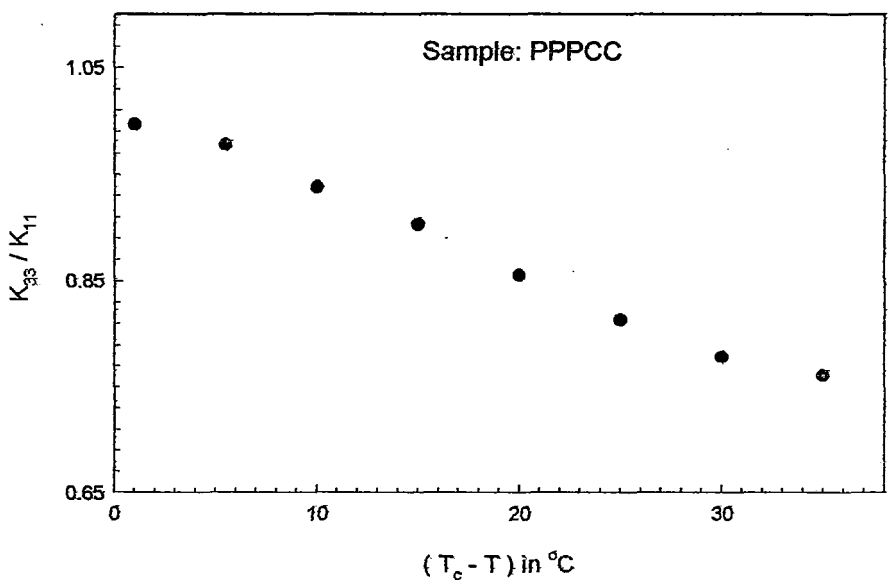

Figure 3.29. Bend to Splay elastic constant ratio (K_{33} / K_{11}) as a function of relative temperature (T_c - T).

Table 3.1a

Density (ρ) and refractive indices (n_o , n_e) at different temperatures of Sample CPPCC.

Temp. in ° C	Density in gm/cc	λ = 6907 Å		λ = 5780 Å	
		n_o	n_e	n_o	n_e
50	1.068	1.464	1.564	1.471	1.571
54	1.066	1.464	1.561	1.471	1.568
58	1.063	1.464	1.557	1.471	1.564
63	1.057	1.464	1.550	1.471	1.557
66	1.053	1.471	1.543	1.479	1.550
69	1.049	1.475	1.536	1.482	1.543
71	1.044	1.493		1.500	

Table 3.1b

Density (ρ) and refractive indices (n_o , n_e) at different temperatures of Sample CPPCC.

Temp. in ° C	Density in gm/cc	λ = 5461 Å		λ = 4358 Å	
		n_o	n_e	n_o	n_e
50	1.068	1.479	1.579	1.489	1.589
54	1.066	1.479	1.575	1.489	1.586
58	1.063	1.479	1.571	1.489	1.582
63	1.057	1.479	1.564	1.489	1.575
66	1.053	1.486	1.557	1.496	1.568
69	1.049	1.489	1.550	1.050	1.561
71	1.044	1.507		1.521	

Table 3.2a

Density (ρ) and refractive indices (n_o , n_e) at different temperatures of Sample CPBCC.

Temp. in ° C	Density in gm/cc	λ = 6907 Å		λ = 5780 Å	
		n_o	n_e	n_o	n_e
30	1.049	1.472	1.592	1.479	1.599
34	1.047	1.472	1.588	1.479	1.595
37	1.045	1.472	1.585	1.479	1.592
43	1.041	1.472	1.577	1.479	1.585
49	1.035	1.472	1.570	1.479	1.577
54	1.032	1.472	1.563	1.479	1.570
59	1.026	1.472	1.556	1.479	1.563
62	1.023	1.474	1.549	1.481	1.556
65	1.019	1.477	1.542	1.484	1.549
67	1.016	1.479	1.535	1.486	1.542
69	1.013	1.493		1.500	

Table 3.2b

Density (ρ) and refractive indices (n_o , n_e) at different temperatures of Sample CPBCC.

Temp. in ° C	Density in gm/cc	λ = 5461 Å		λ = 4358 Å	
		n_o	n_e	n_o	n_e
30	1.049	1.486	1.606	1.496	1.616
34	1.047	1.486	1.602	1.496	1.612
37	1.045	1.486	1.599	1.496	1.609
43	1.041	1.486	1.592	1.496	1.602
49	1.035	1.486	1.585	1.496	1.595
54	1.032	1.486	1.577	1.496	1.588
59	1.026	1.486	1.570	1.496	1.581
62	1.023	1.488	1.563	1.498	1.574
65	1.019	1.491	1.556	1.501	1.567
67	1.016	1.493	1.549	1.504	1.560
69	1.013	1.507		1.518	

Table 3.3a

Density (ρ) and refractive indices (n_o , n_e) at different temperatures of Sample BPPCC.

Temp. in ° C	Density in gm/cc	λ = 6907 Å		λ = 5780 Å	
		n_o	n_e	n_o	n_e
43	0.993	1.452	1.556	1.459	1.563
48	0.989	1.451	1.551	1.458	1.558
51.5	0.985	1.451	1.548	1.457	1.554
55	0.983	1.450	1.544	1.457	1.551
60	0.979	1.449	1.537	1.456	1.544
63	0.976	1.449	1.531	1.456	1.537
68	0.972	1.449	1.524	1.456	1.531
70	0.970	1.456	1.517	1.463	1.524
73	0.964	1.476		1.483	

Table 3.3b

Density (ρ) and refractive indices (n_o , n_e) at different temperatures of Sample BPPCC.

Temp. in ° C	Density in gm/cc	λ = 5461 Å		λ = 4358 Å	
		n_o	n_e	n_o	n_e
43	0.993	1.466	1.570	1.476	1.580
48	0.989	1.465	1.565	1.475	1.575
51.5	0.985	1.464	1.561	1.474	1.571
55	0.983	1.464	1.558	1.474	1.568
60	0.979	1.463	1.551	1.473	1.561
63	0.976	1.463	1.544	1.473	1.554
68	0.972	1.463	1.537	1.473	1.548
70	0.970	1.469	1.531	1.480	1.541
73	0.964	1.490		1.500	

Table 3.4a

Density (ρ) and refractive indices (n_o , n_e) at different temperatures of Sample PPPCC.

Temp. in ° C	Density in gm/cc	λ = 6907 Å		λ = 5780 Å	
		n_o	n_e	n_o	n_e
33	0.981	1.469	1.560	1.476	1.567
36	0.977	1.469	1.559	1.476	1.566
38.4	0.976	1.469	1.559	1.476	1.565
42	0.973	1.469	1.558	1.476	1.565
46	0.970	1.468	1.555	1.475	1.562
49	0.967	1.467	1.553	1.474	1.560
52	0.965	1.467	1.551	1.473	1.558
56	0.962	1.466	1.548	1.472	1.554
60	0.958	1.464	1.544	1.471	1.551
64	0.955	1.463	1.540	1.470	1.547
67	0.952	1.463	1.537	1.469	1.544
71	0.948	1.464	1.531	1.471	1.537
74	0.944	1.466	1.524	1.473	1.531
76	0.941	1.483		1.490	

Table 3.4b

Density (ρ) and refractive indices (n_o , n_e) at different temperatures of Sample PPPCC.

Temp. in ° C	Density in gm/cc	λ = 5461 Å		λ = 4358 Å	
		n_o	n_e	n_o	n_e
33	0.981	1.483	1.573	1.493	1.584
36	0.977	1.483	1.573	1.493	1.583
38.4	0.976	1.483	1.572	1.493	1.582
42	0.973	1.483	1.571	1.493	1.582
46	0.970	1.482	1.569	1.492	1.579
49	0.967	1.481	1.567	1.491	1.577
52	0.965	1.480	1.565	1.490	1.575
56	0.962	1.479	1.561	1.489	1.571
60	0.958	1.478	1.558	1.488	1.568
64	0.955	1.477	1.554	1.487	1.564
67	0.952	1.476	1.551	1.486	1.561
71	0.948	1.478	1.544	1.488	1.554
74	0.944	1.480	1.537	1.490	1.548
76	0.941	1.497		1.507	

Table 3.5

Polarisability (α_o, α_e) at different temperatures of sample CPPCC by Vuks method.

Temp. in ° C	$\lambda = 6907$ Å		$\lambda = 5780$ Å		$\lambda = 5461$ Å		$\lambda = 4358$ Å	
	α_o	α_e	α_o	α_e	α_o	α_e	α_o	α_e
50	27.11	34.28	27.46	34.64	27.82	35.00	28.35	35.51
54	27.19	34.11	27.54	34.48	27.90	34.83	28.43	35.36
58	27.30	33.99	27.65	34.34	28.01	34.70	28.55	35.23
63	27.50	33.70	27.85	34.07	28.22	34.42	28.75	34.96
66	28.04	33.23	28.41	33.59	28.77	33.95	29.31	34.48
69	28.40	32.82	28.77	33.19	29.13	33.55	29.88	34.03

α_o & α_e are in 10^{-24} cm^3 unit.

Table 3.6

Polarisability (α_o, α_e) at different temperatures of sample CPBCC by Vuks method.

Temp. in °C	$\lambda = 6907$ Å		$\lambda = 5780$ Å		$\lambda = 5461$ Å		$\lambda = 4358$ Å	
	α_o	α_e	α_o	α_e	α_o	α_e	α_o	α_e
30	29.29	38.50	29.66	38.88	30.04	39.23	30.59	39.79
34	29.38	38.29	29.75	38.66	30.13	39.04	30.68	39.59
37	29.46	38.16	29.83	38.53	30.21	38.90	30.76	39.45
43	29.63	37.81	30.00	38.19	30.38	38.56	30.94	39.12
49	29.82	37.50	30.20	37.87	30.58	38.25	31.15	38.81
54	29.99	37.13	30.37	37.51	30.75	37.89	31.32	38.45
59	30.21	36.84	30.60	37.22	30.98	37.61	31.55	3 8.17
62	30.46	36.41	30.85	36.79	31.24	37.18	31.81	37.74
65	30.80	35.97	31.18	36.36	31.57	36.74	32.14	37.32
67	31.09	35.54	31.48	35.92	31.86	36.31	32.45	36.89

α_o & α_e are in 10^{-24} cm^3 unit.

Table 3.7

Polarisability (α_o, α_e) at different temperatures of sample BPPCC by Vuks method.

Temp. in ° C	$\lambda = 6907$ Å		$\lambda = 5780$ Å		$\lambda = 5461$ Å		$\lambda = 4358$ Å	
	α_o	α_e	α_o	α_e	α_o	α_e	α_o	α_e
43	33.43	42.83	33.87	43.27	34.29	43.69	34.94	44.34
48	33.52	42.60	33.97	43.02	34.39	43.46	35.04	44.09
51.5	33.62	42.47	34.06	42.91	34.49	43.34	35.15	43.98
55	33.69	42.31	34.13	42.75	34.56	43.18	35.22	43.83
60	33.80	41.92	34.25	42.36	34.69	42.81	35.35	43.46
63	33.97	41.48	34.42	41.93	34.86	42.37	35.53	43.02
68	34.18	41.09	34.62	41.53	35.07	41.98	35.74	42.64
70	34.80	40.47	35.25	40.91	35.70	41.35	36.36	42.01

α_o & α_e are in 10^{-24} cm^3 unit.

Table 3.8

Polarisability (α_o, α_e) at different temperatures of sample PPPCC by Vuks method.

Temp. in ° C	$\lambda = 6907$ Å		$\lambda = 5780$ Å		$\lambda = 5461$ Å		$\lambda = 4358$ Å	
	α_o	α_e	α_o	α_e	α_o	α_e	α_o	α_e
33	39.68	4906	4017	49.54	40.66	50.04	41.39	50.76
36	39.82	49.17	40.32	49.65	40.81	50.15	41.54	50.87
38.4	39.89	49.19	40.39	49.68	40.88	50.17	41.61	50.91
42	40.00	49.23	40.49	49.73	40.99	50.22	41.72	50.96
46	40.07	49.17	40.57	49.67	41.07	50.16	41.81	50.90
49	40.14	49.14	40.64	49.63	41.14	50.13	41.88	50.87
52	40.19	49.08	40.69	49.57	41.19	50.07	41.93	50.81
56	40.24	48.91	40.75	49.41	41.25	49.91	42.00	50.65
60	40.34	48.79	40.85	49.31	41.35	49.80	42.10	50.56
64	40.42	48.61	40.93	49.11	41.44	49.62	42.19	50.37
67	40.53	48.53	41.05	49.03	41.55	49.55	42.31	50.30
71	40.87	48.00	41.39	48.51	41.90	49.02	42.66	49.78
74	41.28	47.49	41.80	48.00	42.31	48.53	43.08	49.29

α_o & α_e are in 10^{-24} cm^3 unit.

Table 3.9

Polarisability (α_o, α_e) at different temperatures of sample CPPCC by Neugebauer method.

Temp. in ° C	$\lambda = 6907$ Å		$\lambda = 5780$ Å		$\lambda = 5461$ Å		$\lambda = 4358$ Å	
	α_o	α_e	α_o	α_e	α_o	α_e	α_o	α_e
50	27.50	33.50	27.85	33.85	28.22	34.19	28.76	34.70
54	27.57	33.36	27.92	33.72	28.29	34.06	28.83	34.57
58	27.66	33.26	28.02	33.61	28.38	33.96	28.92	34.47
63	27.83	33.03	28.19	33.39	28.56	33.74	29.10	34.26
66	28.32	32.67	28.69	33.02	29.05	33.38	29.60	33.90
69	28.64	32.35	29.01	32.71	29.38	33.06	30.11	33.57

α_o & α_e are in 10^{-24} cm^3 unit.

Table 3.10

Polarisability (α_o, α_e) at different temperatures of sample CPBCC by Neugebauer method.

Temp. in °C	$\lambda = 6907$ Å		$\lambda = 5780$ Å		$\lambda = 5461$ Å		$\lambda = 4358$ Å	
	α_o	α_e	α_o	α_e	α_o	α_e	α_o	α_e
30	29.80	37.47	30.18	37.83	30.57	38.18	31.13	38.72
34	29.88	37.30	30.25	37.66	30.64	38.02	31.20	38.55
37	29.94	37.19	30.32	37.55	30.70	37.91	31.27	38.44
43	30.08	36.90	30.46	37.27	30.85	37.63	31.41	38.17
49	30.25	36.65	30.63	37.02	31.02	37.39	31.59	37.93
54	30.38	36.35	30.76	36.72	31.15	37.09	31.72	37.63
59	30.57	36.11	30.96	36.49	31.35	36.87	31.93	37.42
62	30.79	35.76	31.18	36.14	31.57	36.52	32.14	37.07
65	31.08	35.41	31.47	35.79	31.85	36.17	32.44	36.74
67	31.33	35.06	31.72	35.43	32.11	35.82	32.70	36.39

α_o & α_e are in 10^{-24} cm^3 unit.

Table 3.11

Polarisability (α_o, α_e) at different temperatures of sample BPPCC by Neugebauer method.

Temp. in ^{o}C	$\lambda = 6907$ Å		$\lambda = 5780$ Å		$\lambda = 5461$ Å		$\lambda = 4358$ Å	
	α_o	α_e	α_o	α_e	α_o	α_e	α_o	α_e
43	33.93	41.83	34.37	42.25	34.81	42.66	35.46	43.29
48	34.01	41.63	34.45	42.05	34.89	42.47	35.54	43.09
51.5	34.09	41.53	34.53	41.96	34.97	42.39	35.63	43.01
55	34.14	41.40	34.59	41.83	35.03	42.25	35.70	42.88
60	34.23	41.07	34.68	41.50	35.12	41.94	35.79	42.57
63	34.36	40.70	34.81	41.14	35.26	41.57	35.93	42.21
68	34.53	40.37	34.98	40.81	35.43	41.24	36.11	41.90
70	35.10	39.88	35.55	40.32	36.00	40.75	36.67	41.40

α_o & α_e are in 10^{-24} cm^3 unit.

Table 3.12

Polarisability (α_o, α_e) at different temperatures of sample PPPCC by Neugebauer method.

Temp. in °C	$\lambda = 6907$ Å		$\lambda = 5780$ Å		$\lambda = 5461$ Å		$\lambda = 4358$ Å	
	α_o	α_e	α_o	α_e	α_o	α_e	α_o	α_e
33	40.19	48.04	40.69	48.51	41.18	48.99	41.92	49.70
36	40.33	48.15	40.83	48.62	41.33	49.10	42.07	49.81
38.4	40.40	48.18	40.90	48.66	41.40	49.13	42.14	49.85
42	40.50	48.23	41.00	48.71	41.50	49.19	42.25	49.91
46	40.57	48.19	41.07	48.67	41.57	49.15	42.32	49.87
49	40.63	48.17	41.13	48.65	41.64	49.14	42.39	49.86
52	40.67	48.12	41.17	48.60	41.68	49.09	42.43	49.81
56	40.71	47.98	41.22	48.47	41.73	48.96	42.48	49.68
60	40.79	47.89	41.30	48.39	41.82	48.87	42.58	49.61
64	40.86	47.74	41.37	48.23	41.88	48.73	42.65	49.46
67	40.96	47.68	41.47	48.17	41.99	48.68	42.76	49.42
71	41.25	47.25	41.77	47.75	42.28	48.25	43.05	49.00
74	41.61	46.83	42.13	47.34	42.65	47.85	43.43	48.60

α_o & α_e are in 10^{-24} cm^3 unit.

Table 3.13

Order parameter $< P_2 >$ of sample CPPCC at different temperatures by Vuks method.

$(\alpha_{\parallel} - \alpha_{\perp}) = 12.02$ in 10^{-24} cm^3 unit.

Temp. in ^{o}C	$\lambda = 6907$ Å	$\lambda = 5780$ Å	$\lambda = 5461$ Å	$\lambda = 4358$ Å	Average
	$< P_2 >$	$< P_2 >$	$< P_2 >$	$< P_2 >$	$< P_2 >$
50	0.596	0.591	0.597	0.596	.595
54	0.578	0.576	0.576	0.576	0.576
58	0.557	0.557	0.557	0.556	0.557
63	0.516	0.517	0.516	0.517	0.516
66	0.432	0.431	0.431	0.430	0.431
69	0.368	0.367	0.367	0.345	0.362

Table 3.14

Order parameter $< P_2 >$ of sample CPBCC at different temperatures by Vuks method.

$(\alpha_{\parallel} - \alpha_{\perp}) = 13.22$ in 10^{-24} cm^3 unit.

Temp. in ° C	$\lambda = 6907$ Å	$\lambda = 5780$ Å	$\lambda = 5461$ Å	$\lambda = 4358$ Å	Average
	$< P_2 >$	$< P_2 >$	$< P_2 >$	$< P_2 >$	$< P_2 >$
30	0.697	0.697	0.695	0.696	0.696
34	0.675	0.674	0.674	0.673	0.674
37	0.658	0.658	0.657	0.657	0.657
43	0.619	0.619	0.618	0.619	0.619
49	0.580	0.580	0.580	0.579	0.580
54	0.540	0.541	0.540	0.539	0.540
59	0.501	0.501	0.500	0.501	0.501
62	0.449	0.449	0.450	0.449	0.449
65	0.391	0.391	0.391	0.392	0.391
67	0.337	0.336	0.337	0.336	0.337

Table3.15

Order parameter $< P_2 >$ of sample BPPCC at different temperatures by Vuks method.

$(\alpha_{\parallel} - \alpha_{\perp}) = 14.80$ in 10^{-24} cm^3 unit.

Temp. in ° C	$\lambda = 6907$ Å	$\lambda = 5780$ Å	$\lambda = 5461$ Å	$\lambda = 4358$ Å	Average
	$< P_2 >$	$< P_2 >$	$< P_2 >$	$< P_2 >$	$< P_2 >$
43	0.635	0.635	0.635	0.635	0.635
48	0.613	0.611	0.613	0.611	0.612
51.5	0.598	0.598	0.598	0.597	0.598
55	0.582	0.583	0.582	0.581	0.582
60	0.549	0.547	0.549	0.548	0.548
63	0.507	0.507	0.507	0.507	0.507
68	0.467	0.467	0.467	0.467	0.467
70	0.383	0.380	0.382	0.382	0.382

Table 3.16

Order parameter $< P_2 >$ of sample PPPCC at different temperatures by Vuks method.

$(\alpha_{\parallel} - \alpha_{\perp}) = 14.50$ in 10^{-24} cm^3 unit.

Temp. in ° C	$\lambda = 6907$ Å	$\lambda = 5780$ Å	$\lambda = 5461$ Å	$\lambda = 4358$ Å	Average
	$< P_2 >$	$< P_2 >$	$< P_2 >$	$< P_2 >$	$< P_2 >$
33	0.647	0.646	0.647	0.646	0.646
36	0.644	0.643	0.644	0.643	0.643
38.4	0.641	0.641	0.641	0.641	0.641
42	0.637	0.636	0.636	0.637	0.636
46	0.628	0.627	0.627	0.627	0.627
49	0.621	0.620	0.620	0.620	0.620
52	0.613	0.612	0.613	0.612	0.612
56	0.597	0.597	0.597	0.597	0.597
60	0.583	0.583	0.583	0.583	0.583
64	0.565	0.564	0.565	0.564	0.564
67	0.552	0.550	0.551	0.551	0.551
71	0.492	0.492	0.492	0.491	0.492
74	0.428	0.428	0.429	0.428	0.428

Table3.17

Order parameter $< P_2 >$ of sample CPPCC at different temperatures by Neugebauer method.

$(\alpha_{\parallel} - \alpha_{\perp}) = 10.08$ in 10^{-24} cm^3 unit.

Temp. in ° C	$\lambda = 6907$ Å	$\lambda = 5780$ Å	$\lambda = 5461$ Å	$\lambda = 4358$ Å	Average
	$< P_2 >$	$< P_2 >$	$< P_2 >$	$< P_2 >$	$< P_2 >$
50	0.595	0.594	0.593	0.590	0.593
54	0.575	0.574	0.573	0.570	0.573
58	0.556	0.555	0.554	0.551	0.554
63	0.516	0.516	0.514	0.512	0.514
66	0.431	0.430	0.430	0.427	0.429
69	0.367	0.366	0.365	0.342	0.360

Table 3.18

Order parameter $< P_2 >$ of sample CPBCC at different temperatures by Neugebauer method.

$(\alpha_{\parallel} - \alpha_{\perp}) = 11.04$ in 10^{-24} cm^3 unit.

Temp. in ° C	$\lambda = 6907$ Å	$\lambda = 5780$ Å	$\lambda = 5461$ Å	$\lambda = 4358$ Å	Average
	$< P_2 >$	$< P_2 >$	$< P_2 >$	$< P_2 >$	$< P_2 >$
30	0.695	0.693	0.689	0.687	0.691
34	0.673	0.670	0.668	0.666	0.669
37	0.657	0.655	0.653	0.650	0.654
43	0.618	0.617	0.614	0.612	0.615
49	0.580	0.579	0.577	0.574	0.577
54	0.541	0.540	0.537	0.535	0.538
59	0.502	0.501	0.500	0.497	0.500
62	0.451	0.449	0.448	0.447	0.449
65	0.392	0.391	0.390	0.389	0.391
67	0.338	0.336	0.336	0.334	0.336

Table 3.19

Order parameter $< P_2 >$ of sample BPPCC at different temperatures by Neugebauer method.

$(\alpha_{\parallel} - \alpha_{\perp}) = 12.50$ in 10^{-24} cm^3 unit.

Temp. in $^{\circ}$ C	$\lambda = 6907$ Å	$\lambda = 5780$ Å	$\lambda = 5461$ Å	$\lambda = 4358$ Å	Average
	$< P_2 >$	$< P_2 >$	$< P_2 >$	$< P_2 >$	$< P_2 >$
43	0.632	0.630	0.629	0.626	0.629
48	0.610	0.607	0.607	0.604	0.607
51.5	0.595	0.594	0.593	0.590	0.593
55	0.581	0.580	0.578	0.574	0.578
60	0.547	0.546	0.545	0.542	0.545
63	0.507	0.506	0.505	0.502	0.505
68	0.467	0.466	0.465	0.462	0.465
70	0.383	0.382	0.380	0.378	0.381

Table 3.20

Order parameter $< P_2 >$ of sample PPPCC at different temperatures by Neugebauer method.

$(\alpha_{\parallel} - \alpha_{\perp}) = 12.14$ in 10^{-24} cm^3 unit.

Temp. in ^{o}C	$\lambda = 6907$ Å	$\lambda = 5780$ Å	$\lambda = 5461$ Å	$\lambda = 4358$ Å	Average
	$< P_2 >$	$< P_2 >$	$< P_2 >$	$< P_2 >$	$< P_2 >$
33	0.647	0.644	0.643	0.641	0.644
36	0.644	0.642	0.641	0.638	0.641
38.4	0.641	0.639	0.637	0.635	0.638
42	0.637	0.635	0.633	0.631	0.634
46	0.628	0.626	0.624	0.622	0.625
49	0.621	0.619	0.618	0.615	0.618
52	0.614	0.612	0.610	0.607	0.611
56	0.599	0.597	0.595	0.593	0.596
60	0.585	0.584	0.581	0.580	0.583
64	0.567	0.564	0.564	0.562	0.564
67	0.553	0.552	0.551	0.549	0.551
71	0.494	0.493	0.492	0.489	0.492
74	0.431	0.429	0.429	0.427	0.429

Table 3.21

Mean experimental intensity values I (ψ) , in arbitrary units , of CPPCC after background correction.

ψ	I (ψ) values at different temperatures in ° C				
(degree)	50	55	60	65	69
0	4.35	9.45	9.10	6.75	7.40
5	4.10	9.00	8.90	6.65	7.20
10	3.50	8.25	8.30	6.45	7.05
15	2.95	7.25	7.35	6.05	6.50
20	2.40	5.95	6.15	5.45	5.73
25	1.73	4.85	5.25	4.35	4.90
30	1.18	3.80	4.07	3.50	4.05
35	0.85	2.95	3.28	2.80	3.35
40	0.60	2.25	2.80	2.25	2.65
45	0.58	1.75	2.10	1.80	2.35
50	0.48	1.30	1.65	1.35	1.93
55	0.40	1.05	1.28	1.10	1.55
60	0.35	0.85	1.05	0.90	1.35
65	0.33	0.70	0.85	0.75	1.20
70	0.33	0.55	0.75	0.60	1.00
75	0.30	0.45	0.60	0.53	0.70
80	0.29	0.40	0.45	0.43	0.50
85	0.27	0.20	0.20	0.28	0.30
90	0.00	0.00	0.00	0.00	0.00

Table 3.22

Normalised distribution function values f (β) of CPPCC

β (degree)	f (β) values at different temperatures in ° C				
	50	55	60	65	69
0	9.11	6.96	5.71	4.12	4.11
5	8.76	6.84	5.80	4.30	4.22
10	7.72	6.32	5.71	4.61	4.35
15	6.15	5.27	4.95	4.54	4.10
20	4.48	4.02	3.76	3.90	3.44
25	3.07	3.02	2.78	3.08	2.75
30	2.05	2.35	2.23	2.43	2.25
35	1.34	1.84	1.89	1.93	1.88
40	0.86	1.34	1.50	1.46	1.47
45	0.57	0.90	1.03	1.03	1.06
50	0.42	0.59	0.67	0.71	0.76
55	0.35	0.43	0.49	0.53	0.62
60	0.34	0.37	0.43	0.45	0.59
65	0.33	0.32	0.40	0.39	0.56
70	0.31	0.25	0.32	0.31	0.44
75	0.25	0.16	0.19	0.21	0.27
80	0.18	0.09	0.10	0.12	0.13
85	0.14	0.06	0.06	0.08	0.07
90	0.13	0.05	0.04	0.07	0.06

Table 3.23

Mean experimental intensity values I (ψ) , in arbitrary units, of CPBCC after background correction.

ψ	I (ψ) values at different temperatures in degrees								
(deg.)	30.5	35	40	45	50	55	60	65	67.5
0	9.55	9.58	11.80	8.58	10.00	9.90	11.05	7.45	6.35
5	9.20	9.08	11.30	8.43	9.40	9.60	10.85	7.30	6.10
10	8.43	8.27	10.50	7.85	8.45	8.95	10.00	6.98	5.65
15	7.33	7.15	9.30	6.88	7.55	8.20	8.80	6.43	4.90
20	5.98	6.10	7.90	5.53	6.25	6.85	7.75	5.55	4.25
25	4.53	4.40	5.90	4.48	4.95	5.55	6.70	4.58	3.70
30	3.35	3.25	4.15	3.38	4.00	4.20	6.50	3.61	3.15
35	2.35	2.38	3.05	2.48	3.05	3.20	3.80	2.95	2.65
40	1.63	1.73	2.25	1.83	2.35	2.35	2.80	2.33	2.15
45	1.18	1.18	1.65	1.30	1.70	2.00	2.40	1.93	2.00
50	0.75	0.83	1.20	0.98	1.25	1.70	1.95	1.60	1.70
55	0.50	0.63	0.90	0.74	1.00	1.40	1.60	1.30	1.25
60	0.35	0.48	0.63	0.56	0.80	1.20	1.30	1.13	1.05
65	0.24	0.35	0.50	0.43	0.58	0.90	1.10	0.10	0.80
70	0.18	0.25	0.33	0.30	0.40	0.45	0.90	0.83	0.65
75	0.13	0.16	0.23	0.23	0.30	0.35	0.60	0.65	0.40
80	0.10	0.09	0.13	0.15	0.15	0.25	0.30	0.40	0.20
85	0.07	0.06	0.10	0.10	0.10	0.15	0.10	0.15	0.10
90	0.00	0.00	0.00	0.00	0.00	0.00	0.00	0.00	0.00

Table 3.24

Normalised distribution function values f (β) of CPBCC.

β	f (β) values at different temperatures in degrees								
(deg.)	30.5	35	40	45	50	55	60	65	67.5
0	7.85	7.77	6.92	6.87	7.37	6.00	6.19	4.70	5.70
5	7.76	7.73	6.94	6.89	7.20	5.90	5.86	4.84	5.60
10	7.31	7.34	6.76	6.68	6.55	5.57	5.08	5.01	5.16
15	6.26	6.22	6.04	5.80	5.36	5.02	4.23	4.73	4.24
20	4.85	4.70	4.84	4.49	4.05	4.27	3.61	3.91	3.20
25	3.55	3.40	3.57	3.31	3.07	3.39	3.21	2.99	2.46
30	2.56	2.50	2.53	2.48	2.43	2.48	2.80	2.29	2.06
35	1.81	1.81	1.74	1.86	1.93	1.70	2.16	1.81	1.82
40	1.21	1.21	1.16	1.30	1.39	1.14	1.41	1.42	1.52
45	0.75	0.73	0.75	0.83	0.90	0.81	0.85	1.06	1.15
50	0.45	0.45	0.50	0.52	0.58	0.65	0.56	0.77	0.85
55	0.29	0.31	0.37	0.37	0.42	0.57	0.46	0.58	0.70
60	0.20	0.25	0.28	0.30	0.36	0.51	0.46	0.47	0.65
65	0.14	0.21	0.21	0.24	0.30	0.39	0.44	0.37	0.57
70	0.09	0.14	0.13	0.17	0.21	0.24	0.32	0.27	0.39
75	0.05	0.07	0.07	0.09	0.10	0.12	0.16	0.18	0.19
80	0.03	0.03	0.03	0.04	0.05	0.06	0.07	0.11	0.08
85	0.02	0.01	0.02	0.03	0.02	0.03	0.03	0.07	0.04
90	0.01	0.01	0.02	0.02	0.02	0.03	0.02	0.06	0.03

Table 3.25

Mean experimental intensity values I (ψ) , in arbitrary units , of BPPCC after background correction.

ψ (deg.)	I (ψ) values at different temperatures in degrees						
	45	50	55	60	65	70	72
0	9.75	7.90	10.70	8.90	3.35	7.15	2.15
5	9.30	7.75	10.45	8.85	3.25	7.10	2.10
10	9.05	7.25	9.80	8.45	3.00	6.95	2.00
15	7.85	6.15	8.75	7.65	2.57	6.35	1.86
20	5.75	4.92	7.80	6.80	2.22	5.45	1.75
25	4.40	3.80	6.30	5.65	1.92	4.60	1.58
30	2.95	2.76	4.60	4.20	1.47	3.90	1.35
35	2.10	1.90	3.35	3.10	1.03	3.30	1.10
40	1.60	1.50	2.45	2.40	0.82	2.65	0.83
45	1.20	1.20	1.85	1.90	0.63	2.15	0.65
50	1.10	1.00	1.45	1.50	0.53	1.70	0.55
55	0.80	0.85	1.05	1.20	0.48	1.35	0.50
60	0.65	0.65	0.85	0.95	0.44	1.10	0.40
65	0.50	0.55	0.70	0.75	0.43	0.90	0.35
70	0.45	0.32	0.55	0.65	0.19	0.75	0.30
75	0.40	0.25	0.45	0.55	0.37	0.60	0.20
80	0.35	0.20	0.40	0.50	0.30	0.50	0.10
85	0.30	0.10	0.25	0.30	0.23	0.20	0.05
90	0.00	0.00	0.00	0.00	0.00	0.00	0.00

Table 3.26

Normalised distribution function values f (β) of BPPCC.

β (deg.)	f (β) values at different temperatures in degrees						
	45	50	55	60	65	70	72
0	7.14	7.31	5.84	4.95	6.47	4.28	4.21
5	7.32	7.25	5.81	5.02	6.19	4.45	4.08
10	7.47	6.90	5.64	5.08	5.51	4.66	3.76
15	6.76	6.02	5.17	4.84	4.66	4.35	3.43
20	5.10	4.70	4.42	4.22	3.87	3.51	3.16
25	3.35	3.36	3.55	3.40	3.15	2.71	2.93
30	2.12	2.29	2.69	2.59	2.45	2.23	2.60
35	1.38	1.52	1.90	1.87	1.76	1.95	2.12
40	0.94	1.01	1.26	1.29	1.17	1.60	1.56
45	0.66	0.70	0.81	0.87	0.76	1.15	1.06
50	0.47	0.53	0.54	0.61	0.54	0.78	0.75
55	0.36	0.45	0.40	0.47	0.45	0.58	0.62
60	0.30	0.40	0.33	0.40	0.42	0.50	0.58
65	0.25	0.32	0.27	0.34	0.41	0.46	0.10
70	0.19	0.22	0.20	0.26	0.36	0.37	0.52
75	0.14	0.12	0.13	0.18	0.27	0.22	0.42
80	0.09	0.06	0.08	0.11	0.19	0.11	0.28
85	0.07	0.04	0.06	0.08	0.14	0.07	0.15
90	0.06	0.03	0.05	0.07	0.12	0.05	0.05

Table 3.27

Mean experimental intensity values I (ψ) , in arbitrary units, of PPPCC after background correction.

ψ	I (ψ) values at different temperatures in degrees							
(deg.)	40	45	50	55	60	65	70	74
0	15.60	14.90	14.50	16.20	0.65	1.20	1.50	8.20
5	13.40	14.70	14.10	15.80	0.65	1.20	1.50	7.60
10	11.90	13.60	13.00	14.00	0.50	1.15	1.35	7.85
15	9.30	11.20	11.55	11.80	0.40	1.10	1.25	7.40
20	6.30	8.80	9.90	10.10	0.25	0.95	1.10	6.55
25	4.45	6.50	7.95	8.20	0.20	0.80	1.00	5.50
30	3.50	5.00	6.05	6.30	0.20	0.65	0.85	4.40
35	2.60	3.80	4.60	4.50	0.15	0.50	0.70	3.75
40	2.00	2.70	3.10	3.30	0.15	0.35	0.55	3.00
45	1.50	2.20	2.25	2.70	0.10	0.25	0.35	2.50
50	1.20	1.80	1.70	2.20	0.10	0.20	0.30	2.25
55	1.00	1.35	1.20	1.80	0.10	0.20	0.25	1.80
60	0.90	0.90	0.90	1.40	0.05	0.15	0.18	1.35
65	0.75	0.70	0.70	1.10	0.05	0.15	0.16	1.15
70	0.65	0.50	0.50	0.90	0.05	0.10	0.13	0.80
75	0.60	0.40	0.38	0.70	0.03	0.10	0.10	0.60
80	0.40	0.20	0.25	0.50	0.03	0.08	0.10	0.30
85	0.20	0.10	0.13	0.30	0.00	0.05	0.05	0.20
90	0.00	0.00	0.00	0.00	0.00	0.00	0.00	0.00

Table 3.28

Normalised distribution function values f (β) of PPPCC.

β	f (β) values at different temperatures in degrees							
(deg.)	40	45	50	55	60	65	70	74
0	12.14	7.81	6.63	7.81	11.47	4.42	5.35	3.65
5	11.72	7.96	6.57	7.44	11.14	4.49	5.18	3.83
10	10.03	7.83	6.24	6.47	9.37	4.58	4.68	4.17
15	7.06	6.55	5.44	5.27	6.07	4.41	3.96	4.18
20	4.24	4.57	4.37	4.14	3.23	3.94	3.28	3.65
25	2.54	2.99	3.41	3.22	1.84	3.34	2.84	2.92
30	1.74	2.11	2.67	2.45	1.41	2.72	2.58	2.32
35	1.33	1.62	2.01	1.76	1.37	2.06	2.26	1.86
40	0.98	1.20	1.37	1.18	1.30	1.39	1.72	1.45
45	0.64	0.81	0.84	0.78	1.00	0.87	1.12	1.08
50	0.41	0.53	0.52	0.55	0.66	0.57	0.70	0.82
55	0.30	0.39	0.36	0.44	0.50	0.44	0.50	0.69
60	0.28	0.33	0.29	0.39	0.49	0.41	0.41	0.62
65	0.28	0.28	0.24	0.33	0.51	0.40	0.37	0.54
70	0.25	0.19	0.16	0.24	0.39	0.34	0.30	0.37
75	0.16	0.09	0.09	0.15	0.19	0.23	0.20	0.19
80	0.08	0.04	0.04	0.08	0.06	0.13	0.12	0.09
85	0.05	0.02	0.02	0.05	0.02	0.08	0.07	0.04
90	0.04	0.01	0.02	0.04	0.01	0.06	0.06	0.03

Table 3.29

Sample : CPPCC

Variation of $< P_2 >$ and $< P_4 >$ with temperature.

Temperature in ° C	$< P_2 >$	$< P_4 >$
50	0.579	0.297
55	0.561	0.207
60	0.522	0.167
65	0.502	0.140
69	0.453	0.112

Table 3.30

Sample : CPBCC

Variation of $< P_2 >$ and $< P_4 >$ with temperature.

Temperature in ° C	$< P_2 >$	$< P_4 >$
30.5	0.656	0.274
35	0.641	0.268
40	0.629	0.253
45	0.609	0.234
50	0.585	0.211
55	0.553	0.190
60	0.531	0.158
65	0.511	0.147
67.5	0.470	0.115

Table 3.31

Sample : BPPCC

Variation of $< P_2 >$ and $< P_4 >$ with temperature.

Temperature in ° C	$< P_2 >$	$< P_4 >$
45	0.618	0.288
50	0.600	0.253
55	0.579	0.207
60	0.540	0.177
65	0.512	0.196
70	0.477	0.118
72	0.450	0.086

Table 3.32

Sample : PPPCC

Variation of $< P_2 >$ and $< P_4 >$ with temperature.

Temperature in ° C	$< P_2 >$	$< P_4 >$
40	0.640	0.345
45	0.620	0.264
50	0.605	0.219
55	0.576	0.225
60	0.557	0.257
65	0.515	0.156
70	0.498	0.121
74	0.471	0.104

Table 3.33

Apparent molecular length (l_{ap}) at different temperature.

Sample to film distance = 4.46 cm., λ = 1.54051 Å,

Magnetic field = 5 K. Gauss

Sample: CPPCC				
Temp. in °C	l_{ap} in Å	Mean l_{ap} in Å	Model length L in Å	l_{ap}/ L
50	22.62	22.66	16.3	1.39
55	22.59			
60	22.8			
65	22.86			
69	22.93			

Table 3.34

Apparent molecular length (l_{ap}) at different temperature.

Sample to film distance = 4.46 cm., λ = 1.54051 Å,

Magnetic field = 5 K. Gauss

Sample: CPBCC				
Temp. in °C	l_{ap} in Å	Mean l_{ap} in Å	Model length L in Å	l_{ap}/ L
30.5	24.38	24.42	17.2	1.42
35	24.42			
40	24.5			
45	24.42			
50	24.5			
55	24.54			
60	24.53			
65	24.52			
67.5	24.54			

Table 3.35

Apparent molecular length (l_{ap}) at different temperature.

Sample to film distance = 4.46 cm., λ = 1.54051 Å,

Magnetic field = 5 K. Gauss

Sample: BPPCC				
Temp. in °C	l_{ap} in Å	Mean l_{ap} in Å	Model length L in Å	l_{ap}/ L
45	20.7	20.87	19.15	1.09
50	20.77			
55	20.7			
60	20.79			
65	20.82			
70	21.04			
72	21.23			

Table 3.36

Apparent molecular length (l_{ap}) at different temperature.

Sample to film distance = 4.46 cm., λ = 1.54051 Å,

Magnetic field = 5 K. Gauss

Sample: PPPCC				
Temp. in °C	l_{ap} in Å	Mean l_{ap} in Å	Model length L in Å	l_{ap}/ L
37	23.98	24.26	21.1	1.15
40	23.92			
45	24.08			
50	23.98			
55	24.11			
60	24.24			
65	24.14			
70	24.21			
74.5	24.43			

Table 3.37

Experimental values of the density (ρ) , magnetic susceptibility (χ) , susceptibility anisotropy (Δχ) , and the order parameter < P_2 >.

Sample: CPPCC

Temp. in ° C	Density (ρ) in gm/cc	$-\chi_{\parallel}$ x 10^{-7} c.g.s.unit	Δχ x 10^{-8} c.g.s.unit	order parameter < P_2 >
48.5	1.069	6.85	4.8	0.590
52.5	1.067	6.87	4.7	0.570
58.5	1.062	6.88	4.4	0.535
63.0	1.057	6.91	4.0	0.488
67.5	1.051	6.95	3.4	0.420
75.0	1.040	7.18 = $\bar{\chi}_{iso}$		

$\Delta\chi_o$ = 8.22 x 10^{-8} c.g.s.unit ;

Table 3.38

Experimental values of the density (ρ) , magnetic susceptibility (χ) , susceptibility anisotropy (Δχ) , and the order parameter < P_2 >.

Sample: CPBCC

Temp. in ° C	Density (ρ) in gm/cc	$-\chi_{\parallel}$ x 10^{-7} c.g.s.unit	Δχ x 10^{-8} c.g.s.unit	order parameter < P_2 >
38.5	1.044	6.71	5.0	0.643
43.0	1.041	6.72	4.8	0.613
48.0	1.036	6.74	4.6	0.582
53.0	1.034	6.75	4.4	0.558
58.5	1.026	6.77	4.1	0.523
63.0	1.022	6.80	3.6	0.462
67.0	1.016	6.84	3.1	0.393
75.0	1.004	7.05 = $\bar{\chi}_{iso}$		

$\Delta\chi_o$ = 7.85 x 10^{-8} c.g.s.unit;

Table 3.39

Experimental values of the density (ρ) , magnetic susceptibility (χ) , susceptibility anisotropy (Δχ) , and the order parameter < P_2 >.

Sample: BPPCC

Temp. in °C	Density (ρ) in gm/cc	$-\chi_{\parallel}$ x 10^{-7} c.g.s.unit	Δχ x 10^{-8} c.g.s.unit	order parameter < P_2 >
44.0	0.992	6.24	3.8	0.626
49.0	0.988	6.25	3.6	0.594
54.0	0.984	6.27	3.4	0.567
59.0	0.980	6.28	3.2	0.535
63.0	0.976	6.29	3.1	0.509
67.5	0.972	6.32	2.6	0.430
70.5	0.969	6.35	2.2	0.370
78.0	0.960	6.49 = $\bar{\chi}_{iso}$		

$\Delta\chi_o$ = 6.04 x 10^{-8} c.g.s.unit ;

Table 3.40

Experimental values of the density (ρ) , magnetic susceptibility (χ) , susceptibility anisotropy (Δχ) , and the order parameter < P_2 >.

Sample: PPPCC

Temp. in °C	Density (ρ) in gm/cc	$-\chi_{\parallel}$ x 10^{-7} c.g.s.unit	Δχ x 10^{-8} c.g.s.unit	order parameter < P_2 >
39.0	0.975	6.34	4.0	0.644
43.0	0.973	6.35	3.9	0.627
48.0	0.968	6.36	3.8	0.600
53.0	0.964	6.37	3.6	0.575
58.5	0.960	6.38	3.4	0.546
62.0	0.956	6.38	3.3	0.535
67.0	0.952	6.43	3.1	0.493
71.0	0.948	6.45	2.8	0.450
74.0	0.944	6.48	2.6	0.411
81.0	0.938	6.61 = $\bar{\chi}_{iso}$		

$\Delta\chi_o$ = 6.27 x 10^{-8} c.g.s.unit ;

Table 3.41

Experimental values of splay elastic constant (K_{11}) for various (T_c-T) values.

Sample: CPPCC

$T_c = 70^o$ C , Sample thickness = 162 μm, H_c = Threshold magnetic field

T_c - T	H_c in Gauss	$\Delta\chi \times 10^{-8}$ cgs unit	$K_{11} \times 10^{-6}$ dyne
1	715	3.3	0.45
6	750	3.9	0.58
11	770	4.4	0.69
15.5	790	4.6	0.77
21	815	4.9	0.86

Table 3.42

Experimental values of bend elastic constant (K_{33}) for various (T_c - T) values.

Sample: CPPCC

$T_c = 70^o$ C , Sample thickness = 162 μm, H_c = Threshold magnetic field

T_c - T	H_c in Gauss	$\Delta\chi \times 10^{-8}$ cgs unit	$K_{33} \times 10^{-6}$ dyne
1	750	3.3	0.49
6	805	3.9	0.67
11	860	4.4	0.86
15.5	900	4.6	1.00
21	960	4.9	1.20

Table 3.43

Experimental values of splay elastic constant (K_{11}) for various (T_c - T) values.

Sample: CPBCC

T_c = 68.3° C , Sample thickness = 162 μm, H_c = Threshold magnetic field

T_c - T	H_c in Gauss	$\Delta\chi \times 10^{-8}$ cgs unit	$K_{11} \times 10^{-6}$ dyne
1.3	624	3.1	0.32
6.3	660	3.8	0.44
11.3	670	4.2	0.51
16.3	675	4.5	0.54
21.3	685	4.6	0.59
26.3	710	4.7	0.63
30.3	711	5.2	0.69
34.8	720	5.4	0.75

Table 3.44

Experimental values of bend elastic constant (K_{33}) for various (T_c-T) values.

Sample: CPBCC

$T_c = 68.3^{\circ}$ C , Sample thickness = 162 μm, H_c = Threshold magnetic field

T_c - T	H_c in Gauss	$\Delta\chi \times 10^{-8}$ cgs unit	$K_{33} \times 10^{-6}$ dyne
1.3	626	3.1	0.32
6.3	666	3.8	0.44
11.3	686	4.2	0.53
16.3	706	4.5	0.59
21.3	726	4.7	0.66
26.3	756	4.7	0.72
30.3	760	5.2	0.80
34.8	786	5.4	0.89

Table 3.45

Experimental values of splay elastic constant (K_{11}) for various (T_c - T) values.

Sample: BPPCC

$T_c = 72.6^{\circ}$ C , Sample thickness = 101 μm, H_c = Threshold magnetic field

T_c - T	H_c in Gauss	$\Delta\chi \times 10^{-8}$ cgs unit	$K_{11} \times 10^{-6}$ dyne
2.6	1030	2.3	0.25
4.6	1080	2.5	0.30
9.6	1120	3.1	0.40
14.6	1160	3.3	0.45
19.6	1210	3.4	0.52
24.6	1230	3.6	0.57
29.1	1260	3.8	0.62

Table3.46

Experimental values of bend elastic constant (K_{33}) for various (T_c - T) values.

Sample: BPPCC

$T_c = 72.6^{\circ}$ C , Sample thickness = 101 μm, H_c = Threshold magnetic field

T_c - T	H_c in Gauss	$\Delta\chi \times 10^{-8}$ cgs unit	$K_{33} \times 10^{-6}$ dyne
2.6	960	2.3	0.22
4.6	1000	2.5	0.26
9.6	1050	3.1	0.35
14.6	1120	3.3	0.42
19.6	1170	3.4	0.49
24.6	1200	3.6	0.54
29.1	1230	3.8	0.59

Table 3.47

Experimental values of splay elastic constant (K_{11}) for various (T_c- T) values.

Sample: PPPCC

T_c = 75.0° C , Sample thickness = 162 μm, H_c = Threshold magnetic field

T_c - T	H_c in Gauss	$\Delta\chi$ x 10^{-8} cgs unit	K_{11} x 10^{-6} dyne
1	820	2.6	0.46
5.5	880	2.9	0.60
10	950	3.2	0.77
15	1000	3.3	0.88
20	1060	3.5	1.06
25	1120	3.7	1.23
30	1230	3.9	1.55
35	1330	4.0	1.89

Table 3.48

Experimental values of splay elastic constant (K_{33}) for various (T_c - T) values.

Sample: PPPCC

$T_c = 75.0^{\circ}$ C , Sample thickness = 162 μm, H_c = Threshold magnetic field

T_c - T	H_c in Gauss	$\Delta\chi \times 10^{-8}$ cgs unit	$K_{33} \times 10^{-6}$ dyne
1	819	2.6	0.46
5.5	870	2.9	0.59
10	920	3.2	0.72
15	950	3.3	0.79
20	980	3.5	0.90
25	1010	3.7	1.00
30	1085	3.9	1.21
35	1160	4.0	1.44

Table 3.49

Experimental values of the Frank elastic constant ratio (K_{33} / K_{11}) at different relative temperatures (T_c - T).

Sample: CPPCC		Sample: CPBCC	
T_c - T	K_{33} / K_{11}	T_c - T	K_{33} / K_{11}
1	1.10	1.3	1.01
6	1.15	6.3	1.02
11	1.25	11.3	1.05
15.5	1.30	16.3	1.09
21	1.39	21.3	1.12
		26.3	1.13
		30.3	1.14
		34.8	1.19

Table 3.50

Experimental values of the Frank elastic constant ratio (K_{33} / K_{11}) at different relative temperatures (T_c - T).

Sample: BPPCC		Sample: PPPCC	
T_c - T	K_{33} / K_{11}	T_c - T	K_{33} / K_{11}
2.6	0.87	1	1.00
4.6	0.87	5.5	0.98
9.6	0.88	10	0.94
14.6	0.93	15	0.90
19.6	0.93	20	0.86
24.6	0.95	25	0.81
29.1	0.95	30	0.78
		35	0.76

References:

1) Hoffmann-La Roche Catalogue.
2) M. Takahashi, S. Mita and S. Kondo, Mol. Cryst. Liq. Cryst., 132, 53 (1986).
3) M. Mitra, S. Paul and R. Paul, Pramana-J. Phys., 29, 409 (1987).
4) A. J. Leadbetter, R. M. Richardson and C. N. Colling, J. Phys., (Paris) 36, 1 (1975).
5) R. Chang, Mol. Cryst. Liq. Cryst, 30, 155 (1975).
6) D. Revannasiddaiah and D. Krishnamurti, Mol. Cryst. Liq. Cryst, 53, 63 (1979).
7) I. H. Ibrahim and W. Hasse, J. de Physique, C3, 40, C3-164 (1979).
8) I. H. Ibrahim and W. Hasse, Z. Naturforsch, 31a, 1644 (1976).
9) M. Mitra and R. Paul, Mol. Cryst. Liq. Cryst, 148, 185 (1987).
10) A. Scharkowski, H. Schmiedel, R. Stannarius and E. Weisshuhn, Mol. Cryst. Liq. Cryst, 191, 419 (1990).
11) M. Schadt, R. Buchecker, F. Leenhouts, A. Boller, Mol. Cryst. Liq. Cryst, 139, 1 (1986).
12) M. J. Bradshaw, E. P. Raynes, I. Fedak and A. J. Leadbetter, J. Physique, 45, 157 (1984).

CHAPTER- 4

X-ray diffraction studies and measurement of refractive indices, magnetic susceptibility anisotropy, density, splay and bend elastic constant of two members of isothiocyanatobenzenes.

The chemical name, chemical structure and transition temperatures of the mesogenic compounds studied are given below.

I. 4-(trans-4′ - n- decyl cyclohexyl) Isothiocyanatobenzene

(10 CPS in short)

C10H21-Cy-Ph-NCS

$$K \underset{31.6^{\circ}C}{\overset{41.7\ ^{\circ}C}{\rightleftharpoons}} N \overset{50.7^{\circ}C}{\longleftrightarrow} I$$

II. 4-(trans-4′ - n- dodecyl cyclohexyl) Isothiocyanatobenzene

(12 CPS in short)

C12H25-Cy-Ph-NCS

$$K \underset{44^{\circ}C}{\overset{50.8\ ^{\circ}C}{\rightleftharpoons}} N \overset{52.5^{\circ}C}{\longleftrightarrow} I$$

(Ph = Phenyl ring, Cy = Cyclohexane ring)

The chemicals were synthesised by Prof. R. Dabrowski and his co-workers in Institute of Chemistry, Military University of Technology, Warsaw, Poland and was supplied to us in the pure form. These mesogens were used by us without further purification. The transition temperatures were determined by us by observing their textures under polarising microscope using Mettler FP 80/82 thermosystem. The transition temperature obtained by us agreed with those in the literature [1,2] within 1 ^{0}C.

The experimental procedures used and the method of data analysis are given in Chapter 2 and so only the experimental data and calculated values are given in this chapter. The values of density, ordinary and extra-ordinary refractive indices at four different wave lengths for 10CPS are

tabulated in Tables 4.1a and 4.1b. The wavelengths used for refractive index measurements are 4358Å, 5461Å, 5780Å and 6907Å. The density and refractive index values in the isotropic phase of 10CPS are also given in the Tables. The density and refractive indices (at a different wave length of 589 nm) values of 10CPS have already been reported by Baran et al.[3] and their values agree with the present values within experimental errors. However, Baran et al.[3] did not analyse their data to calculate the order parameter of 10CPS, which have been determined by us. Tables 4.2a and 4.2b give the values of density and refractive indices at four different wave lengths for 12CPS in its mesophase and isotropic phase. The temperature variations of density for 10CPS and 12CPS are shown in Figure 4.1 and Figure 4.2 respectively. The density changes at the nematic to isotropic transition are small, the change is indeed very small for 12CPS. The temperature variation of ordinary and extra-ordinary refractive indices for 10CPS and 12CPS are shown in Figure 4.3 and Figure 4.4 respectively. The polarisabilities of 10CPS calculated using Vuks and Neugebauer methods (Chapter2) are tabulated in Table 4.3 and Table 4.4 respectively. The corresponding polarisability values for 12CPS using Vuks and Neugebauer procedure are given in Table 4.5 and Table 4.6 respectively. The order parameters at different temperatures for 10CPS calculated from Vuks and Neugebauer polarisabilities are tabulated in Tables 4.7 and 4.8 respectively. The polarisability anisotropy in the perfectly aligned phase, as obtained from Haller's extrapolation method are also given in the Tables. As seen in the last Chapter (Chapter 3), here also polarisabilty anisotropies calculated by Vuks method are larger than those from Neugebauer method but the order parameters calculated from the two methods are almost identical. Tables 4.9 and 4.10 give the order parameter

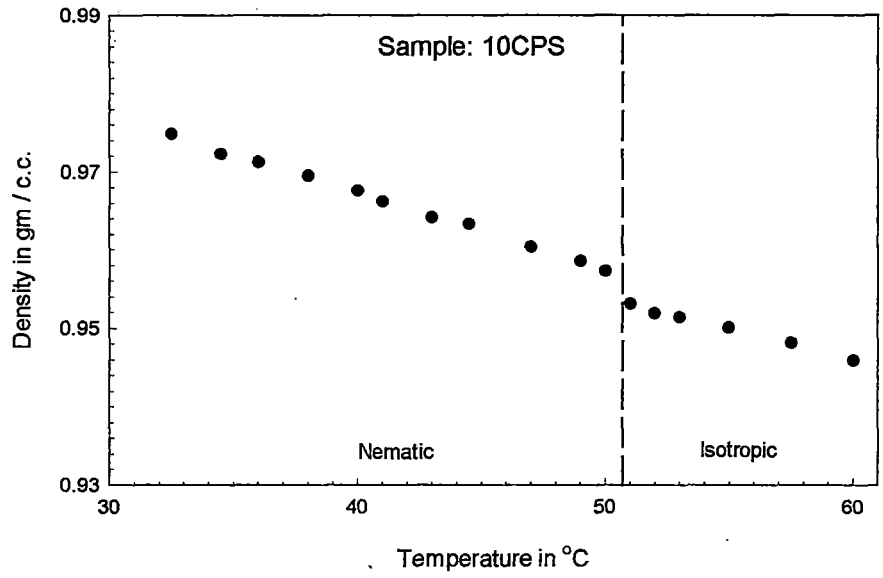

Figure 4.1. Density values as a function of temperature.

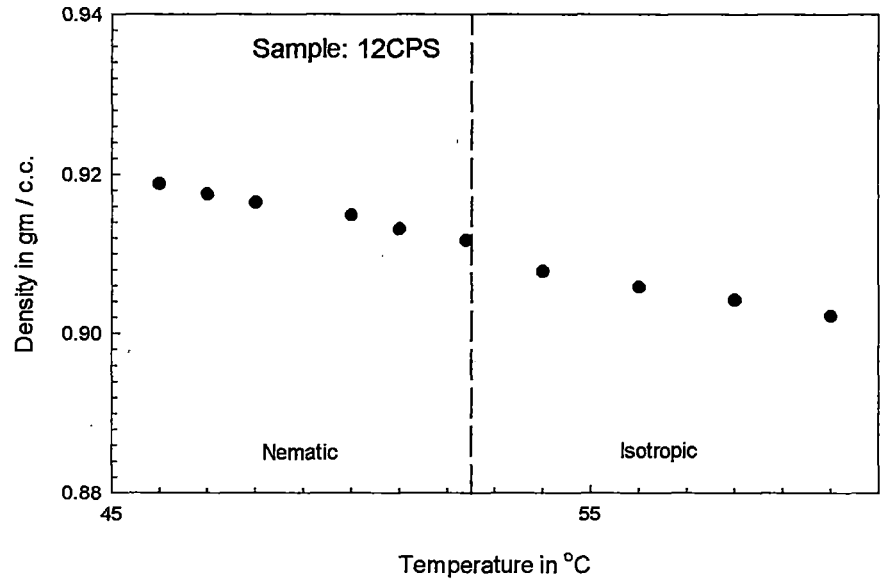

Figure 4.2. Density values as a function of temperature.

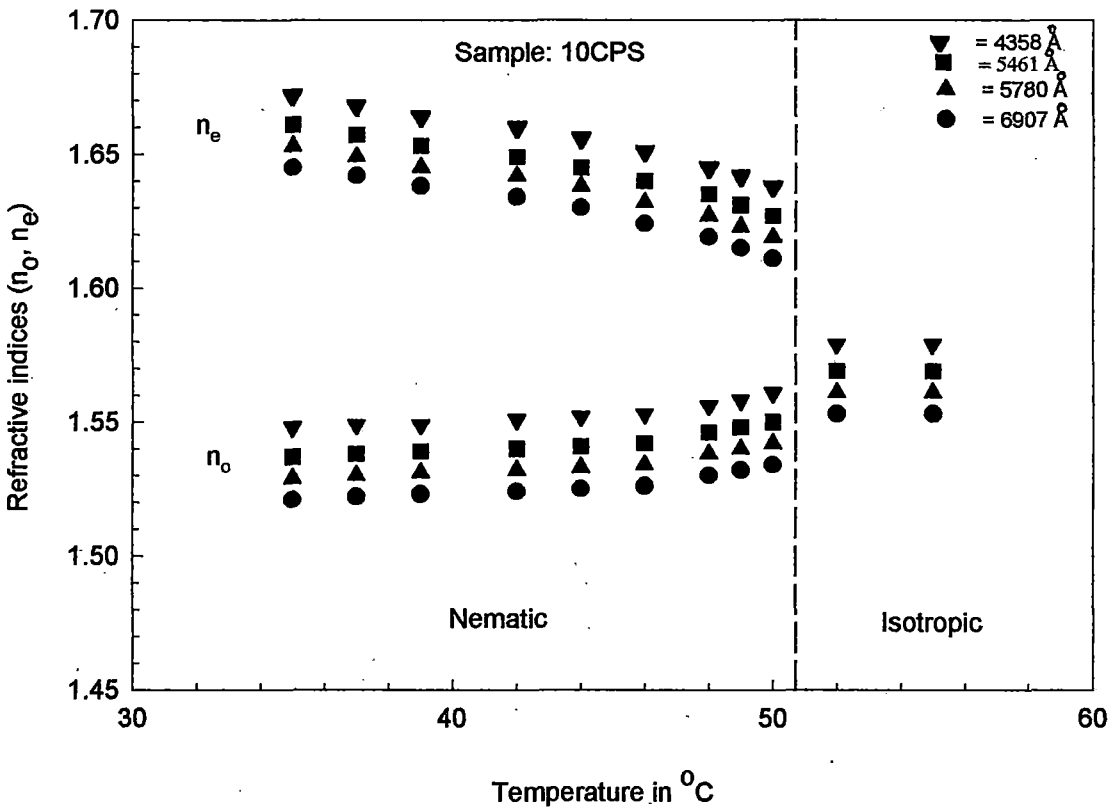

Figure 4.3. Variation of refractive indices (n_o, n_e) with temperature.

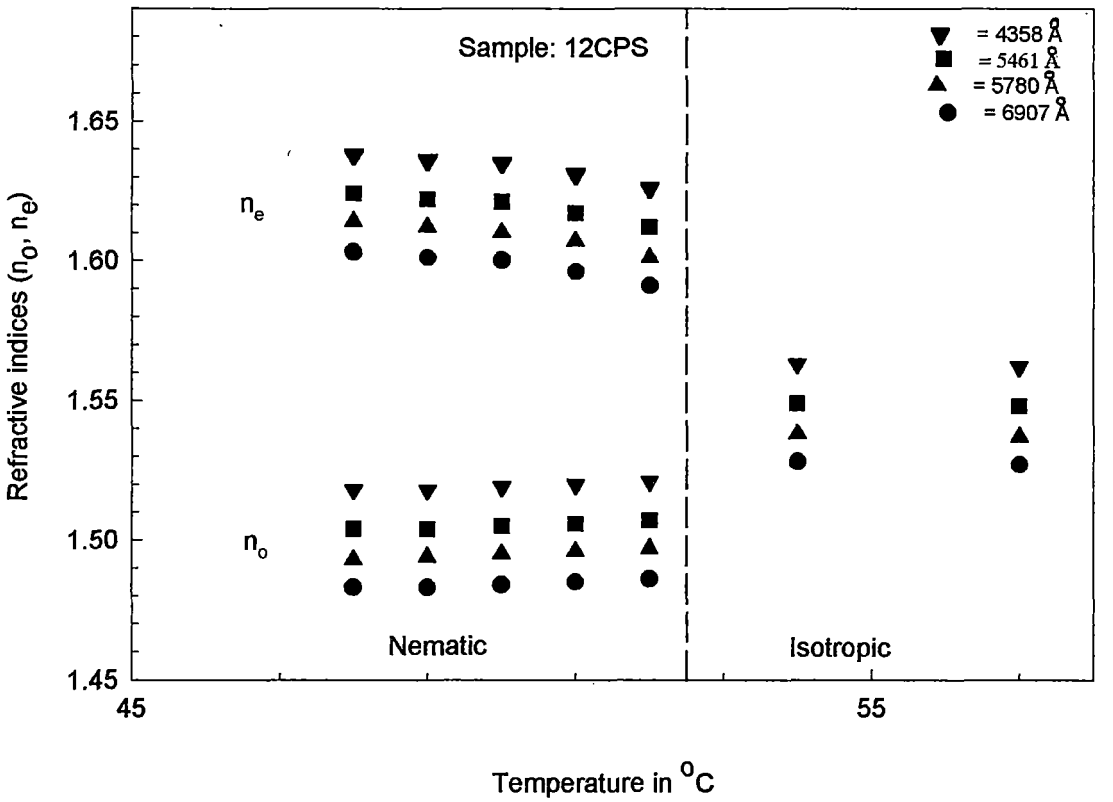

Figure 4.4. Variation of refractive indices (n_o, n_e) with temperature.

values for 12CPS as calculated from Vuks and Neugebauer methods respectively. Extrapolated values of polarisability anisotropy at $< P_2 > =1$ are also given in the Tables. Again the order parameter values from the two procedures agree very well.

X-ray diffraction photographs were taken for the aligned samples of 10CPS and 12CPS in their mesophase. A magnetic field of about 5 Kilogauss was used to align the samples. No x-ray diffraction photograph could be taken in the super cooled nematic phase of 12CPS as the sample crystallised below 50.8^0C. Hence, only one diffraction pattern for the sample was taken between 50.8^0C and 52.5^0C, the clearing temperature. However, for 10CPS x-ray diffraction studies could be performed in the supercooled nematic phase. Plates 4a and 4b show the x-ray diffraction patterns from 10CPS at 46^0C and from 12CPS at $51.5\ ^0$C respectively.

The angular distributions of the x-ray intensity along the outer arc of the diffration pattern for 10CPS after necessary background correction, are tabulated in Table 4.11. The corresponding angular distribution functions calculated using Leadbetter formula (Chapter 2, equation 2.16) are given in Table 4.12. For 12CPS both the angular distribution of x-ray intensity and the corresponding angular distribution function at only one experimental temperature are given in Table 4.13. The order parameter values for 10CPS and 12CPS, calculated following the equation 2.17 are tabluated in Table 4.14 and Table 4.15 respectively. The apparent molecular lengths as calculated from the inner arc of the x-ray diffraction pattern, for 10CPS and 12CPS are given in Table 4.16. The temperature variation of apparent molecular length for 10CPS is shown in Figure 4.5. The single value of apparent molecular length of 12CPS is also plotted in the same figure. It can be seen that apparent molecular length of 10CPS is

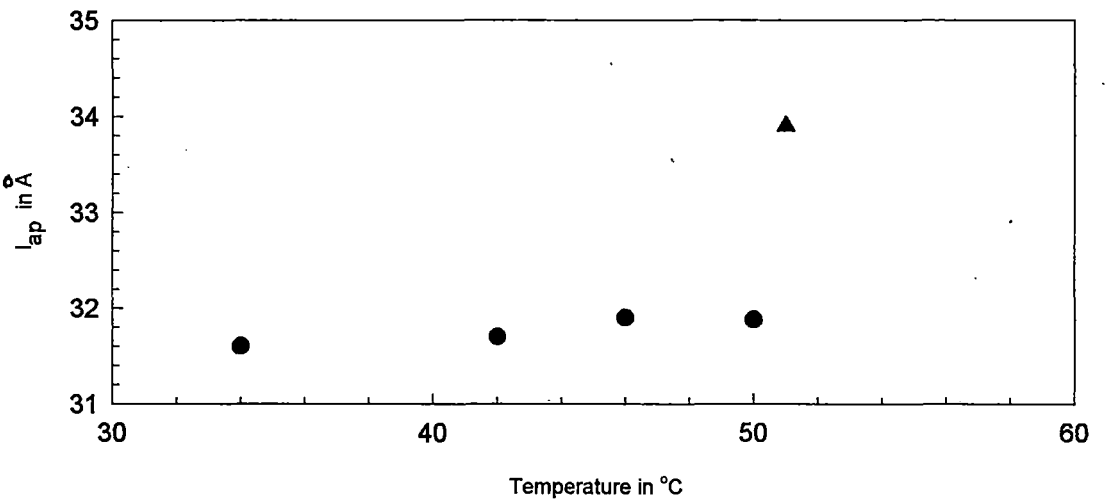

Figure 4.5. Temperature variation of apparent molecular length (l_{ap}).

- ● data for 10CPS
- ▲ data for 12 CPS

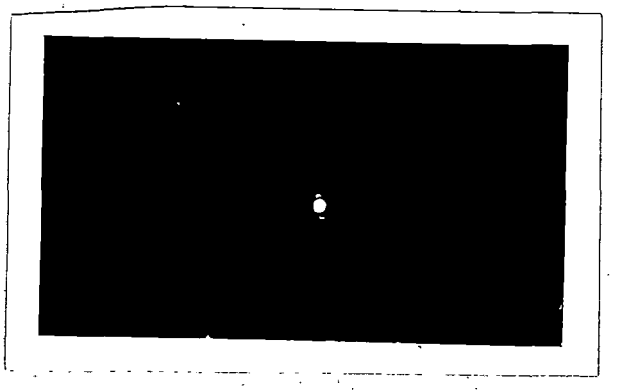

Plate 4a: X-ray diffraction photograph of the oriented sample in the nematic phase of 10CPS at 46°C.

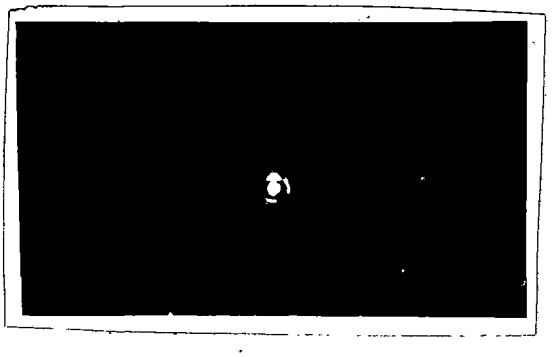

Plate 4b: X-ray diffraction photograph of the oriented sample in the nematic phase of 12CPS at 51.5°C.

almost constant at 31.7 Å . The molecular model length of 10CPS in its fully extended form is 25.7 Å. Thus the ratio of apparent molecular length to the model length is 1.23. The values of apparent molecular length, model molecular length and their ratio for 12CPS are 33.9 Å, 28.1 Å and 1.21 respectively. Thus the ratios of the apparent to model molecular lengths are almost the same for the two CPS compounds and this ratio is much smaller than the value (1.4) in the case of cyanobiphenyls which form dimers. So there is some association of molecules in the mesophases of 10CPS and 12CPS, though it is much weaker than that in cyanobiphenyls.

The magnetic susceptibility along the director, $\chi_{\parallel}$, the magnetic susceptibility anisotropy, $\Delta\chi$, and the order parameter values at different temperatures for 10CPS are tabulated in Table 4.17. The density values given in the Table have been interpolated from our experimental values given in Table 4.1a. The magnetic susceptibility anisotropy for perfectly ordered sample has been obtained by Haller's extrapolation method (described in Chapter 2) and is given in the Table. The magnetic susceptibility $\chi_{\parallel}$, $\Delta\chi$, order parameter and interpolated density values for 12CPS are given in Table 4.18. The experimental values for 12CPS could be obtained at only one temperature in the mesophase since no supercooled nematic phase was observed in the magnetic field. The temperature variation of magnetic anisotropy of 10CPS is shown in Figure 4.6.

The temperature variation of order parameter values for 10CPS as obtained from refractive index, magnetic susceptibility and x-ray diffraction studies, are shown in Figure 4.7. In this figure the Maier-Saupe theoretical values are also shown. The $< P_2 >$ values calculated from x-ray diffraction data agree very well with the Maier-Saupe theoretical values throughout the mesomorphic temperature range. The order parameter

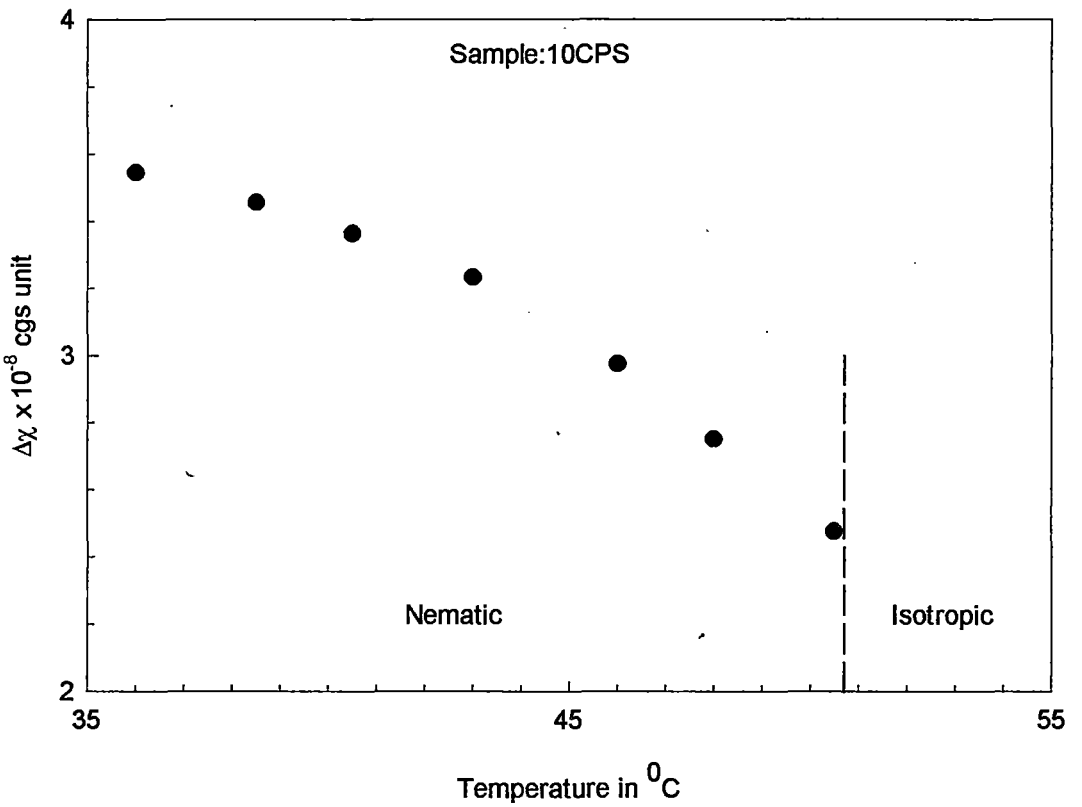

Figure 4.6. Temperature variation of the anisotropy of the diamagnetic susceptibility ($\Delta\chi$).

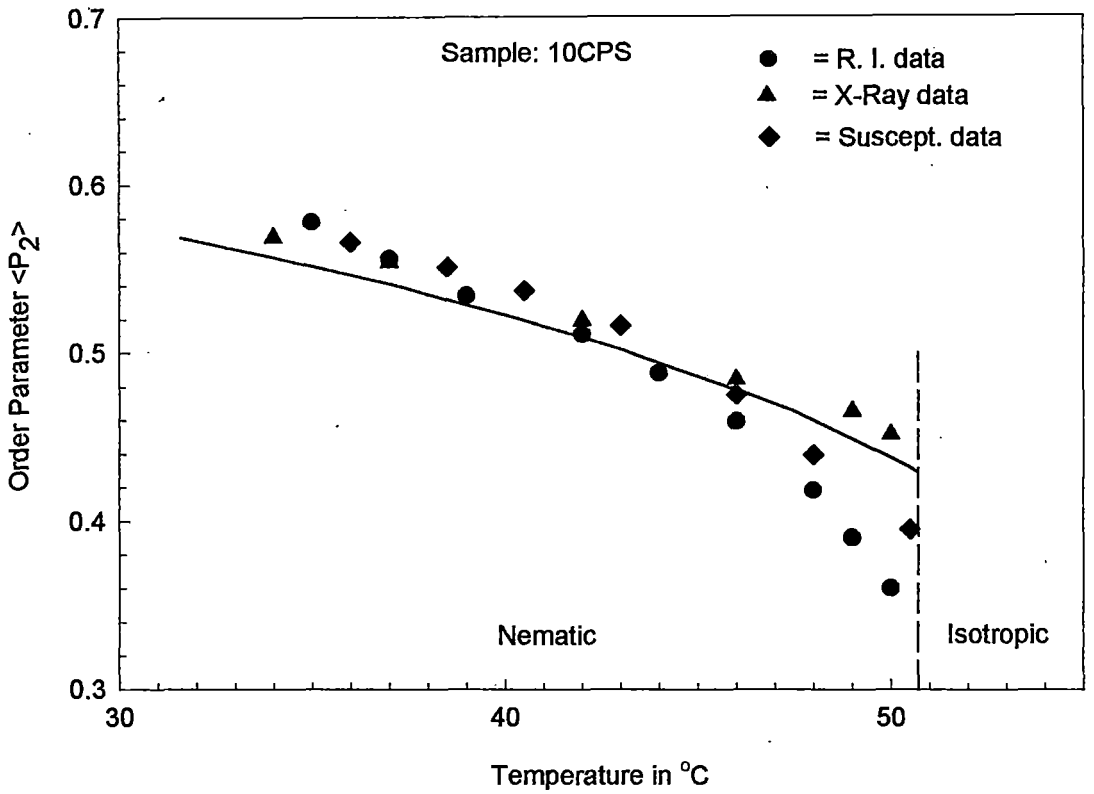

Figure 4.7. Temperature variation of Order Parameter $\langle P_2 \rangle$. Continuous curve corresponds to Maier-Saupe theoretical values.

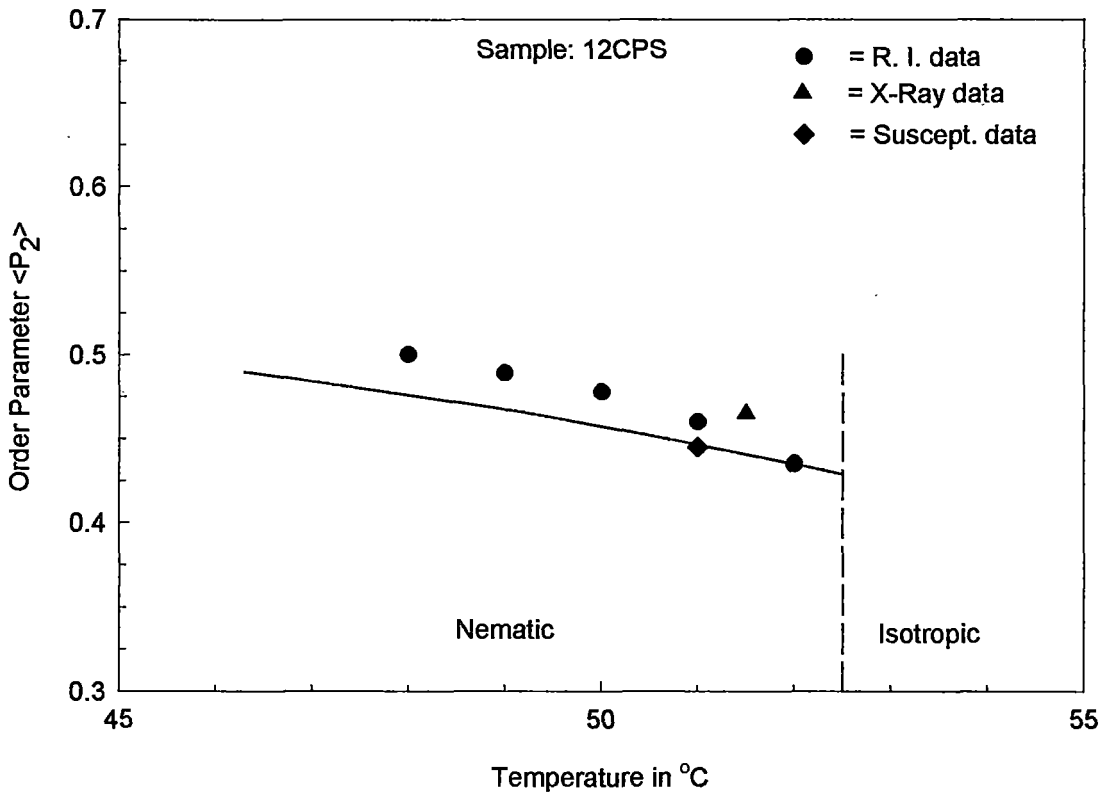

Figure 4.8. Temperature variation of Order Parameter $<P_2>$. Continuous curve corresponds to Maier-Saupe theoretical values.

values obtained from refractive index and magnetic susceptibility measurements agree with the theoretical values at lower temperatures. But, near the nematic to isotropic transition temperature these order parameter values decrease more rapidly than the theoretical values. This trend is more pronounced in the $< P_2 >$ values obtained from the refractive index data.

The temperature variation of order parameter values of 12CPS, obtained from different experimental methods, are shown in Figure 4.8. Since the mesomorphic temperature range of 12CPS is very small, not much can be inferred from this figure. However, like 10CPS for 12CPS also the $< P_2 >$ values obtained from x-ray diffraction data are somewhat greater than those obtained from refractive index and magnetic susceptibility at the same temperature.

The splay and bend elastic constants of these two mesogens were determined by observing Freedericksz transition in magnetic field. The details of the method have already been described in Chapter 2 of the present thesis.

The splay and bend elastic constants at different temperatures for 10CPS are given in Tables 4.19 and 4.20 respectively. The critical magnetic field and the thickness of the sample are also given in the tables. The splay and bend elastic constant values of 12CPS are tabulated in Tables 4.21 and 4.22 respectively for only one temperature, since in a magnetic field the mesophase of 12CPS was stable in the temperature range of $1.7\ ^0C$ only.

The temperature variation of splay and bend elastic constant values of 10CPS are shown in Figure 4.9 and Figure 4.10 respectively. These variations are normal. The temperature variation of bend to splay elastic constants of 10CPS is shown in Figure 4.11 and tabulated in Table 4.23. In

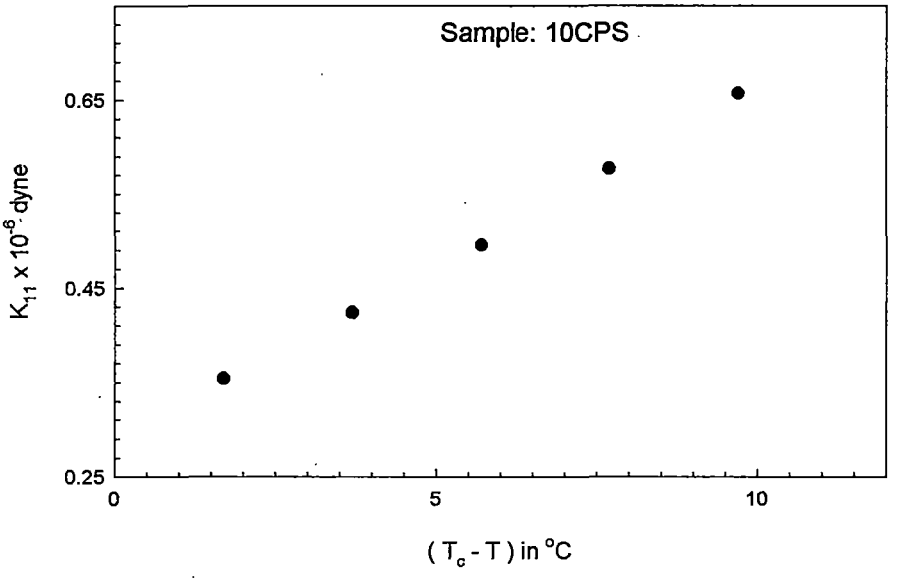

Figure 4.9. Splay elastic constant (K_{11}) as a function of relative temperature (T_c - T).

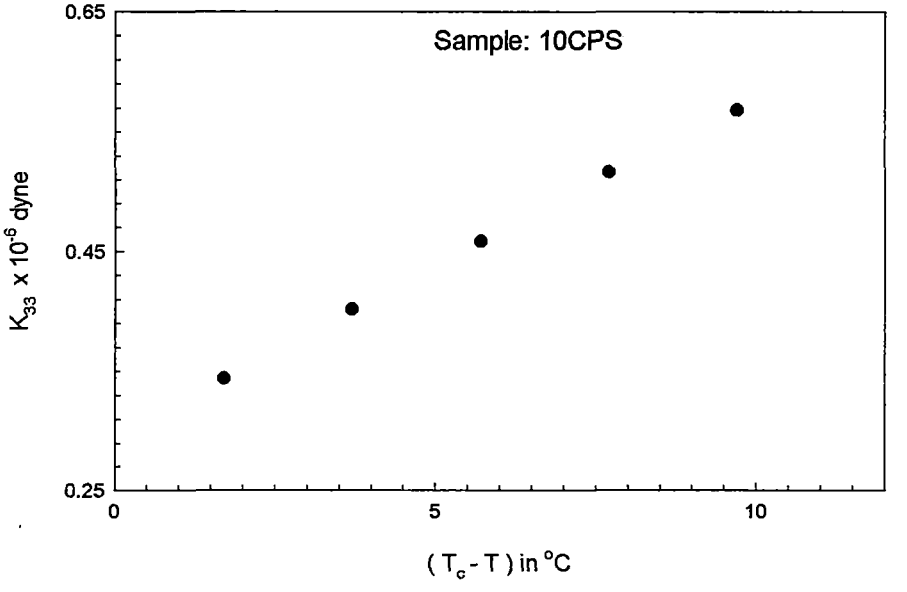

Figure 4.10. Bend elastic constant (K_{33}) as a function of relative temperature (T_c - T).

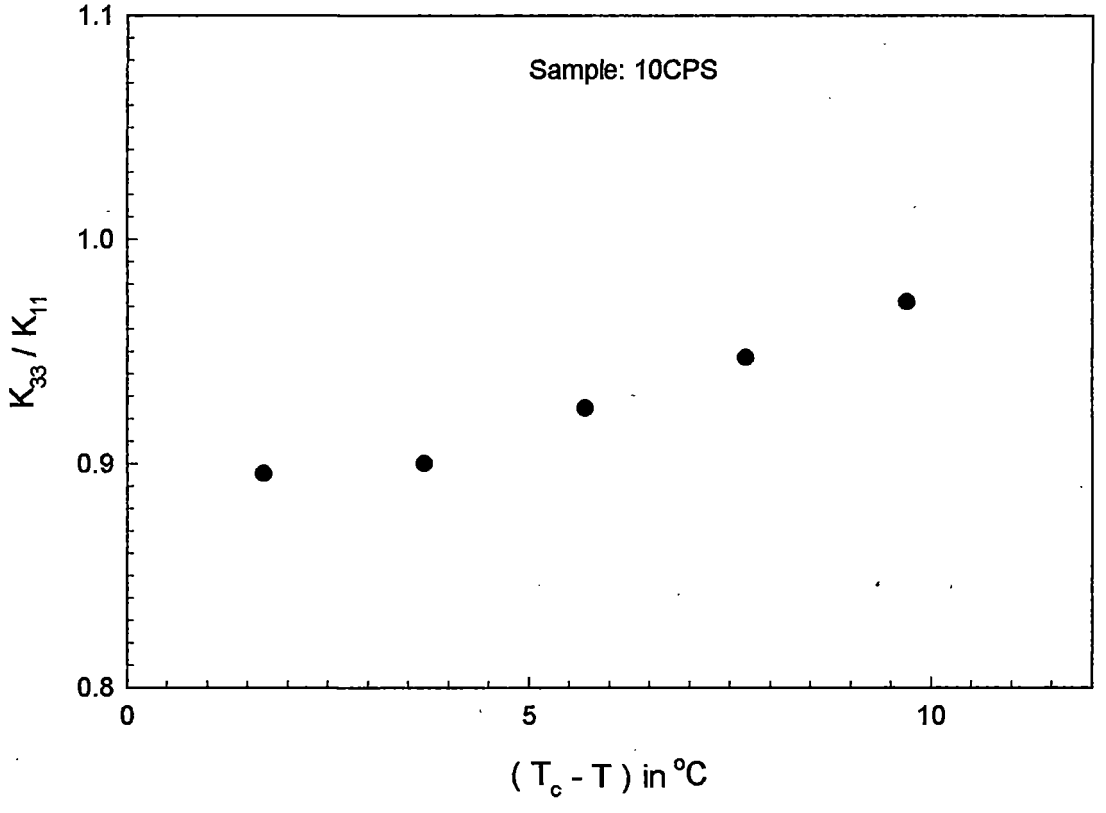

Figure 4.11. Bend to Splay elastic constant ratio (K_{33}/ K_{11}) as a function of relative temperature (T_c - T).

this Table the K_{33}/K_{11} ratio for 12CPS has also been given. It can be seen that the ratios are less than 1 for 12CPS and 10CPS at all temperatures. It may be noted that for cyanophenyl compounds this ratio is larger than 1. In nCPS compounds K_{33} values are much smaller than K_{33} values for corresponding cyanocompounds [4]. According to Schadt et al. [5] the K_{33}/K_{11} ratio decreases with decreasing polarity of the compounds. It has also been found by Schadt et al.[6] that K_{33}/K_{11} ratio is affected by the type of ring structure in the rigid part of the molecules. In non-polar azoxybenzene homologous series, de Jeu et al. [7] found that the K_{33}/K_{11} value decreases with increasing chain length. The K_{33}/K_{11} value for 6CPS is 1.11, at $T_c - T = 21\ ^0C$ [4], whereas for 10CPS our value is 0.972 at $T_c - T = 9.7\ ^0C$. Thus the values of the ratio K_{33}/K_{11}, for 10CPS obtained by us is consistent with the experimental observations of other researchers.

Table 4.1a

Density (ρ) and refractive indices (n_o , n_e) at different temperatures of Sample 10CPS.

Temp. in ° C	Density in gm/cc	λ = 6907 Å		λ = 5780 Å	
		n_o	n_e	n_o	n_e
35	0.972	1.521	1.645	1.529	1.653
37	0.970	1.522	1.642	1.530	1.649
39	0.969	1.523	1.638	1.531	1.645
42	0.965	1.524	1.634	1.532	1.642
44	0.964	1.525	1.630	1.533	1.638
46	0.962	1.526	1.624	1.534	1.632
48	0.960	1.530	1.619	1.538	1.627
49	0.959	1.532	1.615	1.540	1.623
50	0.957	1.534	1.611	1.542	1.619
52	0.953	1.553		1.561	

Table 4.1b

Density (ρ) and refractive indices (n_o , n_e) at different temperatures of Sample 10CPS.

Temp. in ° C	Density in gm/cc	λ = 5461 Å		λ = 4358 Å	
		n_o	n_e	n_o	n_e
35	0.972	1.537	1.661	1.548	1.672
37	0.970	1.538	1.657	1.549	1.668
39	0.969	1.539	1.653	1.549	1.664
42	0.965	1.540	1.649	1.551	1.660
44	0.964	1.541	1.645	1.552	1.656
46	0.962	1.542	1.640	1.553	1.651
48	0.960	1.546	1.635	1.556	1.645
49	0.959	1.548	1.631	1.558	1.642
50	0.957	1.550	1.627	1.561	1.638
52	0.953	1.569		1.579	

Table 4.2a

Density (ρ) and refractive indices (n_o , n_e) at different temperatures of Sample 12CPS.

Temp. in ° C	Density in gm/cc	λ = 6907 Å		λ = 5780 Å	
		n_o	n_e	n_o	n_e
48	0.917	1.483	1.603	1.493	1.614
49	0.916	1.483	1.601	1.494	1.612
50	0.915	1.484	1.600	1.495	1.610
51	0.913	1.485	1.596	1.496	1.607
52	0.912	1.486	1.591	1.497	1.601
54	0.909	1.528		1.538	

Table 4.2b

Density (ρ) and refractive indices (n_o , n_e) at different temperatures of Sample 12CPS.

Temp. in ° C	Density in gm/cc	λ = 5461 Å		λ = 4358 Å	
		n_o	n_e	n_o	n_e
48	0.917	1.504	1.624	1.518	1.638
49	0.916	1.504	1.622	1.518	1.636
50	0.915	1.505	1.621	1.519	1.635
51	0.913	1.506	1.617	1.520	1.631
52	0.912	1.507	1.612	1.521	1.626
54	0.909	1.549		1.563	

Table 4.3

Polarisability (α_o, α_e) at different temperatures of sample 10CPS by Vuks method.

Temp. in $^{\circ}$C	$\lambda = 6907$ Å		$\lambda = 5780$ Å		$\lambda = 5461$ Å		$\lambda = 4358$ Å	
	α_o	α_e	α_o	α_e	α_o	α_e	α_o	α_e
35	43.03	55.92	43.58	56.47	44.13	57.01	44.85	57.72
37	43.21	55.62	43.76	56.16	44.31	56.70	45.04	57.42
39	43.41	55.32	43.96	55.87	44.50	56.41	45.23	57.13
42	43.72	55.11	44.27	55.66	44.81	56.20	45.54	56.93
44	43.91	54.80	44.47	55.35	45.02	55.89	45.75	56.62
46	44.14	54.39	44.71	54.94	45.26	55.49	45.99	56.21
48	44.59	53.92	45.15	54.47	45.70	55.01	46.44	55.74
49	44.82	53.56	45.37	54.10	45.93	54.65	46.67	55.38
50	45.14	53.18	45.70	53.74	46.25	54.28	46.99	55.01

α_o & α_e are in 10^{-24} cm^3 unit.

Table 4.4

Polarisability (α_o, α_e) at different temperatures of sample 10 CPS by Neugebauer method.

Temp. in ° C	λ = 6907 Å		λ = 5780 Å		λ = 5461 Å		λ = 4358 Å	
	α_o	α_e	α_o	α_e	α_o	α_e	α_o	α_e
35	43.82	54.35	44.37	54.88	44.93	55.40	45.67	56.09
37	43.97	54.11	44.52	54.63	45.08	55.15	45.82	55.85
39	44.13	53.88	44.69	54.40	45.24	54.93	45.98	55.63
42	44.41	53.73	44.97	54.26	45.52	54.79	46.26	55.49
44	44.57	53.49	45.14	54.01	45.69	54.54	46.44	55.25
46	44.76	53.15	45.34	53.69	45.89	54.22	46.64	54.93
48	45.15	52.79	45.72	53.33	46.28	53.86	47.02	54.57
49	45.34	52.50	45.91	53.03	46.47	53.57	47.22	54.28
50	45.62	52.21	46.19	52.75	46.75	53.29	47.49	54.00

α_o & α_e are in 10^{-24} cm^3 unit.

Table 4.5

Polarisability (α_o, α_e) at different temperatures of sample 12CPS by Vuks method.

Temp. in °C	$\lambda = 6907$ Å		$\lambda = 5780$ Å		$\lambda = 5461$ Å		$\lambda = 4358$ Å	
	α_o	α_e	α_o	α_e	α_o	α_e	α_o	α_e
48	46.15	60.48	46.99	61.34	47.85	62.17	48.97	63.28
49	46.29	60.33	47.14	61.18	47.99	62.01	49.11	63.11
50	46.43	60.17	47.28	61.01	48.13	61.85	49.25	62.96
51	46.64	59.89	47.50	60.73	48.34	61.57	49.47	62.69
52	46.84	59.35	47.70	60.19	48.54	61.06	49.67	62.17

α_o & α_e are in 10^{-24} cm^3 unit.

Table 4.6

Polarisability (α_o, α_e) at different temperatures of sample 12CPS by Neugebauer method.

Temp. in °C	$\lambda = 6907$ Å		$\lambda = 5780$ Å		$\lambda = 5461$ Å		$\lambda = 4358$ Å	
	α_o	α_e	α_o	α_e	α_o	α_e	α_o	α_e
48	46.96	58.85	47.82	59.68	48.70	60.48	49.83	61.55
49	47.09	58.73	47.95	59.55	48.81	60.35	49.95	61.42
50	47.21	58.61	48.08	59.42	48.94	60.23	50.08	61.31
51	47.39	58.38	48.27	59.19	49.12	60.01	50.26	61.10
52	47.55	57.93	48.42	58.75	49.28	59.59	50.42	60.66

α_o & α_e are in 10^{-24} cm^3 unit.

Table 4.7

Order parameter $< P_2 >$ of sample 10CPS at different temperatures by Vuks method.

$(\alpha_{\parallel} - \alpha_{\perp}) = 22.3$ in 10^{-24} cm^3 unit.

Temp. in $^{\circ}$C	$\lambda = 6907$ Å	$\lambda = 5780$ Å	$\lambda = 5461$ Å	$\lambda = 4358$ Å	Average
	$< P_2 >$	$< P_2 >$	$< P_2 >$	$< P_2 >$	$< P_2 >$
35	0.578	0.578	0.578	0.577	0.578
37	0.556	0.556	0.555	0.555	0.555
39	0.534	0.534	0.534	0.534	0.534
42	0.511	0.511	0.511	0.511	0.511
44	0.488	0.488	0.487	0.487	0.487
46	0.460	0.459	0.459	0.458	0.459
48	0.418	0.418	0.417	0.417	0.417
49	0.392	0.390	0.391	0.391	0.391
50	0.361	0.360	0.360	0.360	0.360

Table 4.8

Order parameter $< P_2 >$ of sample 10CPS at different temperatures by Neugebauer method.

$(\alpha_{\parallel} - \alpha_{\perp}) = 18.25$ in 10^{-24} cm^3 unit.

Temp. in ^{o} C	$\lambda = 6907$ Å	$\lambda = 5780$ Å	$\lambda = 5461$ Å	$\lambda = 4358$ Å	Average
	$< P_2 >$	$< P_2 >$	$< P_2 >$	$< P_2 >$	$< P_2 >$
35	0.577	0.576	0.573	0.571	0.574
37	0.556	0.554	0.552	0.550	0.553
39	0.534	0.532	0.531	0.529	0.532
42	0.511	0.510	0.507	0.506	0.509
44	0.489	0.487	0.485	0.483	0.486
46	0.460	0.458	0.456	0.454	0.457
48	0.419	0.417	0.415	0.414	0.416
49	0.382	0.391	0.389	0.387	0.387
50	0.361	0.360	0.358	0.357	0.359

Table 4.9

Order parameter $< P_2 >$ of sample 12CPS at different temperatures by Vuks method.

$(\alpha_{\parallel} - \alpha_{\perp}) = 28.7$ in 10^{-24} cm^3 unit.

Temp. in ° C	$\lambda = 6907$ Å	$\lambda = 5780$ Å	$\lambda = 5461$ Å	$\lambda = 4358$ Å	Average
	$< P_2 >$	$< P_2 >$	$< P_2 >$	$< P_2 >$	$< P_2 >$
48	0.500	0.500	0.499	0.498	0.499
49	0.489	0.489	0.488	0.488	0.488
50	0.479	0.478	0.478	0.478	0.478
51	0.461	0.460	0.461	0.461	0.461
52	0.436	0.435	0.436	0.435	0.435

Table 4.10

Order parameter $< P_2 >$ of sample 12CPS at different temperatures by Neugebauer method.

$(\alpha_{\parallel} - \alpha_{\perp}) = 23.9$in 10^{-24} cm^3 unit.

Temp. in ° C	$\lambda = 6907$ Å	$\lambda = 5780$ Å	$\lambda = 5461$ Å	$\lambda = 4358$ Å	Average
	$< P_2 >$	$< P_2 >$	$< P_2 >$	$< P_2 >$	$< P_2 >$
48	0.497	0.496	0.493	0.490	0.494
49	0.487	0.485	0.483	0.480	0.484
50	0.477	0.474	0.472	0.469	0.473
51	0.460	0.457	0.456	0.454	0.457
52	0.434	0.432	0.431	0.428	0.431

Table 4.11

Mean experimental intensity values I (ψ) , in arbitrary units , of 10 CPS after background correction.

ψ (deg.)	I (ψ) values at different temperatures in degrees					
	34	37	42	46	49	50
0	1.83	1.60	1.55	1.80	0.75	2.80
5	1.80	1.55	1.55	1.75	0.75	2.75
10	1.55	1.45	1.40	1.65	0.70	2.65
15	1.20	1.30	1.10	1.50	0.55	2.40
20	0.85	1.00	0.80	1.40	0.45	2.10
25	0.65	0.75	0.60	1.30	0.35	2.00
30	0.50	0.60	0.50	1.10	0.25	1.70
35	0.35	0.50	0.40	0.85	0.20	1.40
40	0.35	0.35	0.35	0.70	0.20	1.15
45	0.25	0.30	0.30	0.55	0.18	0.95
50	0.22	0.25	0.25	0.45	0.15	0.80
55	0.20	0.23	0.20	0.35	0.15	0.70
60	0.18	0.20	0.20	0.25	0.12	0.60
65	0.17	0.18	0.18	0.20	0.11	0.40
70	0.14	0.13	0.15	0.15	0.10	0.25
75	0.13	0.08	0.15	0.10	0.10	0.20
80	0.10	0.00	0.10	0.08	0.10	0.10
85	0.05	0.00	0.10	0.00	0.05	0.05
90	0.00	0.00	0.00	0.00	0.00	0.00

Table 4.12

Normalised distribution function values f (β) of 10 CPS.

β (deg.)	f (β) values at different temperatures in degrees					
	34	37	42	46	49	50
0	9.88	6.90	8.18	4.57	6.49	4.51
5	9.75	6.74	8.22	4.50	6.62	4.41
10	8.80	6.24	7.74	4.22	6.55	4.08
15	6.53	5.41	6.02	3.72	5.52	3.59
20	4.03	4.33	3.82	3.19	3.80	3.08
25	2.42	3.18	2.31	2.82	2.39	2.68
30	1.64	2.19	1.59	2.57	1.59	2.37
35	1.27	1.47	1.29	2.26	1.21	2.02
40	1.00	1.04	1.09	1.73	0.99	1.57
45	0.71	0.80	0.85	1.17	0.81	1.56
50	0.50	0.66	0.62	0.79	0.66	0.88
55	0.40	0.55	0.48	0.62	0.57	0.75
60	0.39	0.47	0.44	0.55	0.55	0.69
65	0.40	0.40	0.43	0.47	0.54	0.59
70	0.37	0.32	0.40	0.32	0.49	0.38
75	0.25	0.22	0.30	0.15	0.37	0.18
80	0.14	0.10	0.19	0.06	0.24	0.08
85	0.08	0.04	0.13	0.03	0.17	0.04
90	0.06	0.03	0.11	0.02	0.15	0.03

Table 4.13

Mean experimental intensity values I (ψ) , in arbitrary units , after background correction and Normalised distribution function values f (β) of 12CPS.

ψ in degrees	I (ψ) values at 51.5° C	β in degrees	f (β) values at 51.5°C
0	1.35	0	3.60
5	1.33	5	3.68
10	1.25	10	3.82
15	1.20	15	3.82
20	1.15	20	3.55
25	1.00	25	3.07
30	0.80	30	2.52
35	0.60	35	1.99
40	0.50	40	1.50
45	0.45	45	1.10
50	0.35	50	0.81
55	0.25	55	0.62
60	0.20	60	0.51
65	0.18	65	0.42
70	0.15	70	0.32
75	0.13	75	0.23
80	0.10	80	0.15
85	0.10	85	0.11
90	0.00	90	0.10

Table 4.14

Sample : 10CPS

Variation of $< P_2 >$ and $< P_4 >$ with temperature.

Temperature in ^{o} C	$< P_2 >$	$< P_4 >$
34	0.569	0.293
37	0.554	0.214
42	0.519	0.245
46	0.484	0.089
49	0.465	0.212
50	0.451	0.077

Table 4.15

Sample : 12CPS

Variation of $< P_2 >$ and $< P_4 >$ with temperature.

Temperature in ^{o} C	$< P_2 >$	$< P_4 >$
51.5	0.465	0.102

Table 4.16

Apparent molecular length (l_{ap}) at different temperature.

Sample to film distance = 7.86 cm., λ = 1.54051 Å,

Magnetic field = 5 K. Gauss

Sample: 10CPS Model length L = 25.7 Å				Sample: 12CPS Model length L = 28.1 Å		
Temp. in °C	l_{ap} in Å	Mean length l_{ap} in Å	l_{ap}/L	Temp. in °C	l_{ap} in Å	l_{ap}/L
34	31.6	31.7	1.23	51	33.9	1.21
42	31.7					
46	31.9					
50	31.9					

Table 4.17

Experimental values of the density (ρ) , magnetic susceptibility (χ) , susceptibility anisotropy (Δχ) , and the order parameter < P_2 >

Sample 10CPS

Temp. in °C	Density (ρ)* in gm/cc	$-\chi_{\parallel}$ x 10^{-7} c.g.s.unit	Δχ x 10^{-8} c.g.s.unit	order parameter < P_2 >
36.0	0.971	7.1i	3.5	0.566
38.5	0.969	7.11	3.5	0.551
40.5	0.967	7.12	3.4	0.537
43.0	0.964	7.13	3.2	0.516
46.0	0.962	7.15	3.0	0.475
48.0	0.960	7.16	2.7	0.439
50.5	0.955	7.18	2.5	0.395
52.0	0.952	7.35 = $\bar{\chi}_{iso}$		

$\Delta\chi_o$ = 6.265 x 10^{-8} c.g.s.unit ;

* Interpolated values from Table 4.1a.

Table 4.18

Experimental values of the density (ρ) , magnetic susceptibility (χ) , susceptibility anisotropy ($\Delta\chi$) , and the order parameter $< P_2 >$

Sample 12CPS

Temp. in °C	Density (ρ)* in gm/cc	$-\chi_{\parallel}$ x 10^{-7} c.g.s.unit	$\Delta\chi$ x 10^{-8} c.g.s.unit	order parameter $< P_2 >$
51	0.913	7.626	2.905	0.445
53	0.910	7.820 = $\bar{\chi}_{iso}$		

$\Delta\chi_o$ = 6.528 x 10^{-8} c.g.s.unit ;

* Interpolated values from Table 4.2a.

Table 4.19

Experimental values of splay elastic constant (K_{11}) for various (T_c - T) values.

Sample 10CPS

$T_c = 50.7^\circ$ C , Sample thickness = 162 μm, H_c = Threshold magnetic field.

T_c - T	H_c in Gauss	$\Delta\chi \times 10^{-8}$ cgs unit	$K_{11} \times 10^{-6}$ dyne
1.7	710	2.6	0.35
3.7	746	2.9	0.42
5.7	780	3.1	0.50
7.7	819	3.2	0.58
9.7	860	3.3	0.66

Table 4.20

Experimental values of splay elastic constant (K_{33}) for various (T_c - T) values.

Sample 10CPS

$T_c = 50.7^\circ$ C , Sample thickness = 162 μm, H_c = Threshold magnetic field

T_c - T	H_c in Gauss	$\Delta\chi \times 10^{-8}$ cgs unit	$K_{33} \times 10^{-6}$ dyne
1.7	700	2.6	0.34
3.7	726	2.9	0.40
5.7	750	3.1	0.46
7.7	775	3.2	0.52
9.7	800	3.3	0.57

Table 4.21

Experimental values of splay elastic constant (K_{11}) for various (T_c - T) values.

Sample 12CPS

T_c = 52.5° C , Sample thickness = 162 μm, H_c = Threshold magnetic field

T_c - T	H_c in Gauss	$\Delta\chi$ x 10^{-8} cgs unit	K_{11} x 10^{-6} dyne
1.5	725	2.9	0.41

Table 4.22

Experimental values of splay elastic constant (K_{33}) for various (T_c - T) values.

Sample 12CPS

T_c = 52.5° C , Sample thickness = 162 μm, H_c = Threshold magnetic field

T_c - T	H_c in Gauss	$\Delta\chi$ x 10^{-8} cgs unit	K_{33} x10^{-6} dyne
1.5	720	2.9	0.4

Table 4.23

Experimental values of the Frank elastic constant ratio (K_{33} / K_{11}) at different relative temperatures ($T_c - T$).

Sample: 10CPS		Sample: 12CPS	
$T_c - T$	K_{33} / K_{11}	$T_c - T$	K_{33} / K_{11}
1.7	0.89	1.5	.99
3.7	0.90		
5.7	0.92		
7.7	0.95		
9.7	0.97		

References:

1) R. Dabrowski, J. Dziaduszzek and T. Szczucinski, Mol. Cryst. Liq. Cryst., 102, 155 (1984).
2) R. Dabrowski, private communication.
3) J. W. Baran, Z. Raszewski, R. Dabrowski, J. Kedzierski and J. Rutkowska, Mol. Cryst. Liq. Cryst., 123, 237 (1985).
4) R. Dabrowski, private communication
5) M. Schadt, R. Buchecker, F. Leenhouts, A. Boller, A. Villiger and M. Petrzilka, Mol. Cryst. Liq. Cryst., 139, 1 (1986).
6) M. Schadt, M. Petrzilka, P. R. Gerber and A. Villiger, Mol. Cryst. Liq. Cryst., 122, 241 (1985).
7) W. H. de Jeu and W. A. P. Claassen, J. Chem, Phys., 67, 3705 (1977).

CHAPTER- 5

Magnetic susceptibility anisotropies of two mesogenic mixtures exhibiting induced smectic A_d phase

In this chapter the magnetic susceptibility anisotropy values of two different mesogenic mixture having different compositions have been reported. The mixtures studied have one component as 4-n-pentyl-4-n'-cyanobiphenyl (5CB in short) and the other component being 4-n-pentyl phenyl-4-n'-alkyloxy benzoate (alkyl=pentyl, ME5O.5 in short or alkyl=hexyl, ME6O.5 in short). Both these mixtures show induced smectic A_d phase, i.e., the components in pure form have nematic phases only, but on mixing produce mesogens having both nematic and smectic A_d phases in certain composition range. The mixture of 5CB+ME6O.5 has been extensively studied by Das and Paul [1,2]. They have given the phase diagram of the system as well as measured density and refractive indices at different composition [1]. They have also studied x-ray diffraction pattern from these mixtures and calculated the order parameters and layer thickness as a function of composition. The mixture 5CB+ME5O.5 has also been studied by different workers [3-5]. Dunmer et al.[4] have given the phase diagram of this system. Refractive indices have been measured by Palffy-Muhoray et al.[5], while Das et al.[3] have performed x-ray diffraction studies on this mixture. Orientational order parameters as calculated from refractive index and x-ray diffraction studies of both the mixtures, when plotted against the composition,show a minimum near the equimolar concentration [2,3]. The ratio of bend to splay elastic constants has been determined for one of the mixtures in our laboratory.[6]

The present work was undertaken to see whether $\Delta\chi$ the magnetic susceptibility anisotropy and $\langle P_2 \rangle$, the order parameter calculated from it also show a minimum at equimolar composition of these two mixtures or not. The phase diagrams of 5CB + ME5O.5 and 5CB + ME6O.5 are shown in Figures 5.1 and 5.2 respectively[1,4].

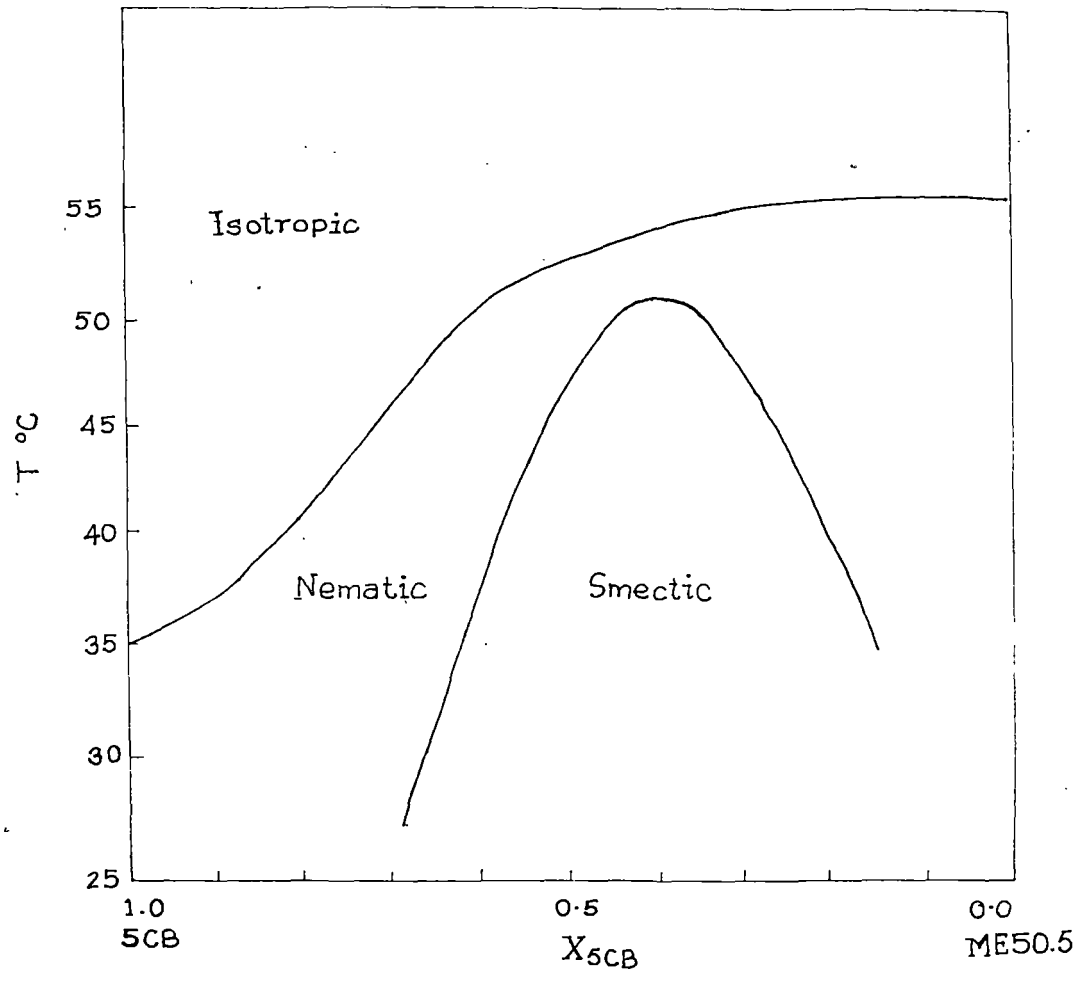

Figure 5.1. Phase diagram of 5CB/ME5O.5 mixture as a function of mole fraction (x_{5CB}) of 5CB [3].

For the study of the system 5CB + ME5O.5 (System I), six mixtures were prepared by mixing the weighed amount of pure components and heating the mixture to its clearing temperature and keeping it at that temperature for 3-4 hours with constant stirring to produce homogenous mixtures. The composition (mole fraction of 5CB) and the transition temperatures of these six mixtures are given below:

I. Mix. A_1 ($x_{5CB} = 0.206$)

$$K \xleftrightarrow{<20^0C} S_A \xleftrightarrow{36.7^0C} N \xleftrightarrow{53.7^0C} I$$

II. Mix. A_2 ($x_{5CB} = 0.303$)

$$K \xleftrightarrow{<20^0C} S_A \xleftrightarrow{45.2^0C} N \xleftrightarrow{53.5^0C} I$$

III. Mix. A_3 ($x_{5CB} = 0.40$)

$$K \xleftrightarrow{<20^0C} S_A \xleftrightarrow{48.8^0C} N \xleftrightarrow{53.7^0C} I$$

IV. Mix. A_4 ($x_{5CB} = 0.501$)

$$K \xleftrightarrow{<20^0C} S_A \xleftrightarrow{46.4^0C} N \xleftrightarrow{52.1^0C} I$$

V. Mix. A_5 ($x_{5CB} = 0.59$)

$$K \xleftrightarrow{<20^0C} S_A \xleftrightarrow{39.6^0C} N \xleftrightarrow{49.7^0C} I$$

VI. Mix. A_6 ($x_{5CB} = 0.702$)

$$K \xleftrightarrow{<20^0C} N \xleftrightarrow{44.1^0C} I$$

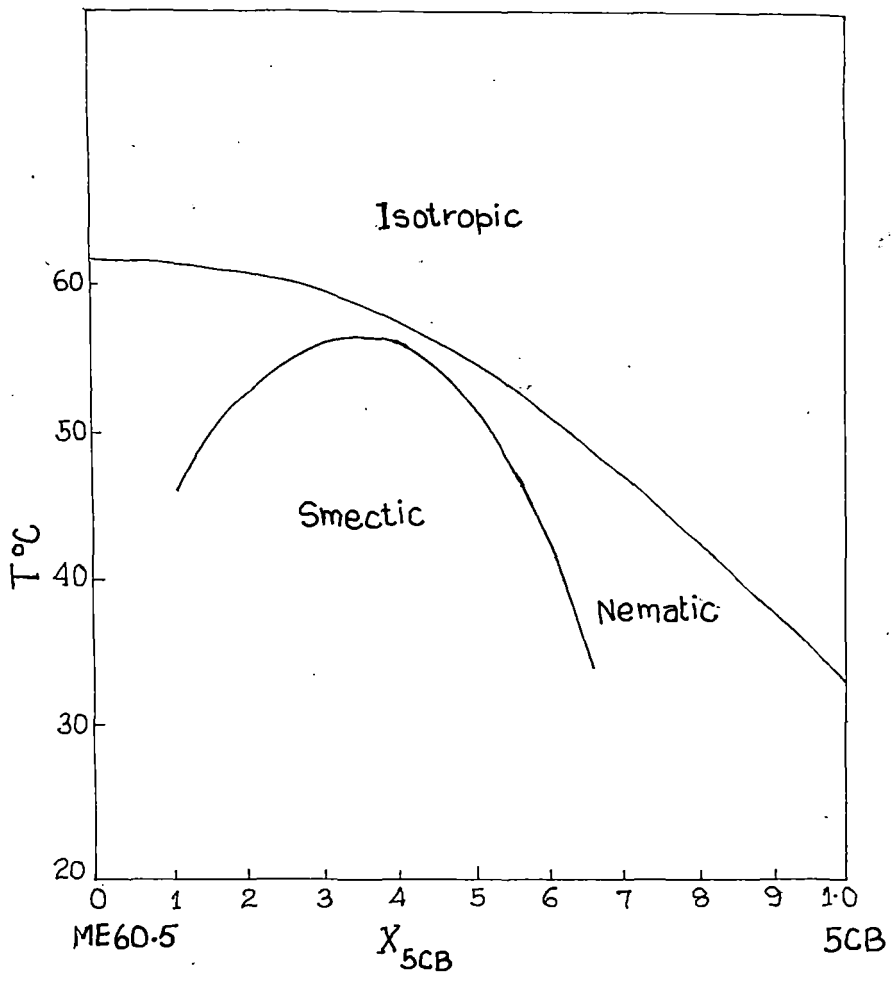

Figure 5.2. Phase diagram of 5CB/ME6O.5 mixture as a function of mole fraction (x_{5CB}) of 5CB [2].

Similarly, for the system 5CB + ME6O.5 (System II), eight mixtures with different compositions were prepared for our study. The composition and the transition temperatures of these eight mixtures are noted below:

I. Mix. B_1 ($x_{5CB} = 0.1845$)

$$K \xleftarrow{<20^0C} S_A \xleftarrow{52.5^0C} N \xleftarrow{61.5^0C} I$$

II. Mix. B_2 ($x_{5CB} = 0.2488$)

$$K \xleftarrow{<20^0C} S_A \xleftarrow{54.7^0C} N \xleftarrow{61.^0C} I$$

III. Mix. B_3 ($x_{5CB} = 0.3025$)

$$K \xleftarrow{<20^0C} S_A \xleftarrow{57.2^0C} N \xleftarrow{60.2^0C} I$$

IV. Mix. B_4 ($x_{5CB} = 0.4008$)

$$K \xleftarrow{<20^0C} S_A \xleftarrow{57.3^0C} N \xleftarrow{59.2^0C} I$$

V. Mix. B_5 ($x_{5CB} = 0.4986$)

$$K \xleftarrow{<20^0C} S_A \xleftarrow{52.8^0C} N \xleftarrow{56.3^0C} I$$

VI. Mix. B_6 ($x_{5CB} = 0.55973$)

$$K \xleftarrow{<20^0C} S_A \xleftarrow{48.1^0C} N \xleftarrow{54.8^0C} I$$

VII. Mix. B_7 ($x_{5CB} = 0.6427$)

$$K \xleftarrow{<20^0C} S_A \xleftarrow{41.9^0C} N \xleftarrow{51.9^0C} I$$

VIII. Mix. B_8 ($x_{5CB} = 0.7075$)

$$K \xleftarrow{<20^0C} N \xleftarrow{48.6^0C} I$$

Some of the mixtures in both the systems show co-existence of both nematic and isotropic phases over a small temperature range (~0.5°C) at the clearing point.

Of the six mixtures of System I, one has only nematic phase, all other have both nematic and smectic A_d phases. The densities and the magnetic susceptibilities were measured using the methods described in detail in Chapter 2.

The experimental values of densities, $\chi_{\|}$, the magnetic susceptibility along the director, $\Delta\chi$, the magnetic susceptibility anisotropy and calculated $\langle P_2 \rangle$ values, for these six mixtures (A_1 to A_6) are tabulated in Tables 5.1 to 5.6 respectively. The extrapolated values [7] of $\Delta\chi$ for perfectly aligned samples are also given in these tables. The magnetic susceptibility of the pure ME5O.5 and ME6O.5 have also been measured, but these values are given in Chapter-7.

Figures 5.3a - 5.3e show the temperature variation of density of the five mixtures. The density of one of the mixture (mix. A_3) is interpolated values from Das et al [3]. In general near mid compositon region, the density changes at nematic to smectic A transition are greater than those at nematic to isotropic transition. Similar result on this system has already been reported[3] for this system at $x_{5CB} = 0.4$.

The temperature variations of $\Delta\chi$ for these mixtures are shown in Figures 5.4a -5.4f. The changes in $\Delta\chi$ values at the smectic A to nematic transition are more pronounced for mixtures A_4 (x=0.501) and A_5(x=0.590). The temperature variations of order parameters are shown in Fig. 5.5a-5.5f.

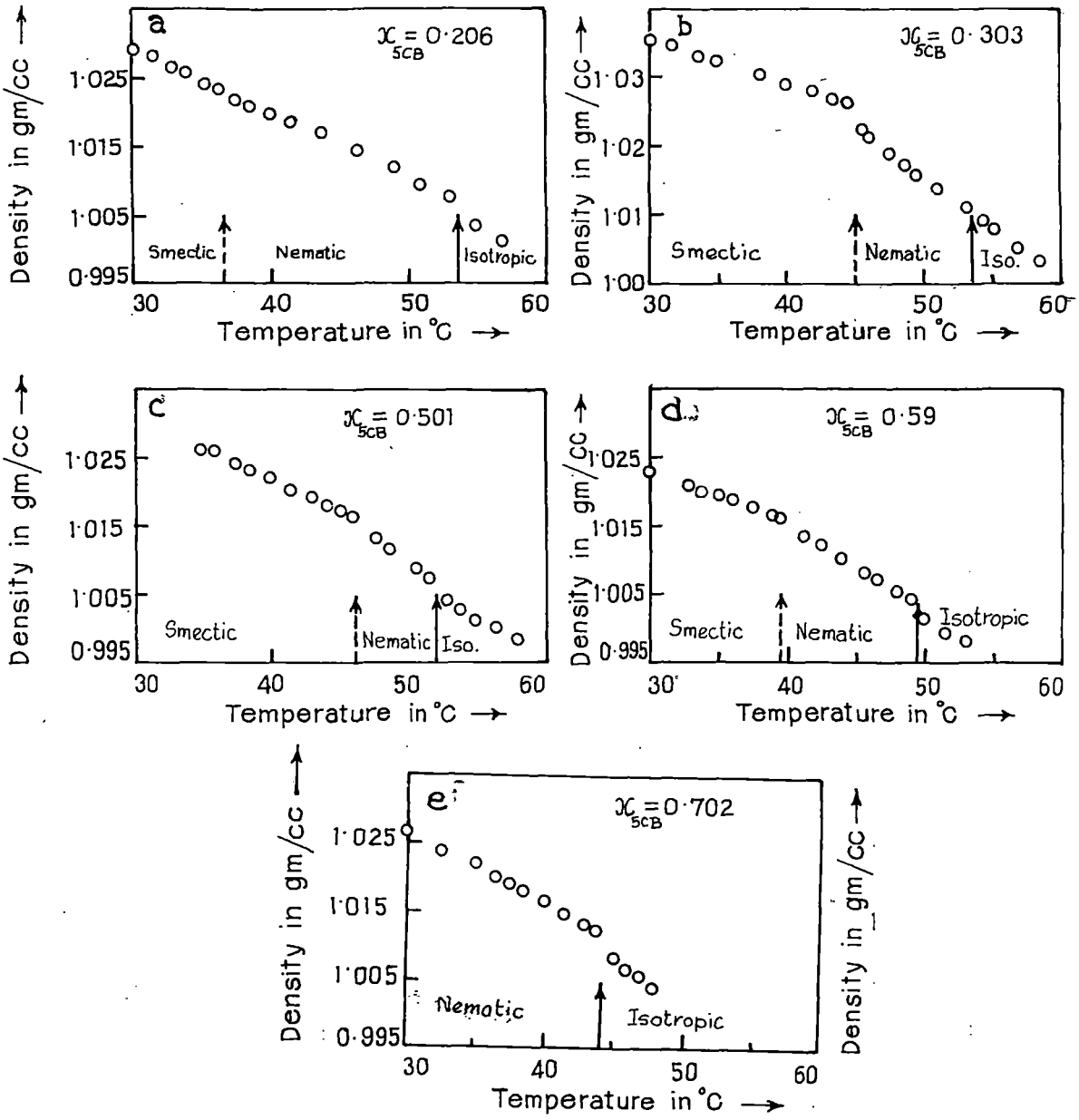

Figure 5.3a- 5.3e. Density values as a function of temperature for 5CB and ME5O.5 mixture.

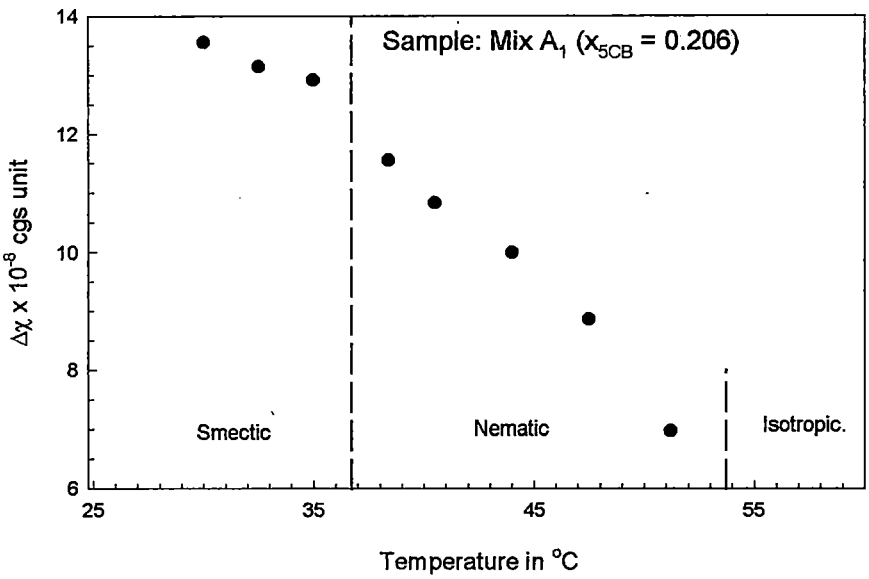

Figure 5.4a. Temperature variation of the anisotropy of the diamagnetic susceptibility ($\Delta\chi$).

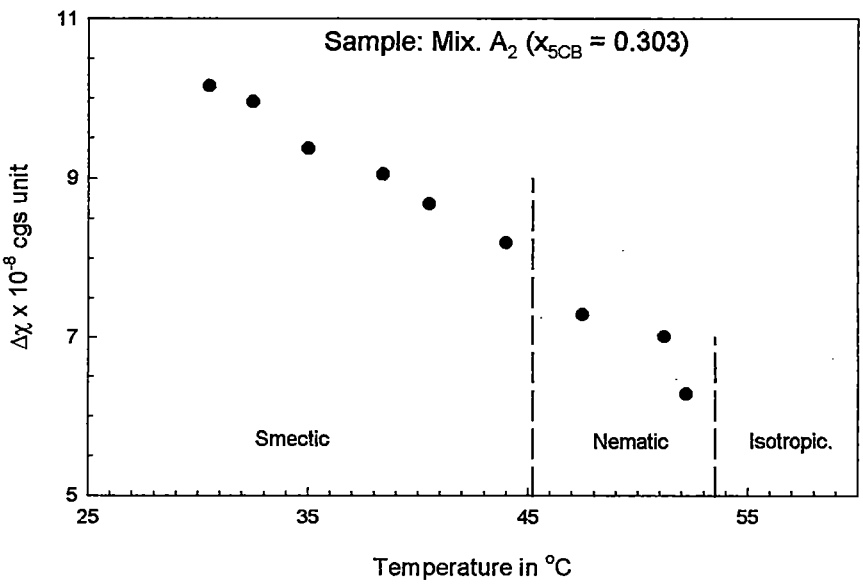

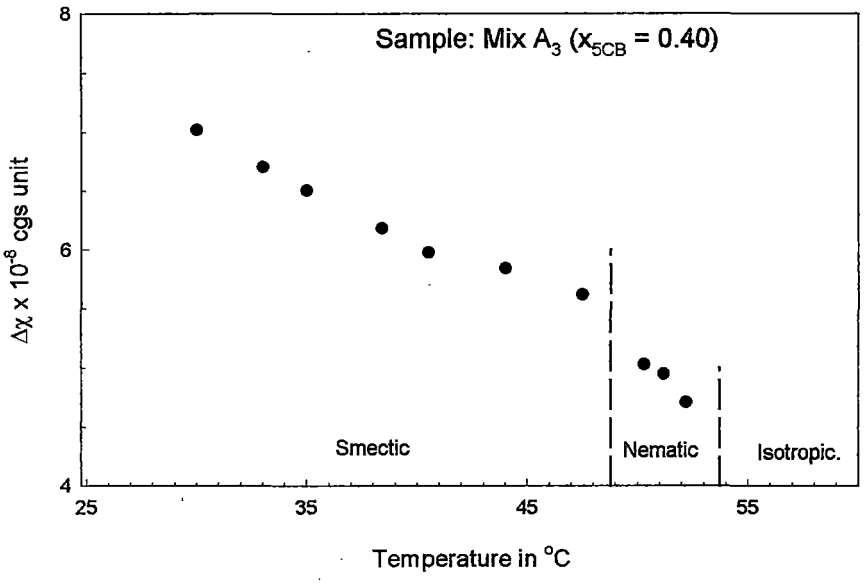

Figure 5.4c. Temperature variation of the anisotropy of the diamagnetic susceptibility ($\Delta\chi$).

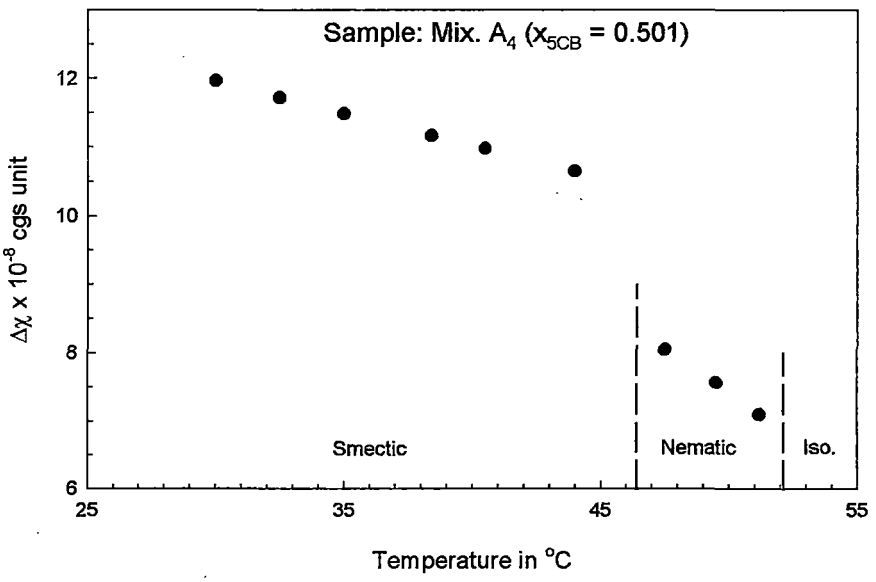

Figure 5.4d. Temperature variation of the anisotropy of the diamagnetic susceptibility ($\Delta\chi$).

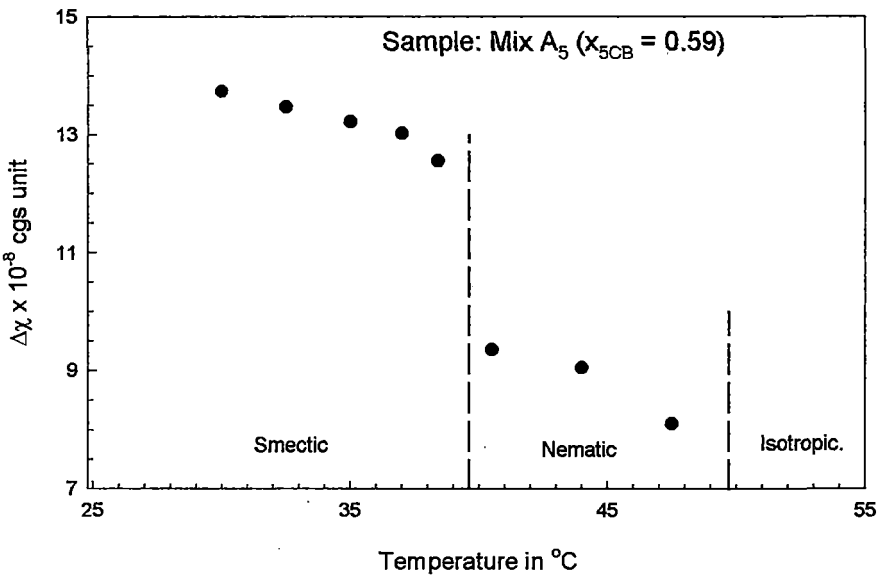

Figure 5.4e. Temperature variation of the anisotropy of the diamagnetic susceptibility ($\Delta\chi$).

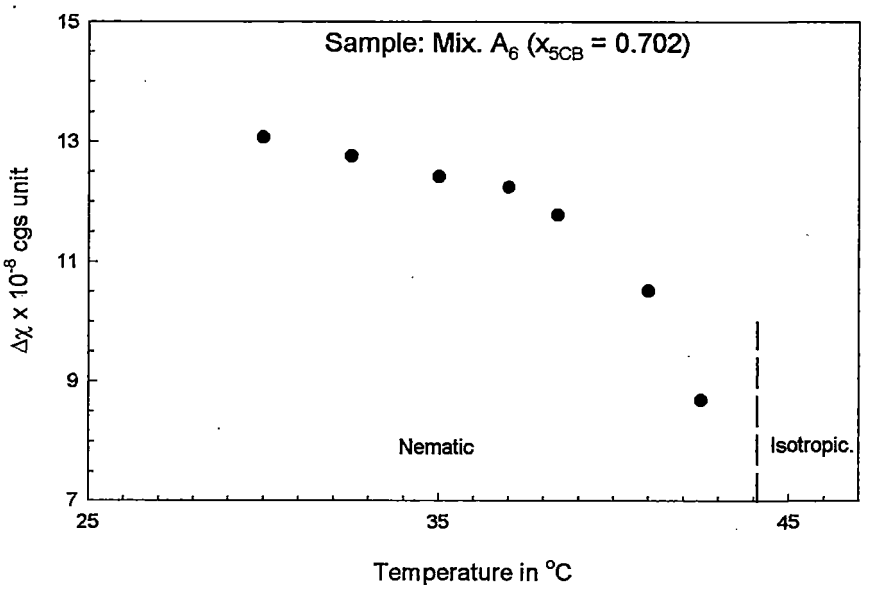

Figure 5.4f. Temperature variation of the anisotropy of the diamagnetic susceptibility ($\Delta\chi$).

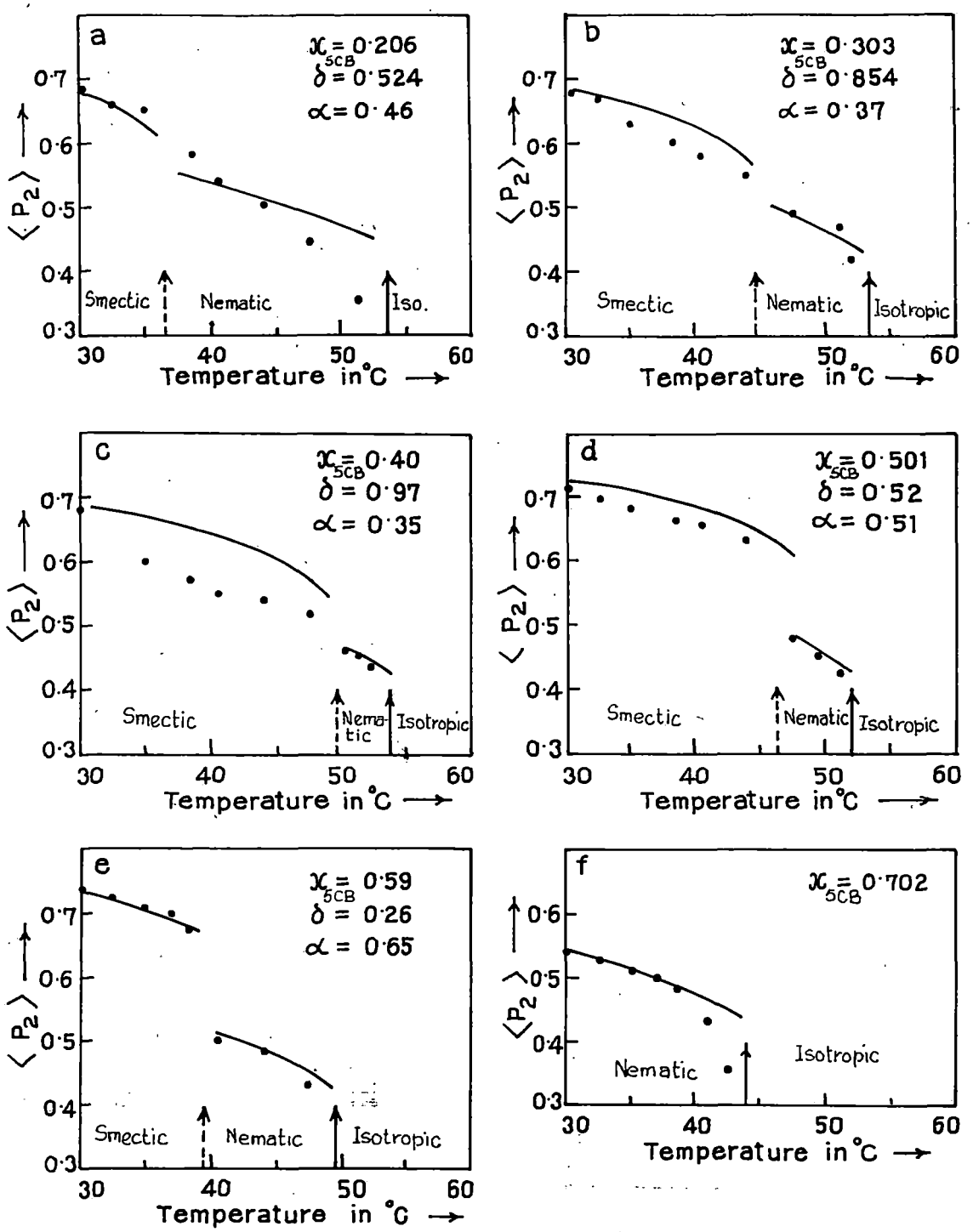

Figure 5.5a-5.5f. Temperature variation of order parameter $\langle P_2 \rangle$ for 5CB and ME 5O.5 mixture.

x_{5CB} is the mole fraction of of 5CB, δ and α are McMillan potential parameter. Solid line in Figure5a-5e indicates McMillan theoretical $\langle P_2 \rangle$ values. Solid line in Figure5f indicates Maier-Saupe theoretical $\langle P_2 \rangle$ values. • = experimental data for $\langle P_2 \rangle$.

We have also tried to fit theoretical McMillan's[8] order parameter values with our experimental values by varying the α and δ parameters of the potential. For mixtures A_2, A_4, A_5 and A_6 the agreements with theoretical values are good. Mixture A_7 has only nematic phase, hence the experimental $<P_2>$ values have been compared with theoretical Maier-Saupe values. In this case agreement is fairly good except near the nematic-isotropic transition temperature. However, the experimental order parameter values for mixture A_1 and A_3 could not be fitted well with McMillan's values with any combination α and δ.

Figure 5.6 shows the composition variation of the order parameter in the mixture 5CB + ME5O.5 at a constant temperature of 35 ^{0}C. The order parameter values of the x-ray diffraction data of Das et al.[3] are also shown in this figure. The two sets of $< P_2 >$ values are consistent within experimental errors. The minimum in $< P_2 >$ values occurs near the mole fraction of 5CB equal to 0.4.

The composition variation of the magnetic susceptibility in the isotropic phase of the mixtures A_1 to A_6 is shown in Figure 5.7. The experimental value of the pure component ME5O.5 is also plotted in the figure, though the experimental value of this mesogen has been given in Chapter 7. I have also measured χ_{iso} value of 5CB and it is included in the figure. It can be seen that χ_{iso} varies linearly with mole fraction as is expected.

Of the eight mixtures of System II, one has only nematic phase, all others have both nematic and smectic A_d phases. The densities of several mixtures of this system have already been reported by Das et al. [1]. The magnetic susceptibilities along the director, $\chi_{\|}$, of all the mixtures were measured using the procedure described in Chapter 2. The density values

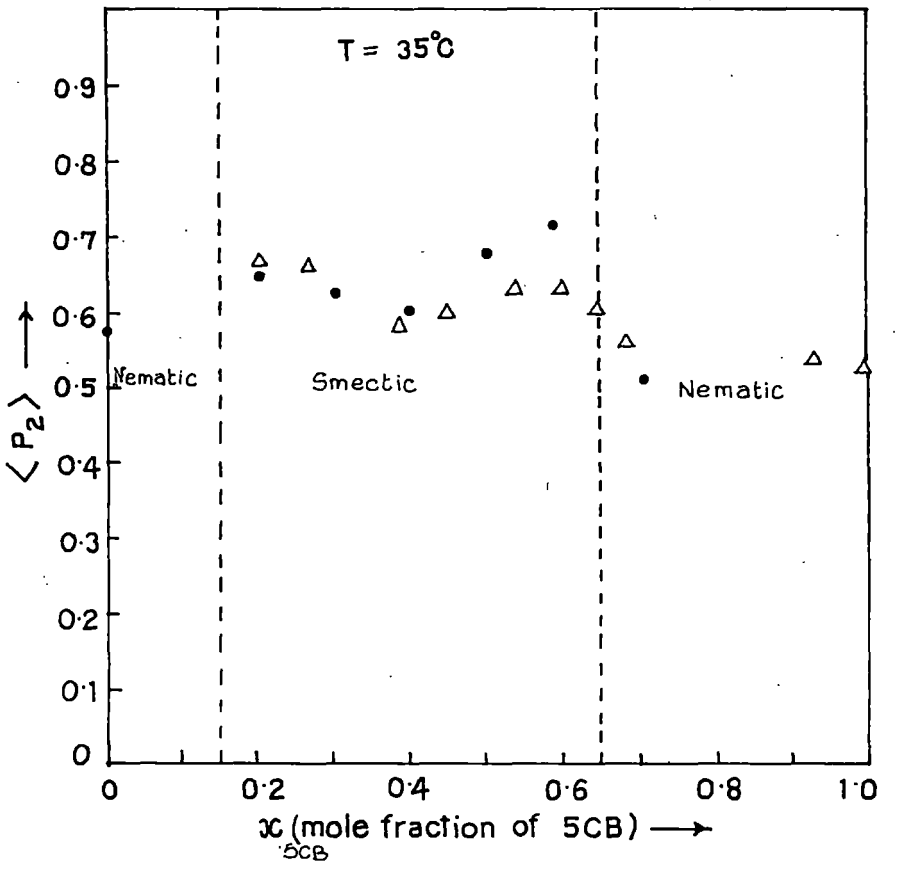

Figure 5.6. Variation of order parameter $\langle P_2 \rangle$ of 5CB and ME 5O.5 mixture with mole fraction of 5CB (x_{5CB}) at a fixed temperature 35°C.

• - present data from magnetic susceptibility ($\Delta\chi$) measurement

Δ - data from x-ray measurement by Das et al. [3].

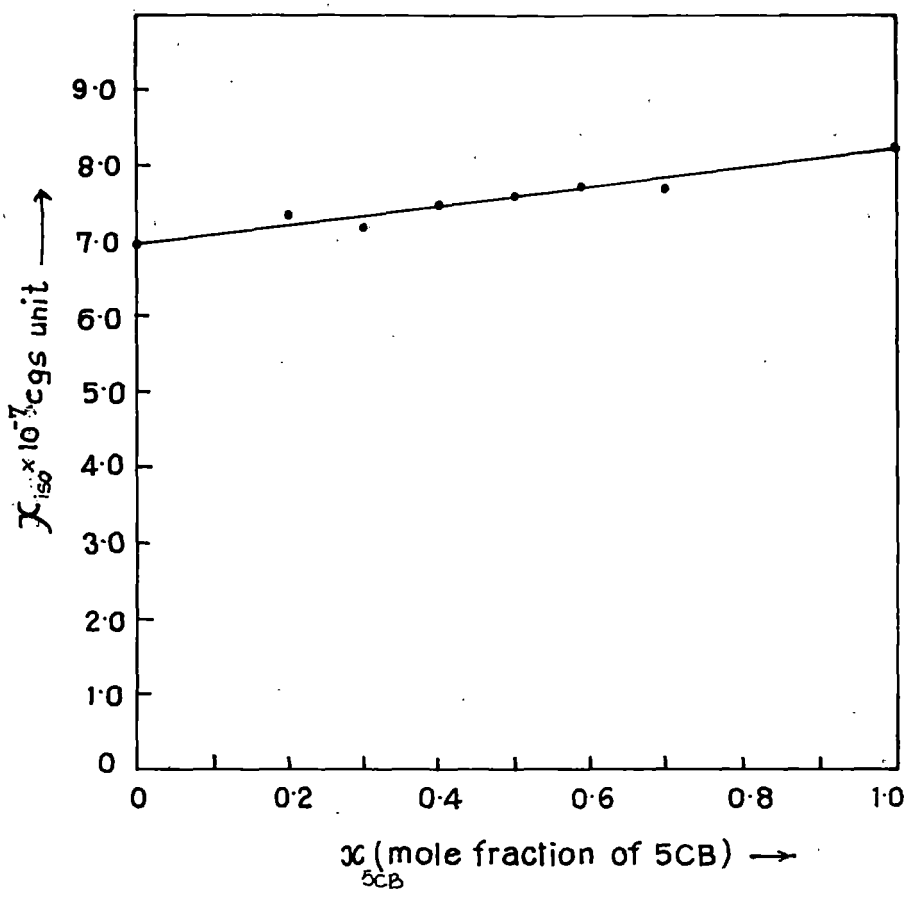

Figure 5.7. Variation of χ_{iso} of 5CB and ME5O.5 mixture with mole fraction of 5CB (x_{5CB}). Straight line is guide to the eye only.

for the present mixtures were interpolated from the values given by Das et al. [2].

The interpolated values of densities and experimetnal $\chi_{\|}$ values together with $\Delta\chi$ and calculated order parameter values at different temperatures for mixtures B_1 to B_8 are tabulated in Tables 5.7 to 5.14.

Mixtures B_1 ($x_{5CB} = 0.1845$) has induced smectic A_d phase. However, magnetic susceptibility values of mixture B_1 in smectic A_d phase have not been shown in Table 5.7. The experimental values in this phase were not consistent and this may be due to the applied magnetic field being not strong enough to align the sample properly. We had no problem in aligning any other smectic A_d phase of these mixtures.

The values of $\Delta\chi$ for perfectly aligned samples, obtained by Hallers [7] extrapolation procedure, are also given in these Tables. The magnetic susceptibility of ME6O.5 has also been measured, but the data are given in Chapter 7.

The temperature variations of magnetic suceptibility anisotropy ($\Delta\chi$) for mixtures B_1 to B_8 are shown in Figures 5.8a -5.8h. Again the changes in $\Delta\chi$ at smectic A_d to nematic phase transition are the largest near the equimolar compositions. The temperature variations of order parameters for mixtures B_1 to B_8 are shown in Figures 5.9a to 5.9h. Again we have tried to fit our experimental order parameter values with the theoretical $\langle P_2 \rangle$ values calculated from McMillan's theory [8] by varying the values of the potential parameters α and δ. The $\langle P_2 \rangle$ values for mixtures B_1 and B_8 have been compared with Maier-Saupe values, since mixture B_8 has only nematic phase and for mixture B_1 the experimental data are avaliable only in the nematic phase. It can be seen that the agreements with theoretical values are good except for mixtures B_3, B_4 and B_5, which are in the middle

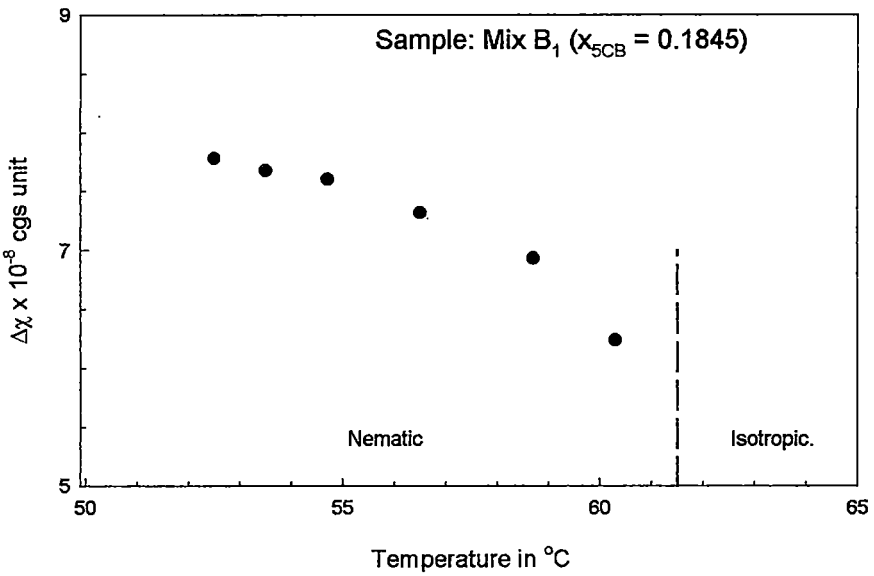

Figure 5.8a. Temperature variation of the anisotropy of the diamagnetic susceptibility ($\Delta\chi$).

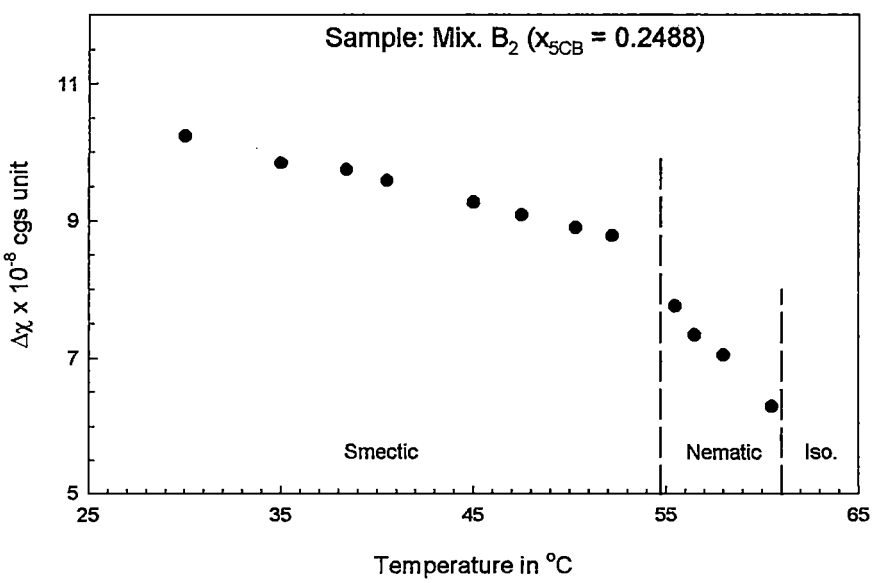

Figure 5.8b. Temperature variation of the anisotropy of the diamagnetic susceptibility ($\Delta\chi$).

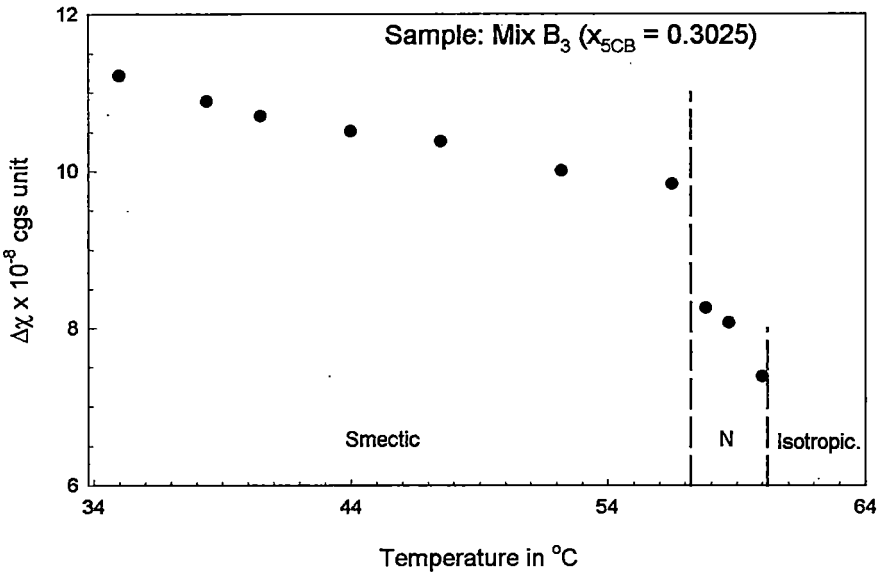

Figure 5.8c. Temperature variation of the anisotropy of the diamagnetic susceptibility ($\Delta\chi$).

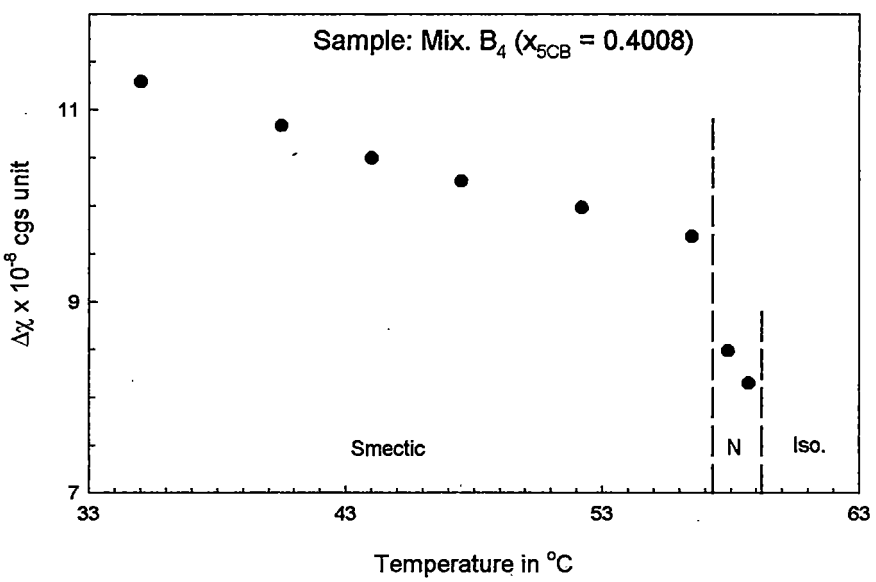

Figure 5.8d. Temperature variation of the anisotropy of the diamagnetic susceptibility ($\Delta\chi$).

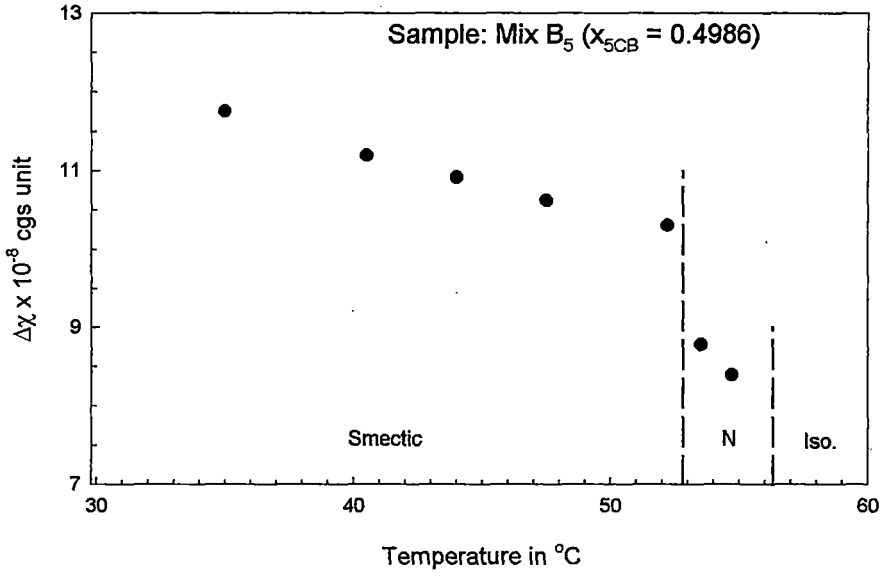

Figure 5.8e. Temperature variation of the anisotropy of the diamagnetic susceptibility ($\Delta\chi$).

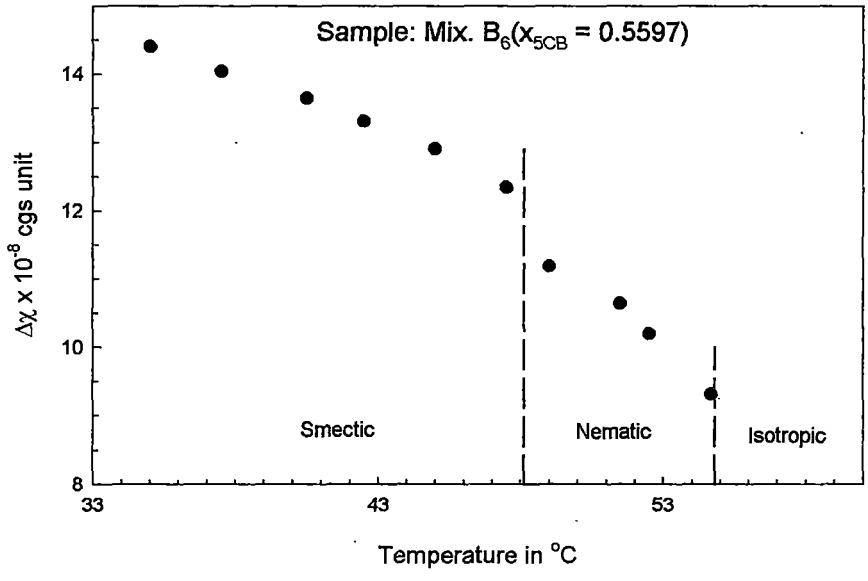

Figure 5.8f. Temperature variation of the anisotropy of the diamagnetic susceptibility ($\Delta\chi$).

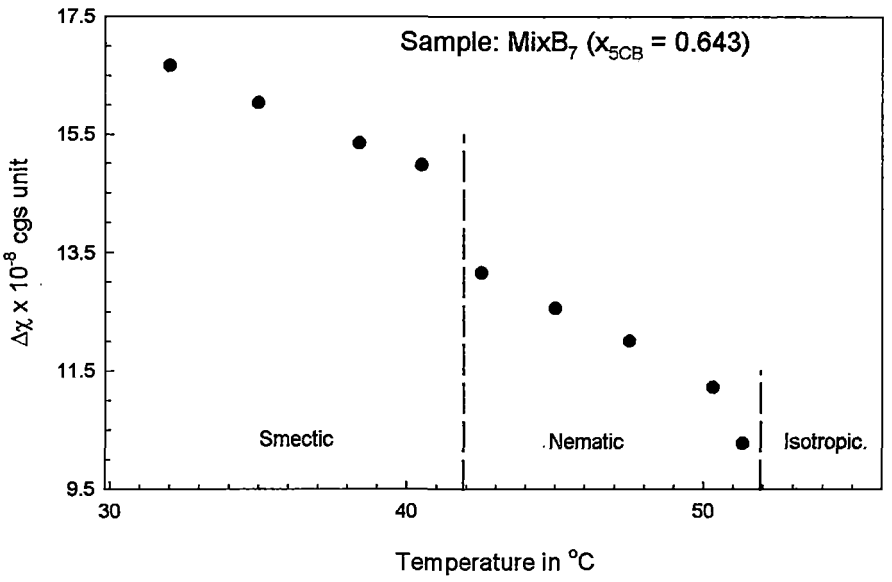

Figure 5.8g. Temperature variation of the anisotropy of the diamagnetic susceptibility ($\Delta\chi$).

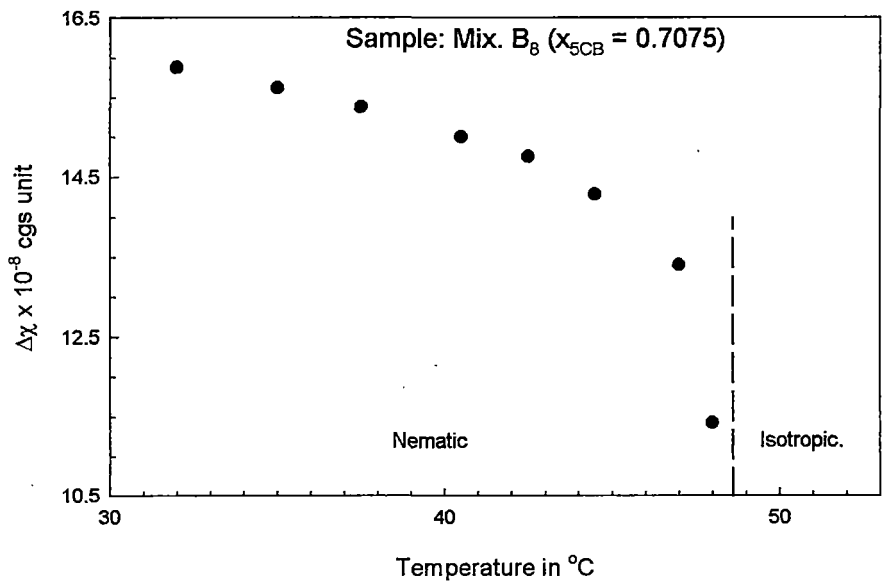

Figure 5.8h. Temperature variation of the anisotropy of the diamagnetic susceptibility ($\Delta\chi$).

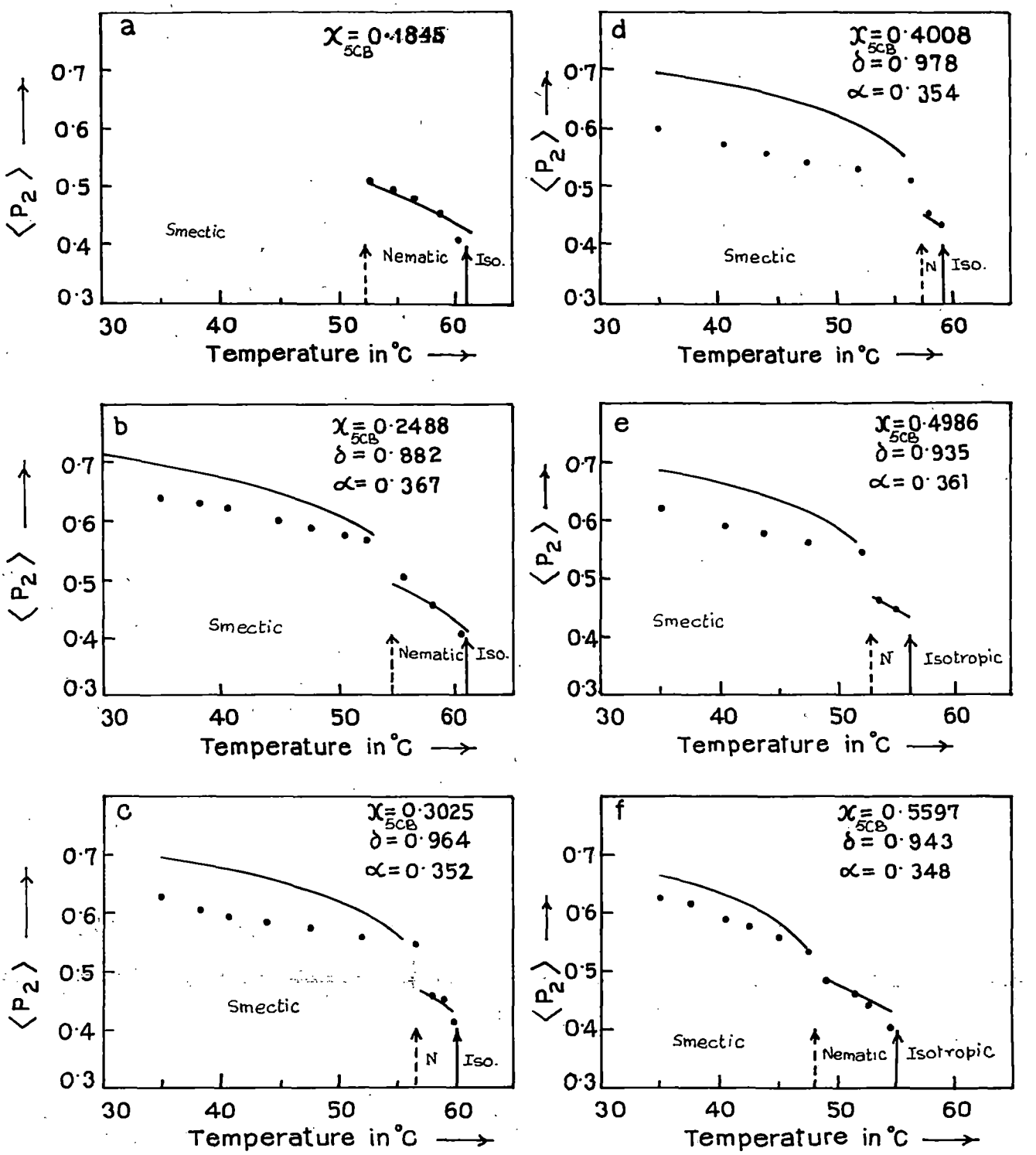

Figure 5.9a-5.9f. Temperature variation of order parameter $\langle P_2 \rangle$ for 5CB and ME 6O.5 mixture.

x_{5CB} is the mole fraction of of 5CB, δ and α are McMillan potential parameter. Solid line in Figure5a-5e indicates McMillan theoretical $\langle P_2 \rangle$ values. Solid line in Figure5f indicates Maier-Saupe theoretical $\langle P_2 \rangle$ values. • = experimental data for $\langle P_2 \rangle$.

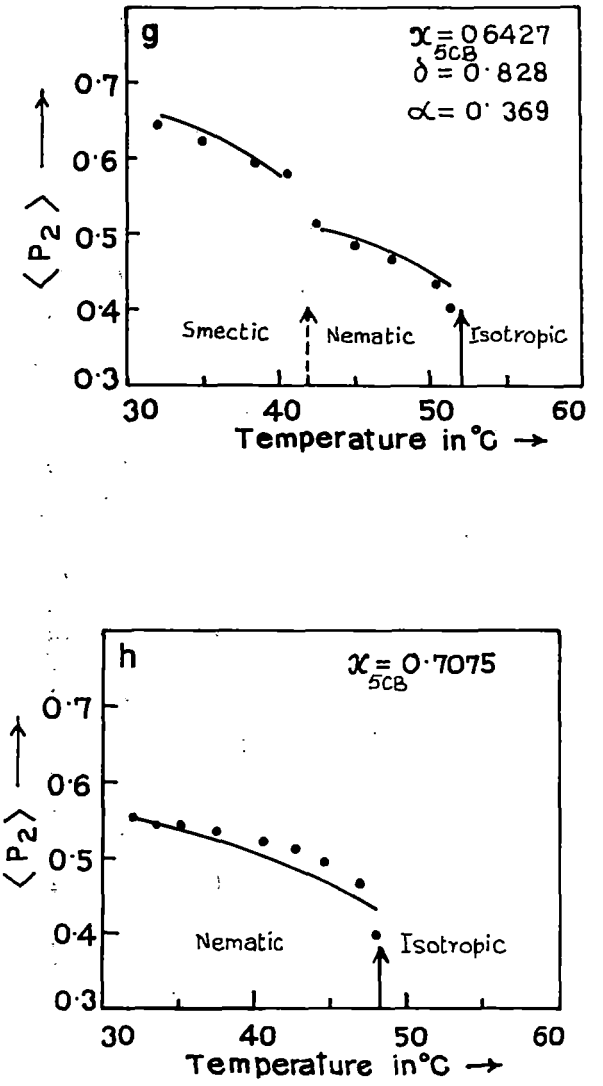

Figure 5.9g-5.9h. Temperature variation of order parameter $\langle P_2 \rangle$ for 5CB and ME 6O.5 mixture.

x_{5CB} is the mole fraction of of 5CB, δ and α are McMillan potential parameter. Solid line in Figure5a-5e indicates McMillan theoretical $\langle P_2 \rangle$ values. Solid line in Figure5f indicates Maier-Saupe theoretical $\langle P_2 \rangle$ values. • = experimental data for $\langle P_2 \rangle$.

composition region. It may not be out of place to mention that in System I also the worse fittings with theoretical values were the mixtures having composition around $x_{5CB} = 0.4$. In particular, in mixtures A_3 ($x_{5CB} = 0.40$) and B_4 ($x_{5CB} = 0.4008$) the agreement are the worst. This is the composition at which the order parameter values show a minimum (Figures 5.6 and 5.10). Figure 5.10 shows the composition variation of order parameter of mixtures B_1 to B_8 at a constant temperatures of 35 ^{0}C. Also shown in the figure are the experimental $\langle P_2 \rangle$ values of Das et al. [2] from x-ray diffraction data. The agreement between two sets of $\langle P_2 \rangle$ values is fair. Again, the minimum value of $\langle P_2 \rangle$ occurs near $x_{5CB} \approx 0.4$.

The composition variation of magnetic susceptibility in the isotropic phase of mixtures B_1 to B_8 is shown in Figure 5.11. The χ_{iso} values for the pure components are also shown in the figure. Again χ_{iso} varies linearly with composition as is expected.

In conclusion, we find that our magnetic susceptibility data corroborats the findings from x-ray diffraction and refractive index studies on these two systems. The maximum in the stability of smectic A_d phases (Please see the phase diagrams Fig.5.1 and 5.2) corresponds to the minimum of the order parameter. The smectic layer spacing shows a minimum in the same compostion range [2,3]. The minimum layer spacing can be attributed to specific interaction between the components of the mixtures, which stabilise the traslationally ordered smectic A_d phases, but in trying to pack the different molecules in layers these interactions in effect lower the orientational order within the layers. This lowering in the order parameter values has been confirmed by our present magnetic susceptibility studies.

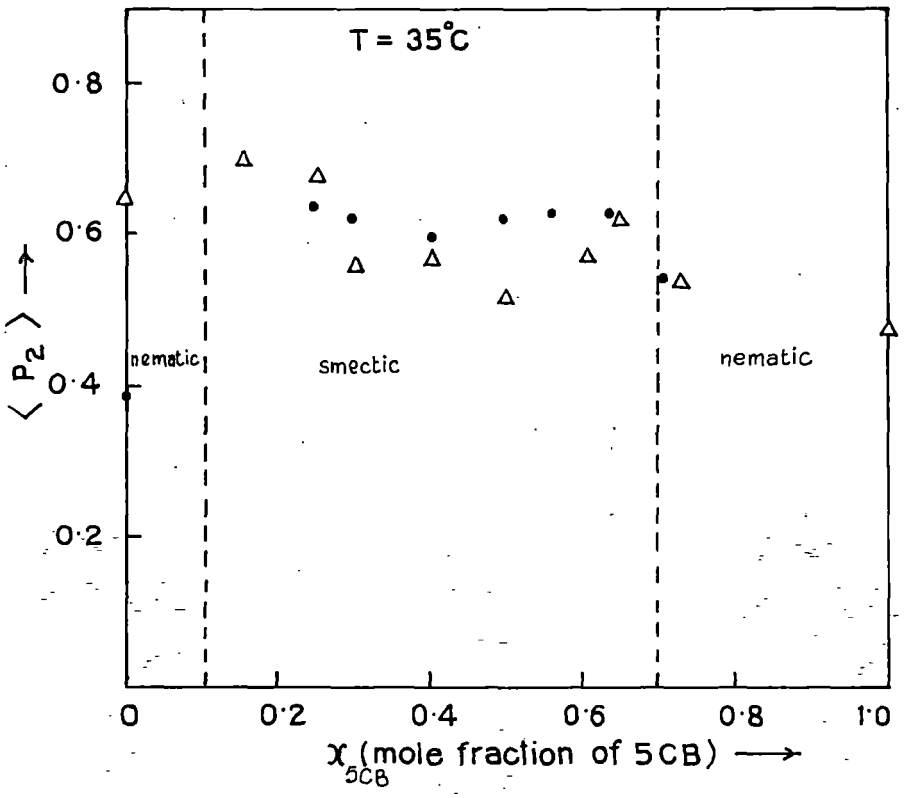

Figure 5.10. Variation of order parameter $\langle P_2 \rangle$ of 5CB and ME 6O.5 mixture with mole fraction of 5CB (x_{5CB}) at a fixed temperature 35°C.

- present data from magnetic susceptibility ($\Delta\chi$) measurement
- data from x-ray measurement by Das et al. [2].

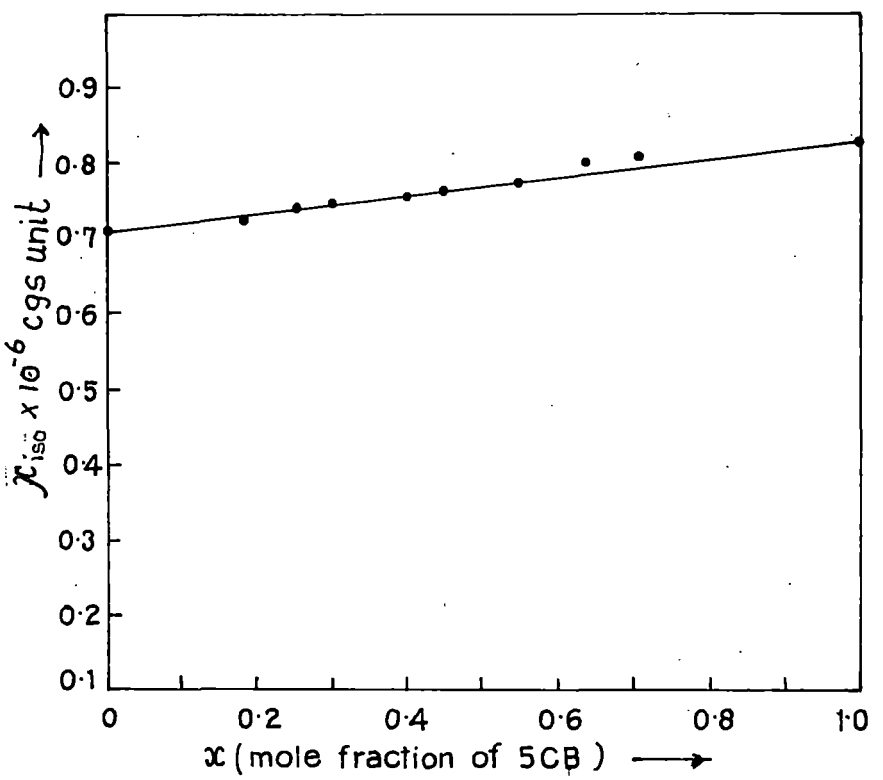

Figure 5.11. Variation of χ_{iso} of 5CB and ME5O.5 mixture with mole fraction of 5CB (x_{5CB}). Straight line is guide to the eye only.

Table 5.1

Experimental values of the density (ρ), magnetic susceptibility (χ), susceptibility anisotropy ($\Delta\chi$), and the order parameter $< P_2 >$

Sample: Mixture (A_1) of ME5O.5 and 5CB

$x_{5CB} = 0.206$

Temp. in °C	Density (ρ) in gm/cc	$-\chi_{\parallel}$ x 10^{-7} c.g.s.unit	$\Delta\chi$ x 10^{-8} c.g.s.unit	order parameter $< P_2 >$
30.0	1.030	6.48	13.5	0.681
32.5	1.027	6.51	13.1	0.661
35.0	1.024	6.53	12.9	0.649
38.4	1.021	6.62	11.5	0.581
40.5	1.020	6.66	10.8	0.544
44.0	1.017	6.72	10.0	0.502
47.5	1.011	6.79	8.9	0.446
51.2	1.009	6.92	7.0	0.350
56.5	1.002	7.38 = $\bar{\chi}_{iso}$		

$\Delta\chi_o = 1.99 \times 10^{-7}$ c.g.s.unit;

Table 5.2

Experimental values of the density (ρ) , magnetic susceptibility (χ) , susceptibility anisotropy ($\Delta\chi$) , and the order parameter $< P_2 >$

Sample: Mixture (A_2) of ME5O.5 and 5CB

$x_{5CB} = 0.303$

Temp. in $^{\circ}$C	Density (ρ) in gm/cc	$-\chi_{\parallel}$ x 10^{-7} c.g.s.unit	$\Delta\chi$ x 10^{-8} c.g.s.unit	order parameter $< P_2 >$
30.5	1.036	6.51	10.1	0.682
32.5	1.034	6.52	9.9	0.669
35.0	1.033	6.56	9.4	0.630
38.4	1.030	6.58	9.0	0.608
40.5	1.029	6.61	8.7	0.583
44.0	1.026	6.64	8. 2	0.551
47.5	1.019	6.70	7.3	0.490
51.2	1.014	6.72	7.0	0.471
52.2	1.013	6.77	6.3	0.422
56.5	1.006	7.187 = $\bar{\chi}_{iso}$		

$\Delta\chi_o$ = 1.488 x 10^{-7} c.g.s.unit;

Table 5.3

Experimental values of the density (ρ), magnetic susceptibility (χ), susceptibility anisotropy ($\Delta\chi$), and the order parameter $< P_2 >$

Sample: Mixture (A_3) of ME5O.5 and 5CB

$x_{5CB} = 0.400$

Temp. in °C	Density (ρ) in gm/cc	$-\chi_{\parallel} \times 10^{-7}$ c.g.s.unit	$\Delta\chi \times 10^{-8}$ c.g.s.unit	order parameter $< P_2 >$
30.0	1.028	7.06	7.0	0.650
33.0	1.026	7.08	6.7	0.620
35.0	1.025	7.09	6.5	0.602
38.4	1.022	7.11	6.2	0.573
40.5	1.021	7.13	6.0	0.554
44.0	1.018	7.14	5.8	0.541
47.5	1.009	7.15	5.6	0.520
50.3	1.008	7.19	5.0	0.466
51.2	1.0075	7.20	4.9	0.458
52.2	1.006	7.21	4.7	0.436
56.5	1.001	$7.52 = \bar{\chi}_{iso}$		

$\Delta\chi_o = 1.08 \times 10^{-7}$ c.g.s. unit;

Table 5.4

Experimental values of the density (ρ) , magnetic susceptibility (χ) , susceptibility anisotropy (Δχ) , and the order parameter < P_2 >

Sample: Mixture (A_4) of ME5O.5 and 5CB

$x_{5CB} = 0.501$

Temp. in °C	Density (ρ) in gm/cc	$-\chi_{\parallel}$ x 10^{-7} c.g.s.unit	$\Delta\chi$ x 10^{-8} c.g.s.unit	order parameter < P_2 >
30.0	1.0315	6.83	11.9	0.712
32.5	1.0290	6.84	11.7	0.693
35.0	1.0265	6.86	11.5	0.683
38.4	1.0233	6.88	11.2	0.664
40.5	1.0212	6.89	11.0	0.653
44.0	1.0188	6.91	10.7	0.634
47.5	1.0129	7.09	8.0	0.479
49.5	1.0100	7.12	7.6	0.450
51.2	1.0075	7.15	7.1	0.423
52.2	1.0061	7.62 = $\bar{\chi}_{iso}$		

$\Delta\chi_o = 1.68 \times 10^{-7}$ c.g.s.unit;

Table 5.5

Experimental values of the density (ρ), magnetic susceptibility (χ), susceptibility anisotropy ($\Delta\chi$), and the order parameter $< P_2 >$

Sample: Mixture (A_5) of ME5O.5 and 5CB

$x_{5CB} = 0.59$

Temp. in °C	Density (ρ) in gm/cc	$-\chi_{\parallel}$ x 10^{-7} c.g.s.unit	$\Delta\chi$ x 10^{-8} c.g.s.unit	order parameter $< P_2 >$
30.0	1.0230	6.79	13.7	0.738
32.5	1.0212	6.81	13.5	0.724
35.0	1.0195	6.83	13.2	0.711
37.0	1.0182	6.84	13.0	0.700
38.4	1.0170	6.87	12.5	0.675
40.5	1.0140	7.08	9.3	0.503
44.0	1.0103	7.11	9.0	0.486
47.5	1.0049	7.17	8.1	0.436
52.2	0.9988	7.71 = $\bar{\chi}_{iso}$		

$\Delta\chi_o = 1.86$ x 10^{-7} c.g.s.unit;

Table 5.6

Experimental values of the density (ρ) , magnetic susceptibility (χ) , susceptibility anisotropy ($\Delta\chi$) , and the order parameter $< P_2 >$

Sample: Mixture (A_6) of ME5O.5 and 5CB

$x_{5CB} = 0.702$

Temp. in ^{o}C	Density (ρ) in gm/cc	$-\chi_{\parallel} \times 10^{-7}$ c.g.s.unit	$\Delta\chi \times 10^{-8}$ c.g.s.unit	order parameter $< P_2 >$
30.0	1.0270	6.85	13.1	0.539
32.5	1.0245	6.87	12.8	0.526
35.0	1.0220	6.90	12.4	0.512
37.0	1.0195	6.91	12.2	0.505
38.4	1.0178	6.94	11.8	0.486
41.0	1.0160	7.02	10.5	0.434
42.5	1.0140	7.15	8.7	0.358
44.5	1.0106	7.72 $= \bar{\chi}_{iso}$		

$\Delta\chi_o = 2.425 \times 10^{-7}$ c.g.s.unit;

Table 5.7

Experimental values of the density (ρ) , magnetic susceptibility (χ) , susceptibility anisotropy ($\Delta\chi$) , and the order parameter $< P_2 >$

Sample: Mixture (B_1) of ME6O.5 and 5CB

$x_{5CB} = 0.1845$

Temp. in °C	Density (ρ)* in gm/cc	$-\chi_{\parallel} \times 10^{-7}$ c.g.s.unit	$\Delta\chi \times 10^{-8}$ c.g.s.unit	order parameter $< P_2 >$
52.5	1.0110	6.72	7. 8	0.511
53.5	1.0095	6.73	7.7	0.504
54.7	1.0076	6.73	7.6	0.499
56.5	1.0050	6.75	7.3	0.481
58.7	1.0030	6.78	6.9	0.455
60.3	1.0020	6.83	6.2	0.410
61.6	1.0010	$7.24 = \bar{\chi}_{iso}$		

$\Delta\chi_o = 1.523 \times 10^{-7}$ c.g.s.unit;

* Interpolated values from reference [1].

Table 5.8

Experimental values of the density (ρ), magnetic susceptibility (χ), susceptibility anisotropy ($\Delta\chi$), and the order parameter $< P_2 >$

Sample: Mixture (B_2) of ME6O.5 and 5CB

$x_{5CB} = 0.2488$

Temp. in °C	Density (ρ)* in gm/cc	$-\chi_{\parallel} \times 10^{-7}$ c.g.s.unit	$\Delta\chi \times 10^{-8}$ c.g.s.unit	order parameter $< P_2 >$
30	1.0372	6.71	10.2	0.664
35	1.0325	6.74	9.8	0.638
38.4	1.0293	6.74	9.7	0.632
40.5	1.0252	6.75	9.6	0.622
45.0	1.0163	6.77	9.3	0.601
47.5	1.0121	6.79	9.1	0.589
50.3	1.0067	6.80	8.9	0.577
52.2	1.0022	6.81	8.8	0.569
55.5	0.9992	6.88	7.7	0.503
56.5	0.9959	6.90	7.3	0.476
58.0	0.9929	6.92	7.0	0.457
60.5	0.9905	6.97	6.3	0.408
63.5	0.9872	$7.39 = \bar{\chi}_{iso}$		

$\Delta\chi_o = 1.542 \times 10^{-7}$ c.g.s.unit;

* Interpolated values from reference [1].

Table 5.9

Experimental values of the density (ρ), magnetic susceptibility (χ), susceptibility anisotropy ($\Delta\chi$), and the order parameter $< P_2 >$

Sample: Mixture (B_3) of ME6O.5 and 5CB

$x_{5CB} = 0.3025$

Temp. in °C	Density (ρ)* in gm/cc	$-\chi_{\parallel} \times 10^{-7}$ c.g.s.unit	$\Delta\chi \times 10^{-8}$ c.g.s.unit	order parameter $< P_2 >$
35.0	1.0305	6.72	11.2	0.625
38.4	1.0278	6.75	10.9	0.607
40.5	1.0260	6.76	10.7	0.596
44.0	1.0217	6.77	10.5	0.585
47.5	1.0118	6.78	10.4	0.578
52.2	1.0110	6.80	10.0	0.557
56.5	1.0025	6.82	9.8	0.547
57.8	1.0000	6.92	8.3	0.460
58.7	0.9963	6.93	8.1	0.449
60.0	0.9900	6.98	7.4	0.411
63.5	0.9767	$6.47 = \bar{\chi}_{iso}$		

$\Delta\chi_o = 1.796 \times 10^{-7}$ c.g.s.unit;

* Interpolated values from reference [1].

Table 5.10

Experimental values of the density (ρ), magnetic susceptibility (χ), susceptibility anisotropy ($\Delta\chi$), and the order parameter $< P_2 >$

Sample: Mixture (B_4) of ME6O.5 and 5CB

$x_{5CB} = 0.4008$

Temp. in $^{\circ}$C	Density (ρ)* in gm/cc	$-\chi_{\parallel} \times 10^{-7}$ c.g.s.unit	$\Delta\chi \times 10^{-8}$ c.g.s.unit	order parameter $< P_2 >$
35.0	1.0270	6.77	11.3	0.598
40.5	1.0225	6.80	10.8	0.574
44.0	1.0189	6.82	10.5	0.556
47.5	1.0140	6.84	10.3	0.544
52.2	1.0082	6.85	10.0	0.529
56.5	1.0015	6.87	9.7	0.513
57.9	1.0000	6.95	8.5	0.450
58.7	0.9970	6.98	8.1	0.432
60.3	0.9920	$7.52 = \bar{\chi}_{iso}$		

$\Delta\chi_o = 1.887 \times 10^{-7}$ c.g.s.unit;

* Interpolated values from reference [1].

Table 5.11

Experimental values of the density (ρ), magnetic susceptibility (χ), susceptibility anisotropy ($\Delta\chi$), and the order parameter $< P_2 >$

Sample: Mixture (B_5) of ME6O.5 and 5CB

$x_{5CB} = 0.4986$

Temp. in ^{o}C	Density (ρ)* in gm/cc	$-\chi_{\parallel} \times 10^{-7}$ c.g.s.unit	$\Delta\chi \times 10^{-8}$ c.g.s.unit	order parameter $< P_2 >$
35.0	1.0177	6.83	11.7	0.622
40.5	1.0157	6.87	11.2	0.592
44.0	1.0124	6.88	10.9	0.577
47.5	1.0110	6.90	10.6	0.562
52.2	1.0060	6.92	10.3	0.545
53.5	1.0028	7.03	8.8	0.464
54.7	0.9991	7.05	8.4	0.444
56.5	0.9971	$7.61 = \bar{\chi}_{iso}$		

$\Delta\chi_o = 1.89 \times 10^{-7}$ c.g.s.unit;

* Interpolated values from reference [1].

Table 5.12

Experimental values of the density (ρ) , magnetic susceptibility (χ) , susceptibility anisotropy ($\Delta\chi$) , and the order parameter $< P_2 >$

Sample: Mixture (B_6) of ME6O.5 and 5CB

$x_{5CB} = 0.560$

Temp. in $^{\circ}$C	Density (ρ)* in gm/cc	$-\chi_{\parallel}$ x 10^{-7} c.g.s.unit	$\Delta\chi$ x 10^{-8} c.g.s.unit	order parameter $< P_2 >$
35.0	1.035	6.76	14.4	0.626
37.5	1.030	6.79	14.0	0.610
40.5	1.023	6.81	13.6	0.593
42.5	1.020	6.83	13.3	0.579
45.0	1.018	6.86	12.9	0.561
47.5	1.015	6.90	12.3	0.537
49.0	1.010	6.98	11.2	0.487
51.5	1.007	7.01	10.6	0.462
52.5	1.006	7.04	10.2	0.443
54.7	1.003	7.10	9.3	0.405
56.5	1.000	7.72 = $\bar{\chi}_{iso}$		

$\Delta\chi_o = 2.30 \times 10^{-7}$ c.g.s.unit;

* Interpolated values from reference [1].

Table 5.13

Experimental values of the density (ρ), magnetic susceptibility (χ), susceptibility anisotropy ($\Delta\chi$), and the order parameter $< P_2 >$

Sample: Mixture (B_7) of ME6O.5 and 5CB

$x_{5CB} = 0.643$

Temp. in °C	Density (ρ)* in gm/cc	$-\chi_{\parallel}$ x 10^{-7} c.g.s.unit	$\Delta\chi$ x 10^{-8} c.g.s.unit	order parameter $< P_2 >$
32.0	1.055	6.90	16.7	0.649
35.0	1.051	6.94	16.0	0.624
38.4	1.048	6.99	15.3	0.597
40.5	1.046	7.01	15.0	0.583
42.5	1.043	7.13	13.1	0.512
45.0	1.041	7.17	12.6	0.489
47.5	1.037	7.21	12.0	0.467
50.3	1.035	7.26	11.2	0.437
51.3	1.030	7.32	10.3	0.400
52.2	1.025	$8.01 = \bar{\chi}_{iso}$		
54.7	1.019	8.01		

$\Delta\chi_o = 2.569 \times 10^{-7}$ c.g.s.unit;

* Interpolated values from reference [1].

Table 5.14

Experimental values of the density (ρ), magnetic susceptibility (χ), susceptibility anisotropy ($\Delta\chi$), and the order parameter $< P_2 >$

Sample: Mixture (B_8) of ME6O.5 and 5CB

$x_{5CB} = 0.7075$

Temp. in °C	Density (ρ)* in gm/cc	$-\chi_{\parallel} \times 10^{-7}$ c.g.s.unit	$\Delta\chi \times 10^{-8}$ c.g.s.unit	order parameter $< P_2 >$
32.0	1.0347	7.02	15.9	0.555
35.0	1.0301	7.04	15.6	0.546
37.5	1.0282	7.05	15.4	0.538
40.5	1.0271	7.08	15.0	0.525
42.5	1.0251	7.09	14.7	0.516
44.5	1.0229	7.13	14.3	0.499
47.0	1.0197	7.18	13.4	0.469
48.0	1.0188	7.32	11.4	0.400
49.5	1.0155	8.0 8 = $\bar{\chi}_{iso}$		

$\Delta\chi_o = 2.86 \times 10^{-7}$ c.g.s.unit;

* Interpolated values from reference [1].

References:

1) M. K. Das and R. Paul, Phase Transitions, 46, 185(1994).
2) M. K. Das and R. Paul, Phase Transitions, 48, 255(1994).
3) M. K. Das, R. Paul and D. A. Dunmur, Mol. Cryst. Liq. Cryst., 258, 239 (1995).
4) D. A. Dunmur, R. G. Walker and P. Palffy-Muhoray, Mol. Cryst. Liq. Cryst., 122, 321(1985).
5) P. Palffy-Muhoray, D. A. Dunmur, W. H. Miller and D. A. Balzarini, Liquid crystals and ordered Fluids, Vol 4, Editors A. C. Griffin and J. F. Johnson, Plenum, N.Y., p615 (1984).
6) B. Adhikari and R. Paul, Mol Cryst. Liq. Cryst., 301, 419 (1997).
7) I. Haller, H. A. Huggins, H. R. Lilienthal and T. R. Mc Guire, J. Phys. Chem., 77, 950 (1973).
8) W. L. McMillan,Phys. Rev. A, 4, 238 (1971); ibid, A, 6, 936 (1972).

CHAPTER-6

X-ray diffraction studies and refractive index measurements on a mesomorphic mixture showing enhanced smectic A_d phase and re-entrant nematic phase.

The phase diagrams of the mixtures of 4 - cyanobiphenyl -4′ alkyl biphenyl - 4 - carboxylates (nCBB) and alkyloxy - 4′ - cyanobiphenyls (nOCB) have been studied extensively by Brodzik and Dabrowski [1]. Some of these mixtures have very interesting property of showing induced smectic A_d phase as well as re-entrant nematic phase in a particular composition range. Some of the mixtures even produce a smectic A_d island in a nematic sea. Hence, these mixtures are well suited for the study of physical properties, which may elucidate the formation of induced smectic A_d phases and re-entrant nematic phases in these mixtures.

The mixtures of 4 - cyanobiphenyl -4′ heptyl biphenyl - 4 - carboxylate (7CBB) and 4 - dodecyloxy- 4 - cyanobiphenyl (12OCB) have been studied by us. Figure 6.1 shows the phase diagram of this mixture as obtained by Brodzik et al.[1]. This system shows enhanced smectic A_d phase as well as re-entrant nematic phase. Whereas, in 12OCB the smectic A_d phase is stable only upto 88.5 ^{0}C, in this mixture at optimum composition the smectic A_d phase can exist upto 264^{0}C. Due to this unusual properties we decided to study this mixture by small angle x-ray diffraction technique and also to measure the density and refractive index of this mixture.

The pure compounds were prepared at the Institute of Chemistry, Military University of Technology, Warsaw. Mixtures were prepared at Physics Department, North Bengal University, where the X-ray diffraction studies and refractive index measurements were performed. Mixtures of 12OCB and 7CBB were prepared with six different compositions all in the range showing enhanced smectic A_d phase. One of the mixtures, having mole fraction of 0.917 of 7CBB, showed re-entrant nematic phase as well. The transition temperature of the mixtures were determined by observing

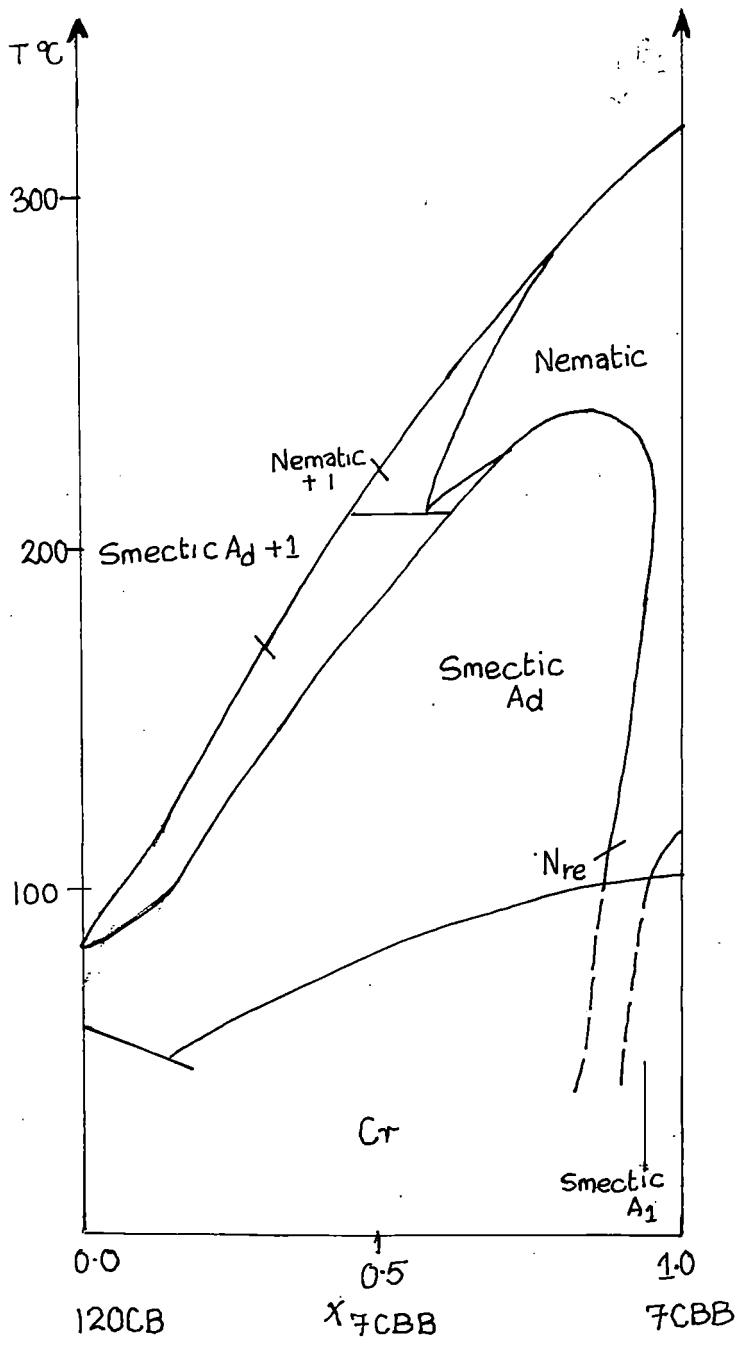

Figure 6.1. Phase diagram of bicomponent mixture (7CBB and 12OCB).

textures under polarising microscope, using Mettler FP 80/82 thermosystem. Unfortunately, at higher temperatures the components decompose, so no high temperature (>200°C) experiments could be performed on these mixtures. The composition of mixtures studied were x_{7CBB} = 0.917 (mix. C_1), 0.80 (mix. C_2), 0.604 (mix. C_3), 0.502 (mix. C_4), 0.296 (mix. C_5), 0.202 (mix. C_6), x_{7CBB} being the mole fraction of 7CBB. The method of refractive index and density measurements and the details of x-ray diffraction set-up used have been described in Chapter 2. Since, mixture C_1, having mole fraction 0.917 of 7CBB, shows both enhanced smectic A_d and re-entrant nematic phases, we studied this mixture more thoroughly. The transition temperatures of the mixtures as observed by us are given below:

I. Mix. C_1

$$K \underset{104.8^\circ C}{\overset{120.1^\circ C}{\rightleftharpoons}} N_{re} \underset{162^\circ C}{\longleftrightarrow} S_{Ad} \underset{\sim 261^\circ C}{\longleftrightarrow} N \underset{\sim 340^\circ C}{\longleftrightarrow} I$$

II. Mix. C_2

$$K \underset{100.1^\circ C}{\overset{116^\circ C}{\rightleftharpoons}} S_{Ad} \underset{\sim 260^\circ C}{\longleftrightarrow} N \underset{\sim 315^\circ C}{\longleftrightarrow} I$$

III. Mix. C_3

$$K \underset{85^\circ C}{\overset{101.8^\circ C}{\rightleftharpoons}} S_{Ad} \underset{\sim 224.7^\circ C}{\longleftrightarrow} N \underset{\sim 251.4^\circ C}{\longleftrightarrow} N+I \underset{2\sim 67.6^\circ C}{\longleftrightarrow} I$$

IV. Mix. C_4

$$K \underset{62^\circ C}{\overset{93.2^\circ C}{\rightleftharpoons}} S_{Ad} \underset{198^\circ C}{\longleftrightarrow} S_{Ad}+I \underset{\sim 238^\circ C}{\longleftrightarrow} I$$

V. Mix. C_5

$$K \underset{32.6^{\circ}C}{\overset{70^{\circ}C}{\rightleftharpoons}} S_{Ad} \overset{140^{\circ}C}{\longleftrightarrow} S_{Ad}+I \overset{181.6^{\circ}C}{\longleftrightarrow} I$$

VI. Mix. C_6

$$K \underset{30.3^{\circ}C}{\overset{65^{\circ}C}{\rightleftharpoons}} S_{Ad} \overset{117.6^{\circ}C}{\longleftrightarrow} S_{Ad}+I \overset{160^{\circ}C}{\longleftrightarrow} I$$

All the transition temperatures agree with the values obtained from the phase diagram [1] for this mixture. The densities and the values of ordinary and extraordinary refractive indices at three different wave lengths (5461 Å, 5780 Å and 6907 Å) for mixture C_1 in the temperature range 120^{0}C to 175 ^{0}C have been tabulated in Table 6.1. Above 175 ^{0}C the sample started to decompose, so experimental data at higher temperatures could not be taken. The temperature variation of the density for mixture C_1 is shown in Figure 6.2. No discontinuity in the density value could be observed at the re-entrant nematic to smectic A_d phase. Hence, this phase transition is probably of the second order. The temperature variation of the ordinary and extraordinary refractive indices at three different wavelengths is given in Figure 6.3. It can be seen that refractive indices also vary continuously across the re-entrant nematic to smectic A_d phase transition. The polarisability values calculated according to Vuks formula (equation 2.24 & 2.25) and Neugebauer formula (equation 2.22 & 2.23) are given in Tables 6.2 and 6.3 respectively. The polarisability and anisotropies in the perfectly ordered state are determined by Haller's extrapolation method. The order parameters calculated using Vuks and Neugebauer procedure are given in Tables 6.4 and 6.5 respectively. Though the two methods give quite different values of $\Delta\chi$ ($= \chi_{\parallel} - \chi_{\perp}$), the order parameter values agree

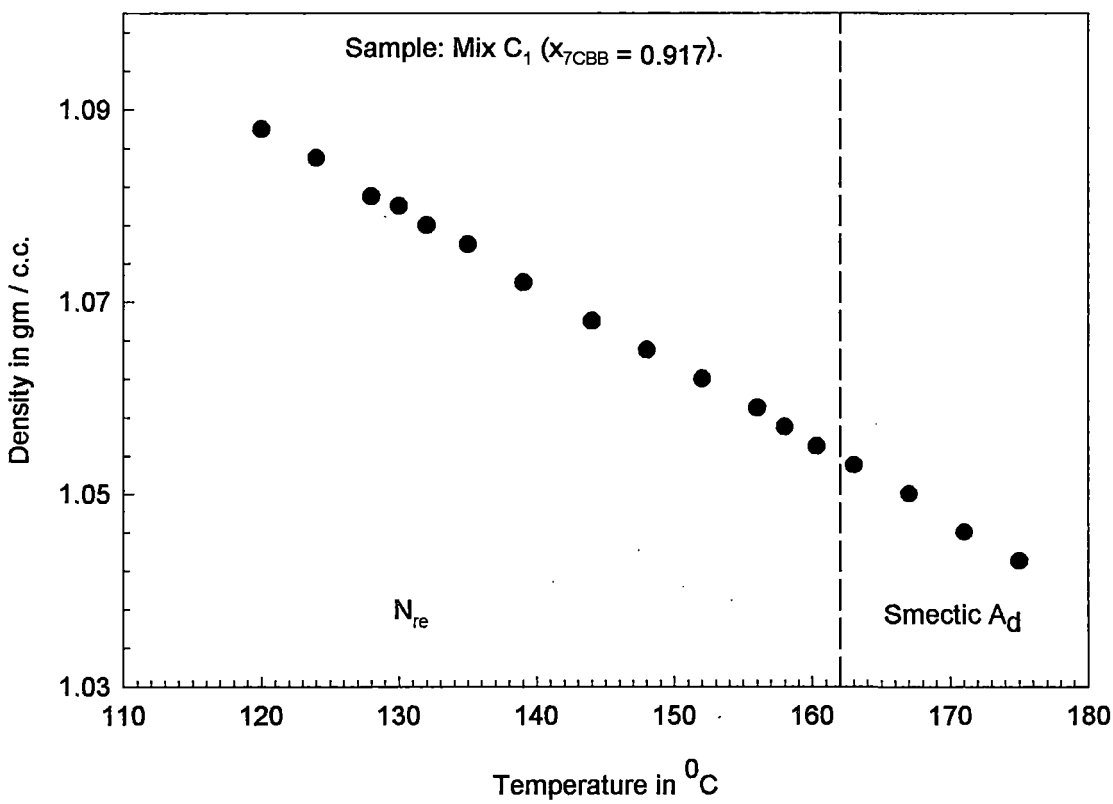

Figure 6.2. Density values as a function of temperature.

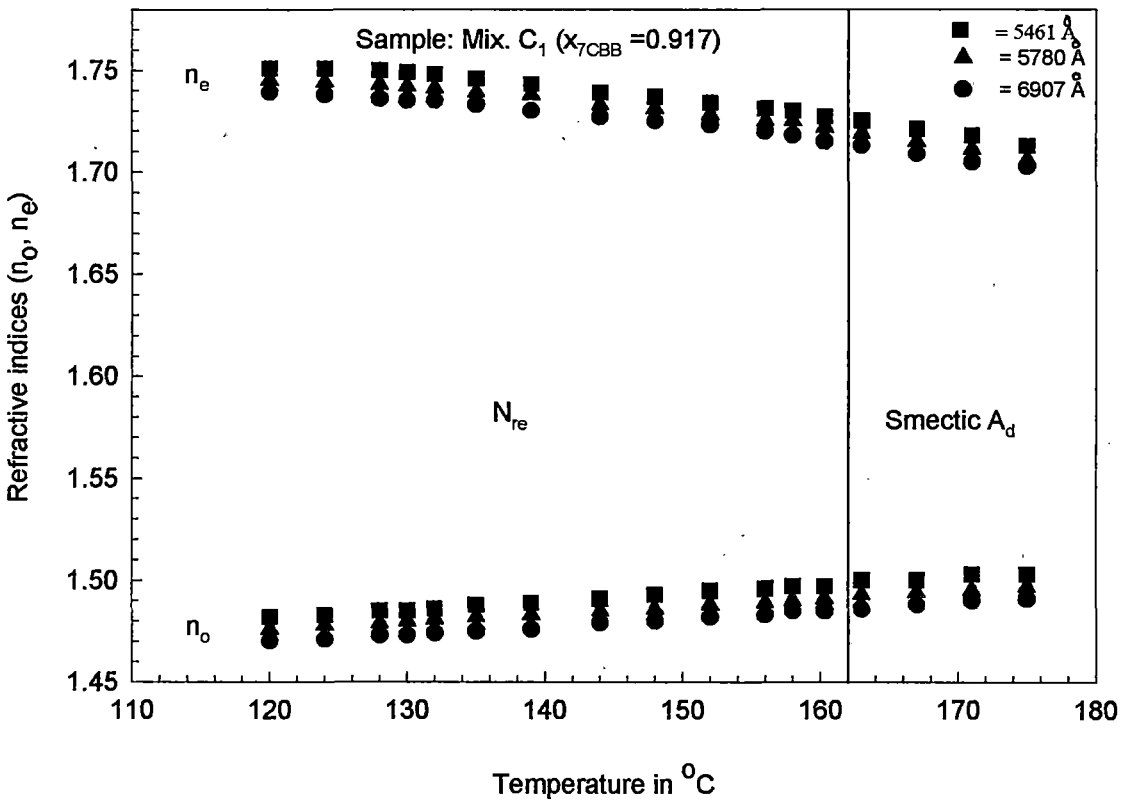

Figure 6.3. Variation of refractive indices (n_o, n_e) with temperature.

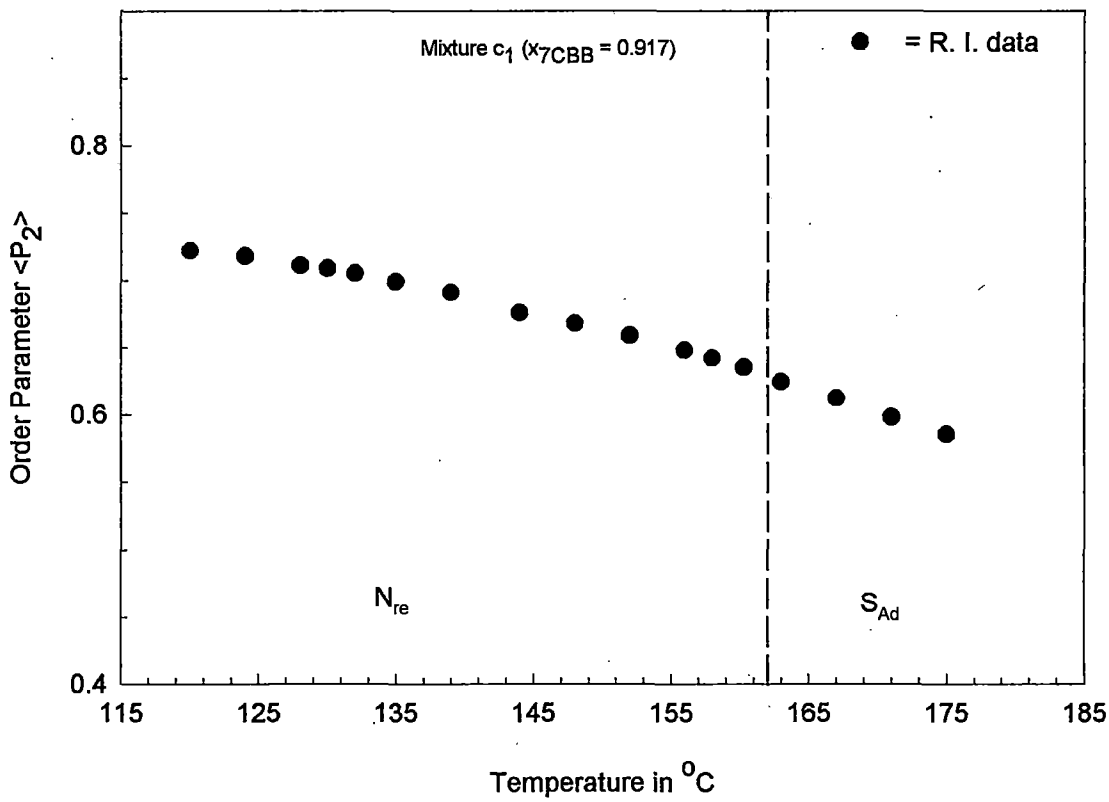

Figure 6.4. Temperature variation of orientational order parameter <P_2> in the re-entrant nematic and induced smectic A_d phase.

almost exactly. Figure 6.4 shows the temperature variation of the order parameter as calculated from refractive index data. Again we find that there is no sudden change in the order parameter value at the re-entrant nematic to smectic A_d phase transition temperature.

X-ray diffraction patterns were recorded for mixture C_1 at ten temperatures between 125^{0}C to 195^{0}C. A magnetic field of 5 kilogauss was applied to align the sample. However, at three temperatures near the re-entrant nematic to smectic A_d phase transition the sample could only be partially aligned. The sample could be taken to higher temperature (195^{0}C) without decomposition, since the sample was sealed in a glass capillary tube, where atmospheric oxygen could not get in to react with the chemicals. In case of refractive index and density measurements, our system was not sealed, hence decomposition set in at a lower (~175^{0}C) temperature.

Angular distribution of the intensities of the outer x-ray diffraction pattern after conversion from optical density to x-ray intensity and correction for the background are tabulated in Tables 6.6 and 6.7. These intensity data have been analysed to obtain angular distribution function using Leadbetter [2] procedure and the angular distribution function values are given in Tables 6.8 and 6.9. The order parameters as calculated from the x-ray data for this mixture (mix.C_1) at different temperatures are tabulated in Table 6.10. Figure 6.5 shows the temperature variation of order parameter for mix.C_1 as obtained from x-ray diffraction and refractive index studies. It can be seen that if the $\langle P_2 \rangle$ values obtained from partially aligned samples be ignored then the agreement between order parameters determined from two different techniques is fair. However, since samples near the N_{re} - Smectic A_d transition could not be aligned for x-ray

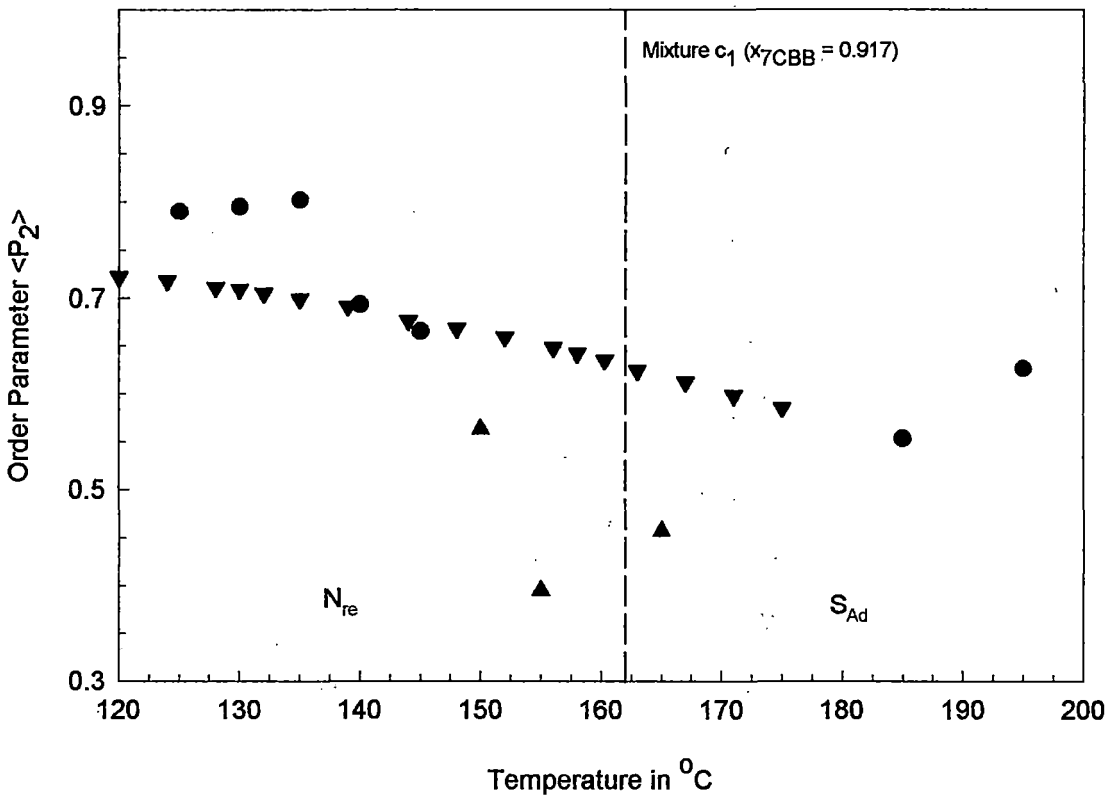

orientational order parameter <P_2> in

diffraction studies, the nature of this phase transition could not be inferred from x-ray studies. But, the density and refractive index show that N_{re} - Smectic A_d transition is most probably of the second order.

The rest five mixtures have only smectic A_d and normal nematic phases at high temperature. None of the mixtures in the smectic phase could be aligned in the magnetic field at our disposal (~5 kilogauss). The x-ray diffraction pattern of the normal nematic phase could not be obtained since the sample started to decompose at higher temperatures. Hence, only layer thickness measurements could be done for these mixtures in their smectic A_d phase from the study of the inner arc of the x-ray diffraction pattern. The layer thickness at different temperatures for all the six mixtures are recorded in Tables 6.11 and 6.12. The apparent molecular lengths in the re-entrant nematic phase of mixture C_1 have also been given in Table 6.11. X-ray diffraction photographs from the mixture C_1 in the re-entrant nematic phase (at 125^0C and 150^0C) and in the smectic A_d phase (185^0C) are shown in Plates 6a-6c. The temperature variation of apparent molecular length in the re-entrant nematic phase and of layer thickness of the smectic A_d phase for mixture C_1 is shown in Figure 6.6. It can be seen that the apparent molecular lenght in the re-entrant nematic phase in mixture C_1 is about 39.8 Å, whereas the layer thickness in the smectic A_d phase of the same mixture is about 38.7 Å. So there is definite re-arrangement of molecular packing at the phase transition. The apparent molecular length in the N_{re} phase very near the transition temperature is almost equal to the smectic layer thickness. This may be due to the pre-transitional effect, when smectic like clusters may be forming in the re-entrant nematic phase. Hence, x-ray diffraction from the re-entrant nematic phase near the transition temperature should be very similar to those from

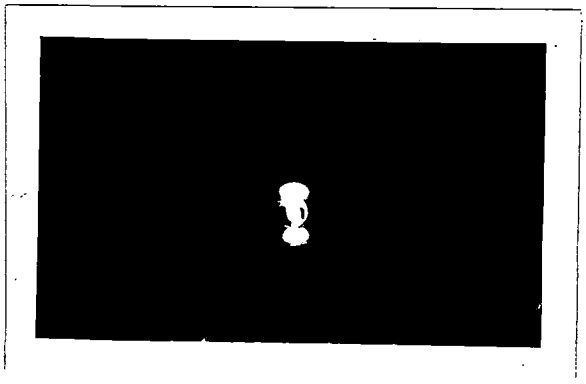

Plate 6a: X-ray diffraction photograph of the oriented sample in the re-entrant nematic phase of 7CBB+12OCB mixture at 125°C.

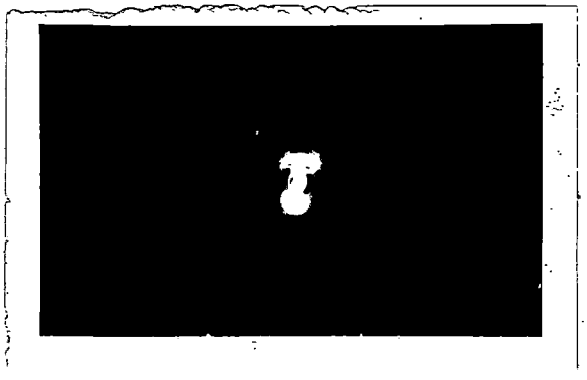

Plate 6b: X-ray diffraction photograph of the oriented sample in the re-entrant nematic phase of 7CBB+12OCB mixture at 125°C.

Plate 6c: X-ray diffraction photograph of the oriented sample in the smectic A_d phase of 7CBB+12OCB mixture at 185°C.

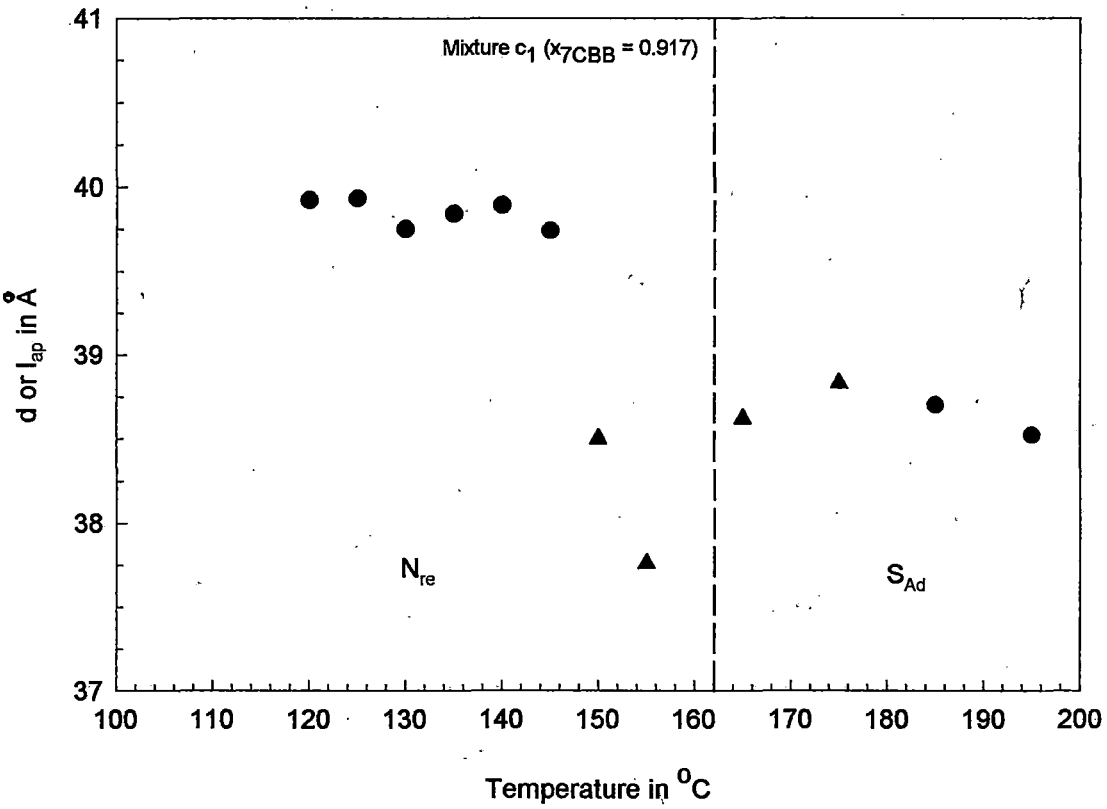

Figure 6.6. Temperature variation of apparent molecular length (l_{ap}) in the re-entrant nematic phase and of layer thickness (d) in the smectic A_d phase from x-ray photographs.

● data from aligned sample

▲ data from partially aligned sample

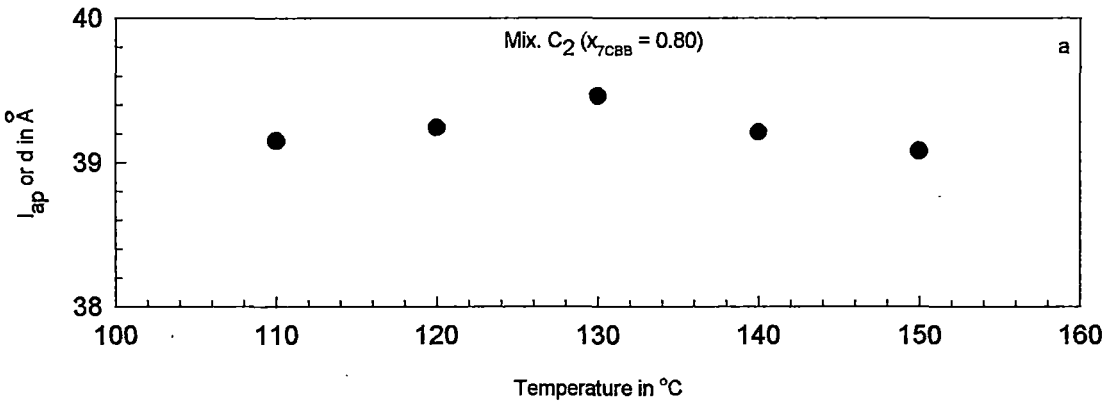

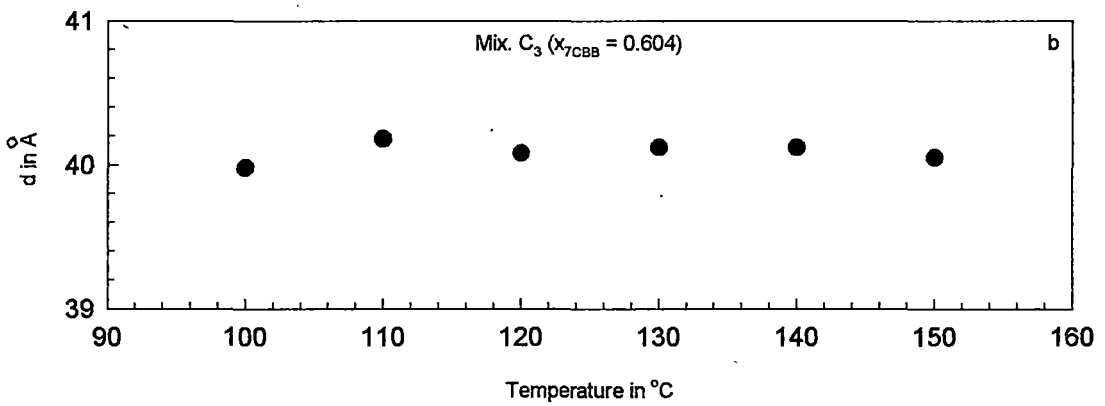

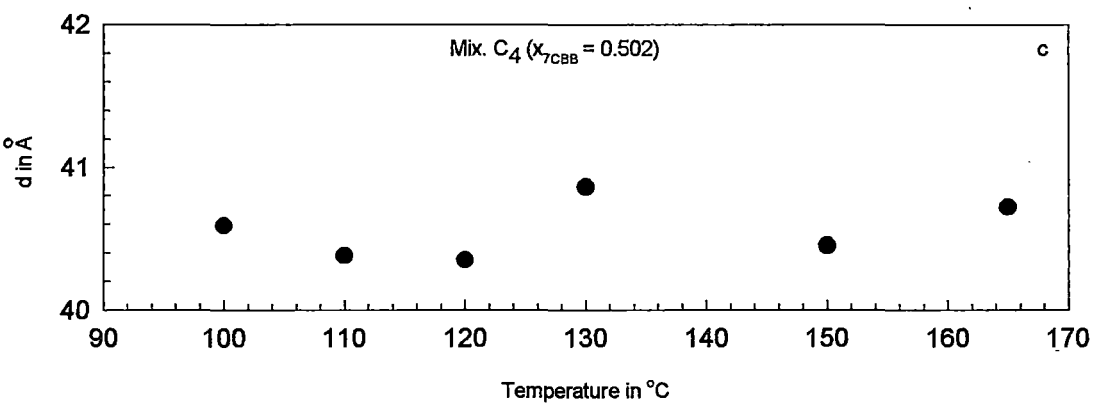

Figure (6.7a - 6.7c). Temperature variation of layer thickness (d).

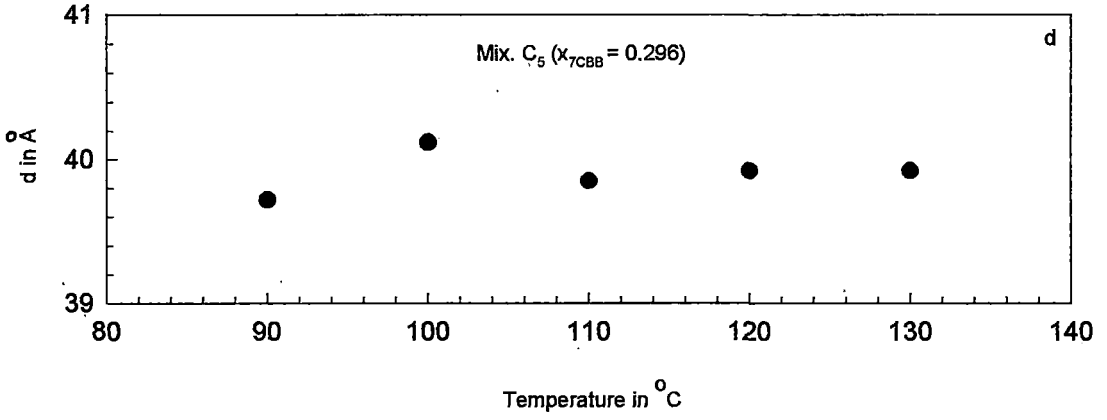

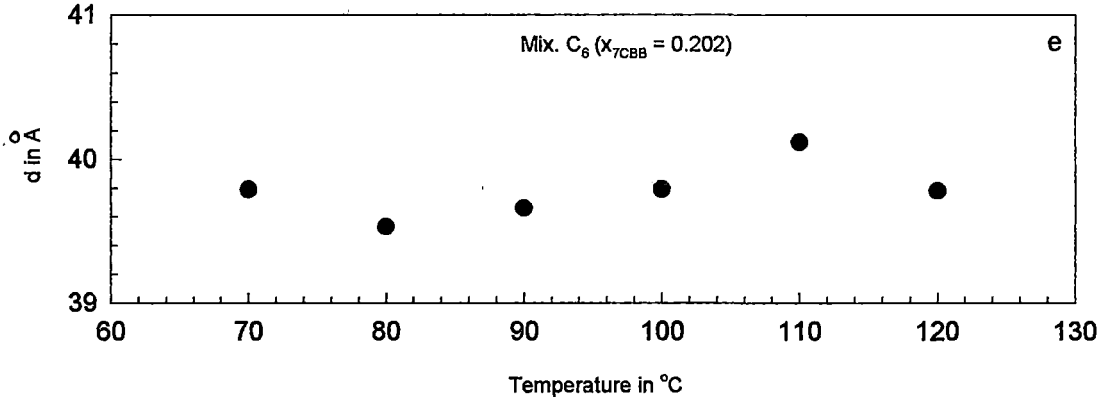

Figure (6.7d - 6.7e). Temperature variation of layer thickness (d).

the smectic A_d phase. Indeed the x-ray diffraction pattern (Plate 6b) from re-entrant nematic phase of mixture C_1 at 150°C does show typical inner spots due to cybotactic clusters.

The temperature variation of the layer thickness in the mixture C_2 to mixture C_6 are shown in Figure 6.7a - 6.7e. It can be seen that the layer thicknesses are almost independent of temperature. This is quite common in smectic A phases. The composition variation of layer thickness at 120°C (except for mixture C_1 for which the layer thickness is at 170°C) is shown in Figure 6.8. The variation shows a broad maximum of ~40Å at about equimolar concentration. This has already been reported by us [5]. This is in contrast to some polar-nonpolar mixtures [3,4] showing induced smectic A_d phase, where the layer thickness shows a minimum at about equimolar composition. However, this maximum is not difficult to explain. The model molecular lengths of 7CBB and 12OCB molecules are 31.5Å and 25.6Å respectively. 7CBB has a latent smectic A_1 phase [1], that means that pure 7CBB, if it forms a smectic phase will have a layer thickness of about 31.5Å. 12OCB forms a partial bilayer smectic (i.e. smectic A_d) phase of layer thickness 37.5Å approximately [6]. However, in the mixture of 7CBB and 12OCB dimer formation between 7CBB and 12OCB will certainely occur. We can assume that in an equimolar mixture 7CBB + 12OCB dimers will predominate in number over 12OCB + 12OCB dimers. The length of 7CBB + 12OCB dimer should be greater than 12OCB + 12OCB dimers and this length should be almost equal to the layer thickness of the smectic phase of equimolar mixture of 7CBB and 12OCB. To estimate the length of 7CBB + 12OCB dimers, we can proceed as follows. The length of 12OCB molecule is 25.6Å and that of its dimer is 37.5Å, if we assume that the layer thickness in the smectic A phase of 12OCB is equal to its

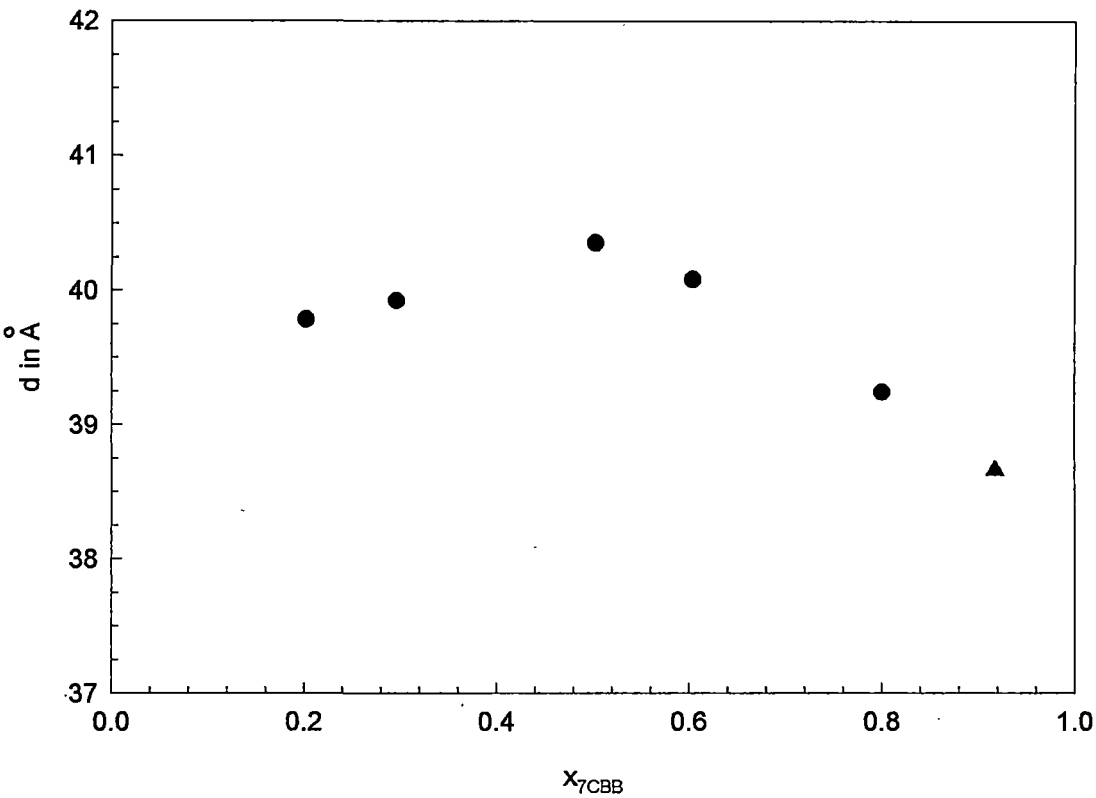

Figure 6.8. Concentration variation of the layer thickness of mixture of 7CBB & 12OCB AT 120 °C { except point x_{7CBB} = 0.917 (▲) for which temperature is about 170 °C }.

dimer length. Then the overlap of the two 12OCB molecules in the dimer is about 14Å. Now 7CBB molecule contains a cyanobiphenyl part identical to that in 12OCB. Since dimer formation is enhanced by the presence of cyanobiphenyl in a molecule, we can assume that in 7CBB + 12OCB dimer an identical overlap of the molecules (16Å) takes place as in 12OCB + 12OCB dimer. Hence, the length of 7CBB +12OCB dimer comes out to be 31.5Å + 25.6Å - 14Å = 43.1Å. This value is slightly greater than the maximum value of the layer thickness (~ 40Å) observed in the in the mixture of 7CBB and 12OCB. If we consider the presence of 12OCB dimers and some 7CBB monomers then the mean layer thickness should be reduced somewhat from 43.1Å. As the composition changes from equimolar, the number of 7CBB + 12OCB dimers reduces and 12OCB + 12OCB dimers increases. Since the 12OCB dimers (37.5Å) are shorter than 7CBB + 12OCB (43.1Å) dimers, it means that the effective layer thickness should be maximum for equimolar mixture. This is exactly what is seen in Figure 6.8. Further work is in progress to explain quantitatively this variation of layer thickness with mole fraction.

Table 6.1

Density (ρ) and refractive indices (n_o, n_e) at different temperatures of mixture C_1 (x_{7CBB} = 0.917) of 7CBB and 12OCB.

Temp. in ° C	Density in gm/cc	λ = 6907 Å		λ = 5780 Å		λ = 5461 Å	
		n_o	n_e	n_o	n_e	n_o	n_e
120	1.088	1.470	1.739	1.476	1.745	1.482	1.751
124	1.085	1.471	1.738	1.478	1.744	1.483	1.751
128	1.081	1.473	1.736	1.479	1.743	1.485	1.750
130	1.080	1.473	1.735	1.480	1.742	1.485	1.749
132	1.078	1.474	1.735	1.481	1.741	1.486	1.748
135	1.076	1.475	1.733	1.482	1.739	1.488	1.746
139	1.072	1.476	1.730	1.483	1.738	1.489	1.743
144	1.068	1.479	1.727	1.485	1.733	1.491	1.739
148	1.065	1.480	1.725	1.486	1.731	1.493	1.737
152	1.062	1.482	1.723	1.488	1.728	1.495	1.734
156	1.059	1.483	1.720	1.489	1.725	1.496	1.731
158	1.057	1.485	1.718	1.490	1.725	1.497	1.730
160.3	1.055	1.485	1.715	1.491	1.722	1.497	1.727
163	1.053	1.486	1.713	1.493	1.719	1.500	1.725
167	1.050	1.488	1.709	1.494	1.715	1.500	1.721
171	1.046	1.490	1.705	1.495	1.711	1.503	1.718
175	1.043	1.491	1.703	1.497	1.706	1.503	1.713

Table 6.2

Polarisability (α_o, α_e) at different temperatures of mixture C_1 ($x_{7CBB} = 0.917$) by Vuks method

Temp. in ^oC	$\lambda = 6907$ Å		$\lambda = 5780$ Å		$\lambda = 5461$ Å	
	α_o	α_e	α_o	α_e	α_o	α_e
120	44.07	76.88	44.56	77.37	45.04	77.86
124	44.31	76.95	44.87	77.48	45.26	78.00
128	44.68	76.99	45.16	77.48	45.64	78.09
130	44.77	76.94	45.34	77.49	45.72	78.09
132	44.91	76.97	45.46	77.50	45.92	78.00
135	45.15	76.97	45.68	77.49	46.16	77.92
139	45.44	76.81	45.93	77.42	46.50	77.81
144	45.89	76.66	46.40	77.08	46.89	77.61
148	46.16	76.61	46.69	77.02	47.19	77.55
152	46.51	76.51	46.99	76.93	47.57	77.43
156	46.75	76.36	47.28	76.78	47.87	77.17
158	47.03	76.18	47.45	76.80	48.05	77.13
160.3	47.18	75.99	47.66	76.57	48.17	76.99
163	47.44	75.83	47.95	76.37	48.54	76.81
167	47.77	75.61	48.28	76.12	48.83	76.62
171	48.16	75.31	48.58	75.87	49.23	76.33
175	48.43	75.26	48.98	75.44	49.47	76.01

α_o & α_e are in 10^{-24} cm^3 unit.

Table 6.3

Polarisability (α_o, α_e) at different temperatures of mixture C_1 ($x_{7CBB} = 0.917$) by Neugebauer method

Temp. in ° C	$\lambda = 6907$ Å		$\lambda = 5780$ Å		$\lambda = 5461$ Å	
	α_o	α_e	α_o	α_e	α_o	α_e
120	46.07	72.89	46.57	73.34	47.08	73.79
124	42.29	72.98	46.88	73.47	47.29	73.94
128	46.65	73.05	47.15	73.50	47.66	74.06
130	46.73	73.02	47.32	73.53	47.74	74.06
132	46.87	73.06	47.43	73.55	47.29	74.01
135	47.09	73.08	47.64	73.52	48.14	73.96
139	47.35	72.98	47.87	73.53	48.45	73.90
144	47.77	72.90	48.29	73.29	48.80	73.78
148	48.02	72.89	48.56	73.28	49.08	73.76
152	48.35	72.85	48.84	73.23	49.43	73.70
156	48.56	72.74	49.10	73.14	49.70	73.51
158	48.81	72.61	49.26	73.17	49.86	73.50
160.3	48.94	72.47	49.45	73.00	49.97	73.40
163	49.18	72.36	49.71	72.85	50.31	73.28
167	49.47	72.21	50.00	72.68	50.56	73.15
171	49.82	72.00	50.27	72.50	50.92	72.94
175	50.07	71.98	50.61	72.18	51.12	72.70

α_o & α_e are in 10^{-24} cm^3 unit.

Table 6.4

Order parameter $< P_2 >$ of mixture $C_1(x_{7CBB} = 0.917)$ at different temperatures by Vuks method.

$(\alpha_{\parallel} - \alpha_{\perp}) = 45.45$ in 10^{-24} cm^3 unit.

Temp. in ^{o} C	$\lambda = 6907$ Å	$\lambda = 5780$ Å	$\lambda = 5461$ Å	Average
	$< P_2 >$	$< P_2 >$	$< P_2 >$	$< P_2 >$
120	0.722	0.722	0.722	0.722
124	0.718	0.717	0.720	0.718
128	0.711	0.708	0.714	0.711
130	0.708	0.707	0.712	0.709
132	0.705	0.705	0.706	0.705
135	0.700	0.698	0.699	0.699
139	0.690	0.693	0.689	0.691
144	0.677	0.675	0.676	0.676
148	0.670	0.667	0.668	0.668
152	0.660	0.659	0.657	0.659
156	0.652	0.649	0.644	0.648
158	0.641	0.646	0.640	0.642
160.3	0.634	0.636	0.634	0.635
163	0.625	0.625	0.622	0.624
167	0.613	0.612	0.611	0.612
171	0.597	0.600	0.596	0.598
175	0.590	0.582	0.584	0.585

Table 6.5

Order parameter $< P_2 >$ of mixture C_1 ($x_{7CBB} = 0.917$) at different temperatures by Neugebauer method.

$(\alpha_{\parallel} - \alpha_{\perp}) = 37.05$ in 10^{-24} cm^3 unit.

Temp. in ° C	$\lambda = 6907$ Å	$\lambda = 5780$ Å	$\lambda = 5461$ Å	Average
	$< P_2 >$	$< P_2 >$	$< P_2 >$	$< P_2 >$
120	0.724	0.723	0.721	0.723
124	0.720	0.718	0.719	0.719
128	0.713	0.711	0.713	0.712
130	0.710	0.707	0.711	0.709
132	0.707	0.705	0.704	0.705
135	0.702	0.699	0.699	0.600
139	0.692	0.693	0.687	0.691
144	0.678	0.675	0.674	0.676
148	0.671	0.667	0.666	0.668
152	0.661	0.659	0.655	0.658
156	0.653	0.649	0.643	0.648
158	0.642	0.645	0.638	0.642
160.3	0.635	0.636	0.632	0.634
163	0.626	0.625	0.620	0.624
167	0.614	0.612	0.610	0.612
171	0.598	0.600	0.595	0.598
175	0.591	0.580	0.582	0.585

Table 6.6

Mean experimental intensity values I (ψ) , in arbitrary units , of 7CBB and 12OCB mixtureC_1 (x_{7CBB} = 0.917) after background correction.

ψ in deg.	I (ψ) values at different temperatures in degrees				
	125	130	135	140	145
0	3.21	3.31	1.54	1.64	1.01
5	2.87	3.04	1.34	1.54	0.90
10	2.22	2.38	1.01	1.29	0.78
15	1.72	1.72	0.95	1.02	0.64
20	1.08	1.13	0.46	0.79	0.51
25	0.68	0.67	0.29	0.60	0.39
30	0.42	0.38	0.18	0.43	0.29
35	0.26	0.19	0.08	0.30	0.22
40	0.16	0.11	0.04	0.21	0.16
45	0.10	0.09	0.03	0.15	0.11
50	0.08	0.07	0.03	0.11	0.08
55	0.07	0.06	0.03	0.07	0.06
60	0.03	0.04	0.02	0.05	0.04
65	0.02	0.04	0.02	0.04	0.03
70	0.01	0.04	0.01	0.03	0.02
75	0.00	0.03	0.01	0.03	0.01
80	0.00	0.01	0.00	0.02	0.00
85	0.00	0.00	0.00	0.01	0.00
90	0.00	0.00	0.00	0.00	0.00

Table 6.7

Mean experimental intensity values I (ψ) , in arbitrary units , of 7CBB and 12OCB mixtureC_1 (x_{7CBB} = 0.917) after background correction.

ψ	I (ψ) values at different temperatures in degrees				
in deg.	150	155	165	185	195
0	3.01	3.08	2.95	2.80	1.57
5	2.96	3.04	2.93	2.75	1.49
10	2.81	3.01	2.88	2.63	1.33
15	2.57	2.92	2.81	2.45	1.10
20	2.28	2.81	2.67	2.20	0.90
25	1.98	2.62	2.51	1.88	0.70
30	1.64	2.42	2.31	1.58	0.53
35	1.30	2.17	2.34	1.20	0.39
40	0.99	1.92	1.60	0.93	0.28
45	0.73	1.62	1.26	0.73	0.21
50	0.52	1.35	0.94	0.50	0.16
55	0.34	1.04	0.69	0.35	0.13
60	0.22	0.75	0.49	0.23	0.08
65	0.14	0.50	0.31	0.15	0.05
70	0.08	0.35	0.20	0.10	0.04
75	0.05	0.23	0.11	0.08	0.04
80	0.04	0.14	0.05	0.05	0.03
85	0.02	0.05	0.01	0.03	0.01
90	0.00	0.00	0.00	0.00	0.00

Table 6.8

Normalised distribution function values f (β) of 7CBB and 12OCB mixture C_1 (x = 0.917).

β in deg.	f (β) values at different temperatures in degrees				
	125	130	135	140	145
0	18.828	19.529	22.266	12.064	11.198
5	17.263	17.139	19.898	11.183	10.498
10	12.250	12.329	14.234	9.206	8.625
15	7.999	8.118	8.375	6.856	6.257
20	5.060	5.265	4.515	4.996	4.294
25	3.162	3.360	2.600	3.668	3.086
30	1.861	1.871	1.651	2.322	2.378
35	0.983	0.825	0.950	1.356	1.817
40	0.781	0.332	0.366	0.825	1.208
45	0.249	0.155	0.099	0.488	0.679
50	0.158	0.094	0.036	0.335	0.388
55	0.126	0.083	0.031	0.297	0.277
60	0.111	0.097	0.035	0.246	0.244
65	0.086	0.101	0.045	0.165	0.209
70	0.050	0.074	0.036	0.093	0.128
75	0.006	0.039	0.014	0.043	0.049
80	0.002	0.013	0.00	0.020	0.012
85	0.00	0.005	0.00	0.014	0.004
90	0.00	0.002	0.00	0.012	0.002

Table 6.9

Normalised distribution function values f (β) of 7CBB and 12OCB mixture C_1 (x = 0.917).

β in deg.	f (β) values at different temperatures in degrees				
	150	155	165	185	195
0	5.388	2.586	3.076	4.716	9.115
5	5.193	2.655	3.097	4.730	8.586
10	4.751	2.767	3.074	4.674	7.300
15	4.284	2.737	2.905	4.385	5.816
20	3.884	2.538	2.677	3.864	4.481
25	3.449	2.332	2.585	3.276	3.359
30	2.839	2.226	2.661	2.730	2.425
35	2.165	2.148	2.652	2.204	1.678
40	1.595	1.935	2.231	1.662	1.135
45	1.153	1.565	1.545	1.159	0.778
50	0.812	1.975	0.999	0.778	0.554
55	0.545	0.942	0.702	0.528	0.406
60	0.340	0.767	0.546	0.365	0.292
65	0.198	0.581	0.404	0.243	0.195
70	0.110	0.353	0.233	0.144	0.119
75	0.060	0.165	0.099	0.077	0.069
80	0.031	0.070	0.036	0.040	0.042
85	0.014	0.030	0.016	0.025	0.029
90	0.009	0.026	0.00	0.021	0.025

Table 6.10

Variation of $< P_2 >$ and $< P_4 >$ with temperature.

Sample:- 7CBB & 12OCB mixture C_1

$x_{7CBB} = 0.917$

Temperature in °C	$< P_2 >$	$< P_4 >$
125	0.790	0.498
130	0.795	0.524
135	0.802	0.534
140	0.693	0.360
145	0.665	0.306
150	0.563 *	----
155	0.395 *	----
165	0.457 *	----
185	0.553	----
195	0.626	0.264

* data from partially aligned sample, magnetic field not sufficient for alignment.

Table 6.11

Apparent molecular length (l_{ap}) or layer thickness (d) at different temperatures for mixtures of 7CBB & 12OCB.

Mix.C_1 ($x_{7CBB} = 0.917$)		Mix.C_2 ($x_{7CBB} = 0.80$)		Mix.C_3 ($x_{7CBB} = 0.604$)	
Temp. in °C	l_{ap} or d in Å	Temp. in °C	d in Å	Temp. in °C	d in Å
120	39.92	110	39.15	100	39.98
125	39.93	120	39.24	110	40.18
130	39.75	130	39.46	120	40.08
135	39.84	140	39.21	130	40.12
140	39.89	150	39.08	140	40.12
145	39.74			150	40.05
150	38.50				
155	37.76				
165	38.62				
175	38.83				
185	38.70				
195	38.52				

Table 6.12

Layer thickness (d) at different temperatures for mixtures of 7CBB & 12OCB.

Mix.C_4 ($x_{7CBB} = 0.502$)		Mix.C_5 ($x_{7CBB} = 0.296$)		Mix.C_6 ($x_{7CBB} = 0.202$)	
Temp. in °C	d in Å	Temp. in °C	d in Å	Temp. in °C	d in Å
100	40.59	90	39.72	70	39.79
110	40.38	100	40.12	80	39.53
120	40.35	110	39.85	90	39.66
130	40.86	120	39.92	100	39.79
150	40.45	130	39.92	110	40.12
165	40.72			120	39.78

Table 6.13

Concentration variation of layer thickness (d) for mixture of 7CBB & 12OCB at 120 °C { except point x_{7CBB} = 0.917 (Δ) for which temperature is about 170 °C }.

x_{7CBB}	l_{ap} or d in Å
0.202	39.78
0.296	39.92
0.502	40.35
0.604	40.08
0.800	39.24
0.917	38.66

References:

1) M. Brodzik and R. Dabrowski, Liq. Cryst., 18, 61 (1995).
2) Chapter 2, equation 2.16.
3) M. K. Das and R. Paul, Phase Trans., 48, 255 (1994).
4) M. K. Das, R. Paul and D. A. Dunmer, Mol. Cryst. Liq. Cryst., 258, 239 (1995).
5) S. K. Giri, N. K. Pradhan, R. Paul, S. Paul, P. Mandal, R. Dabrowski, M. Brodzik and K. Czuprynski, SPIE, 3319, 149 (1998).
6) M. K. Das, S. Paul and R. Paul, Mol. Cryst. Liq. Cryst., 264, 89 (1995).

CHAPTER-7

Magnetic susceptibility, bend and splay elastic constants of four nematogens.

In this chapter I report the temperature variation of magnetic susceptibility anisotropy values for four nematogens. The bend and splay elastic constants of two nematogens have also been reported. The experimental data for magnetic anisotropy have been analysed to calculate the order parameter of the nematogens.

The liquid crystalline compounds studied with their chemical names, chemical structure and transition temperatures are given below:

I. 4 -n- pentyl phenyl- 4 - n′ pentyloxy benzoate.
(ME 5O.5 in short).

C5H11-O-Ph-COO-Ph-C5H11

$$K \underset{<29^{\circ}C}{\overset{40.2^{\circ}C}{\rightleftharpoons}} N \overset{54.9^{0}C}{\longleftrightarrow} I$$

II. 4 -n- pentyl phenyl- 4 - n′ hexyloxy benzoate.
(ME 6O.5 in short).

C6H13-O-Ph-COO-Ph-C5H11

$$K \underset{35.4^{0}C}{\overset{49.5^{0}C}{\rightleftharpoons}} N \overset{62.2^{0}C}{\longleftrightarrow} I$$

III. 3E-n-butane-phenyl-(4-cyclohexane-4′-n-propane)-ether
(3CPOd(3)1 in short).

$$K \underset{25.5^{0}C}{\overset{43^{0}C}{\rightleftharpoons}} N \overset{58^{0}C}{\longleftrightarrow} I$$

IV. 3E-n-butane-phenyl-(4-cyclohexane-4′-n-pentane)-ether
(5CPOd(3)1 in short).

$$K \underset{22.8^{0}C}{\overset{32^{0}C}{\rightleftharpoons}} N \overset{67^{0}C}{\longleftrightarrow} I$$

ME 5O.5 and ME 6O.5 were obtained from E. Merk, U. K. The other two chemicals were donated to us by Hoffmann La Roche, Switzerland. All the chemicals were used without further purification. The transition temperatures were determined by observing their textures under polarising microscope using Mettler FP 80/82 thermosystem. The transition temperatures agreed with the values supplied by the manufacturers. The nematogens ME 5O.5 and ME 6O.5 have been used frequently in liquid crystalline mixtures, which shows induced smectic A_d phases [1-5]. The density and refractive indices of both the compounds in their mesophase have been determined by Adamski [7]. The density and refractive indices of ME 6O.5 have also been reported by other workers [1,8]. Das et al [2,3] have also studied these nematogens and calculated order parameters from x-ray diffraction data.

The refractive indices and elastic constants of the compound 3CPOd(3)1 have been reported by Schadt et al [9,10]. The density and refractive indices of both 3CPOd(3)1 and 5CPOd(3)1 have been determined by Nath et al [11,12]. They have also determined order parameters and other molecular parameters from the x-ray diffraction studies of these two nematogens [11].

Magnetic susceptibility, density and elastic constants of the nematogens were determined following the procedure given in Chapter-2.

The experimental values of density and $\chi_{\parallel}$, the magnetic susceptibility along the director, at different temperatures for ME 5O.5 are Tabulated in Table 7.1. The calculated values of $\Delta\chi$ and order parameters are also shown in the Table. The value of $\Delta\chi$ for perfectly ordered sample was determined by Haller's extrapolation method (Chapter 2) and this value is also given in Table 7.1. The corresponding density, $\chi_{\parallel}$, $\Delta\chi$ and $\langle P_2 \rangle$

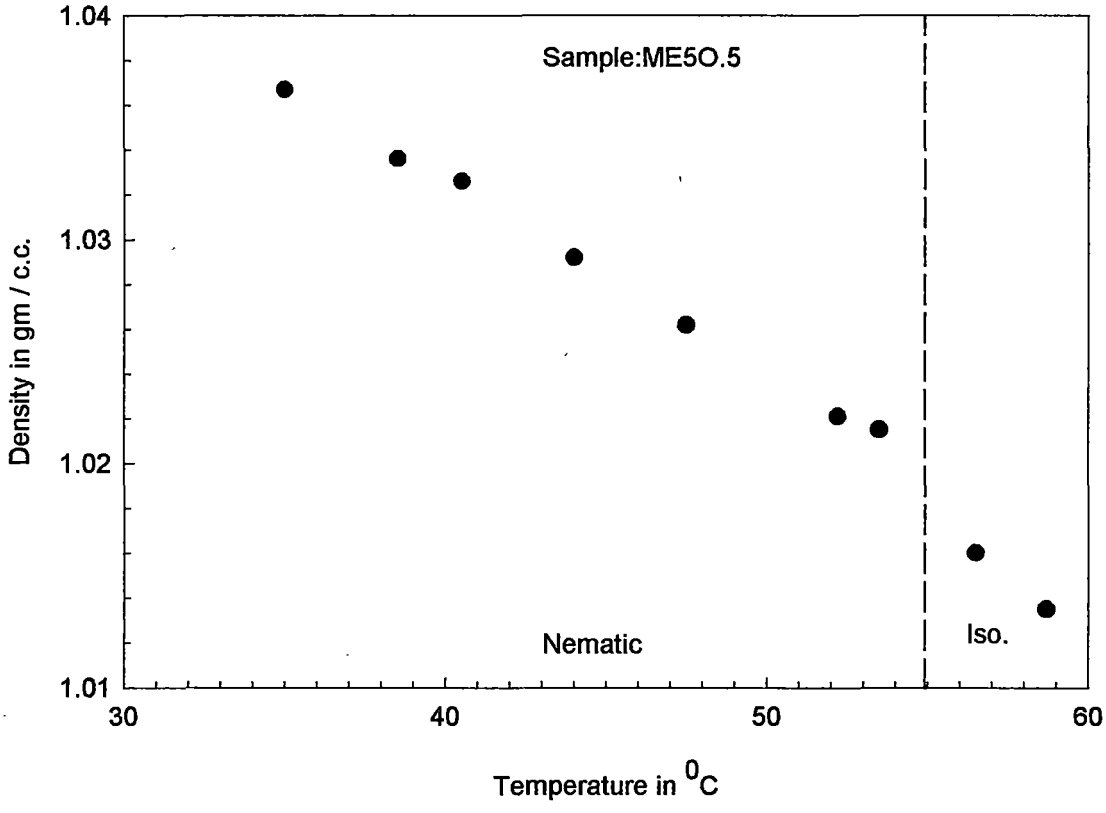

Figure 7.1. Density values as a function of temperature.

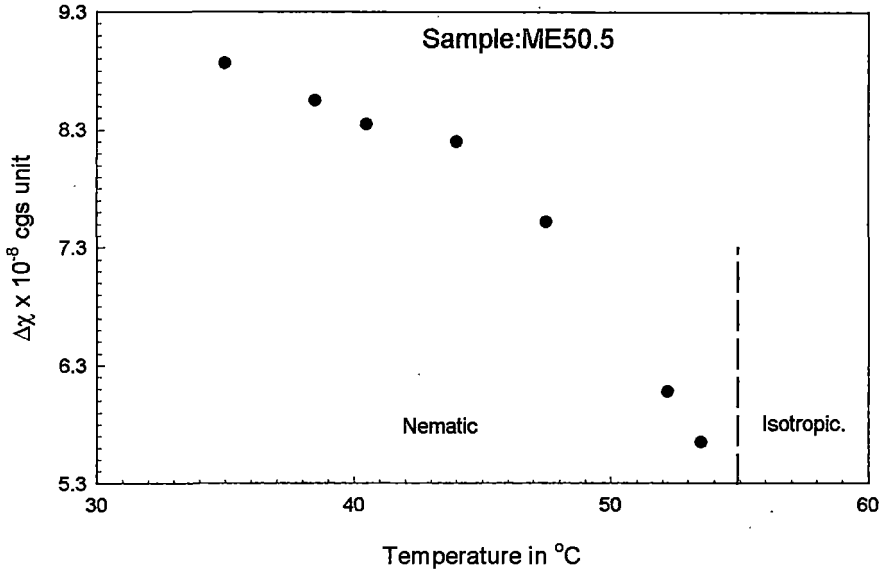

Figure 7.2. Temperature variation of the anisotropy of the diamagnetic susceptibility ($\Delta\chi$).

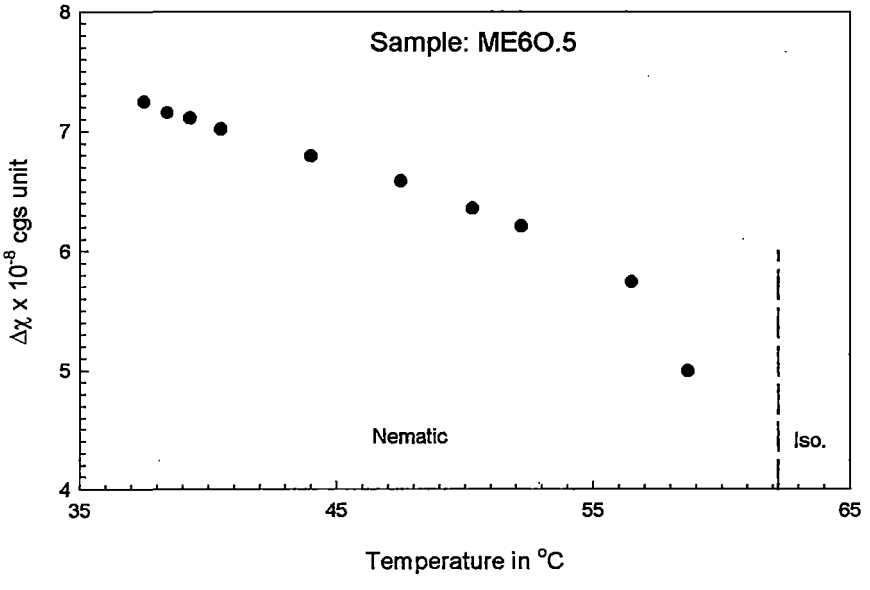

Figure 7.3. Temperature variation of the anisotropy of the diamagnetic susceptibility ($\Delta\chi$).

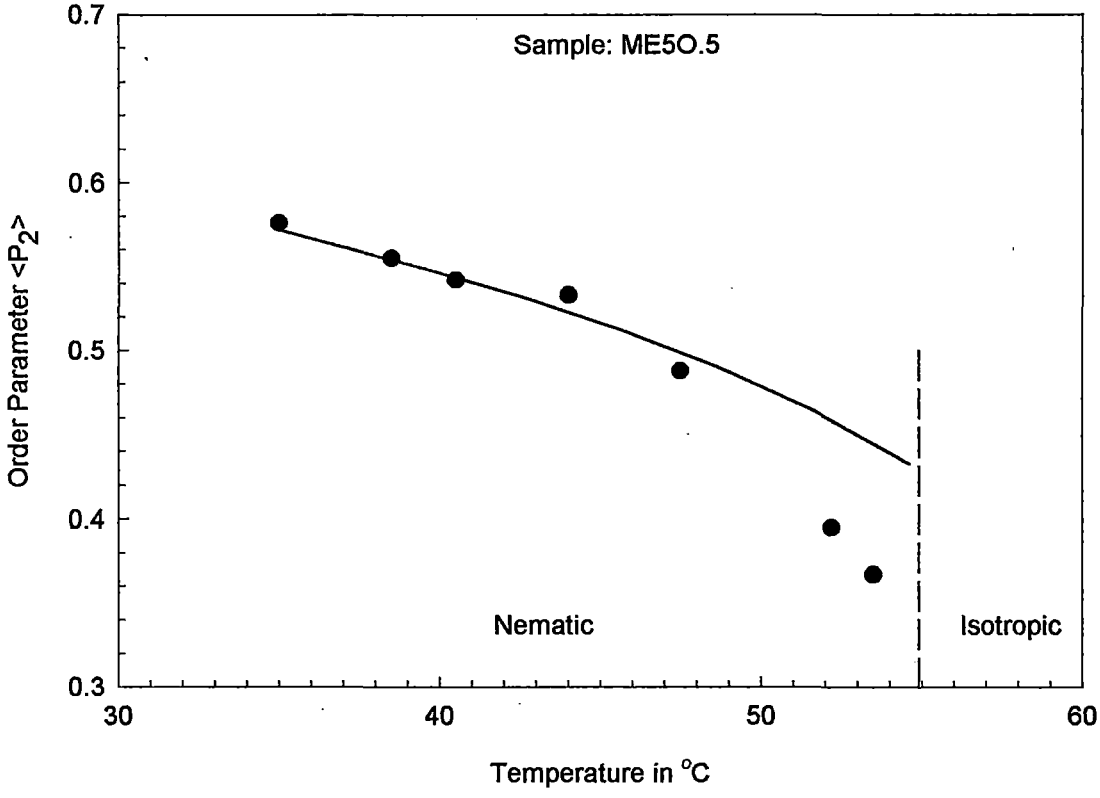

Figure 7.4. Temperature variation of Order Parameter $\langle P_2 \rangle$. Continuous curve corresponds to Maier-Saupe theoretical values.

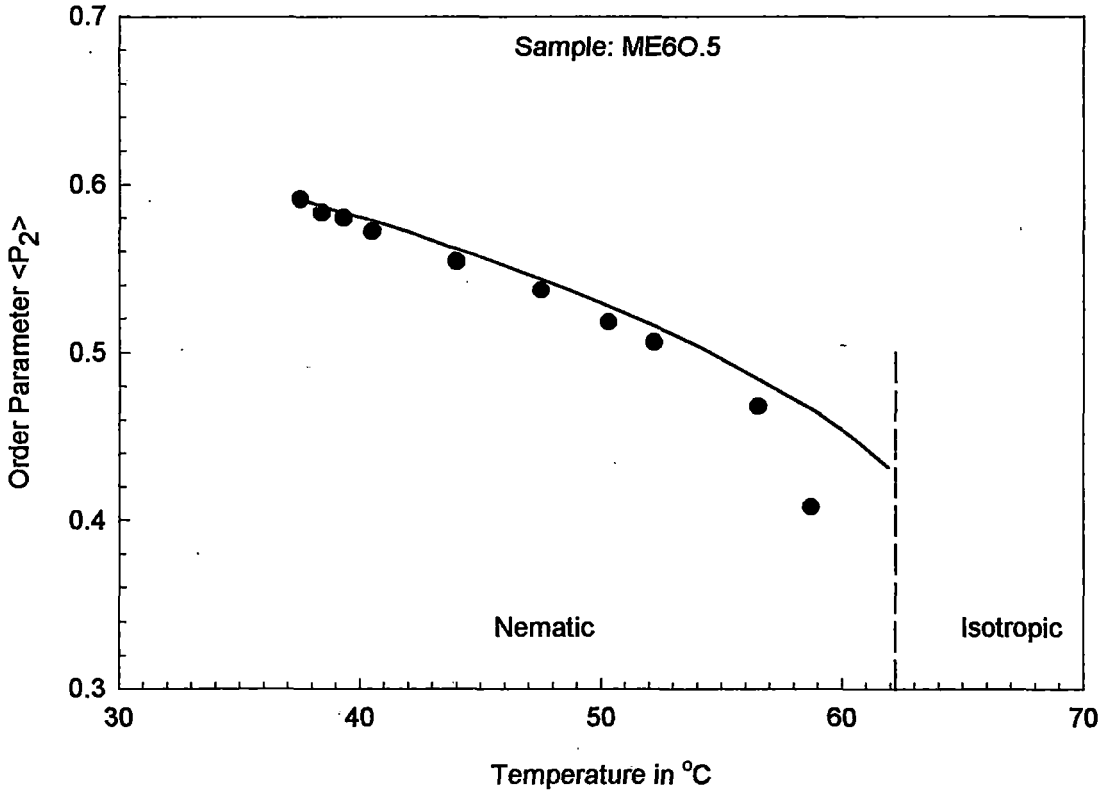

Figure 7.5. Temperature variation of Order Parameter $\langle P_2 \rangle$. Continuous curve corresponds to Maier-Saupe theoretical values.

values for 6O.5 are given Table 7.2. The density values are those interpolated from the data of Das et al [1]. The temperature variation of density of ME 5O.5 is shown in Figure 7.1. Figures 7.2 and 7.3 show the temperature variations of $\Delta\chi$ for ME 5O.5 and ME 6O.5 respectively. Our magnetic susceptibility values for ME 6O.5 are in good agreement with those obtained by Ibrahim and Haase [8]. The temperature variation of order parameters of ME 5O.5 and ME 6O.5 are shown in Figures 7.4 and 7.5 respectively. The theoretical Maier-Saupe order parameter values are also shown in the Figures. The agreement between our experimental values and Maier-Saupe calculated values of $\langle P_2 \rangle$ is good except near the nematic-isotropic transition temperature. This type of behaviour of the order parameters calculated from magnetic susceptibility is quite common (see for example Chapter 3 and Chapter 4 of this thesis). The order parameter values of ME 6O.5 are some what larger than those obtained by Das et al [1] from refractive index data. However, Das et al [2] calculated $\langle P_2 \rangle$ from x-ray diffraction data for ME 6O.5 and found values which are slightly larger than the present $\langle P_2 \rangle$ values obtained from magnetic susceptibility.

The values of splay and bend elastic constants of ME 5O.5 at different temperatures are given in Tables 7.3 and 7.4 respectively. Tables 7.5 and 7.6 show the values of splay and bend elasitic constants respectively. The values of critical magnetic field and the sample thicknesses are also recorded in the respective Tables. The temperature variation of splay elastic constants for ME 5O.5 and ME 6O.5 are shown in Figures 7.6 and 7.7 respectively. Similarly, the temperature variation of bend elastic constants for ME 5O.5 and ME 6O.5 are shown in Figures 7.8 and 7.9 respectively. All the four Figures show normal behaviour, i.e.,

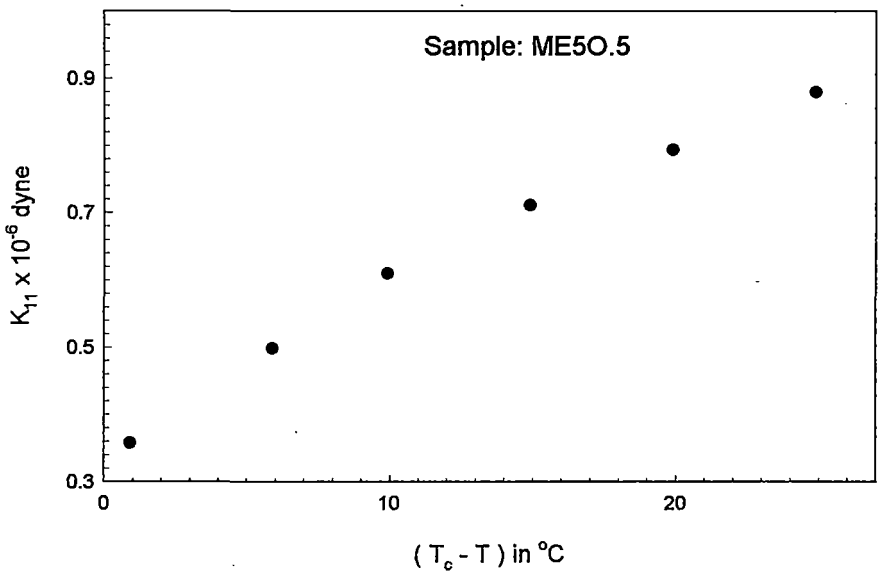

Figure 7.6.Splay elastic constant (K_{11}) as a function of relative temperature (T_c - T).

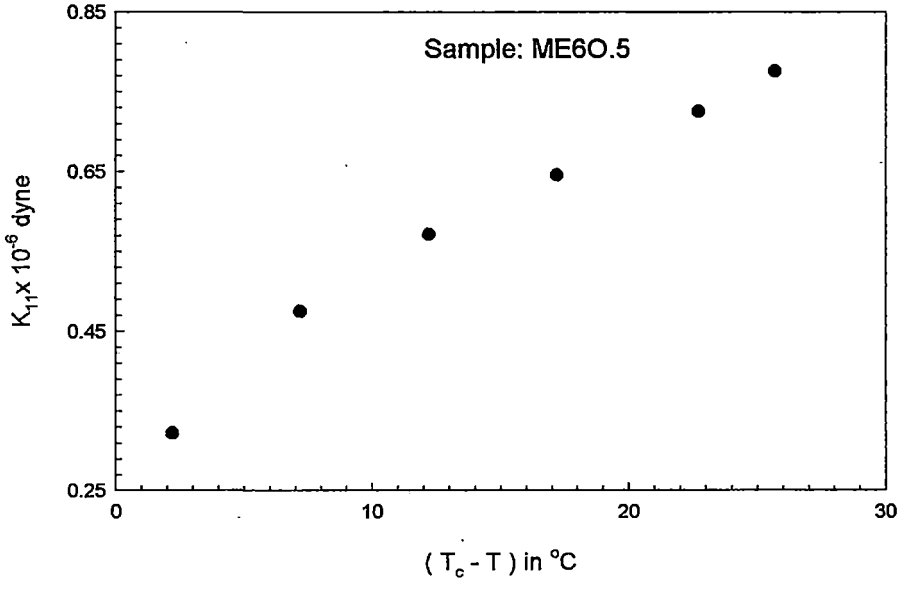

Figure 7.7. Splay elastic constant (K_{11}) as a function of relative temperature (T_c - T).

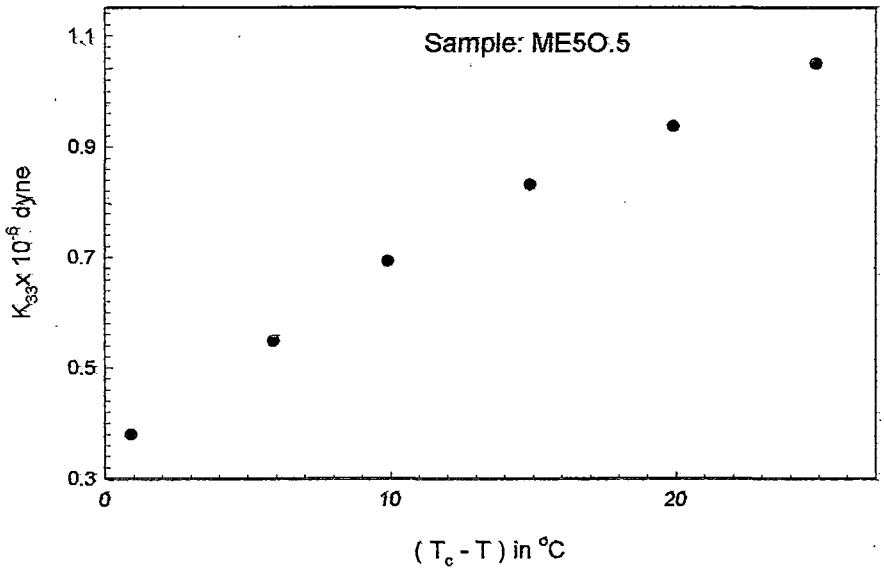

Figure 7.8. Bend elastic constant (K_{33}) as a function of relative temperature (T_c - T).

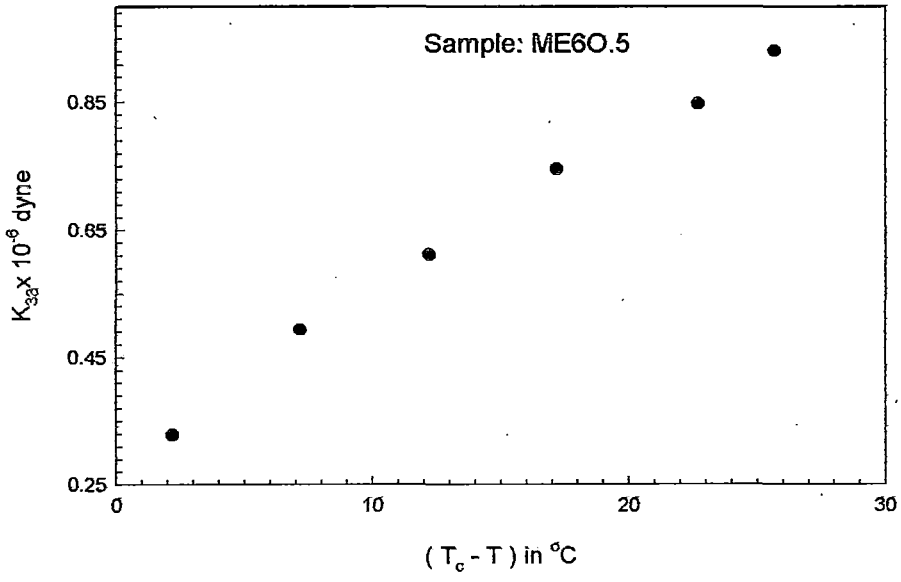

Figure 7.9. Bend elastic constant (K_{33}) as a function of relative temperature (T_c - T).

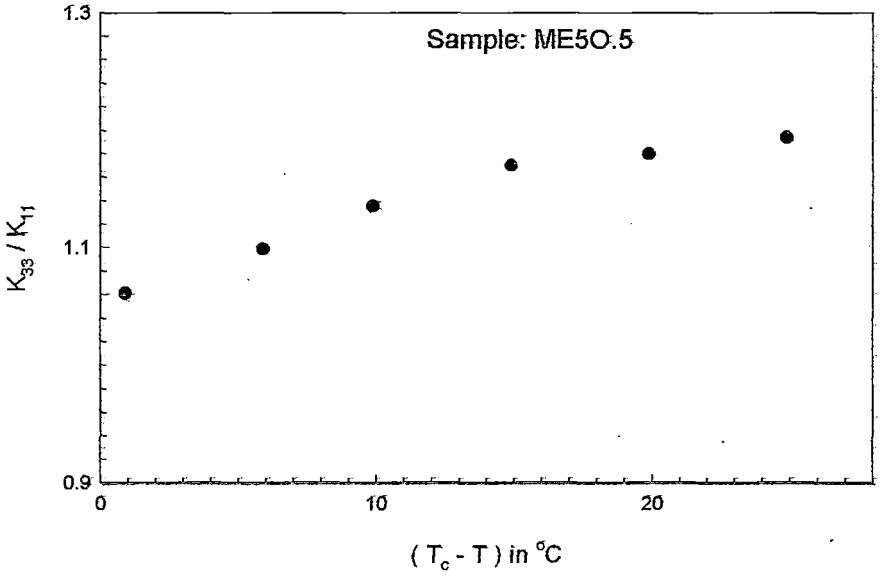

Figure 7.10. Bend to Splay elastic constant ratio (K_{33} / K_{11}) as a function of relative temperature (T_c - T).

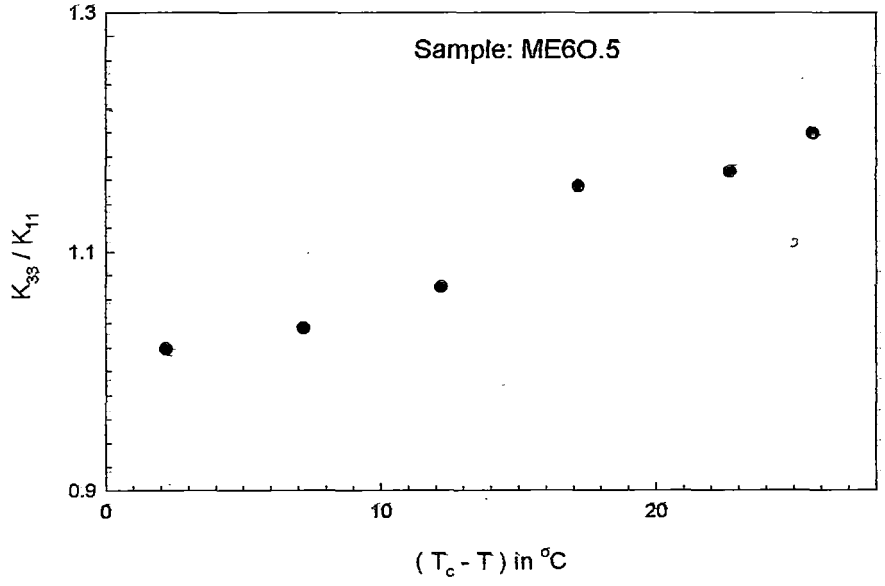

Figure 7.11. Bend to Splay elastic constant ratio (K_{33} / K_{11}) as a function of relative temperature (T_c - T).

elastic constants are increasing with decreasing temperatures. The bend to splay elastic constant ratios for ME 5O.5 and ME 6O.5 are given in Table 7.7 and shown in Figures 7.10 and 7.11 respectively. The K_{33}/K_{11} ratios for both the nematogens are greater than 1 at all temperatures and also increase with decreasing temperatures. This behaviour is quite common in normal nematogens. It is well known [13] that if any alkoxy part in a mesogenic compound is replaced by corresponding alkyl chain, then K_{33}/K_{11} ratio is larger in the alkoxy compound than that in the alkyl compound. It can be seen that if the alkoxy chain in ME 5O.5 is replaced by corresponding alkyl chain then the resulting compound is ME 5.5, whose K_{33}/K_{11} values are given by Bradshaw et al.[13]. One can see that the K_{33}/K_{11} value of ME 5.5 are smaller than those of ME 5O.5 if comparisons are made at the same relative temperature (T_c - T). For example at T_c - T = 24.9 ^{0}C, the K_{33}/K_{11} ratio for ME 5O.5 and ME 5.5 are 1.194 and 1.145 respectively.

The values of density, $\chi_{\parallel}$, $\Delta\chi$, and $< P_2 >$ at different temperatures for 3CPOd(3)1 and 5CPOd(3)1 are tabulated in Tables 7.8 and 7.9 respectively. The values of $\Delta\chi$ for $< P_2 > = 1$ are obtained by Haller's extrapolation method (Chapter 2) and are shown in the Tables. The density values shown in the Tables are interpolated from the density values given by Nath et al.[12]. The temperature variation of $\Delta\chi$ for 3CPOd(3)1 and 5CPOd(3)1 are shown in Figures 7.12 and 7.13 respectively. The values of $\Delta\chi$ changes discontinously at the clearing temperature as it should for nematogens. Figures 7.14 and 7.15 show the temperature variation of order parameter for 3CPOd(3)1 and 5CPOd(3)1 respectively. The order parameter values calculated from Maier-Saupe theory are also shown in the figures. Again, the agreements are very good except near the nematic to

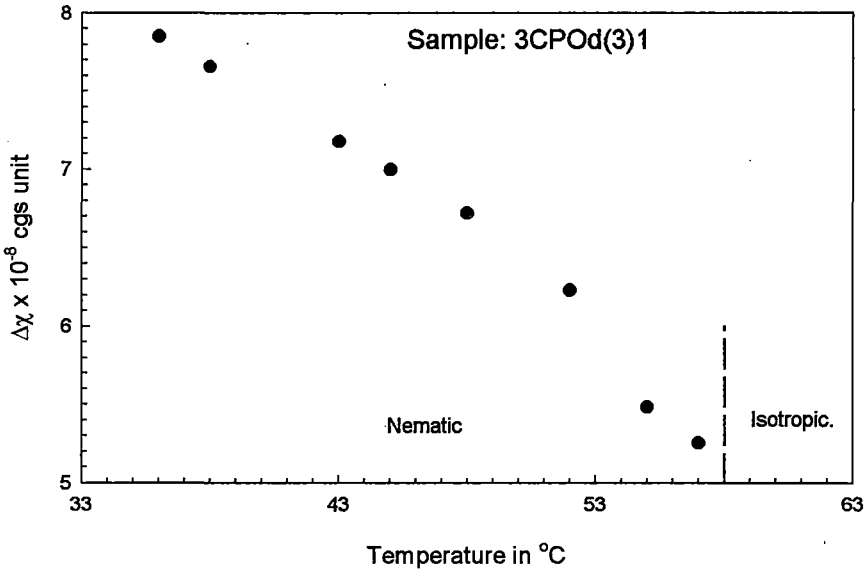

Figure 7.12. Temperature variation of the anisotropy of the diamagnetic susceptibility ($\Delta\chi$).

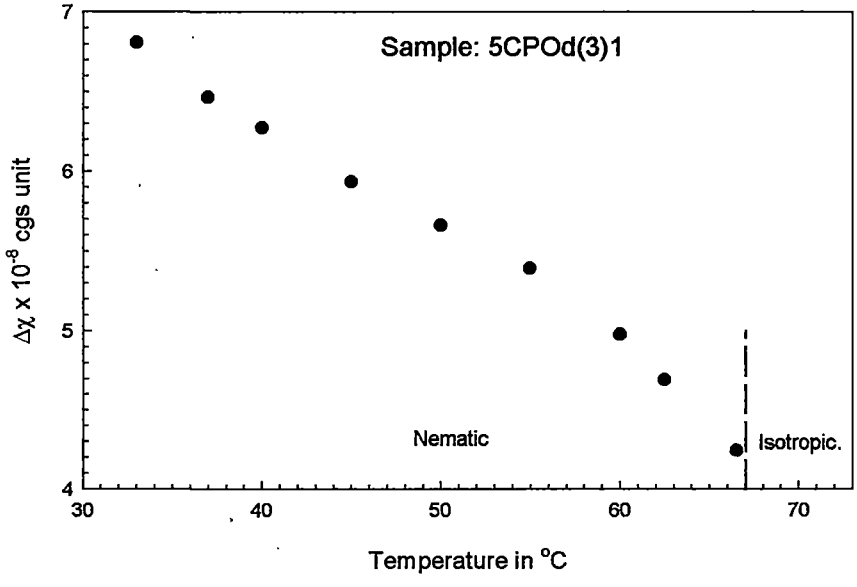

Figure 7.13. Temperature variation of the anisotropy of the diamagnetic susceptibility ($\Delta\chi$).

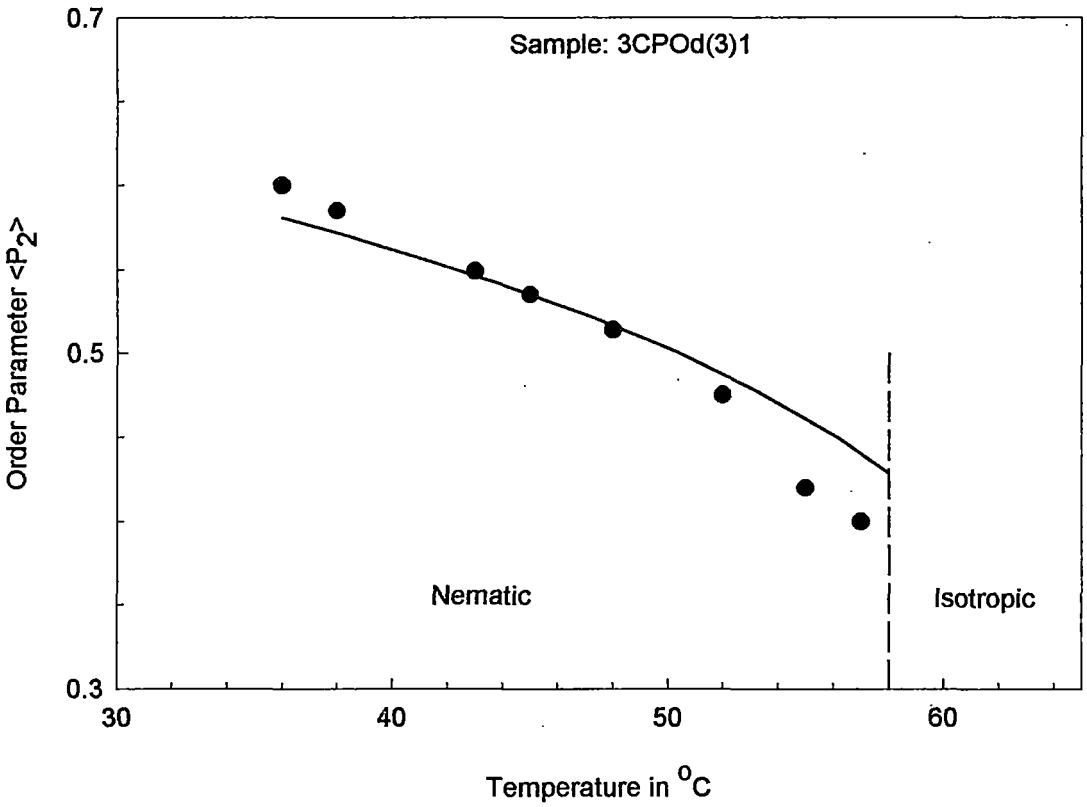

Figure 7.14. Temperature variation of orientational order parameter $\langle P_2 \rangle$ obtained from magnetic susceptibility measurement.

Continuous curves correspond to Maier-Saupe theoretical values.

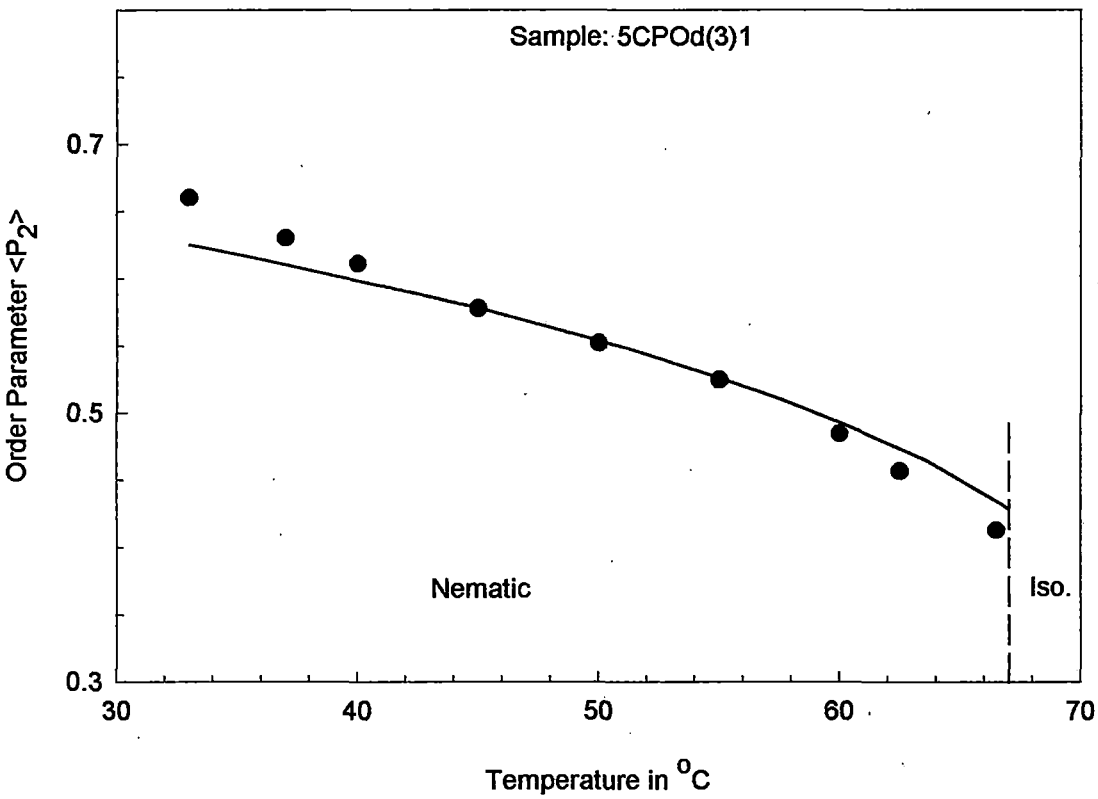

Figure 7.15. Temperature variation of orientational order parameter $\langle P_2 \rangle$ obtained from magnetic susceptibility measurement.

Continuous curves correspond to Maier-Saupe theoretical values.

isotropic transition temperature. The present order parameter values for both the nematogens are slightly lower than the $<P_2>$ values calculated from x-ray diffraction data [11], but are somewhat greater than those determined from refractive index data [11]. This trend in order parameter values obtained from different techniques is also well known and has been discussed in a previous Chapter (Chapter-3) in some detail. The bend and splay elastic constant for 3CPOd(3)1 have been reported earlier [9.10] and those for both 3CPOd(3)1 and 5CPOd(3)1 have been measured in our laboratory [13]. The K_{33}/K_{11} ratio for both the nematogens are greater than 1 and the temperature variation of elastic constants have no abnormal behaviour.

Table 7.1

Experimental values of the density (ρ) , magnetic susceptibility (χ) , susceptibility anisotropy (Δχ) , and the order parameter < P_2 >.

Sample: ME5O.5

Temp. in °C	Density (ρ) in gm/cc	$-\chi_{\parallel}$ x 10^{-7} c.g.s.unit	Δχ x 10^{-8} c.g.s.unit	order parameter < P_2 >
35	1.0367	6.40	8.9	0.576
38.5	1.0336	6.42	8.5	0.555
40.5	1.0326	6.44	8.3	0.542
44	1.0292	6.45	8.2	0.533
47.5	1.0262	6.49	7.5	0.488
52.2	1.0221	6.59	6.1	0.395
53.5	1.0215	6.62	5.6	0.367
56.5	1.0186	6.99 = $\bar{\chi}_{iso}$		

$\Delta\chi_o$ = 1.54 x 10^{-7} c.g.s.unit ;

Table 7.2

Experimental values of the density (ρ) , magnetic susceptibility (χ) , susceptibility anisotropy (Δχ) , and the order parameter < P_2 >.

Sample: ME6O.5

Temp. in °C	Density (ρ)* in gm/cc	$-\chi_{\parallel}$ x 10^{-7} c.g.s.unit	Δχ x 10^{-8} c.g.s.unit	order parameter < P_2 >
37.5	1.0193	6.69	7.2	0.591
38.4	1.019	6.70	7.1	0.583
39.3	1.018	6.70	7.1	0.580
40.5	1.016	6.71	7.0	0.572
44.0	1.014	6.72	6.7	0.554
47.5	1.012	6.74	6.6	0.537
50.3	1.009	6.75	6.4	0.518
52.2	1.007	6.76	6.2	0.506
56.5	1.004	6.79	5.7	0.468
58.7	1.001	6.84	4.8	0.408
63.7	0.992	7.18 = $\bar{\chi}_{iso}$		

$\Delta\chi_o$ = 1.226 x 10^{-7} c.g.s.unit ;

* Interpolated values from reference [1].

Table7.3

Experimental values of splay elastic constant (K_{11}) for various (T_c -T) values.

Sample ME5O.5

T_c = 54.9° C, Sample thickness =162 μm, H_c =Threshold magnetic field

T_c - T	H_c in Gauss	$\Delta\chi$ x 10^{-8} cgs unit	K_{11} x 10^{-6} dyne
0.9	495	5.5	0.36
5.9	515	7.1	0.50
9.9	535	8.0	0.61
14.9	564	8.4	0.71
19.9	580	8.9	0.79
24.9	595	9.3	0.88

Table 7.4

Experimental values of Bend elastic constant (K_3) for various (T_c - T) values.

Sample ME5O.5

T_c = 54.9° C, Sample thickness =162 μm, H_c =Threshold magnetic field

T_c - T	H_c in Gauss	$\Delta\chi$ x 10^{-8} cgs unit	K_{33} x10^{-6} dyne
0.9	510	5.5	0.38
5.9	540	7.1	0.55
9.9	570	8.0	0.69
14.9	610	8.4	0.83
19.9	630	8.9	0.94
24.9	650	9.3	1.05

Table7.5

Experimental values of splay elastic constant (K_{11}) for various (T_c - T) values.

Sample ME6O.5

T_c = 62.2° C, Sample thickness =162 μm, H_c= Threshold magnetic field

T_c - T	H_c in Gauss	$\Delta\chi$ x 10^{-8} cgs unit	K_{11} x 10^{-6} dyne
2.2	515	4. 6	0.32
7.2	550	5.9	0.47
12.2	580	6.4	0.57
17.2	600	6.7	0.64
22.7	620	7.1	0.72
25.7	630	7.3	0.78

Table 7.6

Experimental values of Bend elastic constant (K_3) for various (T_c - T) values.

Sample ME6O.5

T_c = 62.2° C, Sample thickness = 162 μm,H_c =Threshold magnetic field

T_c - T	H_c in Gauss	$\Delta\chi$ x 10^{-8} cgs unit	K_{33} x10^{-6} dyne
2.2	520	4.5	0.33
7.2	560	5.9	0.49
12.2	600	6.4	0.61
17.2	645	6.7	0.74
22.7	670	7.1	0.85
25.7	690	7.3	0.93

Table 7.7

Experimental values of the Frank elastic constant ratio (K_{33} / K_{11}) at different relative temperatures (T_c - T).

Sample: ME5O.5		Sample: ME6O.5	
T_c - T	K_{33} / K_{11}	T_c - T	K_{33} / K_{11}
0.9	1.06	2.2	1.02
5.9	1.10	7.2	1.04
9.9	1.13	12.2	1.07
14.9	1.17	17.2	1.15
19.9	1.18	22.7	1.17
24.9	1.19	25.7	1.20

Table 7.8

Experimental values of the density (ρ) , magnetic susceptibility (χ) , susceptibility anisotropy (Δχ) , and the order parameter < P_2 >

Sample: 3CPOd(3)1

Temp. in ° C	Density (ρ)* in gm/cc	$-\chi_{\parallel}$ x 10^{-7} c.g.s.unit	Δχ x 10^{-8} c.g.s.unit	order parameter < P_2 >
36	0.973	6.37	7.8	0.600
38	0.971	6.39	7.6	0.585
43	0.967	6.42	7.2	0.549
45	0.965	6.43	7.0	0.535
48	0.963	6.45	6.7	0.514
52	0.958	6.48	6.2	0.475
55	0.955	6.53	5.5	0.420
57	0.951	6.55	5.2	0.400
60	0.945	6.90 = $\bar{\chi}_{iso}$		

$\Delta\chi_o$ = 1.308 x 10^{-7} c.g.s.unit ;

* Interpolated values from reference [22].

Table 7.9

Experimental values of the density (ρ) , magnetic susceptibility (χ) , susceptibility anisotropy (Δχ) , and the order parameter < P_2 >

Sample: 5CPOd(3)1

Temp. in °C	Density (ρ)* in gm/cc	$-\chi_{\parallel}$ x 10^{-7} c.g.s.unit	Δχ x 10^{-8} c.g.s.unit	order parameter < P_2 >
33.0	0.963	6.85	6.8	0.660
37.0	0.962	6.87	6.5	0.630
40.0	0.959	6.88	6.3	0.611
45.0	0.955	6.90	5.9	0.578
50.0	0.950	6.92	5.7	0.552
55.0	0.946	6.94	5.4	0.525
60.0	0.942	6.97	5.0	0.485
62.5	0.939	6.99	4.7	0.457
66.5	0.930	7.02	4.2	0.413
70.0	0.925	7.30 = $\bar{\chi}_{iso}$		

$\Delta\chi_o$ = 1.03 x 10^{-7} c.g.s.unit ;

* Interpolated values from reference [22].

References:

1) M. K. Das and R. Paul, Phase Transitions, 46, 185 (1994).
2) M. K. Das and R. Paul, Phase Transitions, 48, 255 (1994).
3) M. K. Das, R. Paul and D. A. Dumur, Mol. Cryst. Liq. Cryst., 258, 239 (1995).
4) D. A. Dunmur, R. G. Walker and P.Palffy-Muhoray, Mol. Cryst. Liq. Cryst., 122, 321 (1985).
5) P. Palffy-Muhoray, D. A. Dunmeur, W. H. Miller and D. A. Bulzarini , Liquid Crystals and Ordered Fluids, vol.4, editor C.A. Griffin and J. F. Johnson, Plenum N.Y., p615 (1984).
6) Present thesis Chapter 5.
7) P. Adamski, Kristallografiya, 37, 791 (1992).
8) H. Ibrahim and W. Haase, Z. Naterforsch, 31a, 1644 (1976).
9) M. Schadt, R. Buchecker, F. Leenhouts, A. Boller, A. Villiger and M. Petrzilka, Mol. Cryst. Liq. Cryst., 139, 1 (1986).
10) M. Schadt, R. Buchecker and K. Muller, Liq. Cryst., 5 . 239 (1989).
11) A. Nath, P. Mandal, and S. Paul, Mol. Cryst. Liq. Cryst., 299, 483 (1997).
12) A. Nath, Ph.D thesis submitted to University of North Bengal (1995) unpublished.

CHAPTER-8

General discussions and conclusion.

In this dessertation I have presented experimental data for ten pure nematogic compounds and three binary mixtures. The study includes x-ray diffraction, refractive indices, density, magnetic susceptibility and Freedericksz transition measurements and analysis of data to calculate orientational order parameters $\langle P_2 \rangle$ (from x-ray diffraction, refractive index and magnetic susceptibility data), apparent molecular length (l_{ap}) or layer thickness in the mesophase, birefringence (Δn), magnetic susceptibility anisotropy ($\Delta\chi$), bend and splay elastic constants and their ratios. All the binary mixtures studied have induced (or enhanced) smectic A_d phases and one has re-entrant nematic phase as well.

The ten pure component nematogens studied can be subdivided into five groups of two members each, from the structural point of view. Table 8.1 presents the five groups with their structural details and the short name of the members of each group. All compounds have two rings with or without a link between them. Four groups of compounds have one phenyl and one cyclohexyl ring, while only one group has two phenyl rings. In three groups the rings are connected through COO link, while in the other groups the rings are directly connected.

Regarding terminal parts, all the compounds have at least one alkyl or alkoxy chain at one end. Two group of compounds have alkyl or alkoxy chains at both ends. In the remaining three groups -CN, -NCS or $-OCH_2CHCHCH_3$ form the other terminal part.

The main features of the results of my experiments for all the pure compounds are tabulated in brief in Table 8.2. I have not tabulated the order parameter values obtained for these nematogens from different experimental studies, since such comparisons have been done in the chapters concerning the related chemicals.

Table 8.1

Structural details of the compounds studied.

Group No. (Short Chem.names)	Left terminal part	Left* ring	Link	Right* ring	Right terminal part
Group I (CPPCC,CPBCC)	n-alkyl	Cy	COO	Ph	CN
Group II (BPPCC,PPPCC)	n-alkyl	Cy	COO	Ph	n-alkoxy
Group III (10CPS,12CPS)	n-alkyl	Cy	-	Ph	NCS
Group IV (3CPOd(3)1, 5CPOd(3)1)	n-alkyl	Cy	-	Ph	$-OCH_2CHCHCH_3$
Group V (ME5O.5, ME6O.5)	n-alkoxy	Ph	COO	Ph	n-alkyl

* Cy stands for cyclohexyl

Ph stands for phenyl

However, one common feature is that the order parameters determined from x-ray diffraction studies agreed well with the Maier-Saupe calculated values, while the $\langle P_2 \rangle$ values calculated from refractive index and magnetic susceptibility data are always much smaller than the theoretical values near the nematic-isotropic transition temperatures. This lowering seems to be more pronounced for the $\langle P_2 \rangle$ values from refractive index measurements. The possible causes for this discrepancy may be director fluctuations or

imperfect alignment of sample in the bulk (in refractive index studies the sample were aligned by surface treatment, whereas, in the other experiments a magnetic field was applied for bulk alignment of the samples) near the transition temperature. It should also be mentioned that the data analysis to calculate $\langle P_2 \rangle$ involve many different assumptions for different experimental techniques, hence there is no reason why two different techniques should yield exactly same order parameter values. From Table 8.2, it can be seen that the ratio of apparent molecular length (l_{ap}) to model molecular length (L) is about 1.4 form the two cyano compounds of Group I. This is in accordance with previous observations on cyanobiphenyl compounds [1,2]. Therefore, the molecules CPPCC and CPBCC form dimers in the mesophases. For Group III molecules with isothiocyanato (-NCS) group there seems to be some association, since the value of l_{ap}/L is little larger than 1.2. The Group II molecules (BPPCC and PPPCC) also show some association in mesophase, having l_{ap}/L between 1.09 to 1.15. However, Group IV and V molecules do not seem to form association in the nematic phase, since for these compounds the apparent molecular lengths are equal to the model lengths.

The refractive indices (n_e) and birefringence of Group III molecules are the largest. It is not surprising since these compounds contain sulphur in -NCS group as well as a phenyl ring. The refractive index (n_e) of Group I molecules are somewhat larger than that of Group II molecules though the birefringence of the two groups seem to be same. The increase in the value of n_e for Group I molecules compare to Group II is due to the -CN terminal part in the Group I molecules.

Regarding magnetic susceptibility ($\chi_{\parallel}$), we again find that the Group III molecules containing isothiocyanato (-NCS) group have the largest value

Table 8.2

Physical properties of the nematogens studied

Name of the compound		$T_{NI} = T_c$ in ^0C	X-ray diffraction		Refractive index at T_c- 5°C		Mag. Susceptibility at T_c- 5°C		Elastic const. at $(T_c$-5)°C	
			l_{ap} in Å	l_{ap} / L	n_e	Δn	$-\chi_{\parallel} \times 10^{-7}$ (cgs unit)	$\Delta\chi \times 10^{-8}$ (cgs unit)	$K_{33} \times 10^{-6}$ (dyne)	K_{33}/K_{11}
Group I	CPPCC	70.0	22.66	1.39	1.552	0.076	6.90	3.7	0.64	1.14
	CPBCC	68.3	24.42	1.42	1.553	0.075	6.80	3.6	0.41	1.02
Group II	BPPCC	72.6	20.87	1.09	1.531	0.075	6.32	2.6	0.26	0.86
	PPPCC	75.0	24.26	1.15	1.535	0.065	6.45	2.9	0.59	0.98
Group III	10CPS	50.7	31.7	1.23	1.632	0.098	7.15	3.0	0.44	0.92
	12CPS	52.5	33.9	1.21	1.614[d]	0.121[d]	7.63[e]	2.9[e]	0.40[e]	0.99[e]
Group IV	ME5O.5	54.9	-	-	-	-	6.53	6.8	0.52	1.09
	ME6O.5	62.2	24.5[a]	1.00[a]	1.061[f]	0.074[f]	6.81	5.5	0.42	1.03
Group V	3CPOd(3)1	58.0	16.8[b]	0.98[b]	1.504[b]	0.068[b]	6.50	6.0	1.27[c]	1.14[c]
	5CPOd(3)1	67.0	19.1[b]	1.00[b]	1.535[b]	0.097[b]	6.99	4.7	0.83[c]	1.01[c]

[a] - value taken from reference [1]. [b] - value taken from reference [9]. [e] - at temperature T_c - 1.5°C.

[c] - value taken from reference [10]. [d] - at temperature T_c - 4°C.

(magnitude) of $\chi_{\parallel}$. Again, this may be due the presence of sulphur. All other molecules have the value of $\chi_{\parallel}$ in the range 6.3 to 6.9 x 10^{-7} c.g.s unit. The Group I molecules with cyano group and Group IV molecules with two phenyl rings have larger value of $\chi_{\parallel}$. The Group II molecules with only one phenyl ring have the lowest $\chi_{\parallel}$ values. Regarding magnetic susceptibility anisotropy ($\Delta\chi$), the Group IV (with two phenyl rings) and Group V (with one phenyl ring connected to alkenyl chain at one end) have largest anisotropies. These large $\Delta\chi$ may be the effect of enhanced dislocation of π electrons over two phenyl rings (Group IV) or between phenyl ring and the alkenyl chain (Group V). This may also be the reason for the birefringence values of the compounds in these two groups (Group IV and Group V) to be quite large. For all other molecules the $\Delta\chi$ values are much smaller.

The values of bend elastic constants at T_c - 5^0C are also shown in Table 8.2. The largest values are of the two alkenyl compounds (Group V). For all pairs of molecules in each group, the K_{33} values decrease with increasing length of alkyl or alkoxy chain, as is expected. The only exception is in Group II, PPPCC has larger K_{33} values compared to BPPCC even if it has longer alkyl or alkoxy chain at both ends. This is due to the fact that PPPCC has a smectic phase at low temperatures and its nematic phase x-ray diffraction pattern shows sign of cybotactic groups (Chapter 3, Plate 3h). The bend to splay elastic constant ratios are greater than one for Group I, IV and V compounds. It is well known that this ratio are larger for molecules having large polarity. Since Group I molecules have a phenyl ring and a cyano group they have large values of K_{33} /K_{11}. The alkenyl compounds (Group V) and Group IV compounds (with two phenyl rings) have also large polarities, hence their K_{33} /K_{11} values are larger than one.

This ratio also should decrease with increasing chain lengths within each group. Except for Group II and III it seems to be the case. In Group II, PPPCC has larger values of K_{33} /K_{11} than BPPCC, since it has cybotactic groups in its nematic phase. In the Group III (10CPS and 12CPS) the comparison cannot be made, since for 12CPS elastic constants could be measured at only one temperature, 1.5°C below the transition temperature.

Mixture studies.

As mentioned earlier three binary mixtures have been studied by me. Two binary mixtures of a terminal polar compound (5CB) and a non polar compound (ME 5O.5 or ME 6O.5) show induced smectic A_d phase and have been studied extensively before by other workers in our laboratory [3,5]. They observed that the orientational order in these mixtures show a minimum in the same composition range where the smectic A_d phase is most stable. They obtained the $\langle P_2 \rangle$ values from x-ray diffraction and refractive index studies. I measured the magnetic susceptibilities of these two mixtures at different compositions and calculated order parameteres from these data. My data fully corroborates the earlier observations regarding $\langle P_2 \rangle$ being minimum at the composition where smectic A_d phase is more stable.

The other binary system studied by me has both the components terminal polar compounds (12OCB and 7CBB, both having -CN group at one end). This mixture has been previously studied by Dabrowski et al.[6] and show an enhanced smectic A_d phase as well as a re-entrant nematic phase in a certain composition range. I have studied in detail a particular mixture ($x_{7CBB} = 0.917$) of this binary system, which showed both re-entrant nematic and smectic A_d phases. I studied density, refractive indices and x-ray diffraction patterns of this particular mixture. My study seems to indicate that the re-entrant nematic to smectic A_d phase transition for this

mixture is continuous. I have also measured variation of layer thickness with both temperature and composition for the mixtures of 7CBB and 12OCB. The main observation is that while the temperature variation of layer thickness at a particular composition is negligible, the composition variation of layer thickness shows a broad maximum near equimolar concentration. This behaviour has been qualitatively explained in Chapter 6, assuming formation of homo dimers (12OCB +12OCB) and hetero dimers (7CBB+12OCB). A calculation which will presumably explain the variation of layer thickness quantitatively in this system as well as in a related system (7CBB+7OCB), which has been studied in our laboratory, [7] is in progress.

Reference:

1) B. Bhattacharjee, S. Paul and R. Paul, Molecular Physics, 44, 139 (1981).
2) A. J. Leadbetter, R. M. Richardson and C. N. Colling, J. Phys., Paris, 36, c1 (1975).
3) M. K. Das and R. Paul, 46, 185 (1993).
4) M. K. Das and R. Paul, 48, 255 (1994).
5) M. K. Das and R. Paul, 258, 239 (1995).
6) M. Brodzik and R. Dabrowski, Liquid Crystals, 18, 61 (1995)
7) S. K. Giri, N. K. Pradhan, R. Paul, S. Paul, P. Mandal, R. Dabrowski, M. Brodzik and K. Czuprynski, SPIE, 3319, 149 (1998).
8) M. K. Das, Ph. D thesis submitted to University of North Bengal (1993), unpublished.
9) A. Nath, Ph. D thesis submitted to University of North Bengal (1995), unpublished.
10) Private communication from S. K. Giri.

Paper published:

1. Small angle x-ray diffraction study of mixtures showing re-entrant nematic phase and induced smectic A_d phase:
   S. K. Giri, N. K. Pradhan, R. Paul, S. Paul, P. Mandal, R. Dabrowski, M. Brodzik and K. Czuprynski, SPIE, 3319, 149 (1998).

Papers to be communicated:

1. Magnetic Susceptibility measurements in two binary mixture systems showing induced smectic A_d phase:
   N. K. Pradhan and R. Paul to be communicated to Mol. Cryst. Liq. Cryst.

2. Refractive index, density and order parameter of two mesomorphic mixtures showing induced smectic A_d phase and re-entrant nematic phase:
   S. K. Giri, N. K. Pradhan, R. Paul, S. Paul, P. K. Mandal, , R. Dabrowski, M. Brodzik and K. Czuprynski. Mol. Cryst. Liq. Cryst., (to be communicated).

3. Physical properties of four cyclohexane carboxylate liquid crystals I, x-ray diffraction studies:
   N. K. Pradhan and R. Paul, Phase Transition (to be communicated).

4. Physical properties of four cyclohexane carboxylate liquid crystals II, refractive index, magnetic susceptibility and elastic constant measurements:
   N. K. Pradhan and R. Paul, Phase Transition (to be communicated).

5. Physical properties of two nematogenic members of isothiocyanatobenzenes:
   N. K. Pradhan et al. Mol. Cryst. Liq. Cryst., (to be communicated).

6. Magnetic susceptibility and elastic constants of four nematogens:
   N. K. Pradhan, S. K. Giri et al, Mol. Cryst. Liq. Cryst., (to be communicated).

Papers presented:

1. Magnetic Susceptibility measurements in two binary mixture systems showing induced smectic A_d phase: N. K. Pradhan and R. Paul.,
   Accepted at 16th International Liquid Crystal Conference, Kent State, June 24-28, 1996, Ohio, USA. Abstract No. D2P.59.

2. Study of liquid crystalline mixture showing re-entrant nematic phase: N. K. Pradhan, R. Paul, S. Paul, R. Dabrowski, and K. Czuprynski.
   Presented at the European Conference on Liquid Crystals- Science and Technology, March 3-8, 1997, Zakopone, Poland. Abstract No. A-11.

3. Small angle x-ray diffraction study of mixtures showing re-entrant nematic phase and induced smectic A_d phase: S. K. Giri, N. K. Pradhan, R. Paul, S. Paul, P. Mandal, R. Dabrowski, M. Brodzik and K. Czuprynski.
   Presented at the National Seminar on Liquid Crystals, 18-20 Dec. 1997, Jammu. Abstract No.13.

4. Refractive index, density and order parameter of two mesomorphic mixtures showing induced smectic A_d phase and re-entrant nematic phase: S. K. Giri, N. K. Pradhan, R. Paul, S. Paul, P. K. Mandal, , R. Dabrowski, M. Brodzik and K. Czuprynski.
   Accepted at 16th International Liquid Crystal Conference, July 19- 24, 1998, Strasbourge, France. Abstract No. P4-198.